PHARMACEUTICAL WASTEWATER TREATMENT BY ELECTROOXIDATION METHOD

A THESIS

Submitted in partial fulfilment of the requirements for the award of the degree

of

DOCTOR OF PHILOSOPHY

in

CHEMICAL ENGINEERING

by

RAVNEET KAUR

DEPARTMENT OF CHEMICAL ENGINEERING
THAPAR INSTITUTE OF ENGINNERING AND TECHNOLOGY
(Deemed to be University)
PATIALA -147004

May, 2019

PHARMACEUTICAL WASTEWATER TREATMENT BY ELECTROOXIDATION METHOD

A THESIS

Submitted in partial fulfilment of the requirements for the award of the degree

of

DOCTOR OF PHILOSOPHY

in

CHEMICAL ENGINEERING

by

RAVNEET KAUR

DEPARTMENT OF CHEMICAL ENGINEERING
THAPAR INSTITUTE OF ENGINNERING AND TECHNOLOGY
(Deemed to be University)
PATIALA -147004

May, 2019

CANDIDATE'S DECLARATION

I hereby certify that the work which is being presented in the thesis entitled **"PHARMACEUTICAL WASTEWATER TREATMENT BY ELECTROOXIDATION METHOD"** in partial fulfillment of the requirements for the award of the degree of Doctor of Philosophy and submitted in the Department of Chemical Engineering, Thapar Institute of Engineering and Technology, Patiala is an authentic record of my own work carried out during a period from July 2014 to May 2019 under the supervision of Dr. J. P. Kushwaha, Associate Professor, Department of Chemical Engineering and Dr. Neetu Singh, Associate Professor, Department of Chemical Engineering, Thapar Institute of Engineering and Technology, Patiala.

The matter presented in the thesis has not been submitted by me for the award of any other degree of this or any other Institute.

Ravneet Kaur

(RAVNEET KAUR)

This is to certify that the above statement made by the candidate is correct to the best of our knowledge.

Dr. J. P. Kushwaha
Supervisor

Dr. Neetu Singh
Supervisor

ABSTRACT

Advancement in medical science over years has led to bulk production and consumption of pharmaceutical compounds all over the world. Antibiotics, particularly have become an indispensable part of human and animal health systems, which are intended to treat bacterial infections. As per a report published in 2018, over a period of fifteen years (2000 – 2015), antibiotic consumption in India increased by 103%. Moreover, India was the largest consumer of antibiotics in the world in 2010, with cephalosporins, broad-spectrum penicillins and fluoroquinolones among the top three categories of antibiotics being consumed by Indians Such large production and intake of antibiotics has led to their occurrence and accumulation in aquatic environment.

Scientific communities worldwide have conducted comprehensive studies and reported occurrence of antibiotics in effluents from waste water treatment plants, sewage treatment plants, sea water, river water, lakes and ground water, which proved the incapability of conventional treatment technologies to remove antibiotics. This alarming issue requires immediate attention due to growing antibiotic resistance in native bacterial population. Over the years, this problem has worsened in India, leading to highest number of deaths caused by antibiotic resistance.

Electro-oxidation (EO) has fetched much attention of researchers in past two decades. EO is a type of electrochemical AOP, which utilizes strong oxidant species (•OH, H_2O_2, O_3) generated on anode for pollutant degradation in a much simpler equipment and without involvement of any hazardous chemicals. Moreover, it is an environmentally benign technology as no sludge generation takes place. In present study, two commonly prescribed antibiotics: ofloxacin (OFLX) and amoxicillin trihydrate (AMT), belonging to fluroquinolone and penicillin category, respectively, were chosen as model pollutants for testing the degradation/mineralization efficiency of EO cell comprising of Ti/RuO_2 electrodes in batch as well continuous mode of treatment.

In case of batch EO treatment of antibiotics (OFLX and AMT), treatment efficiency was evaluated in terms of antibiotic removal efficiency (%ARE), TOC removal efficiency (%TRE), specific energy consumption (SEC, kW h (g TOC removed)$^{-1}$) and mineralization current efficiency (%MCE). The effects of operating parameters such as applied current (*I*, 0.25–1.0 A), initial pH of wastewater (2–9) and supporting electrolyte (NaCl) concentration

(S_0, 0.5–2 g L^{-1}), on ARE, TRE, SEC and MCE were systematically studied. Effect of initial antibiotic concentration (C_0, 10–50 mg L^{-1}) and applied current (*I*) on kinetics of antibiotic degradation was analysed. Analysis of transformation products of antibiotics formed during EO was done by ultra-performance liquid chromatography coupled with mass spectrometry (UPLC-Q-TOF-MS).

In case of batch EO treatment of OFLX, optimum pH and current were found to be 6.8 ± 0.1 (natural pH of OFLX wastewater) and 1 A, at which 80% ARE and 46.3% TRE were achieved in 30 min and 240 min of electrolysis, respectively. MCE decreased from 7.8 to 4.9% with increase in *I* value from 0.25 to 1 A. De-fluorination, breaking of piperazinyl ring and dealkylation or replacement by •OH and Cl^- led to the formation of seven major OFLX transformation products. Whereas, when batch EO of AMT was performed, 60% of antibiotic and 48% of TOC removal took place in 60 and 240 min, respectively, at optimum conditions of 1 A of applied current and neutral pH 7.0. MCE decreased from 11.77 to 7.67% with increase in applied current from 0.25 to 1.0 A. This was attributed to increase in undesirable but inevitable reactions occurring simultaneously during EO, which consumed a considerable part of energy. Three major transformation products of AMT were identified which were generated after hydroxylation of AMT molecule and attack of active chlorine on aromatic moiety. Degradation of both the drugs followed pseudo-first order kinetics. Increase in applied current resulted in rapid degradation, which was proved by increase in k_f value. SEC decreased with the increase in NaCl concentration. The operating cost of EO process for removal of 1 g of TOC was found to be INR 35.38 ($ 0.54) and INR 28.88 ($ 0.44) for OFLX and AMT, respectively.

The reactor set-up for continuous EO treatment was similar to batch except that an inlet and outlet points were incorporated in the reactor, and a continuous supply of wastewater from reservoir to reactor at required flow-rate (corresponding to retention time) was facilitated by a peristaltic pump. The continuous EO of antibiotics was performed after designing the experiments by response surface methodology (RSM) based on five level central composite design (CCD) . Set of 30 experiments with 6 replications were performed for each antibiotic. Individual and interactive effects of operating parameters (independent variables): pH (2–10), *I* (0.25–1.25 A), retention time (R_T, 15 – 195 min) and elapsed time (*t*, 20 -180 min), on the responses %TOC removal (Z_1), % antibiotic removal (Z_2) and SEC (Z_3) were investigated. Synthetic wastewater comprising 50 mg L^{-1} of drug and 2 g L^{-1} of

NaCl was freshly prepared before each experiment. As suggested by ANOVA, the quadratic model was found to be significant for both the antibiotics. The optimum condition for continuous EO treatment of OFLX as found by RSM was: pH = 6.0, I = 0.64 A, R_T = 157.68 min and **t** = 170 min. The experimental values of the responses (Z_1 = 23.85%, Z_2 = 76.78%, Z_3 = 0.706 kW h (g TOC removed)$^{-1}$) were in good agreement with the predicted values (Z_1 = 23.94%, Z_2 = 78.16%, Z_3 = 0.658 kW h (g TOC removed)$^{-1}$). Seven major reaction intermediates of OFLX were identified and a plausible degradation scheme was proposed. In case of AMT, optimum condition achieved by RSM was: pH = 7.53, I = 0.7 A, R_T = 175.6 min and t = 128.89 min. The experimental values of the responses (Z_1 = 38.36%, Z_2 = 52.86%, Z_3 = 0.385 kW h (g TOC removed)$^{-1}$) were in good agreement with the predicted values (Z_1 = 37.82%, Z_2 = 51.64%, Z_3 = 0.408 kW h (g TOC removed)$^{-1}$). MCE at optimum run came out to be 5.07 and 9.81% for OFLX and AMT, respectively. Decay kinetics of both the antibiotics as well as mineralization at optimum run of continuous EO followed pseudo-first order kinetic model. However, degradation was found to be almost five times faster than mineralization of antibiotics by Ti/RuO_2 electrodes. A plausible degradation mechanism was proposed on the basis of eight major reaction intermediates of AMT. Apart from direct degradation at anode surface, the AMT molecule was indirectly oxidized by active chlorine leading to opening of its beta-lactam ring. The chlorinated transformation products underwent reduction at the Ti/RuO_2 cathode, leading to their de-chlorination. The operating cost of continuous EO treatment of antibiotics came out to be INR 102.69 (US $ 1.57) (OFLX) and INR 56.5 (US $ 0.87) (AMT) for removal of 1 g of TOC from the wastewater.

The characterization of fresh and used Ti/RuO_2 electrodes was done by SEM–EDX and XRD analysis. SEM images revealed that the morphology of electrodes was same, except diminutive loss of RuO_2 coating after performing EO treatment reactions. EDX study of used electrode indicated increase in amount of carbon content as compared to fresh electrode, which could be attributed to •OH mediated EO. XRD pattern of fresh and used electrode exhibited Ti, TiO_2 and RuO_2 rich broad and symmetric peaks. The peak positions in used electrode remained intact, signifying unaltered micro structure, however the intensity of peaks was slightly diminished.

ACKNOWLEDGEMENTS

First and foremost I want to thank the almighty for always blessing me with the best of opportunities and abilities, which empowered me to successfully complete this work.

I would like to express my sincere gratitude to my supervisors **Dr. Jai Prakash Kushwaha** and **Dr. Neetu Singh** for their guidance and expertise in supervising the thesis. I appreciate all their contributions of time, knowledge, ideas and encouragement to make my Ph.D. experience productive and stimulating. Their useful criticism and constant help extended in hours of need had been immensely beneficial.

I express my sincere thanks to **Prof. H. Bhunia** (Head of the Chemical Engineering Department), who has always been very supportive. I am also thankful to **Prof. R. K. Gupta** (Former Head of the Chemical Engineering Department), and members of my IRB committee: **Dr. B. N. Chudasama**, **Dr. S. Barman** and **Dr. S. K. Singh**, for their valuable suggestions throughout the course of this work. I greatly appreciate the support from all the faculty members and technical staff of the Chemical Engineering Department. I would also like to thank entire staff of **SAI Labs** for facilitation in analytical analysis.

I gratefully acknowledge the financial support provided by **University Grants Commission** of India and **Thapar Institute of Engineering and Technology, Patiala**. The institute provided me with a conducive research environment.

I also owe my thanks to **Mr. Nazre Heyat,** HRMS Lab, IIT Ropar, for his help and assistance in UPLC-MS analysis.

A deep appreciation goes to **Surinder Singh,** who dutifully helped me to commute to the institute during this entire period.

A very special gratitude goes out to my colleagues and friends **- Sehaspreet, Bandhana, Kamaljeet, Suman, Parminder, Steffi, Meenakshi and Metali**, for their motivation, support and cheerfulness which enabled me to carry out this work smoothly. It was great sharing lunch with all of you during the period of this work. I would also like to thank my friends **Fiza** and **Nikita**, who are no less than family and have been my emotional support system always.

This thesis would never have been possible without the unbeatable love, support and sacrifices of my father-in-law **Inderjit Singh** and mother-in-law **Sukhjinder Kaur**. I am

also thankful to my sister-in-laws **Satinder** and **Jasdeep** and brother-in-law **Jaskirat Singh** for constantly encouraging me throughout this phase.

I would like to say a heartfelt thanks to my parents **Jagjit Singh** and **Kanwaljit Kaur** for being the wind beneath my wings, and my brother **Hardilmohan Singh** for always believing in me and encouraging to follow my dreams. Needless to say that it is your infinite love, sacrifices and support behind all that I have accomplished today.

Last but by no means least, I am much thankful to my husband **Barjinder Singh,** who has been by my side throughout this Ph.D. It's your selfless love and kindness which always kept me moving. Thank you for always helping me in whatever way you could during this challenging period. Finally, a big thanks to my adorable son **Jahaan Singh** for being such a good little baby for past year, and making it possible for me to complete what I started.

RAVNEET KAUR

CONTENTS

LIST OF TABLES

LIST OF FIGURES

NOMENCLATURE

ABBREVIATIONS

ADP	Amoxicillin degradation product
AMT	Amoxicillin trihydrate
ANOVA	Analysis of variance
AO	Anodic oxidation
AOP	Advanced oxidation processes
ARE	Antibiotic removal efficiency
ARI	Amoxicillin reaction intermediate
BDD	Boron doped diamond
CCD	Central composite design
COD	Chemical oxygen demand
DC	Direct current
DF	Degree of freedom
DWTP	Drinking water treatment plant
EDX	Energy-dispersive x-ray spectroscopy
EF	Electro-Fenton
EO	Electro-oxidation
MCE	Mineralization current efficiency
MPSD	Marquardt's percent standard deviation
OFLX	Ofloxacin
ORI	Ofloxacin reaction intermediate
OTP	Ofloxacin transformation product
RSM	Response surface methodology
SEC	Specific energy consumption
SEM	Scanning electron microscopy
TOC	Total organic carbon
TRE	Total organic carbon removal efficiency
UPLC-Q-TOF-MS	Ultra-performance-quadrupole-time of flight-mass spectrometry
WWTP	Wastewater treatment plant
XRD	X-ray diffraction

NOTATIONS

I	Applied current (A)
C_0	Initial antibiotic concentration (mg L^{-1})
C_f	Final antibiotic concentration (mg L^{-1})
TOC_0	Initial TOC concentration (mg L^{-1})
TOC_f	Final TOC concentration (mg L^{-1})
S_0	Supporting electrolyte concentration (g L^{-1})
U	Average cell potential (V)
t	Elapsed time (min)
V_R	Volume of wastewater in reactor (L)
R^2	Coefficient of determination
k_f	Pseudo-first order rate constant
Z_1	TOC removal (%)
Z_2	Antibiotic removal (%)
Z_3	Specific energy consumption (kW h (g TOC removed)$^{-1}$)
R_T	Retention time (min)

Chapter – 1

INTRODUCTION

1.1. GENERAL

In view of betterment of living standard, humans have accelerated the process of industrialization and urbanization, involving extensive utilization of water. As a consequence, humungous amount of wastewater is being generated worldwide, leading to severe environmental pollution. This has become a matter of serious concern due to its alarming effects on aquatic life along with humans and animals. Fresh water demand has also increased manifold owing to population growth. Many countries, including India, are already experiencing moderate to severe water shortage.

Advancement in medical science over years has enabled people to live healthier and longer lives. Hence, pharmaceutical manufacturing industries have emerged as utmost important part of any economy. However, bulk production and consumption of drugs has unfortunately contaminated our biosphere, as in past three decades, more than 200 synthetic pharmaceutical compounds such as analgesics, anti-inflammatory drugs, beta-blockers, antibiotics, blood lipid regulators, steroids and hormones, etc., have been detected in aquatic streams of different parts of the globe (Petrie et al., 2015). Wastewater treatment plants (WWTPs) are not designed for removal of drugs and alike compounds, consequently releasing them into the environment (Homem and Santos, 2011; Michael et al., 2013). In 1976, Garrison et al., was the first to report the occurrence of a pharmaceutical "clofibric acid" in treated wastewater in USA (Nikolaou et al., 2007). Presence of pharmaceuticals in aquatic environments leads to adverse eco-toxicological effects on aquatic and terrestrial faunas such as feminization in fish and alligators (Guillette et al., 2000). The vulture population in Indian subcontinent is on the verge of extinction due to exposure to diclofenac (anti-inflammatory drug) residues in environment (Oaks et al., 2004). Considering pharmaceuticals as potentially hazardous contaminants in waterbodies, scientific communities worldwide have conducted comprehensive studies and reported their occurrence in effluents from WWTPs, sewage treatment plants, sea water, river water, lakes and ground water, in the range from few ng L^{-1} to 100 mg L^{-1} (Hirsch et al., 1999; Kummerer, 2001; Petrovic et al., 2005; Khetan and Collins, 2007; Larsson et al., 2007; Fick et al., 2009; Kummerer, 2009; Lin and Tsai, 2009; Mutiyar and Mittal, 2013; Petrie et al., 2015). This issue is attracting global attention of concerned authorities as pharmaceuticals still remain

unregulated or are presently undergoing a regularization process, even though the directives and legal frameworks are not yet set-up.

1.2. ANTIBIOTICS – EMERGING WATER POLLUTANTS

Antibiotics, also termed as antimicrobials, are used to treat bacteria induced infections and diseases, by either inhibiting further growth of bacteria or by destroying them. The role of antibiotics in modern medical science has amplified in past few decades, as they support crucial tasks such as surgeries, organ replacement and cancer treatment (Laxminarayan et al., 2016a). Consequently, antibiotics have become an indispensable part of human and animal health system, thus leading to exponential rise in their production and consumption in past two decades.

Over a period of fifteen years (2000 – 2015), antibiotic consumption in India increased by 103%, from 3.2 to 6.5 billion defined daily doses, which was globally the highest, followed by China (79%) and Pakistan (65%) (Klein et al., 2018). Moreover, India was the largest consumer of antibiotics in the world in 2010, with cephalosporins, broad-spectrum penicillins and fluoroquinolones among the top three categories of antibiotics being consumed by Indians (Van Boeckel et al., 2014). Population growth has also triggered aggravation in antibiotics' usage in livestock and animal husbandries, due to rising demand of feed and meat. Such large production and intake of antibiotics has led to their occurrence and accumulation in aquatic environment.

1.2.1. Sources of Antibiotics in Environment

As discussed above, massive use of antibiotics in living beings intensifies the possibility of environmental pollution by such compounds. The contamination routes followed by antibiotics are illustrated in Fig. 1.1. Humans and animals can excrete up to 90% of antibiotic content through urine and faeces, without undergoing metabolism in liver, thus releasing it into the environment (Hirsch et al., 1999; Kemper 2008). Human excreta goes into the sewage network systems connected to WWTPs, where conventional physico-chemical and biological treatment processes are incapable of eradicating antibiotics due to their highly polar and bio-refractory nature (Michael et al., 2013, Homem and Santos, 2011; Zorita et al., 2009). Similarly, manure formed from animal excreta is administered in agricultural fields as fertilizer, which contaminates soil with antibiotics and subsequently

surface and ground water via run-off and leaching (Kemper, 2008). Improper disposal of excess and expired antibiotics from hospitals and households causes their deposition in landfills, consequently letting them enter groundwater through leaching. Sludge generated during wastewater treatment ends up either in landfills or in fields as manure causing further contamination of surface and ground water. Discharge of inefficiently treated effluent generated at manufacturing industries further magnifies this issue. Drinking water treatment plants (DWTPs) treat surface waters for removal of potential pollutants in order to make water suitable for human consumption, however, their design is not efficient for removal of antibiotics (Homem and Santos, 2011). Antibiotics, ultimately enter the food chain through animal food products such as chicken, meat and milk (Kakkar and Rogawski, 2013) and via plant uptake from contaminated soil.

1.2.2. Occurrence in Aquatic Environment – Scenario in India

Occurrence of antibiotics in aquatic environment is ubiquitous as proved by several researcher groups. More than three decades ago (1982), Watts et al., reported first case of contamination of surface water by antibiotics belonging to macrolide, sulphonamide and tetracycline class at concentration of 1 µg L^{-1}, in samples collected from a river in England (Sarmah et al., 2006). Following this, a number of research studies conducted worldwide reported presence of antibiotics in different varieties of aquatic streams (Hirsch et al., 1999 (Germany); Sacher et al., 2001 (Germany); Costanzo et al., 2005 (Australia); Brown et al., 2006 (USA); Cha et al., 2006 (USA) ; Kim and Carlson, 2006 (USA); Larsson et al., 2007 (India); Xu et al., 2007 (China); Smith et al., 2007 (UK); Lin et al., 2008 (Taiwan); Tamtam et al., 2008 (France); Lin and Tsai, 2009 (Taiwan); Fick et al., 2009 (India); Watkinson et al., 2009 (Australia); Behera et al., 2011 (Korea); Mutiyar and Mittal, 2013 (India)).

A decade ago, two research groups from Sweden reported a comprehensive study on contamination of surface, ground, and drinking water by effluent from around 90 bulk drug manufacturing industries situated in Hyderabad, India (Larsson et al., 2007; Fick et al., 2009). This pharmaceutical industry hub is one of the world's largest suppliers of generic drugs to Europe, USA and other countries (Larsson and Fick, 2009). Effluent generated from all the manufacturing units is transported to a WWTP (PETL) for treatment before its discharge into south Indian rivers. The results in both the studies were extremely shocking and alarming. The effluent from WWTP was reported to have antibiotic (ciprofloxacin)

concentration as high as 31 mg L^{-1} (Table 1.1). The maximum level of contamination by antibiotics in surface waters around the region was reported to be 2.8 mg L^{-1} (lake water) and 2.5 mg L^{-1} (river water) (Table 1.2). These are the highest reported antibiotic concentrations in WWTP effluents and surface waters across the world, to the best of my knowledge. Moreover, the samples collected from wells of six villages around *Patancheru* area were reported to have positive results in terms of presence of antibiotics, with their levels in the range of 0.2 – 14 µg L^{-1} (Table 1.2). As listed in tables (Table 1.1 and 1.2), other categories of pharmaceuticals were also detected in all the samples, but the levels of antibiotics were severely high. The WWTP was thus categorically ineffectual for degradation and removal of antibiotics from the pharmaceutical industry wastewater.

Wastewater from hospitals is another primary source of water pollution by antibiotics (Fig. 1.1). Presence of eight different antibiotics in hospital wastewater samples collected from two different hospitals in Madhya Pradesh, India, was reported by Diwan et al., 2009, with maximum contamination level of 236.6 µg L^{-1} (Table 1.3). The occurrence of such high levels of antibiotics in different aquatic matrices in India is appalling, due to continuous rise in antibiotic resistance in native bacterial population.

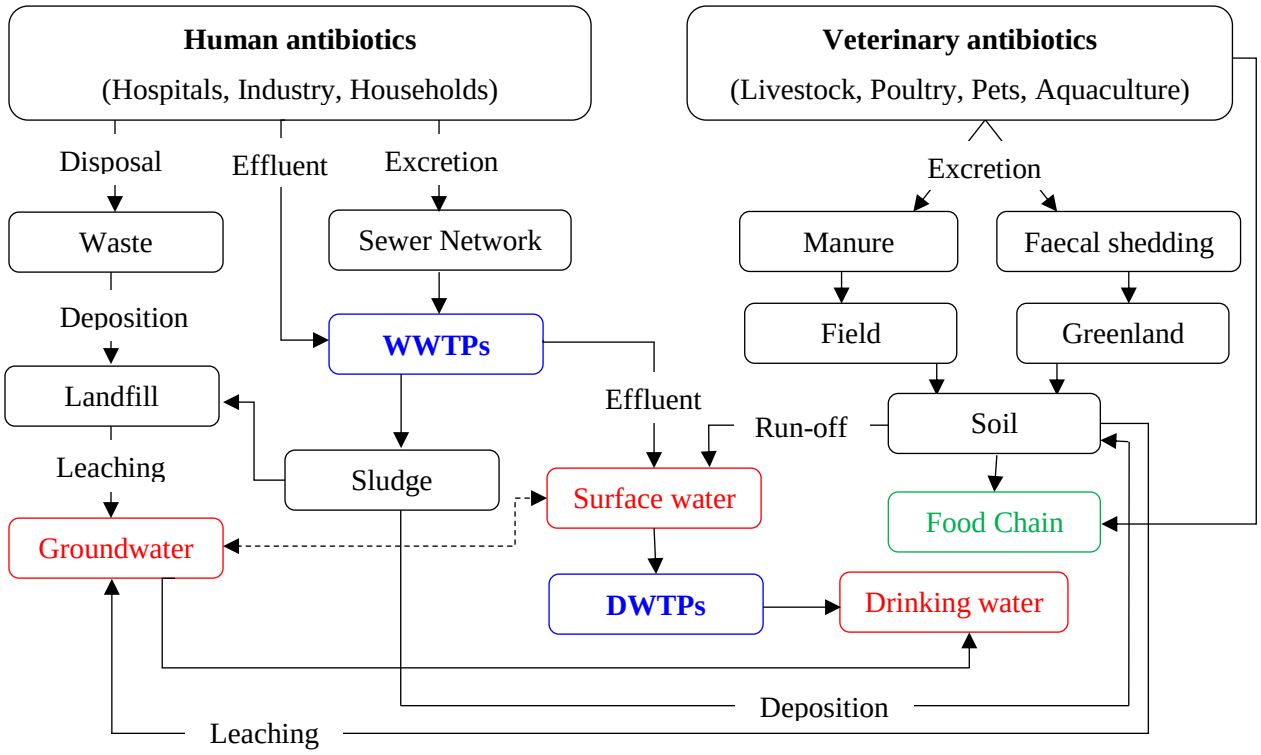

Fig. 1.1. Origin and possible contamination routes of antibiotics.
Source: Homem and Santos, 2011

Table 1.1. Levels of pharmaceutical residues reported in effluent from wastewater treatment plant, PETL, Hyderabad, India (all values are in µg L^{-1})

Compound	Class	Larsson et al., 2007	Fick et al., 2009
Cetirizine	Antihistamine	1,300 – 1,400	2,100
Ciprofloxacin	Antibiotic, fluoroquinolone	28,000 – 31,000	14,000
Citalopram	Selective serotonin reuptake inhibitor	770 – 840	430
Enalapril	Angiotensin-converting enzyme inhibitor	ND	2.2
Enrofloxacin	Antibiotic, fluoroquinolone	780 – 900	210
Erythromycin	Antibiotic, macrolide	1.0 – 10	ND
Lomefloxacin	Antibiotic, fluoroquinolone	150 – 300	8.8
Losarton	Angiotensin II receptor antagonist	2,400 – 2,500	ND
Metoprolol	Beta-adrenoreceptor antagonist	800 – 950	4
Norfloxacin	Antibiotic, fluoroquinolone	390 – 420	25
Ofloxacin	Antibiotic, fluoroquinolone	150 – 160	55
Ranitidine	H_2-receptor antagonist, acid reducer	90 – 160	ND
Terbinafine	Antimycotic	ND	0.12
Trimethoprim	Antibiotic, folic acid synthesis inhibitor	ND	4.4

PETL – Patancheru Enviro Tech. Ltd.; ND – not determined

Table 1.2. Levels of pharmaceuticals reported in lake, river and well water, Patancheru, India (all values are in µg L^{-1})

Compound	Class	Lake water	River water	Well water
Cetirizine	Antihistamine	1,200	530	28
Ciprofloxacin	Antibiotic, fluoroquinolone	2,800	2,500	14
Citalopram	Selective serotonin reuptake inhibitor	8	76	1.4
Enalapril	Angiotensin-converting enzyme inhibitor	1	1.5	-
Enoxacin	Antibiotic, fluoroquinolone	160	66	1.9
Enrofloxacin	Antibiotic, fluoroquinolone	25	30	0.07
Lomefloxacin	Antibiotic, fluoroquinolone	-	1.1	0.04
Metoprolol	Beta-adrenoreceptor antagonist	7	0.24	0.09
Norfloxacin	Antibiotic, fluoroquinolone	520	4.7	0.03
Ofloxacin	Antibiotic, fluoroquinolone	11	10	0.5
Terbinafine	Antimycotic	15	0.2	1.8
Trimethoprim	Antibiotic, folic acid synthesis inhibitor	-	4	0.06

Source: Fick et al., 2009

Table 1.3. Levels of antibiotic residues reported in hospital wastewater, Madhya Pradesh, India (all values are in µg L^{-1})

Compound	Class	UCTH	CRGH
Ceftriaxone	Cephalosporin	58.3 – 59.5	0
Ciprofloxacin	Fluoroquinolone	7.6 – 31	64.8 – 236.6
Levofloxacin	Fluoroquinolone	70.7 – 80.5	1.6 – 6.8
Metronidazole	Nitroimidazole	2.5	1.4 – 3.8
Norfloxacin	Fluoroquinolone	5.7	20.6 – 22.8
Ofloxacin	Fluoroquinolone	66 – 73.2	1.5 – 7.5
Tinidazole	Nitroimidazole	13.6	50.4 – 88.4
Sulfamethoxazole	Sulfonamide	2.7 – 5.7	36.7 – 81.1

UCTH - Ujjain Charitable Trust Hospital, CRGH – Chandrikaben Rashmikant Gardi Hospital
Source: Diwan et al., 2009

1.2.3. Antibiotic Resistance – A Consequential Health Threat

Efficacy of antibiotics in treatment of bacterial infections is continuously declining, as extensive use of antibiotics and their proliferating presence in environmental matrices has led to development of antibiotic resistant bacterial strains. In developing countries like India, burden of infectious diseases is comparatively high due to lack of proper sanitation conditions, clean water and nutrition, particularly in rural areas, which has led to widespread usage of antibiotics (Laxminarayan et al., 2016a). The consequence is increase in prevalence of resistant bacteria in the country. In a course of six years (2008 – 2013), *Escherichia coli* resistance to cephalosporin and fluoroquinolone class of antibiotics amped from 70% to 83%, and 78% to 85%, respectively (CDDEP, 2015). Fluoroquinolone resistance among *Klebsiella pneumoniae* isolates also increased from 57% to 73% (CDDEP, 2015). Firstly reported in 2008, New Delhi metallo-β-lactamase (NDM) enzymes, responsible for making bacteria resistant to a wide range of β-lactam antibitoics, are now found globally (Nordmann et al., 2011). *Salmonella Typhi* isolates (responsible for typhoid fever) improved their resistance to fluoroquinolones from 8% (2008) to 28% (2014). Repercussions are such that

the number of deaths from neonatal sepsis caused by bacterial resistance to first-line antibiotics, are unfortunately the highest in India (≈56,000 every year) (Laxminarayan et al., 2016b). The situation thus demands for immediate attention and solution, to curb such high death rate of neonates, and to prevent further growth in resistant pathogens in the country.

1.3. TREATMENT TECHNIQUES

Endemic occurrence of antibiotics in aqueous eco-systems has proven the incompetence of wastewater treatment techniques employed in sewage treatment plants, WWTPs and DWTPs in terms of antibiotic removal. Conventional treatment techniques broadly include physico-chemical and biological treatment processes.

1.3.1. Physico-chemical Treatment Methods

Filtration, coagulation, flotation, flocculation, adsorption and chemical oxidation are some common physico-chemical techniques used in WWTPs. Filtration generally removes suspended solid particles present in wastewater by passing it through some membranes or granular media. However, membranes and their cleaning is quite expensive (Cannizares et al., 2006; Baghel et al., 2018). Coagulation and flocculation of wastewater is done by using chemicals such as iron salts, alum, lime or polymers, which bind and precipitate the pollutants to form colloids, subsequently letting them to settle down in the treatment chamber, thus resulting in sludge formation, which is nothing but solid waste comprising of the pollutants removed from wastewater. Similarly, adsorption process also involves removal of pollutant from the wastewater by adsorbing it on to some solid adsorbent with high surface area (usually activated carbon), which consequently concentrates the pollutant on to solid phase, without its degradation or mineralization, again generating a new form of waste. Chemical oxidation involves transportation and storage of hazardous chemicals which are not environmental friendly. Thus, expensive adsorbents, chemicals, coagulants, membranes, inefficiency to remove dissolved organic pollutants and generation of secondary pollutants are major drawbacks of physico-chemical wastewater treatment techniques (Panizza and Cerisola, 2009). Nevertheless, subsequent treatment of effluent is required for complete eradication of contaminants (Homem and Santos, 2011; Sahu et al., 2019).

1.3.2. Biological Treatment Process

Industries commonly treat effluents using biological treatment systems involving activated sludge technology, employing either aerobic or anaerobic micro-organisms to degrade pollutants. However, these processes are not proficient in antibiotic degradation because of their toxic and recalcitrant nature for microbes. Moreover, high level of controlling and energy requirement, and sludge generation limits the use of biological treatment methods (Kushwaha et al., 2010).

1.3.3. Advanced Oxidation Processes

As found in open literature, much attention has been given to advanced oxidation processes (AOPs) in past three decades. These processes are based on generation of highly reactive free radicals (•OH, $•O_2^-$, $HO_2•$), primarily hydroxyl radicals (•OH), which non-selectively destroy toxic and recalcitrant organic pollutants present in wastewater, owing to its high oxidation potential. AOPs are categorized on the basis of technique responsible for generation of these free radicals, such as wet air oxidation, UV and gamma radiation based AOPs, ozone based AOPs, and electrochemical AOPs.

1.3.3.1. Electrochemical AOPs: These are energy intensive processes as they involve application of electrical power for generation of free radicals from water discharge. Electrochemical AOPs (EAOPs) for wastewater treatment can broadly be classified into two categories: (a) electro–Fenton (EF) method, and (b) electro–oxidation (EO) method (Fig. 1.2).

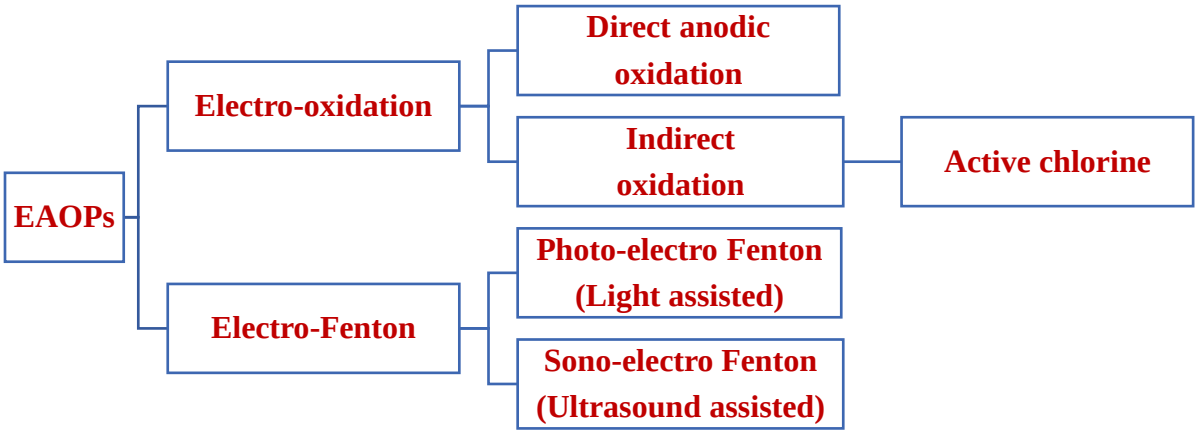

Fig. 1.2. Classification of electrochemical advanced oxidation processes.

(a) Electro-Fenton method: EF method involves heterogeneous catalytic reactions of hydrogen peroxide with ferric or ferrous ions, acting as catalysts, for generation of hydroxyl radicals via free radical chain reactions. As compared to traditional Fenton's process, addition of iron salts in EF is limited because of regeneration of ferrous ions at the cathode surface. The produced hydroxyl radicals then non-selectively destroy the organic content in the wastewater. Efficiency of EF is further improved when assisted by UV radiation/sunlight (photo-electro Fenton) or ultrasonic radiation (sono-electro Fenton) (Brillas, 2014). However, the major drawback of EF method is its dependency on pH (efficient in pH value ≈ 3) and possibility of generation of some iron sludge (Gadipelly et al., 2014).

(b) Electro-oxidation method: EO method is based on electrochemical generation of powerful oxidising agents, such as hydroxyl radicals (•OH) directly on-site using only water, salt and energy, which are then able to destroy organics up to their mineralization to carbon dioxide and water. It is also termed as green method for wastewater treatment. Major advantages of EO are listed below (Martinez-Huitle and Ferro, 2006, Anglada et al., 2009, Sires et al., 2014):

- No sludge generation, hence environmentally benign technology
- Minimum or no addition of chemicals required
- Versatile – can be used to treat any wastewater with chemical oxygen demand (COD) values in the range of 0.1 to 100 g/L
- Cost effective
- Amenability to automation
- Easy handling because of simple equipment
- Safety – operates under mild conditions (room temperature and pressure)
- Robustness – the reaction can be terminated easily in seconds by cutting off the power and resumed immediately after solving any operational problem

Hence, EO represents a useful solution when the presence of bio-refractory and toxic pollutants prevents the use of conventional treatment techniques.

EO technique destroys organic pollutants by two different oxidation mechanisms, i.e., "direct oxidation" at the anode surface, and "indirect oxidation" in the bulk solution by oxidizing agents generated on the anode surface (Fig. 1.3) (Martinez-Huitle and Ferro, 2006, Panizza and Cerisola, 2009; Bocos et al., 2014, 2016). Direct anodic oxidation of pollutants

occurs after pollutant adsorption on anode surface and its destruction via electron transfer. The mechanism of direct oxidation of target pollutant strongly depends on process conditions and type of electrodes (active or non-active) employed for the purpose. The hydroxyl radicals generated by water discharge either get physisorbed on the anode surface (A) (Eq. 1.1) or chemisorbed by forming a covalent bond with the anode (Eq. 1.3) (Martinez-Huitle and Panizza, 2018). Physisorption is predominant in non-active anodes. Whereas, chemisorption dominates in case of active anodes (Nideesh et al., 2019). Physisorbed •OH leads to complete mineralization of organic pollutant to CO_2 (Eq. 1.2). However, the chemisorbed radicals lead to electrochemical conversion of organic pollutants (Eq. 1.4) (Comninellis, 1994, Brillas and Martinez-Huitle, 2015).

$$A + H_2O \rightarrow A(\bullet OH) + H^+ + e^- \quad (\textit{Physisorption}) \quad \textbf{(1.1)}$$

$$A(\bullet OH) + R \rightarrow nCO_2 + mH^+ + ze^- + \text{Inorganic ions} + A \quad (\textit{Combustion}) \quad \textbf{(1.2)}$$

$$A + H_2O \rightarrow AO + 2H^+ + 2e^- \quad (\textit{Chemisorption}) \quad \textbf{(1.3)}$$

$$AO + R \rightarrow RO + A \rightarrow \text{Reaction intermediates} + A \quad (\textit{Conversion}) \quad \textbf{(1.4)}$$

In case of indirect oxidation, strong oxidant species are generated in-situ through oxidant precursor or mediator, which instantly destroy the organic pollutants in the bilk solution (Fig. 1.3). Commonly generated oxidant species include hydrogen peroxide (H_2O_2) and ozone (O_3). In wastewaters comprising chlorides, reactive chlorine species (Cl_2, HOCl, ClO^-) play an imperative part in pollutant degradation via indirect oxidation. The dominance of these species is highly pH dependent (Fig. 1.4) (Deborde and Von Gunten, 2008). Apart from generation of oxidants and pollutant destruction, the undesirable but inevitable reactions of oxygen and hydrogen evolution occur simultaneously in the electrochemical cell, resulting in curtailed performance of EO process.

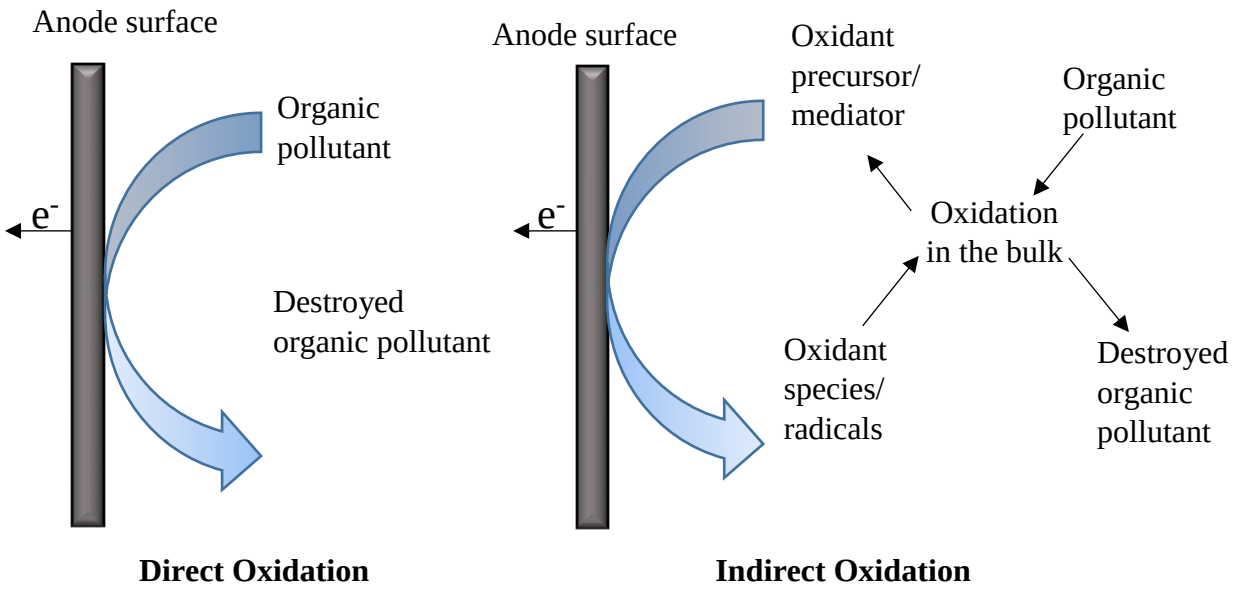

Fig. 1.3. Direct and indirect oxidation mechanisms in EO treatment

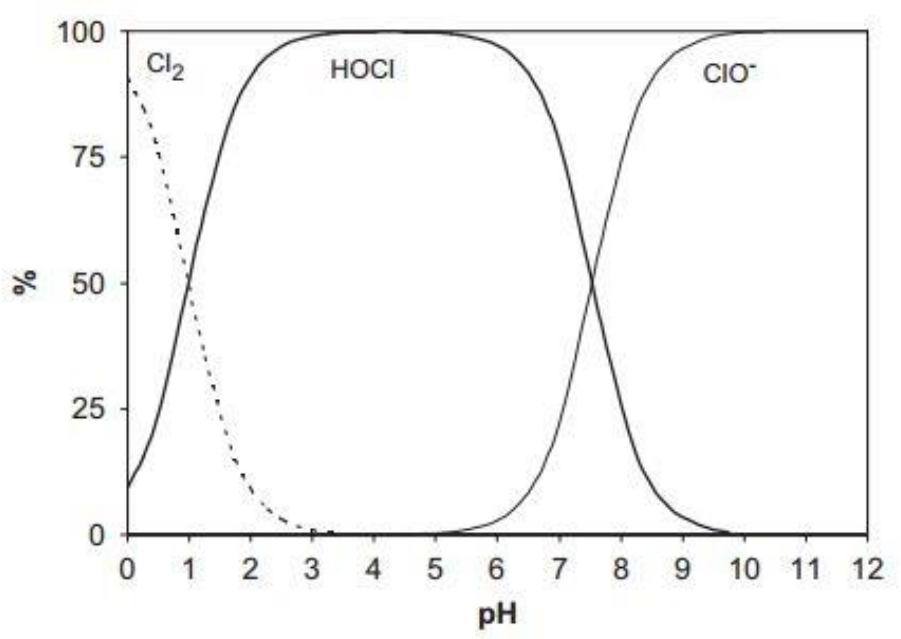

Fig. 1.4. Relative distribution of aqueous chloro-oxidant species with respect to pH

Several research groups have investigated the application of electro-oxidation treatment technique for abatement of different categories of pharmaceutical compounds including antibiotics, using different electrode materials and operating conditions. The following chapter discusses the corresponding literature in detail.

Chapter – 2

LITERATURE REVIEW

2.1. GENERAL

This chapter presents the review of research studies based on removal/degradation and mineralization of different types of antibiotics and other pharmaceutical compounds using EO treatment method. Subsequently, areas which require further research and attention have been identified.

2.2. EO TREATMENT OF ANTIBIOTICS

Since past decade, EO technique has fetched much attention of scientific groups for removal of antibiotics from aqueous media. The choice of electrodes and range of EO process parameters are of paramount importance. Major parameters include applied current, pH of the wastewater, substrate concentration and conductivity of the wastewater. In case of EO treatment using continuous reactor set-up, retention time and elapsed time are additional parameters which play a pivotal role. Anodes are broadly classified in to two categories – active and non-active. Anodes are considered non-active when the active oxygen species generated on anode surface during electrolysis do not involve in chemical bonding with the anode and are only physically adsorbed on to its surface. Such anodes are poor catalysts for evolution of oxygen, i.e., the oxygen evolution overpotential of these anodes is relatively high. The weakly physisorbed active oxygen species destroy the organics on the anode surface resulting into their mineralization to CO_2 and H_2O (*electrochemical combustion*) (Comninellis, 1994; Martinez-Huitle and Ferro, 2006; Panizza and Cerisola, 2009). Common examples of non-active anodes are boron-doped diamond (BDD), lead dioxide (PbO_2) and tin dioxide (SnO_2). On the other hand, active anodes (Pt, graphite, IrO_2 and RuO_2) comparatively have lower oxygen evolution overpotential, and reactive oxygen species chemically bond with their surface (chemisorption) forming higher oxide. The chemisorbed active oxygen favours partial oxidation of pollutants (*electrochemical conversion*) (Comninellis, 1994; Martinez-Huitle and Ferro, 2006; Panizza and Cerisola, 2009). However, practically most anodes demonstrate mixed behaviour exhibiting pollutant oxidation as well as oxygen evolution (Panizza and Cerisola, 2009).

Studies on removal of different classes of antibiotics, such as penicillins, fluoroquinolones, sulphonamides and tetracyclines, by EO using different anode materials have been reported in literature which are discussed in detail in following section.

2.2.1. Penicillins

Antibiotics comprising of beta-lactam ring (four membered cyclic amide) in their molecular structure are termed as beta-lactam antibiotics. Important members of this antibiotic class are penicillin derivatives, cephalosporins, monobactams and carbapenems. Penicillins are one of the most widely prescribed beta-lactam antibiotics and their mechanism is based on inhibiting the biosynthesis of cell wall of the bacteria, and thus killing them.

Efficiency of EO method for degradation of penicillins was first investigated by Wirzal et al. (2013). Effect of pH on degradation of ampicillin and penicillin G antibiotics was explored by performing anodic oxidation using titanium based mixed metal oxides as anode (Ru-Ir-TiO_2 (40:10:50) and Ru-Ir-TiO_2 (20:30:50)), and titanium as cathode. 100% degradation of ampicillin was achieved in 15 min for the latter anode. The best medium for degradation of ampicillin was pH 4 for both anodes. Whereas degradation of penicillin G took place in highly alkaline medium, as pH 10 and 12 were found to be optimum for its degradation using Ru-Ir-TiO_2 (20:30:50) and Ru-Ir-TiO_2 (40:10:50) respectively.

Boron-doped diamond (BDD) anodes have been extensively utilized by researchers for treatment of different varieties of wastewaters. Diamond coating is usually deposited on materials like glassy carbon, silicon, titanium, niobium and tantalum. Infusion of boron atoms is done into the diamond films, enabling them to become conducting in nature, for utilization in EO treatment as anode material. Major advantages of non-active BDD electrodes include chemical and electrochemical stability, longer service life and a wide potential window for water discharge. The oxygen evolution overpotential of BDD anodes is 2.3 V, which is higher than other electrode materials in application.

Application of conductive diamond EO for treatment of wastewater comprising antibiotics have been extensively studied by several research groups (Table. 2.1). BDD has shown promising results not only in terms of antibiotic degradation, but also in terms of total organic carbon (TOC) removal, i.e., mineralization. Sopaj et al. (2015) tested the ability of different anode materials (carbon-felt, carbon-fiber, carbon-graphite, platinum, lead

dioxide, Ti/RuO_2-IrO_2 and BDD) for degradation of amoxicillin. BDD electrode was reported to be the best among all with almost 100% degradation and complete mineralization of amoxicillin in less than 100 min. Korbahti and Tasyurek (2015) also employed BDD as anode to study the degradation of ampicillin. They optimized the EO process conditions using response surface methodology (RSM). 97.1 % ampicillin removal was reported at optimum conditions (antibiotic concentration: 618 mg L^{-1}, supporting electrolyte (NaCl) concentration: 3.6 g L^{-1}, current density: 13.4 mA/cm^2 and, temperature: 36 °C). In another study, Frontistis et al. (2017) also performed statistical evaluation of operating parameters (current density: 30–50 mA cm^{-2}, initial COD concentration: 1–2 g L^{-1}, treatment time: 15–90 min, initial pH: 3–9 and NaCl concentration: 2–4 g L^{-1}) using Minitab for BDD oxidation of amoxicillin. The most significant effects on COD removal were found to be single effects of current density, initial COD concentration and treatment time, and interactive effect between COD and treatment time. Oxidation pathway of amoxicillin by BDD was proposed based on identified transformation by-products.

Apart from BDD, several other non-active and active anodes have been inspected in order to degrade and mineralize antibiotic content in aquatic medium (Table 2.2). Efficiency of sub-stoichiometric titanium oxide (Ti_4O_7) to degrade amoxicillin was compared with BDD and other anode materials such as Pt and DSA (dimensionally stable anode) by Ganiyu et al., (2016). TOC removal efficiencies of 36%, 41%, 69% and 94% were reported for DSA, Pt, Ti_4O_7 and BDD, respectively. Oxidation products of amoxicillin were identified using HPLC and GC-MS, and subsequently mechanism of antibiotic mineralization by Ti_4O_7 anode was proposed.

Lately, Silva et al., (2019) compared performance of EO process with photolysis (irradiation by ultraviolet light) and sonolysis (irradiation by ultrasound waves). The group reported complete degradation and mineralization of two beta-lactam antibiotics – ampicillin and amoxicillin (100 mg L^{-1}) using diamond electrodes. The removal efficiency increased with the increase in applied current density from 15 to 60 mA cm^{-2}. Complete degradation of both the antibiotics was attained in less than 30 min in chlorine media. However, removal rate was slower in media comprising sulphates. Moreover, the results achieved by electrolysis were far superior to photolysis and sonolysis.

2.2.2. Fluoroquinolones

Fluoroquinolones belong to quinolone family of synthetic broad-spectrum antibacterial drugs, which have a fluorine atom attached to the central ring system. These are widely prescribed for certain microbial infections as they are effective against both gram-positive and gram-negative bacteria. These are also bactericidal antibiotics like penicillins. Studies on EO treatment of wastewater comprising important fluoroquinolones such as ofloxacin, enrofloxacin, ciprofloxacin and norfloxacin, which have also been detected in surface, ground and drinking water, are available in literature.

The first ever study on degradation of a fluoroquinolone by EO was reported more than a decade ago by Jara et al. (2007). The research team conducted electrochemical oxidation of ofloxacin in a divided cell using different anode materials (Ti/Pt, graphite, $Ti/IrO_2/Ta_2O_5$ and three dimensional granular activated carbon bed (3D-GAC)), and stainless steel plate as cathode. Ofloxacin was efficiently oxidized up to 99.99% over all tested anodes. The electro-oxidation was found to occur with 1^{st} order kinetics. Time requirement for abatement of ofloxacin was minimum for 3D-GAC and maximum for $Ti/IrO_2/Ta_2O_5$. A few years later, the same research group derived and applied a mathematical cost estimation model in order to optimize current density for EO of ofloxacin by employing Ti/Pt as anode (Jara and Fino, 2010). Ofloxacin removal by BDD anode was reported by Chen et al. (2013). The process was dependent on applied current density, as degradation increased with increase in current density. Complete drug degradation occurred in 60 min of EO at 100 mA cm^{-2} of current density. Recently, a novel electrode – TiO_2-based SnO_2-Sb/polytetrafluoroethylene (PTFE) resin-PbO_2, fabricated by Xie et al. (2017), was tested for ofloxacin (20 mg L^{-1}) degradation by EO. More than 99% of antibiotic removal efficiency was reported in 90 min at applied current density of 30 mA cm^{-2}.

Degradation of enrofloxacin (1,580 mg L^{-1}) using different oxidation techniques was explored by Guinea et al. (2009). The group compared conductive-diamond electrochemical oxidation (CDEO, using BDD anode), ozonation and Fenton oxidation method. All the three processes reduced the organic content of synthetic wastewater comprising of the drug. However, CDEO using Si/BDD anode was found to be most efficient in terms of mineralization. Furthermore, this research team reported a comparative study on enrofloxacin degradation (158 mg L^{-1}) at pH = 3.0, using different EAOPs – anodic

oxidation with electrogenerated hydrogen peroxide (AO-H_2O_2), electro-Fenton (EF), photo-electro Fenton (PEF) and solar photo-electro Fenton (SPEF) (Guinea et al., 2010). Anode material chosen for the study was either Pt or BDD, and cathode material was carbon-PTFE cloth fed with O_2 for H_2O_2 generation. EAOPs were more effective with BDD than Pt anode. SPEF demonstrated best results amongst all with almost complete degradation and mineralization of antibiotic. In case of AO-H_2O_2 using BDD, 67% and 28% of organic carbon content was oxidized in stirred tank reactor and batch recirculation flow reactor, respectively.

Electrochemical degradation of an important fluoroquinolone ciprofloxacin was explored by Wang et al. (2016) using titanium coated with antimony doped tin dioxide (Ti/SnO_2-Sb) anode prepared in their laboratory. After applying 30 mA cm^{-2} of current density for 120 min, 99.5% of antibiotic content (initial concentration = 50 mg L^{-1}) was degraded in the electrochemical cell. COD and TOC removal efficiencies were reported to be 86% and 70%, respectively. Degradation of antibiotic was found to be much dependent on applied current density. The proposed mechanism of degradation of ciprofloxacin was based on action of •OH radical on its quinolone moiety and fluorine atom. Application of another non-active anode Ti/PbO_2 was tested for ciprofloxacin (36 mg L^{-1}) removal by Rahmani et al. (2018). Using 32 mA cm^{-2} of current density, 70% drug was degraded in 120 min and only 50% COD removal was attained in 180 min. Much recently, Wachter et al. (2019) degraded ciprofloxacin using double sided β-PbO_2 anode and nickel plate as cathode in a flow reactor. Complete removal of antibiotic was reported within 2 h of electrolysis with applied current density of 30 mA cm^{-2}. However, ~75% of TOC was removed after 5 h of EO.

Norfloxacin degradation was recently studied using BDD anodes by da-Silva et al. (2019) and Mora-Gomez et al. (2019). Complete removal of antibiotic and COD from synthetic wastewater was achieved by former research crew in ~140 min of EO using 20 mA cm^{-2} of current density. The latter research group compared the performance of BDD with another non-active Sb-SnO_2 ceramic anode. TOC removal efficiencies of 92% and 63% were attained using BDD and Sb-SnO_2 anode, respectively.

2.2.3. Sulfonamides

Sulfonamides are synthetic antimicrobial agents, comprising of sulfonyl group attached to amine group in their molecular structure. These are among the most widely used veterinary antibiotics in aquaculture and animal husbandry, and also in human medicine in developing countries. Sulfonamides are bacteriostatic antibiotics, which inhibit the growth of bacteria instead of killing them. Degradation of sulphonamides, particularly sulfamethoxazole (SMX), by EO has been widely reported.

SMX was degraded using BDD as anode by several researchers. Li et al. (2008) reported 73% degradation of SMX (253 mg L^{-1}) and 32% TOC removal by EO after applying 2.86 mA cm^{-2} of current density for 210 min, using stainless steel as the counter electrode to BDD. Similar set of electrodes as Li et al. (2008) were used to reduce the concentration of SMX (100 mg L^{-1}) by De Vidales et al. (2012). As per their results, anodic oxidation was able to reduce the concentration of antibiotic below 0.1 mg L^{-1} at 15 mA cm^{-2} within 100 min. Formation of nine reaction intermediates was reported in the electrochemical system, identified by LC-TOF-MS (Liquid chromatography-time of flight-mass spectrometry). Subsequently, a pathway for EO of SMX was proposed. Application of BDD as anode for SMX degradation was further explored by De Amorim et al. (2013). They performed anodic oxidation on the mixture of two antibiotics: SMX and trimethoprim. Degradation efficiency of 96% and 92% for SMX and trimethoprim, respectively was reported at pH 5.0 and current density 36 mA cm^{-2}. HPLC and GC-MS analysis of treated samples revealed that 6 aromatic and 3 aliphatic organic compounds were formed during EO treatment. This research group also reported complete degradation of another sulphonamide antibiotic – sulfadiazine, under similar experimental conditions (De Amorim et al. 2014).

Apart from BDD as anode, EO performance in terms of SMX removal was also investigated using other anode materials. Lin et al. (2013) made use of two different matrices for degradation of SMX (100 mg L^{-1}): contaminated lake water and deionized water. The set of Ti/SnO_2-Sb/Ce-PbO_2 and Ti plate was implemented as anode and cathode respectively. Complete mineralization of drug was reported for current densities higher than 10 mA cm^{-2}. SMX degradation followed pseudo-first order kinetics. Also, degradation of SMX was reported to be faster in case of contaminated lake water. Hussain et al. (2015)

tested the application of dimensionally stable and commercial mixed oxide anode – $Ti/Ru_{0.3}Ti_{0.7}O_2$, for electro-oxidation of SMX. At pH 3 and current densities ≥20 mA cm^{-2} more than 98% of antibiotic was degraded within 30 min of EO. Important reaction intermediates of SMX were identified and degradation route involving action of active oxygen and chlorine species was proposed.

El- Ghenymy et al. (2013a, 2013b) tested the degradation of two sulphonamides, namely sulphanilamide and sulfamethazine, in two different research studies. However, the operating conditions were kept similar in both the studies: BDD as anode, stainless steel as cathode, and acidic medium (pH = 3.0). In a divided electrochemical cell, around 97 – 98% TOC reduction was reported in case of sulphanilamide (239 mg L^{-1}) for all applied current densities (33.3 – 150 mA cm^{-2}) (El-Ghenymy et al., 2013a). However, TOC abatement is quite faster in case of applied current densities above 66 mA cm^{-2}.Similarly, in case of sulfamethazine (El-Ghenymy et al., 2013b), 98% mineralization was achieved for current densities greater than 66 mA/cm^2. Aromatic intermediates, carboxylic acids and inorganic ions were determined using GC-MS and HPLC. Mineralization pathway of both the antibiotics in acidic medium was proposed by authors. Fabianska et al. (2014) chose five different sulfonamides (sulfadiazine, sulfathiazole, sulfamerazine, sulfamethazine and sulfadimethoxine) to test their degradation using Si/BDD anode, using either 6.1 g/L Na_2SO_4 or municipal WWTP's effluent as electrolyte medium. 14% COD removal was reported for mixture of all antibiotics in Na_2SO_4. When separately degraded using Na_2SO_4, 74, 75, 66, 65, 75% COD removal was achieved for sulfadiazine, sulfathiazole, sulfamerazine, sulfamethazine and sulfadimethoxine, respectively. Whereas, with municipal WWTP's effluent, more efficient results were reported, as 72% COD removal was achieved in this case (almost 5 times better results than Na_2SO_4).

2.2.4. Tetracyclines

Tetracyclines are broad-spectrum antibiotics, extensively used for disease control due to their great therapeutic values and affordability. They are also widely used in livestock feed to prevent diseases and promote growth.

Degradation of tetracyclines by EO has been widely studied by researchers using both active and inactive anode materials. Efficacious removal and mineralization of tetracycline antibiotics by inactive BDD electrodes have been reported by a few researchers

(Table 2.1). PbO_2 based inactive anodes were also tested for their application in tetracycline abatement. Comparison of Ti/PbO_2 anode with active Ti/IrO_2 anode in terms of tetracycline degradation has been reported by two different research groups. Kitazono et al. (2012) examined electrochemical oxidation of tetracycline antibiotics in milk (as diary industry disposes large volumes of waste milk with antibiotic residues) using both active (Ti/IrO_2) and inactive (Ti/PbO_2) anodes. Removal efficiencies of 83% and 93% were achieved using Ti/IrO_2 and Ti/PbO_2, respectively. Comparison of same set of electrodes as used by Kitazono et al. (2012) was done by Zaviska et al. (2013), but using chlorotetracycline as model pollutant and distilled water as matrix. At similar operating conditions, nearly 78% and 96% degradation was reported for Ti/IrO_2 and Ti/PbO_2 anodes, respectively. Therefore, the performance of Ti/PbO_2 electrode was clearly better than Ti/IrO_2 electrode. Yahiaoui et al. (2013) investigated the effect of current density, temperature and initial concentration of tetracycline hydrochloride on its degradation using Pb/PbO_2 as anode and grid Pt as cathode. Increasing the current density and temperature increased the degradation of the drug while increase in initial concentration of drug had negative effect on its removal. Optimum conditions reported by the authors for removal of drug were: temperature = 26 °C, current density = 25 mA cm^{-2}, initial concentration = 100 mg L^{-1} and agitation speed of 720 rpm. 86.7% mineralization efficiency was attained at these conditions.

Mixed metal oxide anodes have been found to be dimensionally stable and active in nature. Zhang et al. (2009) used one such anode, Ti/RuO_2-IrO_2, for studying the effect of varying initial concentration of antibiotic. They reported that with the increase in initial concentration of antibiotic tetracycline the degradation decreased. 89.1% removal efficiency at initial concentration of 50 mg L^{-1} was achieved. Whereas for initial concentration of 200 mg L^{-1}, 82.2% removal efficiency was reported. Likewise, Wu et al. (2012) also degraded tetracycline using Ti/RuO_2-IrO_2 anode and carbon felt cathode. After 480 minutes of electrolysis 100% degradation of antibiotic was achieved and 33% COD removal was reported.

However, to best of my knowledge, there are just two reported studies in literature which have incorporated Ti/RuO_2 anode, and reported excellent results in terms of antibiotic diminution from wastewater (Rossi et al., 2009; Hussain et al., 2015). Rossi et al. (2009) conducted Ti/RuO_2 based anodic oxidation of oxytetracycline hydrochloride. Complete

degradation of antibiotic was achieved and antibiotic activity of the drug was lost after only 120 min of electrolysis. Thus, dimensionally stable RuO_2 based electrodes have proven their potential for antibiotic degradation and offer themselves as a great alternative to super expensive BDD anodes. Hussain et al. (2015) treated wastewater comprising SMX and has been discussed earlier in section **2.2.3**.

2.2.5. Other antibiotics

Besides penicillins, fluoroquinolones, sulphonamides and tetracyclines there are other antibiotics which are quite important from therapeutic point of view such as lincosamides, macrolides, glycopeptides etc. Degradation of lincomycin (lincosamide) was investigated by Jara at al. (2007) using different anodes (Ti/Pt, graphite, $Ti/IrO_2/Ta_2O_5$, 3D GAC) and stainless steel as cathode. Lincomycin was hardly oxidized (COD removal = 30%) with slow overall kinetics. Gonzalez et al. (2011) tested the capability of BDD to degrade trimethoprim. Complete degradation of antibiotic was attained in acidic pH 3.0 using current density of 207 mA cm^{-2}.

Table 2.1. EO treatment of different types of antibiotics using BDD as anode material

Antibiotic	Concentration	Cathode	Current density	%Removal	Reference
Penicillins					
Ampicillin	618 mg L^{-1}	Nb/BDD	13.4 mA cm^{-2}	Drug: 97.1% COD: 92.5%	Korbahti and Tasyurek, (2015)
Amoxicillin	36.5 mg L^{-1}	Stainless steel	20.8 mA cm^{-2}	Drug: 100% TOC: 100%	Sopaj et al. (2015)
Amoxicillin	COD: 1000 mg L^{-1}	Stainless steel	50 mA cm^{-2}	COD: 80.2%	Frontistis et al. (2017)
Ampicillin	50 mg L^{-1}	Carbon-PTFE	5 mA cm^{-2}	Drug: 68%	Vidal et al. (2019)
Fluoro-quinolones					
Enrofloxacin	1580 mg L^{-1}	Stainless steel	50 mA cm^{-2}	TOC: ≈85% in 15 h	Guinea et al. (2009)
Enrofloxacin	158 mg L^{-1}	Carbon-PTFE cloth	33 mA cm^{-2}	TOC: Stirred tank reactor: 67% Batch recirculation flow reactor: 28%	Guinea et al. (2010)
Ofloxacin	50 mg L^{-1}	Platinum wire	100 mA cm^{-2}	Drug: 100%	Chen et al. (2013)
Norfloxacin	100 mg L^{-1}	Stainless steel	83 mA cm^{-2}	TOC: 92%	Mora-Gomez et al. (2019)
Norfloxacin	100 mg L^{-1}	Stainless steel	10 mA cm^{-2}	TOC: 90% in 5 h	Sanchez-Montes et al. (2018)
Norfloxacin	0.1 mM	Stainless steel	20 mA cm^{-2}	Drug: 100% COD: 100%	da Silva et al. (2019)

Antibiotic	**Concentration**	**Cathode**	**Current density**	**%Removal**	**Reference**
Sulfonamides					
Sulfamethoxazole	1 mM	Stainless steel	2.86 mA cm^{-2}	Drug: 73% TOC: 32%	Li et al. (2008)
Sulfamethoxazole	1 mM	Stainless steel	5.33 mA cm^{-2}	TOC: 78%	Boudreau et al. (2010a)
Sulfamethoxazole	100 mg L^{-1}	Stainless Steel	15 mA cm^{-2}	Drug: 100% TOC: 80%	De Vidales et al. (2012)
Sulfamethoxazole Trimethoprim	250 mg L^{-1} 50 mg L^{-1}	Stainless Steel	36 mA cm^{-2}	Drug: 96% Drug: 92%	De Amorim et al. (2013)
Sulfamethazine	193 mg L^{-1}	Stainless steel	66.6 mA cm^{-2}	TOC: 98%	El-Ghenymy et al. (2013a)
Sulfanilamide	239 mg L^{-1}	Stainless steel	66.6 mA cm^{-2}	TOC: 97%	El-Ghenymy et al. (2013b)
Sulfachloro-pyridazine	0.2 mM	Carbon-felt	16 mA cm^{-2}	TOC: 95%	Haidar et al. (2013)
Sulfadiazine Sulfathiazole Sulfamerazine Sulfamethazine Sulfadimethoxine	50 mg L^{-1} each	Stainless Steel	5 mA cm^{-2}	Mixture COD: 72% Drugs(COD): 74, 75, 66, 65 and 75% in the order as mentioned	Fabianska et al. (2014)
Sulfadiazine	250 mg L^{-1}	Stainless Steel	36 mA cm^{-2}	Drug: 100%	De Amorim et al. (2014)
Tetracyclines					
Tetracycline	100 mg L^{-1}	Stainless steel	300 A m^{-2}	COD: 86% TOC: 83% Drug: 99.8%	Brinzila et al. (2012)
	150 mg L^{-1}	Stainless steel	300 A m^{-2}	COD: 93% TOC: 87% Drug: 100% after 4 h	

Antibiotic	**Concentration**	**Cathode**	**Current density**	**%Removal**	**Reference**
Tetracycline	100 mg L^{-1}	Carbon-felt	20.83 mA cm^{-2}	TOC: 98% in 6 h	Oturan et al. (2013)
Tetracycline	150 mg L^{-1}	BDD	8.5 mA cm^{-2}	TOC: 94% in 13 h	Vedenyapina et al. (2014)
Tetracycline	50 mg L^{-1}	Stainless steel	50 A m^{-2}	TOC: 80% in 2 h	Vasilie et al. (2018)
Other antibiotic(s)					
Trimethoprim	0.17 mM	Si/BDD	207 mA cm^{-2}	Drug: 100%	Gonzalez et al. (2011)

Table 2.2. EO treatment of antibiotics using different anodes

Antibiotic	Class	Concentration	Operating conditions	Results	Reference
Ofloxacin	Fluoro-quinolone	50 mg L^{-1}	Anodes: Ti/Pt, graphite, $Ti/IrO_2/Ta_2O_5$ (DSA) or 3D GAC Current density: 400 A m^{-2}	99.9% drug removal over all anodes Fastest removal at 3D-GAC and slowest at DSA Pseudo-first order kinetics	Jara et al. (2007)
Oxytetra-cycline hydro-chloride	Tetracycline	2 mM	Anode/cathode: $Ti/RuO_2/Ti$ Current density: 50 mA cm^{-2} Stirred tank reactor	100% TOC removal. Antibacterial activity is lost after 120 min. Pseudo first order kinetics.	Rossi et al. (2009)
Tetracycline	Tetracycline	50 and 200 mg L^{-1}	Anode: Ti/RuO_2-IrO_2 Cathode: Stainless steel Stirred tank reactor	Drug removal: 89.1% and 82.2% for 50 and 200 mg L^{-1}	Zhang et al. (2009)
Sulfamethoxa-zole	Sulfonamide	1.3 mM	Pt mesh as anode, carbon-felt cathode pH = 3.0 Batch reactor	91% TOC removal. Reaction pathway was proposed.	Dirany et al. (2010)
Tetracycline	Tetracycline	100 mg L^{-1}	Ti/IrO_2 as anode, Ti plate as cathode 1.5 A for 6 h Stirred tank reactor	Drug removal: *Aqueous solution:* >99.4% in 6 h *Livestock wastewater:* >99.3% in 6 h	Miyata et al. (2011)
Tetracycline	Tetracycline	100 mg L^{-1}	Ti/RuO_2-IrO_2 as anode, carbon-felt as cathode Stirred tank reactor	COD removal: 33% in 480 min Drug removal: 100% in 480 min	Wu et al. (2012)

Antibiotic	**Class**	**Concentration**	**Operating conditions**	**Results**	**Reference**
Ampicillin Penicillin G	Penicillin	0.01 M	Mixed metal oxide anodes: (a) Ru-Ir-TiO_2 (20:30:50) or (b) Ru-Ir-TiO_2 (40:10:50) Cathode: Ti	Optimum pH for 100% removal: Ampicillin: pH 4 Penicillin G: pH 12 and 10 for anode (a) and (b), respectively	Wirzal et al. (2013)
Chloro-tetracycline	Tetra-cycline	10 mg L^{-1}	Ti/IrO_2 or Ti/PbO_2 as anode, Ti plate as cathode	Ti/PbO_2 was better than Ti/IrO_2 96% drug removal in 49 min using Ti/PbO_2	Zaviska et al. (2013)
Ciprofloxacin	Fluoro-quinolone	50 mg L^{-1}	Ti/SnO_2-Sb anode Current density: 30 mA cm^{-2} Stirred tank reactor	100% drug removal in 2 h 70% TOC removal in 2 h	Wang et al. (2016)
Ciprofloxacin	Fluoro-quinolone	36 mg L^{-1}	Ti/PbO_2 anode Current density: 32 mA cm^{-2} Stirred tank reactor	70% drug removal in 2 h 50% COD removal in 3 h	Rahmani et al. (2018)
Ciprofloxacin	Fluoro-quinolone	50 mg L^{-1}	Double sided Ti-Pt/β-PbO_2 anode pH 10 Current density: 30 mA cm^{-2}	100% drug removal in 2 h 75% TOC removal in 5 h	Watcher et al. (2018)

Table 2.3. EO treatment of different pharmaceutical compounds

Drug	Class	Concentration	Operating conditions	Results	Reference
Paracetamol	Analgesic	157 mg L^{-1}	Anode: Pt or BDD 300 mA current for 6 h Stirred tank reactor	TOC removal: Pt: 19% BDD: 98%	Brillas et al. (2005)
Clofibric acid	Metabolite of blood lipid regulators	179 mg L^{-1}	Anode: Pt or BDD	TOC removal: BDD: 100% Pt: 30% Drug removal: BDD: 100% Pt: 100%	Sires et al. (2006)
Paracetamol	Analgesic	1 mM	Anode: BDD or Ti/SnO_2 or Ti/IrO_2 200 mA for 210 min Plug-flow reactor	TOC removal: Ti/IrO_2: 1% Ti/SnO_2: 40% BDD: 73%	Waterson et al. (2006)
17 β-estradiol	Estrogen steroid hormone	500 μg L^{-1}	Anode: BDD Current density: 50 mA cm^{-2}	100% TOC removal in 4.5 h Optimum pH: 10	Muruganantham et al. (2007)
Ibuprofen	NSAID	1.75 mM	Anode: $Ti/Pt/PbO_2$ or Si/BDD Current density: 30 mA cm^{-2} Batch reactor	TOC removal: $Ti/Pt/PbO_2$: 75% Si/BDD: 92%	Ciriaco et al. (2009)
Diclofenac	NSAID	30 mg L^{-1}	Anode: BDD	100% drug removal in 4 h 72% TOC removal in 4 h	Zhao et al. (2009)
Paracetamol	Analgesic	1 mM	Anode: BDD/ Ti/RuO_2; 80 mA current; 300 min Stirred reactor	TOC removal: Ti/RuO_2: 28% BDD: 55%	Boudreau et al. (2010b)

Drug	**Class**	**Concentration**	**Operating conditions**	**Results**	**Reference**
Diclofenac	NSAID	175 mg L^{-1}	Anode: Pt or BDD 300 mA current for 360 min pH: 6.5 Stirred tank reactor	TOC removal: Pt: 46% BDD: 97% Pseudo first order kinetics	Brillas et al. (2010)
Ketoprofen	NSAID	50 mg L^{-1}	Anode: Si/BDD Current density: 235 mA cm^{-2}	Drug removal: 100% COD removal: 38%	Dominguez et al., 2010
17 α-ethinylestra-diol	Estrogen	2 mg L^{-1}	Anode: Ti/SnO_2 Current density: 10 mA cm^{-2} Batch reactor	78.5% TOC removal in 8 h	Feng et al. (2010)
Ketoprofen	NSAID	5.0 μM	Anode: BDD or Pt Stirred tank reactor	100% TOC removal	Muruganant han et al. (2010)
Ibuprofen	NSAID	30 mg L^{-1}	Anode: BDD, glassy carbon (GC), carbon nanotubes (CNTs)	Drug removal: BDD: 50% GC: 45% CNT: 75%	Motoc et al. (2012)
Diclofenac	NSAID	150 mg L^{-1}	Anode: BDD Flow reactor	100% TOC removal 78% current efficiency	Coria et al. (2014)

Pharmaceutical compounds such as analgesics, non-steroidal anti-inflammatory drugs (NSAIDs), β-blockers, etc. have also been tested from their degradation and mineralization point of view using the process of EO (Table 2.3). As illustrated in Tables 2.1 and 2.3, most of the research teams have incorporated BDD as anode material in their respective studies and reported successful EO treatment of pharmaceuticals. Despite being so advantageous, practical application of BDD anodes at large scale is yet dubious due to their excessively high cost in comparison to other dimensionally and chemically stable electrode materials (Panizza and Cerisola, 2009). Performance of other inactive anodes such as SnO2 and PbO2 for degradation of pharmaceuticals is reported to be good (Yahiaoui et al., 2013, Wang et al., 2016, Rahmani et al., 2018). However, they have certain drawbacks such as inability to resist corrosion and instability and poor performance in wastewaters comprising chlorides (Cossu et al., 1998, Chen et al., 2004, Anglada et al., 2009). Degradation performance of active IrO2 anodes has been reported to be quite poor due to their low oxygen evolution overpotential (1.6 V) and electro-catalytic activity (Waterson et al., 2006).

Interestingly, Ti/RuO_2 electrodes have demonstrated remarkable potency in degradation and mineralization of a variety of organic pollutants including tetracycline antibiotics (Rossi et al., 2009, Kim et al., 2010, Kaur et al., 2015, Kumar et al., 2015, Goyal et al., 2017). These electrodes possess certain characteristic properties which favour the EO treatment such as strong mechanical and chemical stability even in highly acidic medium (Goyal et al., 2017, Kaur et al., 2017), relatively high oxygen evolution overpotential of ~ 1.9 V (Anglada et al., 2009, Santos et al., 2011), and high electro-catalytic activity for generation of strong oxidant species (•OH, H_2O_2, O_3, Cl_2, HOCl, OCl^-) (Panizza and Cerisola, 2009, Kumar et al., 2015, Goyal et al., 2017, Kaur et al., 2017). Moreover, Ti/RuO_2 electrodes offer themselves as a cost effective alternative to supremely claimed BDD anodes. For treatment of wastewaters comprising chlorides, besides direct electro-oxidation on the anode surface through cleanest reagent – electron, the pollutant species are also degraded via indirect oxidation in the bulk through chloro-oxidant species (Cl_2, HOCl, OCl^-) generated on the surface of Ti/RuO_2 anode surface (Goyal et al., 2017).

According to literature survey, major parameters scrutinized under EO technique are current density, pH of wastewater and substrate concentration. The effect of these parameters was found to vary significantly depending on the pollutant involved in the study. Even after using same anode material, the effect of pH on degradation and mineralization efficiency of

EO was reported to be diverse for different organic contaminants. Moreover, application of EO over a wide range of current density (2 – 200 mA cm^{-2}), and initial antibiotic concentration (1 – 2000 mg L^{-1}) has been reported by different research groups.

The economic viability of any treatment process is of utmost importance. Apart from cost of electrodes, the operational cost of EO includes the expenses of energy consumed during the process. Energy consumption during EO depends on the average potential of the electrochemical cell during treatment. The cell potential in turn depends on two factors: 1) applied current, and 2) conductivity of wastewater. In order to minimize the operational cost, conductivity of wastewater is enhanced by addition of some harmless salts, such as Na_2SO_4 and NaCl. Moreover, Ti/RuO_2 electrodes have shown enhanced performance in wastewaters comprising chlorides (Kaur et al., 2017, Kaur et al., 2018). However, to the best of my knowledge, there is no study on determination of cost effectiveness of Ti/RuO_2 based EO treatment of pharmaceutical wastewater.

Ofloxacin (OFLX) is a second generation fluoroquinolone antibiotic, widely prescribed for treatment of bronchitis, pneumonia, chlamydia, gonorrhoea, skin infections, urinary and respiratory tract infections pelvic inflammatory disease, infectious diarrhoea, ear and eye infection (Goyne et al., 2005). Amoxicillin trihydrate (AMT) is a semi-synthetic broad spectrum antibiotic belonging to penicillin class. It is one of the most prescribed antibiotics for children, adults and animals, for a number of bacterial infections, such as pneumonia, middle ear infections, strep throat, skin infections and urinary tract infections. Less than 20% of OFLX and AMT content is metabolised in human body and rest is excreted (Benito-Pena et al., 2006). Both these antibiotics are among the most prescribed ones in India and have been detected in different aquatic streams in the country as well (Fick et al., 2009; Mutiyar and Mittal, 2014). Few studies have reported degradation of OFLX and AMT by EO, using different anode materials. However, a detailed parametric study involving evaluation and mechanism of EO treatment process, identification of transformation by-products and degradation pathway was missing.

On the basis of the review of literature, research gaps and areas demanding further investigation were identified, and subsequently objectives for the present study were established.

2.3. RESEARCH GAPS

On the basis of literature discussed above following research gaps have been identified:

1. Application of electrooxidation for abatement of various pharmaceuticals using BDD electrode has been extensively studied by a number of researchers. BDD has shown excellent performance for degradation and mineralization of a variety of pharmaceutical compounds. Nonetheless, its high cost makes its application at large-scale dubious. Therefore, there is a need to investigate alternative anode material which is comparatively cheaper and surmount the limitations of BDD.
2. Cost effective Ti/RuO_2 electrodes have shown promising results in terms of organic pollutants' removal from wastewater. Efficacy of this anode material further needs to be explored for degradation of antibiotics commonly detected in environmental matrices
3. Mechanism of degradation, pathway followed and analysis of intermediates which may be formed during electrooxidation need to be studied in order to check the toxicity level of final product. Beta-lactams and fluoroquinolones are among those drugs which need to be explored on the above mentioned grounds. Their study is also important because these are reported to be the highest selling drugs in India according to a report published in 2014.
4. Most of the researchers have used batch reactor for electrooxidation of pharmaceuticals. Very few studies have investigated EO process in a continuous reactor. This needs to be explored for testing the applicability of EO at industrial level. Moreover important design parameters like residence time and steady state time were not explored.

2.4. OBJECTIVES

In view of literature survey and necessity of developing a treatment process for pharmaceutical wastewater comprising antibiotics, following objectives have been set for present study:

a) Treatment of pharmaceutical wastewater (synthetically prepared using ofloxacin and amoxicillin trihydrate antibiotics) in batch EO reactor:
    - To study the effect of Ti/RuO_2 electrodes on TOC removal, ofloxacin and amoxicillin trihydrate removal and specific energy consumed.
    - To study the effect of various operating parameters such as current density, detention time, initial pH of wastewater and electrical conductivity on TOC removal, ofloxacin and amoxicillin trihydrate removal and specific energy consumed.
    - To study the kinetics of degradation and modelling.

b) To study the treatment performance of pharmaceutical wastewater in continuous EO reactor.

Chapter – 3

MATERIALS AND METHODS

3.1. GENERAL

This chapter describes the materials and methods used in treatment of synthetic pharmaceutical wastewater comprising of either ofloxacin (OFLX) or amoxicillin trihydrate (AMT) as a model pollutant using electro-oxidation technique. Preparation of synthetic wastewater, experimental set-up for batch and continuous mode of treatment, and analytical techniques are explained in detail.

3.2. MATERIALS

3.2.1. Wastewater and Chemicals

Synthetic wastewater was prepared freshly for each experiment at room temperature. Pre-determined quantity of antibiotic (ofloxacin or amoxicillin trihydrate) was dissolved in 1.5 L of double distilled water with the help of magnetic stirrer. To enhance the conductivity of synthetic wastewater, pre-determined quantity of sodium chloride (NaCl) was added as supporting electrolyte. For batch mode of electrolysis, effect of initial antibiotic concentration (C_0, mg L^{-1}) and supporting electrolyte concentration (S_0, g L^{-1}) was investigated, using the range as: C_0 = 10 – 50 mg L^{-1}, and S_0 = 0.5–2 g L^{-1}. However, for continuous mode of treatment, C_0 and S_0 were fixed as 50 mg L^{-1} and 2 g L^{-1}, respectively. The initial pH of wastewater was adjusted using 0.1 M hydrochloric acid (HCl) or 0.1 M sodium hydroxide (NaOH).

Both the antibiotics used in the study were obtained from their respective manufacturing industries in the purest available powder forms. Ofloxacin (99.9%) was procured from Shri Ramesth Industries, a unit of Zhen Heal Craft Private Ltd., Himachal Pradesh, India. Amoxicillin Trihydrate (99%) was procured from DSM Sinochem Pharmaceuticals, Punjab, India. The chemicals - NaCl, HCl and NaOH were of analytical reagent grade (AR) and purchased from Loba Chemie Pvt. Ltd., Mumbai, India. Formic acid (HCOOH) and acetonitrile (CH_3CN) were of LC–MS (liquid chromatography–mass spectrometry) grade and purchased from Fluka Sigma–Aldrich and Fluka Honeywell, respectively.

3.2.2. Electrodes

Set of four titanium plates coated with ruthenium dioxide (Ti/RuO_2) was purchased from Titanium Tantalum Products Limited, Chennai, India. The dimensions of these plates

were – 100 mm × 85 mm × 1.5 mm, with surface area of 85 cm^2. All four electrodes were connected in parallel such that two alternate electrodes were connected to the positive terminal of the power supply, and hence acted as anodes, while the other two were connected to negative terminal, thus serving as cathodes. Therefore, the total effective anodic area was 170 cm^2.The set of electrodes was properly washed with distilled water and air dried at room temperature before conducting each EO experiment.

3.2.3. Instruments and Analytical Techniques

Residual antibiotic concentration in the wastewater during and after the treatment was determined using a double beam UV–visible spectrophotometer (Perkin Elmer, Lambda 35). The UV visible spectra of OFLX and AMT revealed that the wavelengths corresponding to maximum absorbance of light (λ_{max}) were 288 and 228 nm, respectively. A calibration curve for both the antibiotics were prepared at their respective λ_{max} values (Fig. 3.1a and b) using samples of different known concentrations. Therefore, the dependent variable i.e., absorbance, was plotted along y-axis, and known concentrations along x-axis. Regression equations analogous to the calibration plot of OFLX (y = 0.0739x) and AMT (y = 0.0227x) enabled to determine the unknown antibiotic concentration in the aliquots collected from the electrochemical reactor, simply from the value of absorbance conveyed by the spectrophotometer.

The amount of total organic carbon (TOC) in the samples was determined using TOC-VCPH, PC controlled TOC analyser (Shimadzu, Japan). It utilized the technique of combustion of sample by platinum catalysed oxidation at 680 °C followed by determination of CO_2 by non-dispersive infrared sensor.

The transformation products or reaction intermediates of antibiotics formed during electro-catalytic oxidation were analysed by ultra-performance liquid chromatography coupled with mass spectrometry using UPLC-XEVO-G2-XS/QTOF-MS (Waters) equipped with equipped with BEH (ethylene bridged hybrid) C18 analytical column (100 mm × 2.1 mm; 1.7 µm particle size). The mobile phase comprised of 0.1% formic acid in water (A) and acetonitrile (B). The chromatographic method held the initial mobile phase condition (10% B) constant for 2.50 min, followed by a linear gradient to 50% B up to 5.50 min, then a linear increase to 90% B and kept for 2 min at 90% B. Finally, the mobile phase was returned to initial conditions of 10% B for 2 min. The flow rate was 0.3 mL min^{-1}. The MS analyser was operated in positive ion mode across the range 100 – 1000 m/z with a capillary

voltage of 2000 V and cone voltage of 30 V. The source and desolvation temperature of MS analyzer were set as 120 ^{o}C and 350 ^{o}C, respectively. Nitrogen was employed as carrier gas with cone gas flow of 60 L h^{-1}.

The pH of wastewater was measured using Thermo Scientific Orion 5 star pH meter. Conductivity measurements were performed using Benchtop Water Quality Meter – 860033, equipped with a conductivity probe.

The morphology and elemental distribution of Ti/RuO_2 electrodes was examined by performing SEM (Scanning electron microscopy) and EDX (Energy dispersive x-ray spectroscopy) analysis. The make of SEM used in present study was Zeiss ultra 55 FE-SEM with oxford EDX system. The micro structure and crystal orientation of electrodes was analyzed by conducting x-ray diffraction over electrode samples. Panalytical X'pert pro diffracto-meter with angular range of 20° to 80° and copper-K-α as x-ray energy was used for the purpose.

3.3. EXPERIMENTAL SET-UP

3.3.1. Batch Electro-oxidation

Synthetic wastewater was treated in a cuboid reactor (13 cm × 13 cm × 13 cm) fabricated from acrylic sheet, with working volume of 1.5 L (Fig. 3.2). The set of electrodes was mounted over the top of the reactor in a way that its distance from the reactor bottom was 2 cm, thus allowing enough space for the magnetic bead to rotate. The inter-electrode gap was maintained as 1 cm. The reactor equipped with electrodes was placed over magnetic stirrer for homogeneous mixing of the wastewater solution throughout the EO process. Current was supplied through a regulated DC power supply (DIGITECH, Roorkee, India, Model: 4818A10; 0–20 V, 0–5 A).

3.3.2. Continuous Electro-oxidation

The reactor set-up used in continuous EO experiments was similar to the one used in batch EO, but with inlet and outlet pipes attached to it as shown in Fig. 3.3. Synthetic wastewater was continuously supplied to the reactor from a reservoir through inlet pipe. The flow rate of wastewater corresponding to required retention time (R_T) was set using a peristaltic pump (Miclin PP 20 EX). Once the reactor was filled with synthetic wastewater up to the outlet point, treatment process was started by switching on the power supply.

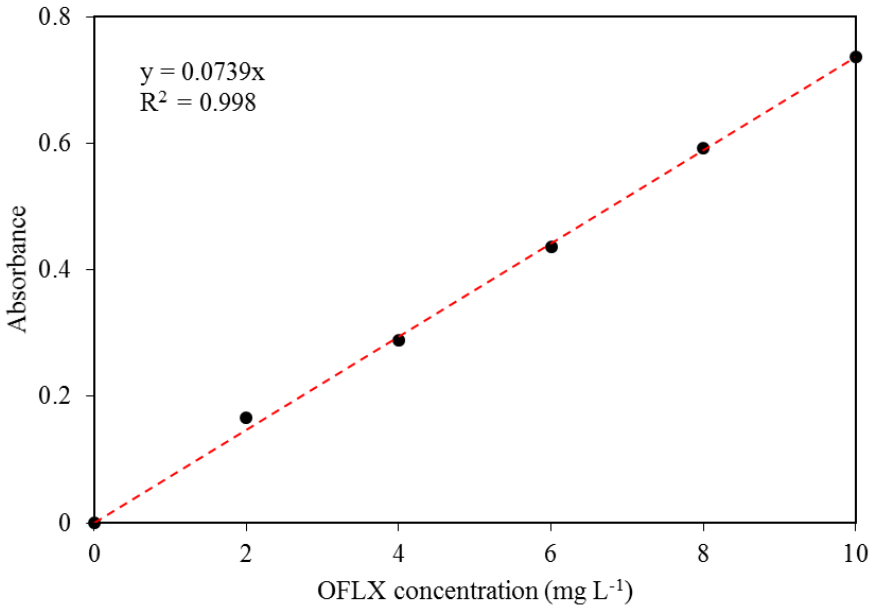

(a)

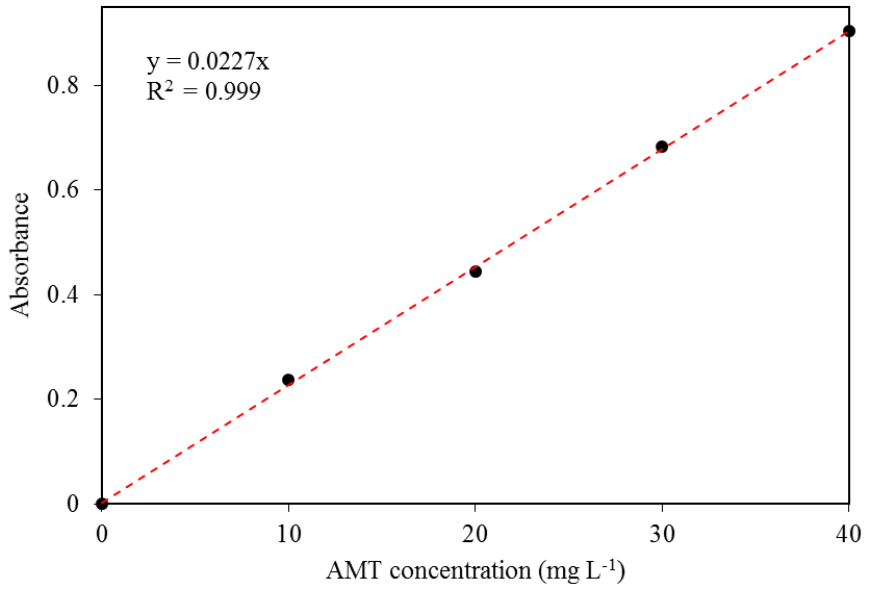

(b)

Fig. 3.1. Calibration curve of (a) OFLX and (b) AMT antibiotic.

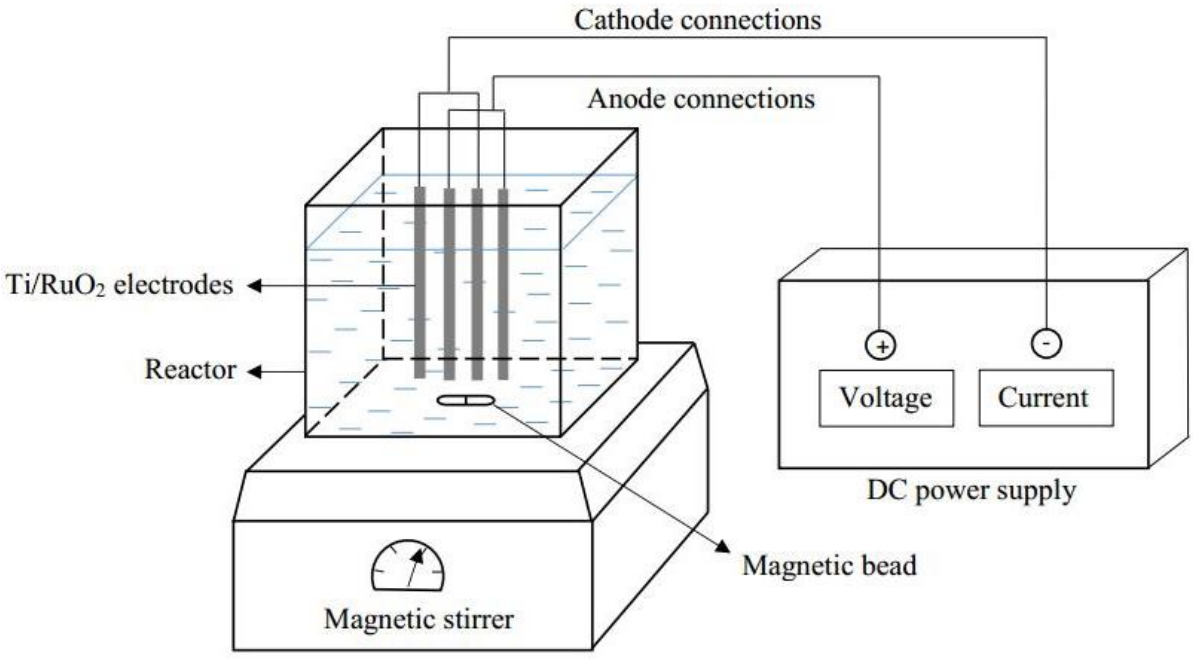

Fig. 3.2. Schematic diagram of experimental set-up for batch EO

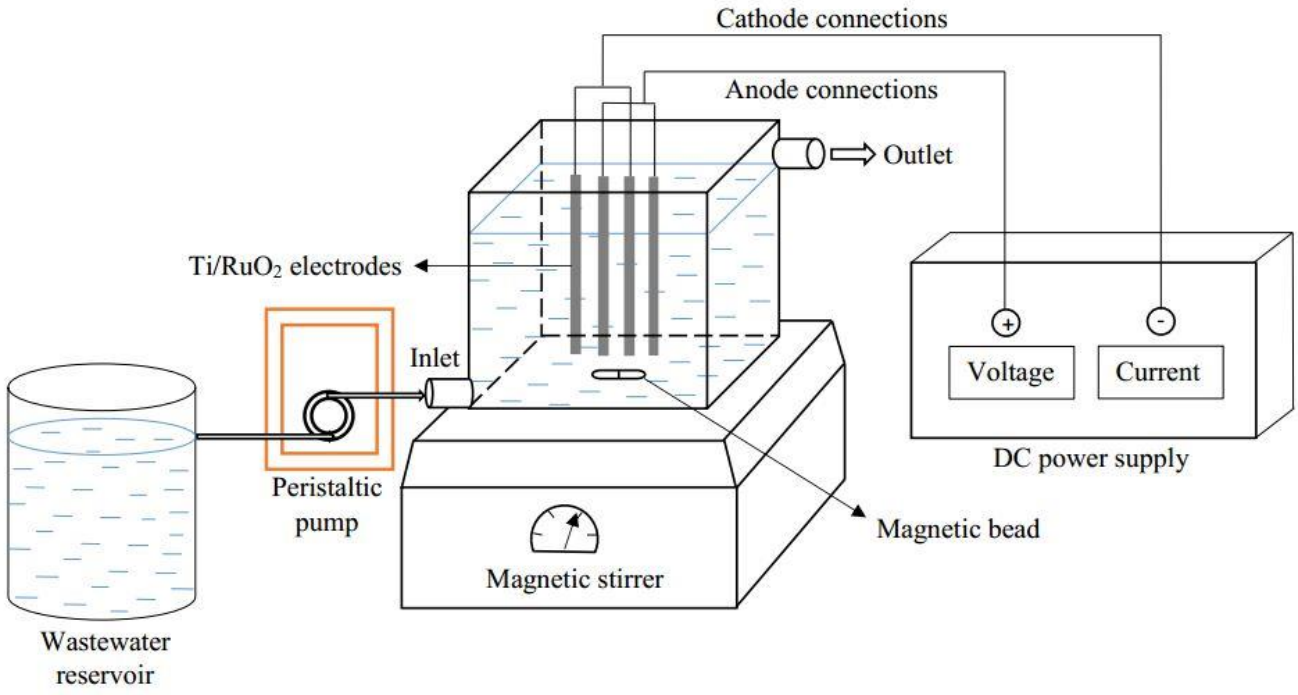

Fig. 3.3. Schematic diagram of experimental set-up for continuous EO

3.4. EXPERIMENTAL PROCEDURE AND ANALYSIS

3.4.1. Batch electro-oxidation

The batch EO experiments were performed over a range of operating parameters such as: initial pH: 2–9, applied current (*I*): 0.25–1 A, initial antibiotic concentration (C_0): 10–50 mg L^{-1} and supporting electrolyte (NaCl) concentration (S_0): 0.5–2 g L^{-1}. The process conditions were optimized in a way that the effect of a particular parameter within its defined range was evaluated by keeping other parameters constant. Effects of operating parameters on antibiotic and TOC removal efficiency, specific energy consumption (SEC) and mineralization current efficiency (MCE) were explored in detail. Furthermore, the mechanism of oxidation of antibiotics in electrochemical cell was elucidated.

Residual antibiotic concentration in samples withdrawn from the reactor after pre-defined time interval was determined using UV-visible spectrophotometer. Antibiotic removal efficiency (ARE) was calculated using Eq. 3.1.

$$ARE\ (\%) = \frac{C_0 - C_f}{C_0} \times 100 \quad \textbf{(3.1)}$$

Where, C_0 and C_f denote initial and final concentration of antibiotic (mg L^{-1}) in the synthetic wastewater.

Degree of mineralization of treated wastewater by EO was evaluated by examining TOC removal efficiency (TRE) over a period of time using Eq. 3.2.

$$TRE\ (\%) = \frac{TOC_0 - TOC_f}{TOC_0} \times 100 \quad \textbf{(3.2)}$$

Where, TOC_0 and TOC_f stand for TOC concentration (mg L^{-1}) in the synthetic wastewater before and after the EO treatment, respectively.

The economic viability of EO treatment process was assessed by calculating SEC according to Eq. 3.3. SEC is defined as the amount of energy consumed in kWh for reduction of 1 g of organic load from wastewater.

$$SEC\ (kWh(g\ TOC\ removed)^{-1}) = \frac{UIt}{(TOC_0 - TOC_f)\ \times V_R} \quad \textbf{(3.3)}$$

Where, U is average electrochemical cell potential (V), I is applied current intensity (A), t is the electrolysis time (h) and V_R is the volume of wastewater in the reactor.

Mineralization of an organic pollutant is its complete transformation to CO_2 and other inorganic ions. The antibiotics, OFLX ($C_{18}H_{20}O_4N_3F$) and AMT ($C_{16}H_{19}N_3O_5S.3H_2O$), underwent mineralization during electro-oxidation treatment according to following reactions (Eqs. 3.4 and 3.5).

$$C_{18}H_{20}O_4N_3F + 32H_2O \rightarrow 18CO_2 + F^- + 3NH_4^+ + 72H^+ + 74e^- \quad \textbf{(3.4)}$$

$$C_{16}H_{19}N_3O_5S.3H_2O + 28H_2O \rightarrow 16CO_2 + 3NH_4^+ + SO_4^{2-} + 69H^+ + 70e^- \quad \textbf{(3.5)}$$

Mineralization current efficiency of EO treatment process was computed using Eq. 3.6. MCE is defined as ratio of the charge used for mineralization of a pollutant to total charge passed during electrolysis.

$$MCE\ (\%) = \frac{(TOC_0 - TOC_f)zFV_R}{4.32 \times 10^7 nIt} \times 100 \quad \textbf{(3.6)}$$

Where, z is the number of electrons involved in mineralization of antibiotic (OFLX: z = 74 (Eq. 3.4); AMT: z = 70 (Eq. 3.5)), F is Faraday's constant (96,487 C mol^{-1}), n is the number of carbon atoms in antibiotic molecule (OFLX: n = 18; AMT: n = 16) and 4.32×10^7 is the conversion factor (3,600 s h^{-1} × 12,000 mg mol^{-1} carbon).

Samples were withdrawn from the reactor after fixed interval of time in order to identify the transformation products of antibiotics formed during EO by UPLC-MS. Subsequently, plausible degradation pathways of both the antibiotics were proposed.

3.4.2. Continuous Electro-oxidation

The continuous EO experiments were designed based on five level full factorial central composite design (CCD), by response surface methodology (RSM) using Design-Expert software 6.0.8 (STAT-EASE Inc. Minneapolis, US). RSM is a statistical and mathematical tool used for assessment of individual and interactive effects of different operating parameters (independent variables) of a process on designated responses, by designing experiments. Paramount objective of RSM software is to reduce the number of experiments necessary to provide sufficient information to optimize the process. Full factorial experimental strategy varies operating parameters (independent variables) together, instead of one at a time. The correlation of responses and independent variables

was estimated using quadratic model (which also includes linear model), given by second order polynomial equation (Eq. 3.7).

$$Z = \beta_0 + \sum_{i=1}^{k} \beta_i v_i + \sum_{i=1}^{k} \beta_{ii} v_i^2 + \sum\sum_{i<j} \beta_{ij} v_i v_j + E_r \qquad \textbf{(3.7)}$$

Where, Z is the predicted response; β_o is the constant coefficient, v_i are the linear terms corresponding to independent variables' effects, v_i^2 correspond to effect of squared terms, $v_i v_j$ are interaction terms and correspond to effect of each paired combination of variables, β_i, β_{ii} and β_{ij} are the coefficients, and E_r represents the error value. The interaction of a response with input parameters can be represented graphically, either in a three dimensional space or in the form of contour plots. The model establishes a relationship between response and individual and interactive effects of variables by testing of hypothesis. In addition to Eq. 3.6, analysis of variance (ANOVA) was used to analyze the significant model terms and interaction between operating parameters and responses. The quality of fit of the quadratic model was scrutinized on the basis of values of R^2 (coefficient of determination) and values of predicted and adjusted R^2. The F value and P value (Prob > F) determine significance of the model and model terms. For a model or model term to be significant, P value should be less than 0.05. "Lack of fit" should not be significant for a model, i.e. the P value should be greater than 0.1. Optimization of process conditions or variables was then performed in order to minimize or maximize a response as per requirements.

The synthetic wastewater comprising 50 mg L^{-1} of antibiotic and 2 g L^{-1} of NaCl was freshly prepared using double distilled water for each experimental run of continuous EO. The operating parameters selected for designing continuous EO experiments were: initial pH, applied current (I), retention time (R_T) and elapsed time (t). The range and levels of these parameters are enlisted in Table 3.1. The responses on which individual and interactive effects of operating parameters were investigated were: TOC removal efficiency (Z_1) (Eq. 3.2), antibiotic removal efficiency (Z_2) (Eq. 3.1) and SEC (Z_3) (Eq. 3.3). Based on the effects of different parameters on treatment performance of continuous EO method in terms of the three responses, oxidative mechanism of both the antibiotics was interpreted. Thereafter, multi-response optimization was performed by RSM to simultaneously maximize TOC and antibiotic removal efficiency, and minimize energy consumption.

Comparison of response values predicted by model with actual experimental values at optimum run was done in order to check the suitability of optimization. Thereafter, MCE for optimum run was calculated using Eq. 3.6.

Table 3.1. Range and levels of operating parameters in continuous EO

Operating Parameters	**Levels**				
	(-2)	**(-1)**	**(0)**	**(1)**	**(2)**
pH: V_1	2	4	6	8	10
Applied current, I (A): V_2	0.25	0.5	0.75	1.0	1.25
Retention time, R_T (min): V_3	15	60	105	150	195
Elapsed time, *t* (min): V_4	20	60	100	140	180

Samples from the outlet of reactor were withdrawn after fixed interval of time in order to identify the transformation products of antibiotics formed during EO by UPLC-MS. Subsequently, plausible degradation pathways were proposed.

Characterization of Ti/RuO_2 electrodes was done to analyze their stability after their usage in multiple experiments (batch and continuous) of EO treatment of synthetic pharmaceutical compounds. The structural, physical and chemical composition of electrodes before and after EO treatment was examined by scanning electron microscopy (SEM), energy-dispersive x-ray spectroscopy (EDX) and x-ray diffraction (XRD) analysis.

Chapter – 4

RESULTS AND DISCUSSION

4.1. GENERAL

This chapter presents the detailed analysis of results obtained during EO treatment (batch and continuous) of antibiotics (OFLX and AMT). It includes effects of important operating parameters on process performance in terms of antibiotic degradation, mineralization and energy consumption. Consequently, mechanism of oxidation of antibiotics was well elucidated. This was further followed by study of decay kinetics of antibiotics, identification of their transformation products formed during EO treatment and proposition of plausible degradation pathways.

4.2. BATCH EO TREATMENT OF WASTEWATER COMPRISING OFLX

4.2.1 Effect of Initial pH

The pH value of the aqueous solution is an important controlling parameter in the EO p5rocess. The effect of pH was studied at initial OFLX concentration (C_0) = 50 mg L^{-1}, applied current (I) = 1 A and NaCl concentration (S_0) = 2 g L^{-1}, by varying the initial pH of synthetic wastewater comprising OFLX antibiotic in the range of 2 – 9. Antibiotic removal efficiency (ARE, %) and TOC removal efficiency (TRE, %) were calculated for entire pH range and are shown in Fig. 4.1.

Very rapid removal of OFLX can be seen during first 15 min of EO. Further, for time > 30 min of EO treatment, no significant changes in the ARE value were observed. This may be seen true for all the values of pH studied (Fig. 4.1a). Furthermore, as shown in Fig. 4.1a, solutions with lower initial pH showed higher ARE than those with higher initial pH. Nearly 88.6% OFLX degradation was achieved within 30 min of EO at highly acidic pH (pH = 2.0), whereas for strongly basic condition (pH = 9.0), ≈68.6% OFLX was degraded in 30 min. However, almost similar ARE values (≈79±1.5%) were observed within 30 min of EO in the pH range of 4 – 8. Moreover, the OFLX removal rate increased with decrease in initial pH.

Various oxidants are generated during the EO process. Subsequently, by the action of generated oxidants, the organics are first degraded to lower intermediate organic compounds and finally mineralized to produce CO_2.

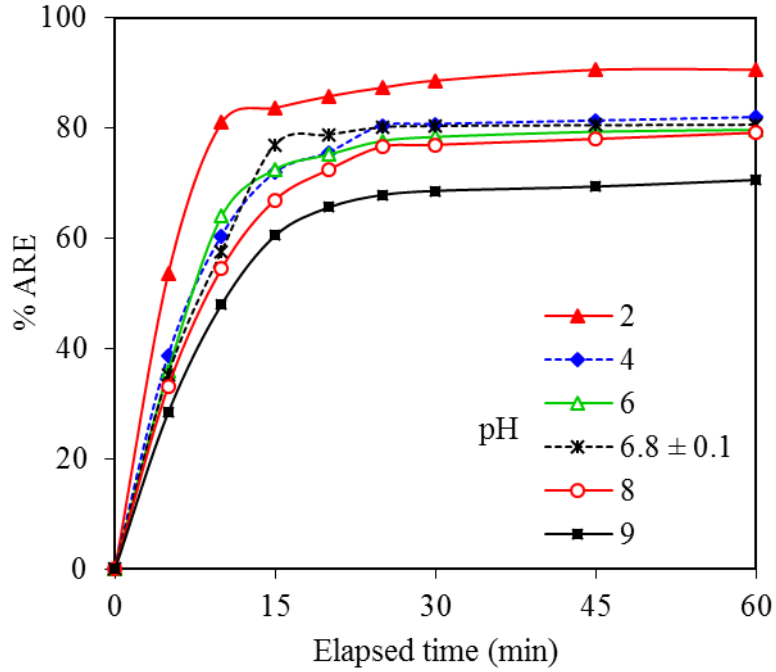

(a)

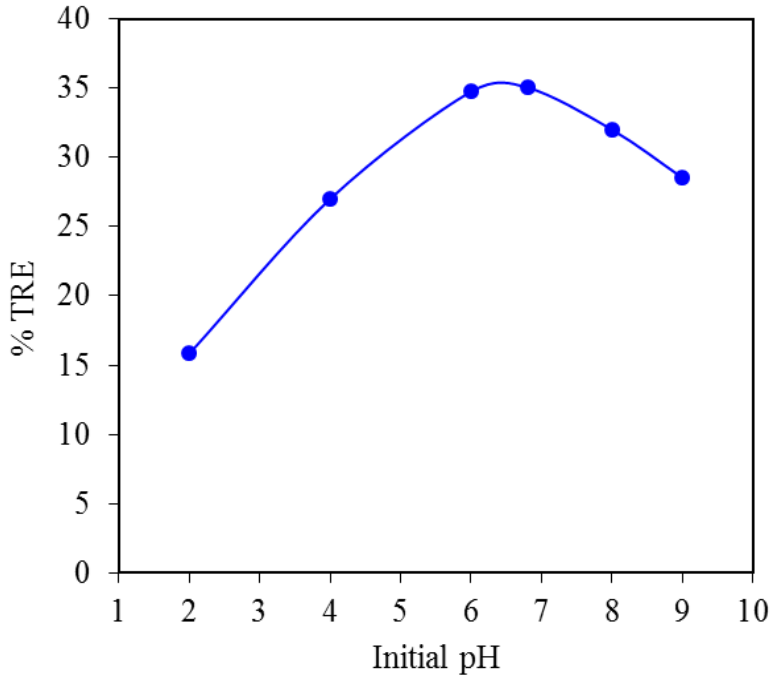

(b)

Fig. 4.1. Effect of initial pH on (a) %ARE and (b) %TRE for EO treatment of OFLX wastewater.

The degradation/mineralization of organic pollutant by EO treatment technique using Ti/RuO_2 electrodes can follow the route of direct oxidation at the anode surface and/or indirect oxidation in the bulk solution. Direct anodic oxidation takes place via direct electron transfer from anode to organic pollutant molecule (R) as shown in following reaction (Eq. 4.1).

$$Ti/RuO_2 + R \rightarrow Ti/RuO_2.(R)_{ad} \rightarrow nCO_2 + yH^+ + ze^- + \text{inorganic ions} \quad \textbf{(4.1)}$$

Electrolysis of water produces active oxygen in the form of hydroxyl radical at the anode surface which can either get physisorbed on to anode surface (Eq. 4.2) or can get chemisorbed into the oxide matrix of the Ti/RuO_2 anode, thus resulting in formation of Ti/RuO_3 (Eq. 4.3). When the pollutant species (R) come in contact with the physisorbed active oxygen, it results into complete mineralization (*electrochemical combustion*) of that molecule as shown in Eq. 4.4. However, when pollutant molecule reacts with chemisorbed •OH, it gets oxidized to form RO, which is also called "*electrochemical conversion*" (Eq. 4.5). Further oxidation of RO would lead to formation of CO_2, H_2O and other degradation products and ions.

$$Ti/RuO_2 + H_2O \rightarrow Ti/RuO_2.(\bullet OH)_{ad} + H^+ + e^- \quad \textbf{(4.2)}$$

$$Ti/RuO_2.(\bullet OH)_{ad} \rightarrow Ti/RuO_3 + H^+ + e^- \quad \textbf{(4.3)}$$

$$Ti/RuO_2.(\bullet OH)_{ad} + R \rightarrow Ti/RuO_2 + nCO_2 + \text{oxidation products} + yH^+ + ze^- \quad \textbf{(4.4)}$$

$$Ti/RuO_3 + R \rightarrow Ti/RuO_2 + RO \quad \textbf{(4.5)}$$

Furthermore, in the presence of chlorides in wastewater, Ti/RuO_2 electrodes exhibit high electrocatalytic activity for generation of reactive chlorine species which play an important role in indirect oxidation of organic pollutants (Martinez-Huitle and Ferro, 2006; Panizza and Cerisola, 2009; Sundarapandiyan et. al., 2010). Chlorine is electro-generated by direct oxidation of Cl^- ion on the anode surface as demonstrated in following reactions (Eq. 4.6 and 4.7) (Trasatti, 1987; Rajkumar et al., 2003; Jeong et al., 2009). Reaction of chlorine with water results in formation of hypochlorous acid (HClO) in the bulk solution (Eq. 4.8). Furthermore, deprotonation of HOCl generates hypochlorite ion (ClO^-) (Eq. 4.9)

$$Ti/RuO_2 + Cl^- \rightarrow Ti/RuO_2.(\bullet Cl)_{ad} + e^- \quad \textbf{(4.6)}$$

$$2Ti/RuO_2.(\bullet Cl)_{ad} \rightarrow 2Ti/RuO_2 + Cl_2 \quad \textbf{(4.7)}$$

$$Cl_2 + H_2O \rightarrow HOCl + H^+ + Cl^- \quad \textbf{(4.8)}$$

$$HOCl + OH^- \rightarrow ClO^- + H_2O \quad \textbf{(4.9)}$$

The oxygen transfer to molecules of pollutant species can also take place through adsorbed oxy-chloro radicals as shown in following reactions (Eq. 4.10 and 4.11):

$$Ti/RuO_2 + HOCl \rightarrow Ti/RuO_2.(\bullet OCl)_{ad} + H^+ + e^- \quad \textbf{(4.10)}$$

$$Ti/RuO_2.(\bullet OCl)_{ad} \rightarrow Ti/RuO_3 + Cl^- \quad \textbf{(4.11)}$$

The stability and dominance of these species is highly pH dependent. Cl_2 is predominant in highly acidic conditions (pH<1), whereas, HOCl dominates in the range of 3<pH<5 and ClO^- in pH>9 (Comninellis, 1994; Deborde and Von Gunten, 2008; Sires at al., 2014). Furthermore, in alkaline pH, other lower valued oxidants such as hydrogen peroxide (H_2O_2) and hydroperoxyl radical ($HO_2\bullet$) are produced from •OH, due to the high reactivity as well as high instability of •OH (Eqs. 4.12 – 4.14) (Sires et al., 2014; Singh et al., 2013).

$$2H_2O \rightarrow 2\bullet OH + 2H^+ + 2e^- \quad \textbf{(4.12)}$$

$$2\bullet OH \rightarrow H_2O_2 \quad \textbf{(4.13)}$$

$$\bullet OH + H_2O_2 \rightarrow HO_2\bullet + H_2O \quad \textbf{(4.14)}$$

High ARE value for OFLX at highly acidic pH could be attributed to oxidation of OFLX via direct mechanism by chemisorbed •OH in the lattice of Ti/RuO_2 anode, and partially via indirect oxidation mediated by Cl_2 and HOCl. In highly alkaline pH, %ARE value for OFLX is reduced due to the predomination of lower potential ClO^- oxidant in comparison to HOCl. Also, the lower valued oxidants such as H_2O_2 and $HO_2\bullet$ (as described above) formed (Eq. 4.13 and 4.14) participate in OFLX oxidation.

Fig. 4.1b shows the trend of %TRE with change in initial pH of the solution. Maximum TRE value of ≈35 % can be observed at natural pH (6.8 ± 0.1) after 120 min of EO. For all the pH values beyond the neutral pH, change in pH continuously decreased TOC removal. However, high ARE value of ≈88.6% was observed in highly acidic pH (pH = 2.0), opposite to TOC removal efficiency trend (Fig 4.1a). Therefore, it is obvious that the degraded OFLX during EO process is partially mineralized, and un-mineralized degraded

compounds or OFLX transformation products remain in the solution contributing to the TOC content.

This mineralization behaviour in EO process can be explained by several electrochemically generated oxidants (•OH, H_2O_2, HO_2•, Cl_2, HOCl and ClO^-). The mineralization of organics depends on the type, concentration and oxidation potential of various oxidants produced. In highly acidic pH, the degradation and mineralization is via direct oxidation mechanism involving chemisorbed •OH, Cl_2 and HOCl, while at nearly neutral pH, the oxidation is mediated by H_2O_2 and HO_2•, HOCl and ClO^- and chemisorbed •OH. In highly acidic pH, OFLX is transformed/degraded to lower molecular weight compounds via indirect oxidation by action of oxidants with higher oxidation potential such as HOCl and direct oxidation by chemisorbed •OH, which results in lower TOC removal. At natural pH range (6.8 ± 0.1), TRE value is improved due to OFLX oxidation mediated by H_2O_2 and HO_2•, however, ClO^- mediated transformation/degradation of OFLX to lower molecular weight compounds lower the TOC removal. In highly alkaline pH, predomination of ClO^- mediated oxidation further lowered the TOC removal.

From the above explained results, it may be concluded that the highly acidic pH favours OFLX degradation, while at neutral pH maximum mineralization occurred. Therefore in present study, natural pH conditions (6.8 ± 0.1) were used to carry out further experiments.

4.2.2. Effect of applied Current Intensity (*I*)

Effect of applied current intensity (*I*, A) on OFLX and TOC removal efficiency with Ti/RuO_2 anode was studied by varying *I* from 0.25 – 1 A at C_0 = 50 mg L^{-1}, pH = 6.8 ± 0.1, and S_0 = 2 g L^{-1}. The ARE and TRE values calculated with time for different values of applied *I* are shown in Fig. 4.2.

OFLX degradation increased from 20% at 15 min to 55% at 60 min for *I* = 0.25 A. Almost 80% content of OFLX was degraded in 120 min. Further increase in electrolysis time did not improve the ARE value. As *I* was increased from 0.25 A, OFLX decay rate drastically increased showing maximum ARE value of ≈80% in 60 and 30 min at 0.5 A and 0.75 A, respectively (Fig. 4.2a). Therefore, to achieve ≈80% of ARE, it took only 30 min of electrolysis at 0.75 A, whereas it was 120 min for applied current of 0.25 A. With further increase in *I* value to 1 A, although, OFLX removal rate was improved, however,

equilibrium electrolysis time was not decreased significantly (≈80% RE was observed in 25 min).

Apparently, once 80% of OFLX was destroyed, there was no further degradation for all values of applied I. This could be probably attributed to the fact that the process is substrate limiting, and the maximum removable OFLX (≈80%) is removed by the EO. Thus, for the applied *I* values of 0.25, 0.5, 0.75 and 1 A, the electrolysis time for ≈80% OFLX removal are 120, 60, 30 and 25 min respectively.

As discussed in section 4.2.1, the degradation/oxidation of OFLX near neutral pH is mainly due to mediated/indirect oxidation by H_2O_2 and HO_2•, HOCl and ClO^- and partially by direct oxidation mechanism with chemisorbed •OH. The generation rate of these oxidants increases with increase in applied *I*, which in turn increases the OFLX removal. However, increase in OFLX removal rate at higher *I* value range is slighter than that at lower *I* value range. This may be attributed to the dominance of inevitable but undesirable oxygen evolution reaction, in competition with oxidants' generation at anode, at higher applied *I* via the following reactions (Eqs. 4.15 and 4.16):

$$Ti/RuO_2.(\bullet OH)_{ad} \rightarrow Ti/RuO_2 + 1/2O_2 + H^+ + e^- \quad \textbf{(4.15)}$$

$$Ti/RuO_{2+1} \rightarrow Ti/RuO_2 + 1/2O_2 + H^+ + e^- \quad \textbf{(4.16)}$$

During the EO process, OFLX is first degraded to intermediate compounds and finally oxidized to CO_2. Therefore, it is important to study the mineralization efficiency. In order to study the effect of applied *I* on mineralization of OFLX, mineralization efficiency of EO process was calculated in terms of TRE (Fig. 4.2b) at the extended electrolysis time continued up to 240 min. It was observed that TRE value increased from just 5.71% to 24.82% in 60 min, when applied *I* was increased from 0.25 to 1 A. After 240 min of EO, 46.31% of TOC content was eliminated from the OFLX wastewater at I = 1 A. Higher production rate of hydroxyl radicals and hence chemisorbed •OH and chloro-oxidant species at higher applied current could be the most probable reason behind the results achieved (Lin et al., 2013; Fabianska et al., 2014).

The usefulness of applied current in mineralization of organics during EO treatment is assessed by calculation of mineralization current efficiency (MCE, %). The oxygen evolution rate increases with the increase in applied *I*. Consequently, due to oxygen evolution competition reaction with oxidants' generation at anode at higher applied *I*, the

mineralization current efficiency (MCE, %) is continuously decreasing with increase in applied *I* (Fig. 4.3). The MCE value decreased from 7.8% to 4.9% with increase in *I* value from 0.25 – 1 A, after 120 min of electrolysis. Lower MCE values indicate that a much smaller part of applied current is used for mineralization/combustion of OFLX, while its major part is being utilized in degradation/transformation of the antibiotic. Moreover, as shown in Fig. 4.3, after 120 min of EO treatment of synthetic wastewater comprising OFLX, specific energy consumption (SEC) increased significantly from 0.334 to 0.759 kW h (g TOC removed)$^{-1}$ with increase in applied current intensity from 0.25 to 1 A. This could be attributed to increase in value of average cell potential with the increase in *I* value. As discussed above, much part of electrical energy got consumed in amplification of unavoidable reactions (Eqs. 4.13 – 4.16) occurring at elevated values of *I*, thus resulting in lower MCE and higher SEC.

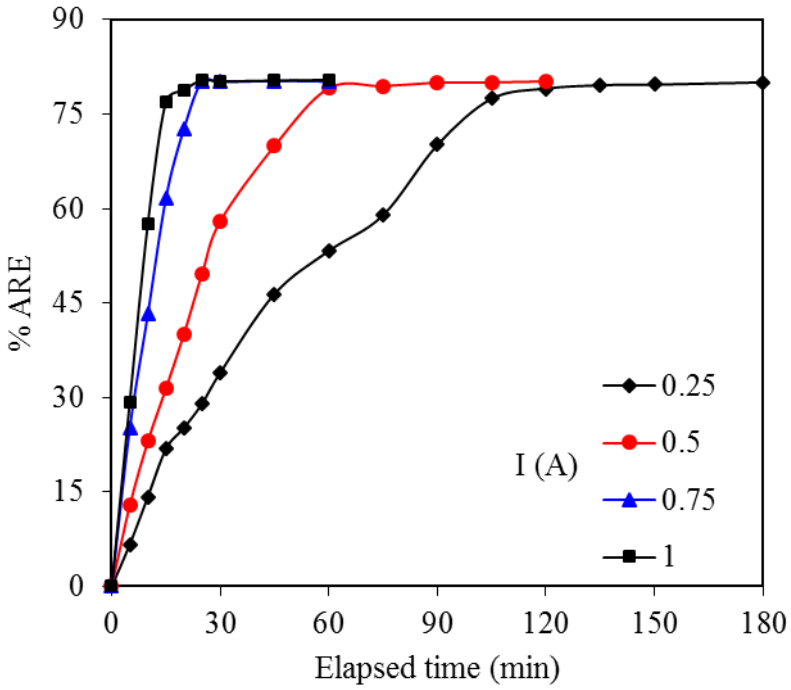

(a)

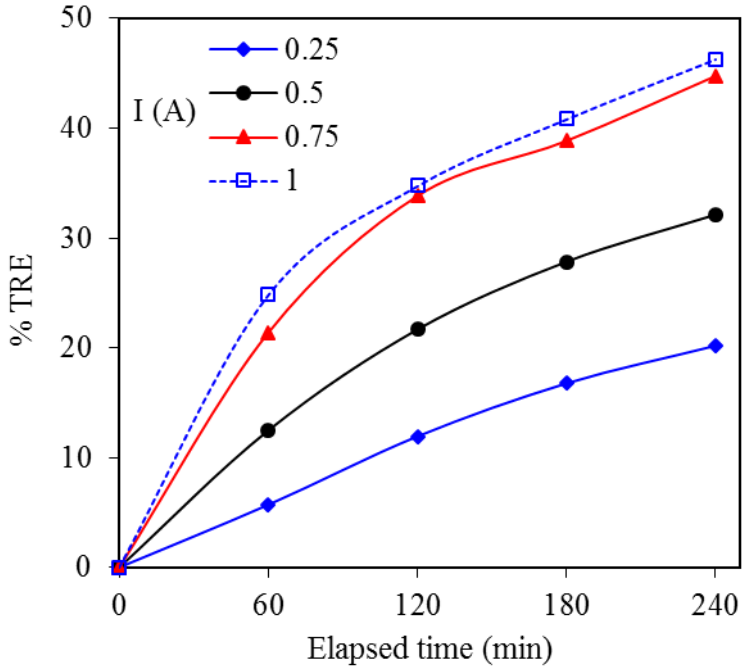

(b)

Fig. 4.2. Effect of applied current (*I*) on (a) %ARE and (b) %TRE for EO treatment of OFLX wastewater.

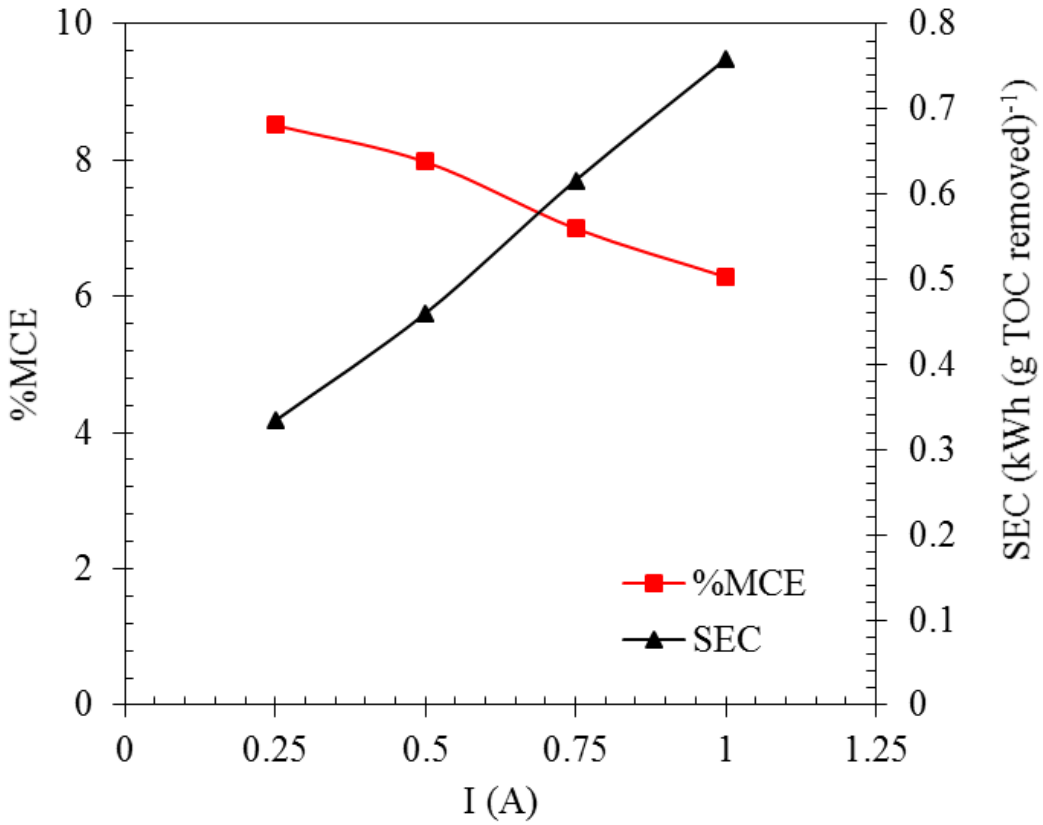

Fig. 4.3. Effect of applied current (*I*) on %MCE and SEC (kW h (g TOC removed)$^{-1}$) for EO treatment of OFLX wastewater.

4.2.3. Effect of Supporting Electrolyte Concentration (S_0)

For the present study, NaCl was employed as a supporting electrolyte for all EO experiments. It served two purposes: (1) enhancement of electrical conductivity of the synthetic wastewater to perform the electrolysis; (2) deliver active chlorine species as oxidizing agents for abatement of organic pollutant present in synthetic wastewater. The effect of NaCl concentration on OFLX removal efficiency and TOC removal efficiency (Fig. 4.4) by EO process was observed by varying the NaCl concentration from 0.5 to 2 g L^{-1} under the following operating conditions: C_0 = 50 mg L^{-1}, I = 1 A, pH = 6.8 ± 0.1.

At a given value of S_0, ARE value was found to increase with electrolysis time, and ultimately reaching a limiting value (Fig. 4.4a). Further, increased NaCl concentration at any electrolysis time always improved ARE value from 73% (S_0 = 0.5 g L^{-1}) to ≈81% (S_0 = 2 g L^{-1}). Fig. 4.4b shows the variation in TOC removal efficiency with increase in NaCl concentration. In a similar trend as ARE, TRE increased from ≈14% to 35% with the increase in S_0 value from 0.5 to 2 g L^{-1}. Rise in NaCl concentration resulted in increase in generation of chloro-oxidant species according to Eqs. 4.6 – 4.9. Increase in values of ARE and TRE with increase in NaCl concentration is thus attributed to mediated degradation/mineralization of OFLX molecules by active chlorine species.

Simultaneous effect of S_0 on %MCE and SEC (kW h (g TOC removed)$^{-1}$) values is illustrated in Fig. 4.5. SEC value continuously decreased from 3.83 to 0.775 kW h (g TOC removed)$^{-1}$) with increase in NaCl concentration from 0.5 to 2 g L^{-1}. As explained in section 4.2.1, the degradation/oxidation of OFLX near neutral pH is largely due to oxidation by H_2O_2 and HO_2•, HOCl, ClO^- and chemisorbed •OH. Increase in amount of NaCl not only enhanced the conductivity of OFLX solution (from 1.26 mS cm^{-1} for S_0 = 0.5 g L^{-1} to 3.87 mS cm^{-1} for S_0 = 2 g L^{-1}) which decreased SEC value by decreasing the average cell potential value (U), but also increased the amount of active chlorine species responsible for carrying the mediated oxidation of OFLX. With increase in NaCl concentration in synthetic wastewater, efficiency of EO cell to mineralize OFLX was also enhanced almost three times with its value rising from 2.59% (S_0 = 0.5 g L^{-1}) to 6.55% (S_0 = 2 g L^{-1}) (Fig. 4.5). Summing up, increase in S_0 value improved the %MCE of EO method by Ti/RuO_2 electrodes and decreased the overall treatment cost.

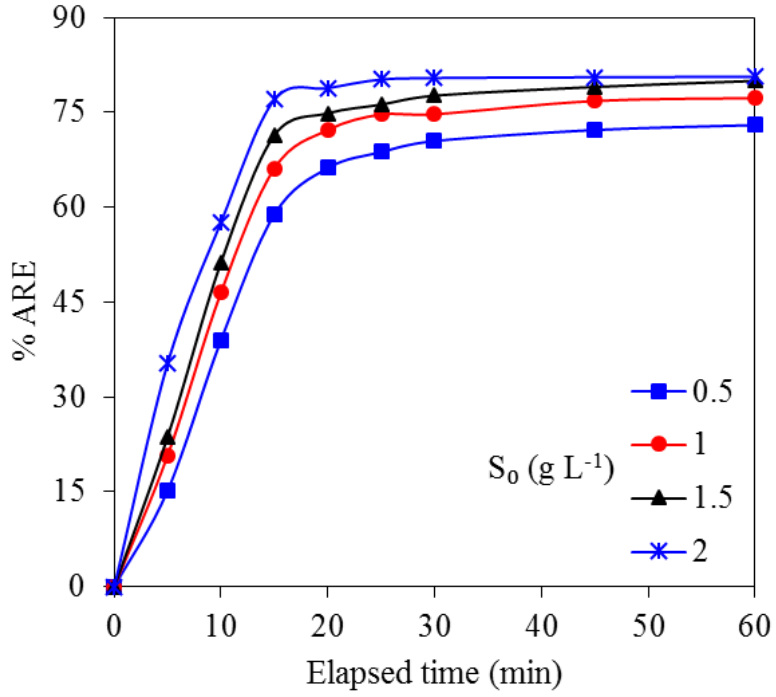

(a)

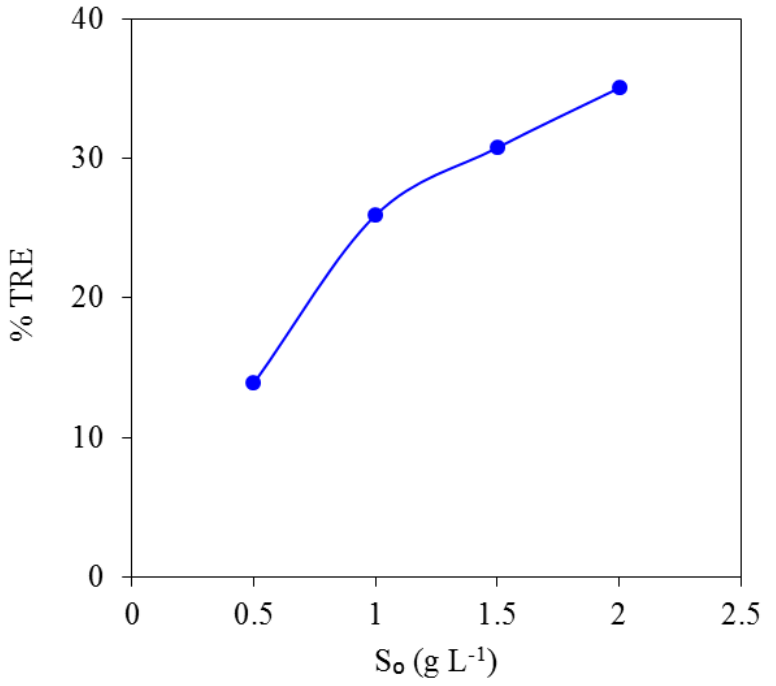

(b)

Fig. 4.4. Effect of NaCl concentration (S_0) on (a) %ARE and (b) %TRE for EO treatment of OFLX wastewater.

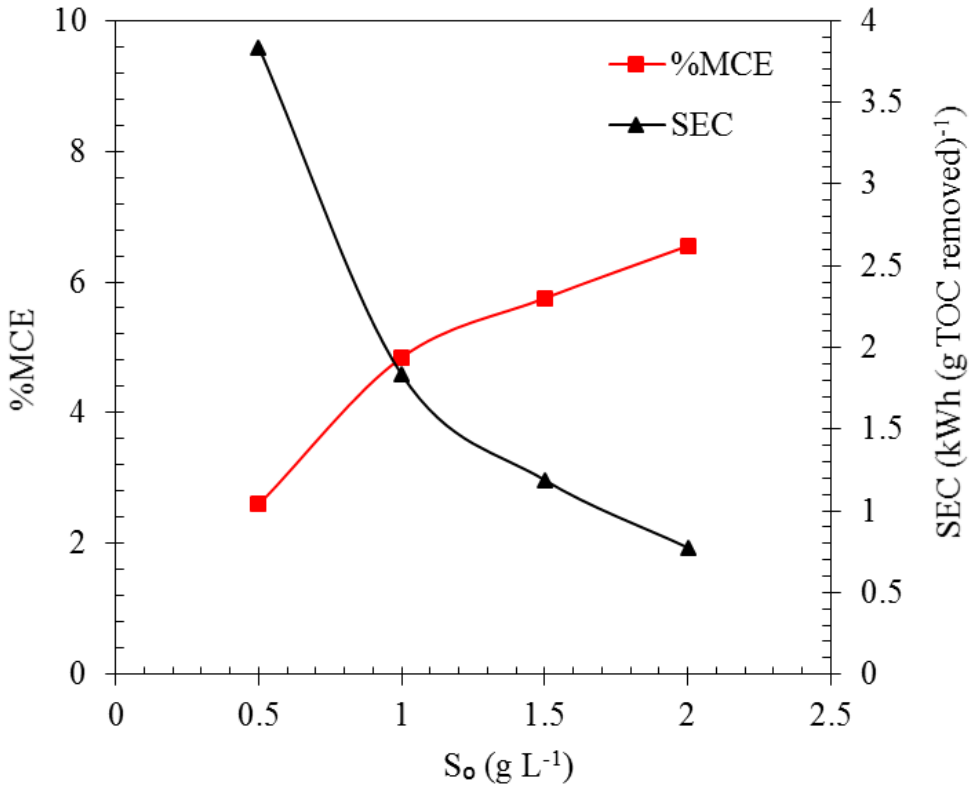

Fig. 4.5. Effect of NaCl concentration (S_0) on %MCE and SEC (kW h (g TOC removed)$^{-1}$) for EO treatment of OFLX wastewater.

4.2.4. Effect of Initial OFLX Concentration (C_0) and Decay kinetics

The OFLX removal from synthetic wastewater by EO method at any instant of time (t) can be represented by pseudo-first-order model which is given as:

$$\frac{-dC}{dt} = kC \qquad \textbf{(4.17)}$$

Where, C is the concentration of OFLX in synthetic wastewater. The above equation can be rewritten as:

$$\ln\frac{C_0}{C_t} = kt \qquad \textbf{(4.18)}$$

At any value of C_0 and applied I, the OFLX removal first increases and then becomes constant reaching an equilibrium value of C_e, and leaving behind a fraction of initial OFLX (C_0) which is not removable at given experimental conditions. Therefore, the above Eq. 4.18 can be modified to following Eq. 4.19, in a more appropriate way (Lucas and Peres, 2009):

$$C_{Rt} = C_{\mathrm{Re}}[1-e^{k_f t}] \qquad \textbf{(4.19)}$$

Where, C_{Rt} and C_{Re} (mg L^{-1}) denote the amount of OFLX removed at any time (t), and at equilibrium condition, respectively, and k_f is the pseudo-first-order rate constant. The experimental data collected were then fitted to Eq. 4.20 by applying non-linear regression using Marquardt's percent standard deviation (MPSD) error function (Marquardt, 1963):

$$MPSD = 100\sqrt{\frac{1}{n-p}\sum_{i=1}^{n}\left(\frac{C_{Rt,i,exp}-C_{Rt,i,cal}}{C_{Rt,i,exp}}\right)^2} \qquad \textbf{(4.20)}$$

Where, the subscripts 'exp' and 'cal' represent the experimental and calculated values of C_{Rt}, n is the number of measurements, and p is the number of parameters in the model.

Kinetic study for degradation of OFLX was performed by varying initial OFLX concentration (C_0) in the range of 10-50 mg L^{-1} at I = 1 A, pH = 6.8 ± 0.1 and S_0 = 2 g L^{-1}; and applied I in the range of 0.25 – 1 A at C_0 = 50 mg L^{-1}, pH = 6.8 ± 0.1 and S_0 = 2 g L^{-1}. Fig. 4.6a and b depict the kinetic data fitted to pseudo-first order kinetic model for degradation of OFLX by varying C_0 and applied I, respectively, by solid line; and the best-fit values of kinetic parameters along with the correlation coefficients and MPSD values are given in Table 4.1.

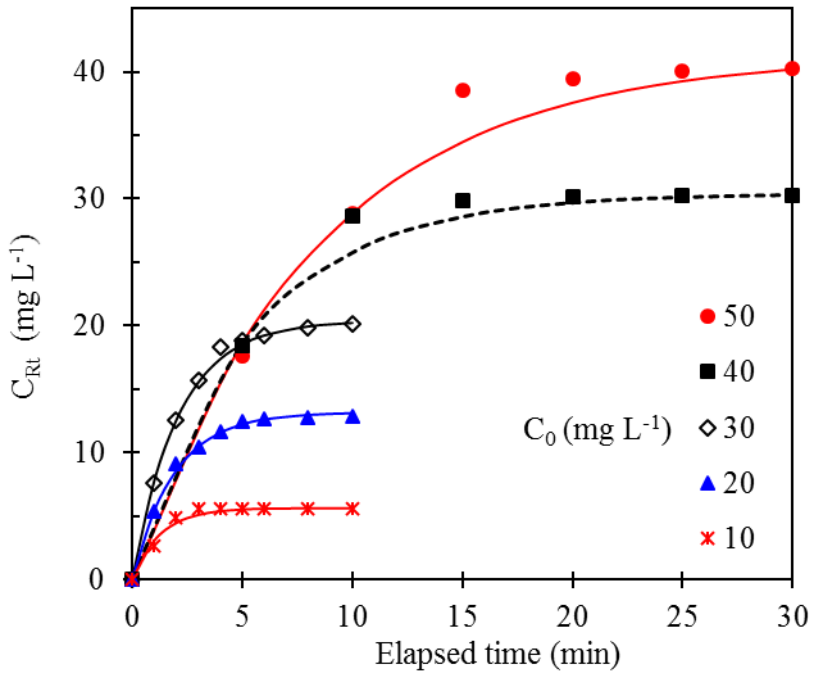

(a)

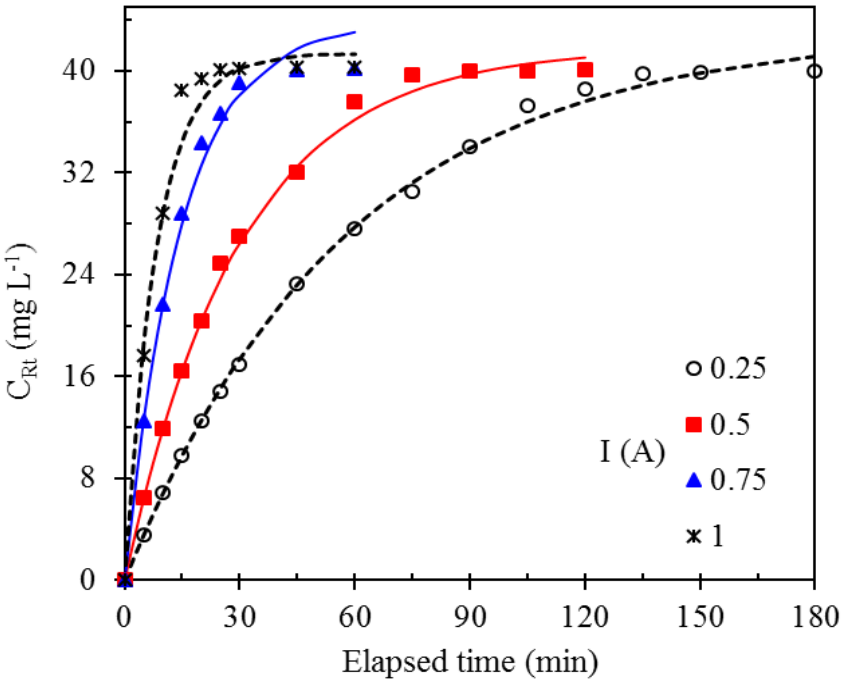

(b)

Fig. 4.6. Degradation kinetics of OFLX (a) Effect of initial OFLX concentration (C_0) (b) Effect of applied current (*I*).

Table 4.1. Kinetic parameters for OFLX degradation at different operating conditions.

Parameter	k_f (min^{-1})	$C_{Re,\ exp}$ (mg L^{-1})	$C_{Re,\ cal}$ (mg L^{-1})	R^2	MPSD
C_0 (mg L^{-1})					
10	0.78	5.57	5.61	0.99	20.21
20	0.52	12.81	13.16	0.998	6.19
30	0.48	20.14	20.39	0.998	5.07
40	0.19	30.27	30.38	0.995	7.82
50	0.12	40.22	41.37	0.993	12.21
***I* (A)**					
0.25	0.02	40.02	43.12	0.999	4.95
0.50	0.03	40.1	41.83	0.998	5.95
0.75	0.07	40.19	43.79	0.995	9.44
1.00	0.12	40.32	40.22	0.993	12.21

Since, the equilibrium for initial OFLX concentration, C_0 = 10, 20 and 30 mg L^{-1} was attained in 10 min, therefore kinetics of OFLX degradation was studied within this time range. However, for higher C_0, 40 and 50 mg L^{-1}, equilibrium was achieved in 30 min, hence the time range for kinetic study for higher concentration of OFLX was 30 min (Fig. 4.6a).

Lower MPSD and high R^2 (≈0.99) values (Table 4.1) at all the C_0 and applied *I* studied indicates the adequacy of the pseudo-first-order kinetic model for degradation of OFLX by EO method using Ti/RuO_2 electrodes. Also, very closer values of $C_{Re,\ exp}$ and $C_{Re,\ cal}$ advocate the suitability of pseudo-first order kinetic model. Furthermore, the k_f values were found to decrease from 0.78 to 0.12 min^{-1} when the C_0 was increased from 10 to 50 mg L^{-1}. This signifies faster degradation rate of OFLX by EO at its lower C_0 values. At a fixed value of applied *I*, the oxidizing species (H_2O_2 and HO_2•, HOCl, ClO^- and •OH) generation rate at the anode remain the same. Hence, for lower C_0 values, these oxidants are in abundance, thus resulting in faster degradation by attacking OFLX molecules. For higher

concentration of OFLX, the ratio of amount of oxidising species to OFLX content in wastewater decreases, hence resulting in slower degradation.

However, increasing applied *I*, increases the oxidizing species (H_2O_2 and HO_2•, HOCl, ClO^- and •OH) generation rate, consequently faster degradation rate can be observed (Fig. 4.6b). The k_f values were found to increase from 0.017 to 0.12 min^{-1} when applied *I* was increased from 0.25 to 1 A (Table 4.1). This signifies faster degradation rate of OFLX by EO at higher *I*.

4.2.5. Identification of Transformation Products and Proposed Degradation Pathway

In order to study the transformation products of OFLX during EO process, 200 mg L^{-1} of antibiotic solution with 2 g L^{-1} of NaCl was subjected to EO at its natural pH and at 1 A of applied current for 60 min. This experiment was conducted using high concentration of OFLX as it enabled to detect the reaction intermediates with higher level of accuracy. Samples from the solution under reaction were withdrawn at predetermined time intervals and analysed by UPLC-Q-TOF-MS. The retention time of OFLX (molar mass [M] = 361) was 5.4 min (Fig. 4.7). The corresponding mass spectrum showed a peak with mass/charge ratio (m/z) of 362 attributable to protonated molecular ions $[M+H]^+$ (Fig. 4.8). Two other peaks with m/z of 318 and 261 correspond to OFLX fragmentation ions $[M - CO_2 + H]^+$ and $[M - CO_2 + H]^+$ – piperazinyl ring, respectively. UPLC-MS spectra of samples withdrawn after 30 min (Fig. 4.9a) and 45 min (Fig. 4.9b) of EO revealed the presence of seven major reaction intermediates or OFLX transformation products (OTP 1 – OTP 7). The retention time, elemental composition and structure of these OTPs are listed in Table 4.2.

During EO of wastewater comprising NaCl, there are different oxidative species playing their part in degradation of organics such as Cl_2, HOCl and •OH (Deborde et al., 2008; Sundarapandiyan et al., 2010; Rivera-Utrilla et al., 2013). Hence, multiple reactions occur during EO leading to mediated/indirect or direct oxidation of OFLX molecule. Based on OTPs identified, a possible degradation pathway involving attack of active chlorine and hydroxyl radicals on OFLX molecule has been proposed (Fig. 4.10). In one possible route of degradation, the addition of •OH radical to the aromatic ring of OFLX would lead to defluorination, also called the "ipso attack" (Santoke et al., 2009). As shown in Fig. 4.10, further reaction of •OH would break the piperazinyl ring of OFLX molecule leading to dealkylation and formation of two OTPs with m/z 337 (OTP 1) and 326 (OTP 2) as listed in Table 4.2. The breaking of ring was due to attack of hydroxyl radicals on nitrogen atoms

of piperazinyl moiety and formation of unstable alcohol intermediates because of oxidation of adjacent alkyl groups (Zhu et al., 2016). In another route of degradation, attack of active chlorine leads to decarboxylation of OFLX molecule, which would form a reaction intermediate with m/z 352 (OTP 4). Dealkylation and subsequent hydroxylation of OTP 4 would form OTP 5 with m/z 314. Complete dealkylation of OTP 4 would result into formation of a reaction intermediate whose reaction with hydroxyl radicals would lead to replacement of fluorine atom (ipso attack) and methyl group and thus formation of OTP 7 (m/z 269). Besides, there is also a possibility of •OH radicals attacking the entire substituted piperazinyl moiety in OTP 5, causing the formation of OTP 6 with m/z 272. OTP 3 (m/z 304) was formed after dealkylation of OTP 1 by attack of active chlorine and also the replacement of substituted piperazinyl ring by active chlorine. According to the chromatograms, the intensity and peak area of OTPs with higher m/z values of 352 (OTP 4) and 326 (OTP 2), were found to be quite lower in case of 45 min of EO than in 30 min of EO. Whereas, the peak area of OTPs with lower m/z values of 304 (OTP 3) and 272 (OTP 6) increased as the EO progressed from 30 to 45 min. This pattern is also justified by the significant TOC removal from OFLX solution by EO treatment. All the OTPs would undergo further oxidation leading to formation of aliphatic compounds, certain acids such as oxalic acid, acetic acid and formic acid, inorganic ions such as NH_4^+ and F^-. Further oxidation of aliphatic compounds and acids would yield CO_2 and H_2O. Moreover, the chlorinated OTPs would undergo reduction at Ti/RuO_2 cathode, leading to their de-chlorination.

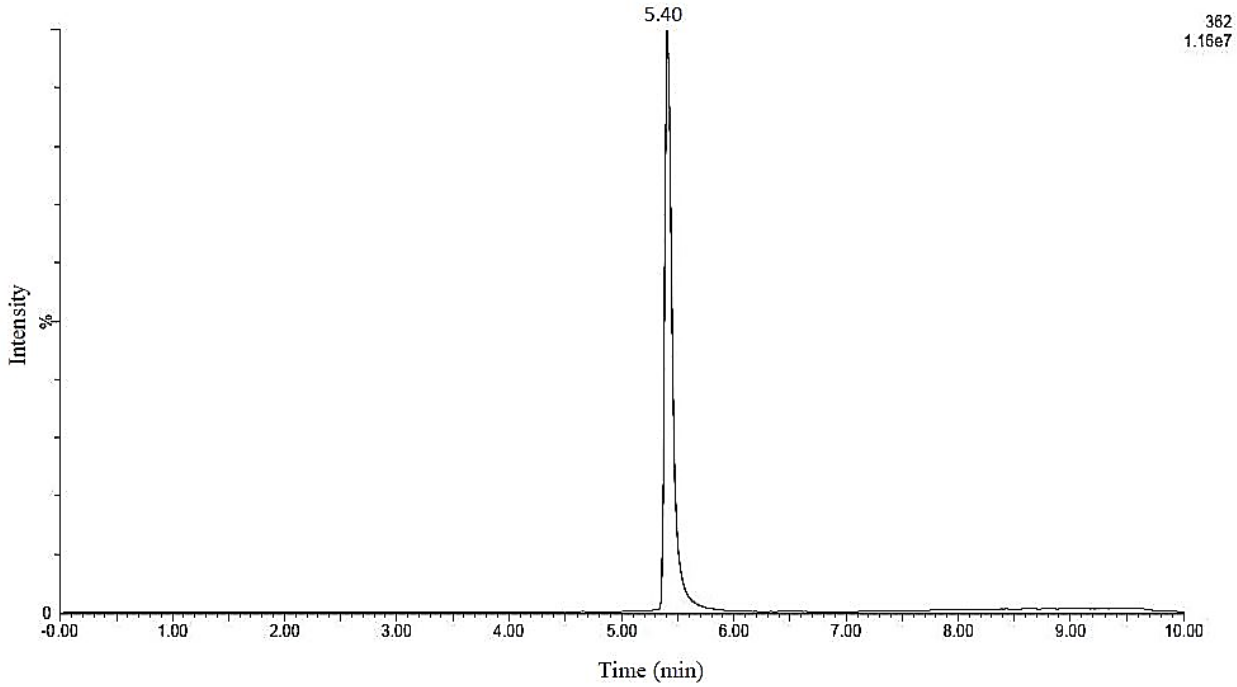

Fig. 4.7. UPLC-Q-TOF-MS chromatogram of OFLX (Retention time = 5.4 min).

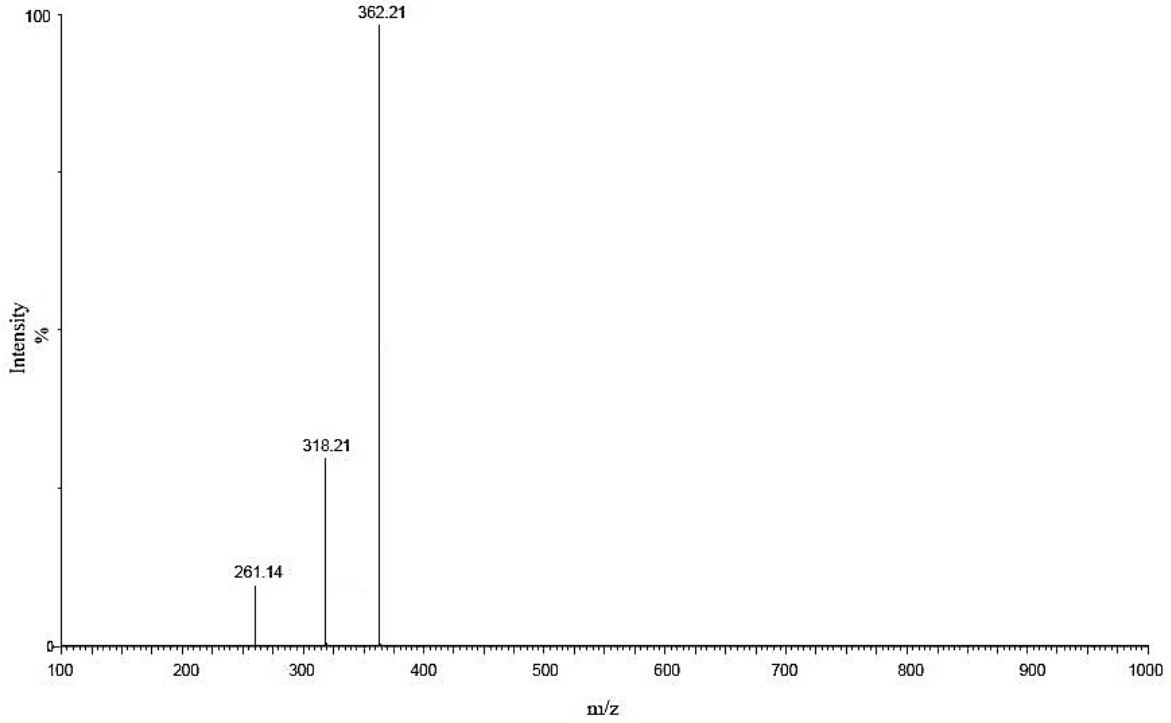

Fig. 4.8. Mass spectrum of OFLX (m/z $[M+H]^+$ = 362).

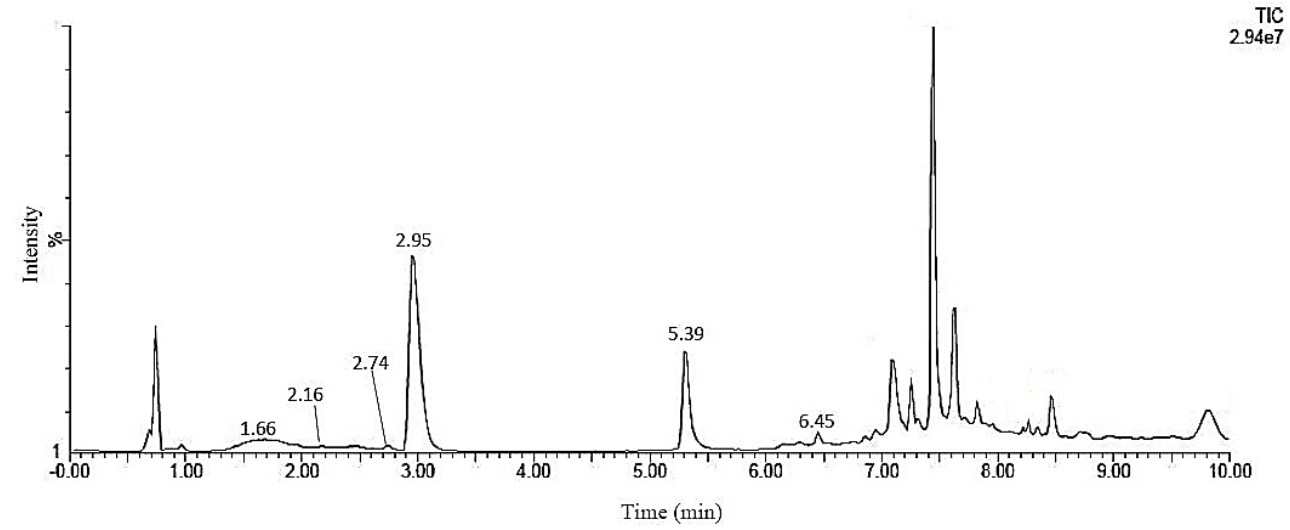

(a)

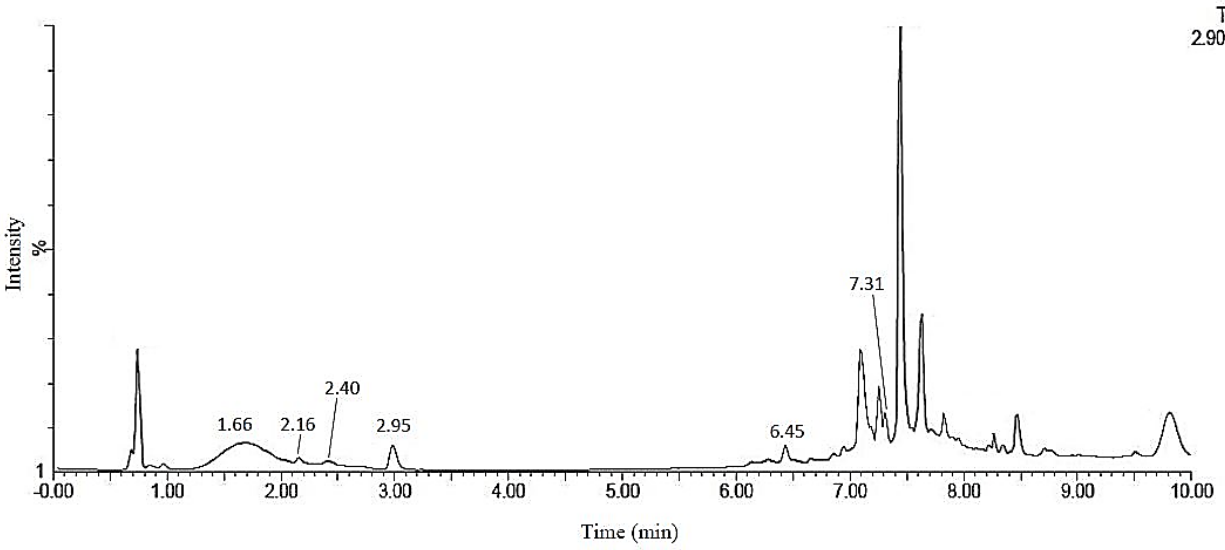

(b)

Fig. 4.9. UPLC-Q-TOF-MS chromatograms of samples taken after (a) 30 min and (b) 45 min of batch EO treatment of OFLX wastewater.

Table 4.2. Major OFLX transformation products (OTPs) formed during batch EO process.

Compound	Retention time (min)	m/z $[M+H]^+$	Elemental composition	Proposed Structure
OTP 1	2.161	337	$C_{15}H_{16}N_2O_7$	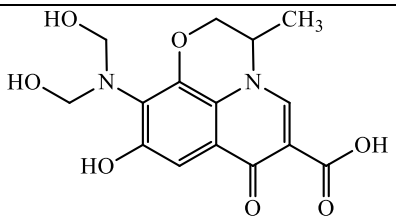
OTP 2	2.744	326	$C_{13}H_{15}N_3O_7$	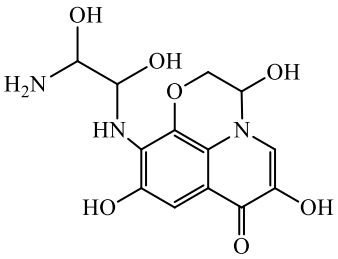
OTP 3	1.663	304	$C_{11}H_7NO_5Cl_2$	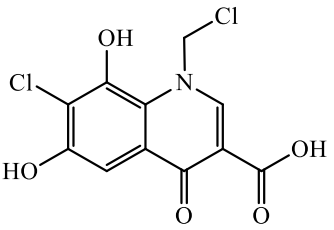
OTP 4	2.950	352	$C_{17}H_{19}N_3O_2FCl$	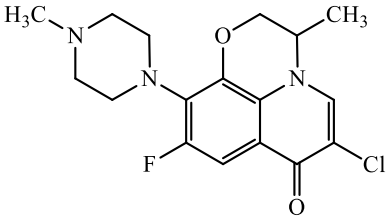
OTP **5**	2.401	314	$C_{13}H_{13}N_3O_3FCl$	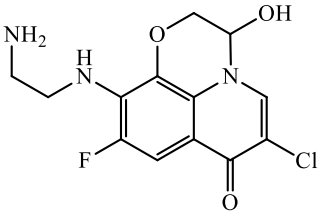
OTP 6	7.307	272	$C_{11}H_7NO_4FCl$	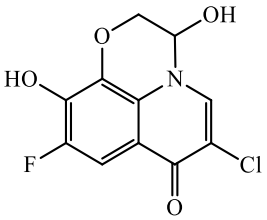
OTP 7	6.450	269	$C_{11}H_9N_2O_4Cl$	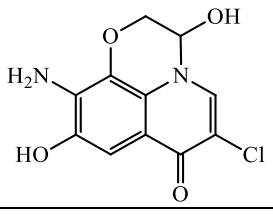

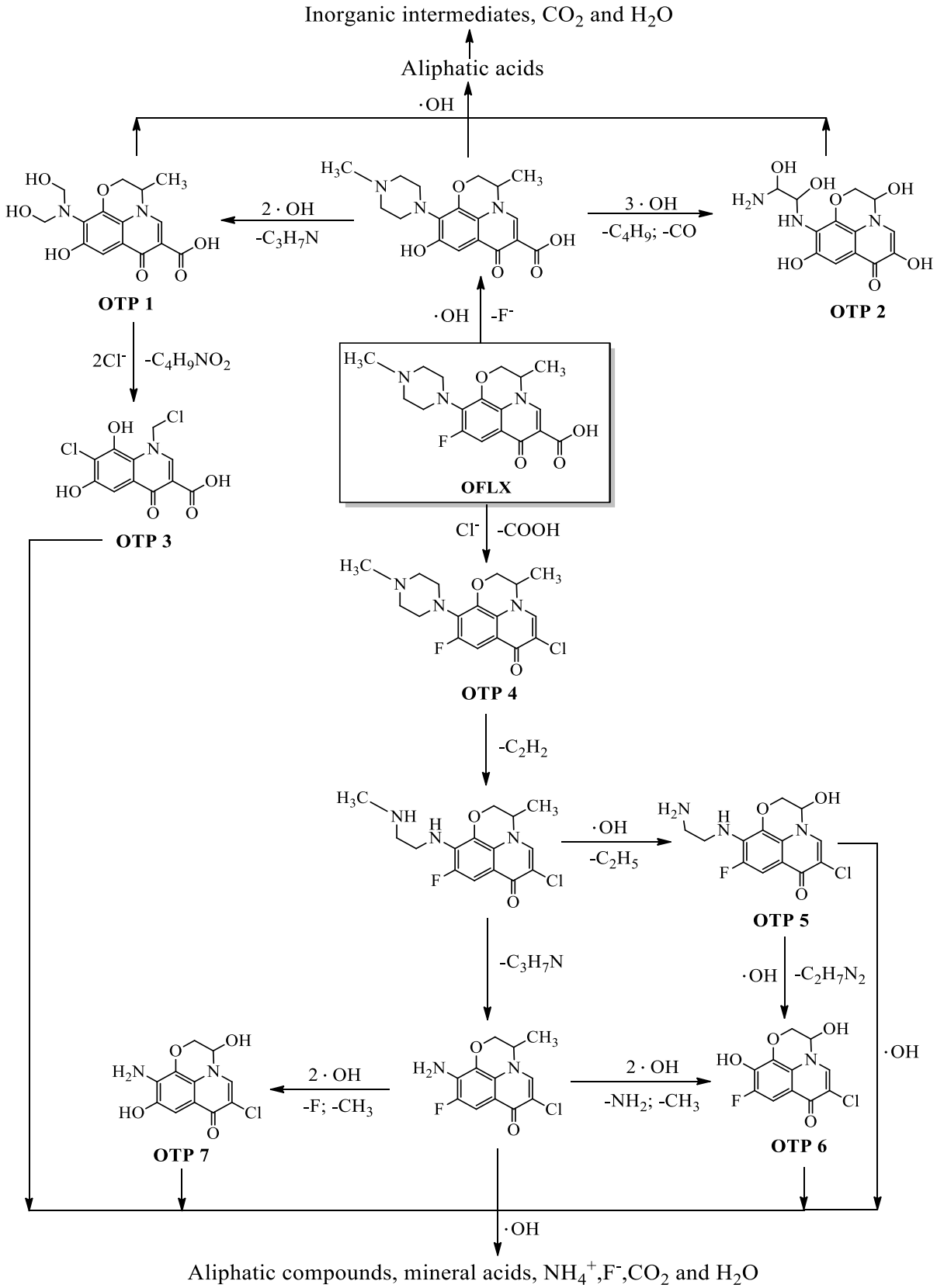

Fig. 4.10. Proposed pathway for degradation of OFLX during batch EO treatment.

4.2.6. Operating Cost Analysis

Economic feasibility of any treatment technique is essential for its applicability at high scale. For a WWTP based on EO technique, apart from the fixed cost, other operational costs include cost of electrical energy consumed, electrodes cost, pumping cost, mixing cost and wages. Amongst these, the cost of anode material and electrical energy are of much important. Therefore, in the present study, based on the electrical power consumed and cost of anode material, operating cost for EO treatment of synthetic pharmaceutical wastewater was calculated.

For removal of 1 g of TOC from wastewater at optimum conditions (I = 1 A, pH = 6.8 ± 0.1, S_0 = 2g L^{-1}), 0.542 kW h of electrical energy was consumed in 1 h. Since, price of electrical energy in Punjab, India is INR ~5.00 per kW h, therefore cost of electrical energy (C_{EE}) becomes INR 2.71 (g TOC removed)$^{-1}$.

Secondly, electrode cost for EO treatment technology needs to be calculated. Two Ti/RuO_2 (Dimensions: 10 cm × 8.5 cm; thickness: 1.5 mm) electrodes of cost INR 2,500 each, were employed as anodes for removal of OFLX from wastewater. According to manufacturer, life of electrodes at optimum condition (I = 1 A, pH = 6.8 ± 0.1) is 2.5 years. Since, ~25% TOC removal efficiency was attained at optimum conditions in 1 h of EO, therefore cost of Ti/RuO_2 electrodes (C_{EL}) is INR 32.67 (g TOC removed)$^{-1}$.

Combining the electricity and electrode cost, total operating cost (C_{EE} + C_{EL}) for removal of 1 g of TOC would to be INR 35.38 (~ US $ 0.54 (g TOC removed)$^{-1}$. In the available literature, operating cost has been reported by different authors. Fill et al. (2014) reported the operating cost of $ 17.06 (kg COD removed)$^{-1}$ for treatment of pistachio processing industry wastewater using graphite anode. For textile wastewater, Pillai and Gupta (2017) estimated the operating cost to be in the range of $10.2 – 5.83 m^{-3}. However, using Ti/RuO_2 anode, Kaur et al. (2017) reported the operating cost of $ 3.66 for treatment of 1 m^3 of textile wastewater. Thus, the calculated operating cost in the present study is comparable to those reported by other authors.

4.3. BATCH EO TREATMENT OF WASTEWATER COMPRISING AMT

4.3.1 Effect of Initial pH

Efficiency of electrooxidation process for abatement of organic pollutants is highly pH dependent. The nature of various oxidation species generated on the anode surface and in the bulk solution strongly depends on the pH of wastewater under treatment. Effect of initial pH (2 – 9) of the solution on %ARE and %TRE with time was studied at I = 1 A, S_0 = 2 g L^{-1} and C_0 = 50 mg L^{-1}, and is shown in Fig. 4.11a and b, respectively. As shown in Fig. 4.11a, %ARE increased with an increase in pH of the solution from 2 to 7. After 120 min of EO process, 33.22% of AMT was degraded at pH = 2, whereas, at pH = 7, similar removal was achieved in just 10 min of EO. Almost 60% of AMT was degraded in 45 min of EO at pH = 7. Thereafter no significant increase in %ARE was observed. AMT degradation of 40.77%, 48.89% and 52.59% was achieved in 120 min of electrolysis for pH values of 3, 4 and 5.5 (natural pH of synthetic wastewater), respectively. With further rise in pH (8 and 9), there was no improvement in removal efficiency. Similar trend was observed in case of %TRE values (Fig. 4.11b). In case of highly acidic medium (pH = 2), 11.53% of TOC was removed in 120 min of EO. However, for the similar electrolysis time and conditions, a significant enhancement in %TRE was observed when pH was raised up to neutral level 7, as 41.21% of TOC content in synthetic wastewater got degraded. For pH values of 3, 4 and 5.5, 18.07%, 27.29% and 37.53% of TRE was achieved in 120 min, respectively. TRE value of ~40% was attained for pH values of 8 and 9. Therefore, no significant change in TRE was observed when pH was raised above 7.0.

Ti/RuO_2 electrodes exhibit high electrocatalytic activity for generation of reactive chlorine species (Section 4.2.1, Eqs. 4.6 – 4.9), which actively degrade the organic pollutant through indirect/mediated oxidation. (Trasatti, 1987, Martinez-Huitle and Ferro, 2006; Panizza and Cerisola, 2009). Oxidation of AMT in acidic conditions mainly occurs through Cl_2, which has low oxidation potential, and chemisorbed hydroxyl radical according to Eq. 4.9, which are predominant in acidic conditions. Furthermore, dissolved chlorine gets reduced in acidic conditions, resulting in oxygen evolution in the solution, which resulted in low removal efficiency of EO system for AMT and TOC content (Trasatti, 1987).

$$2Cl_2 + 2H_2O \rightarrow O_2 + 4HCl \qquad \textbf{(4.21)}$$

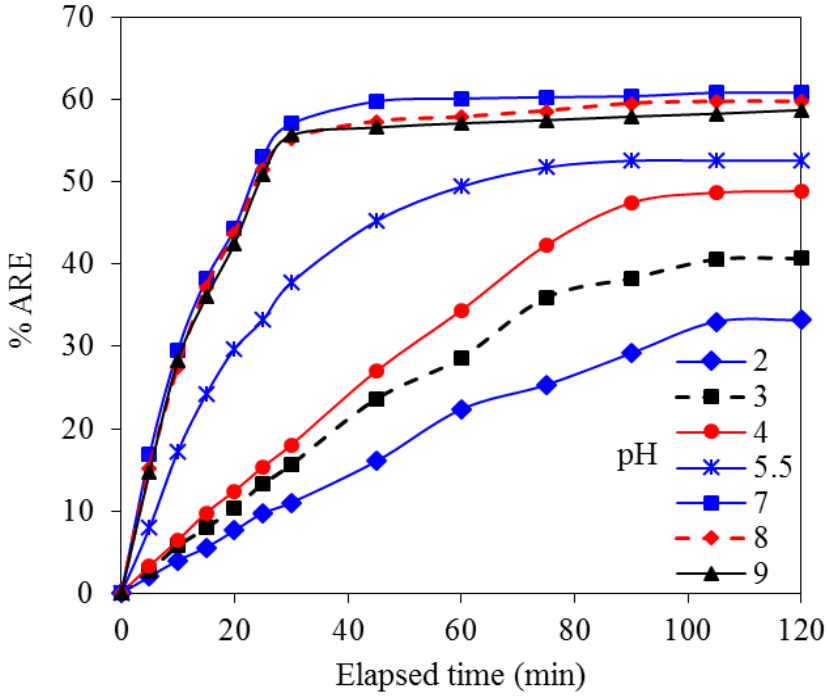

(a)

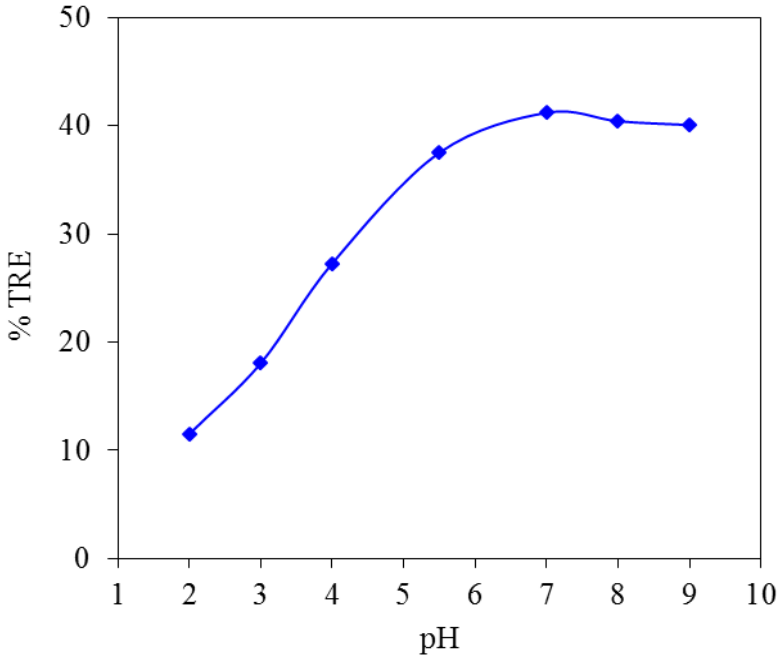

(b)

Fig. 4.11. Effect of initial pH on (a) %ARE, and (b) %TRE for EO treatment of AMT wastewater.

Chemisorbed hydroxyl radicals lead to partial conversion of AMT molecules (Eq. 4.21), hence resulting in quite low value of %TRE as compared to %ARE. After the pH is raised, hypochlorous acid becomes the major chloro-oxidant (Eq. 4.8) responsible for degradation of AMT in synthetic wastewater, whose oxidation potential is higher than that of Cl_2. Thus, a significant increase in values of %ARE and %TRE was observed with increase in pH values up to 7. Moreover, in this pH range, physisorbed active oxygen and physisorbed oxy-chloro species play their part in AMT degradation and mineralization (Eqs. 4.4, 4.10 and 4.11). The increase in amount of •OH radicals with increase in pH is also a key factor behind improved values of %ARE and %TRE (Kumar et al., 2015).

As discussed above, %ARE and %TRE increased with the increase in initial pH of the wastewater up to pH 7.0, with no significant difference for higher pH values of 8 and 9. Thus, the optimum pH value for the present study was found to be 7 and further experiments were conducted at neutral pH only.

4.3.2. Effect of applied current intensity (*I*)

The effect of applied current intensity *I* (0.25 A – 1.0 A) on EO process efficiency in terms of antibiotic removal, TOC removal, mineralization current efficiency and specific energy consumption was studied systematically, using Ti/RuO_2 electrodes at pH = 7, C_0 = 50 mg L^{-1}, S_0 = 2 g L^{-1}. Fig. 4.12a shows the effect of different values of applied *I* (A) on %ARE values with electrolysis time. Significant increase in %ARE values was observed when *I* value was increased from 0.25 A to 1.0 A. AMT removal improved from 9.77% at 30 min to 22.75% at 120 min for *I* = 0.25 A. When EO was carried on further, 26.32% of AMT content got degraded in 150 min, with no further increase up to 180 min. Similarly, for *I* = 0.5 A, equilibrium was attained in 150 min of EO with 38.44% ARE. However, for *I* values of 0.75 A and 1.0 A, equilibrium stage was achieved in 75 min and 45 min, with 53.65% and 61% AMT removal, respectively. AMT removal rate got enhanced with the increase in applied current because the amount of oxidant species (chemisorbed and physisorbed •OH, Cl_2, HOCl, ClO^-) generated at the anode surface according to Eqs. 4.2, 4.3 and 4.6 – 4.11, increased substantially when applied current intensity was increased. However, not more than ~61% of ARE was attained for 1 A of applied current for present experimental conditions. This might be because of the inevitable reaction of oxygen evolution taking place at anode surface at higher values of current intensity (Eqs. 4.15 and 4.16).

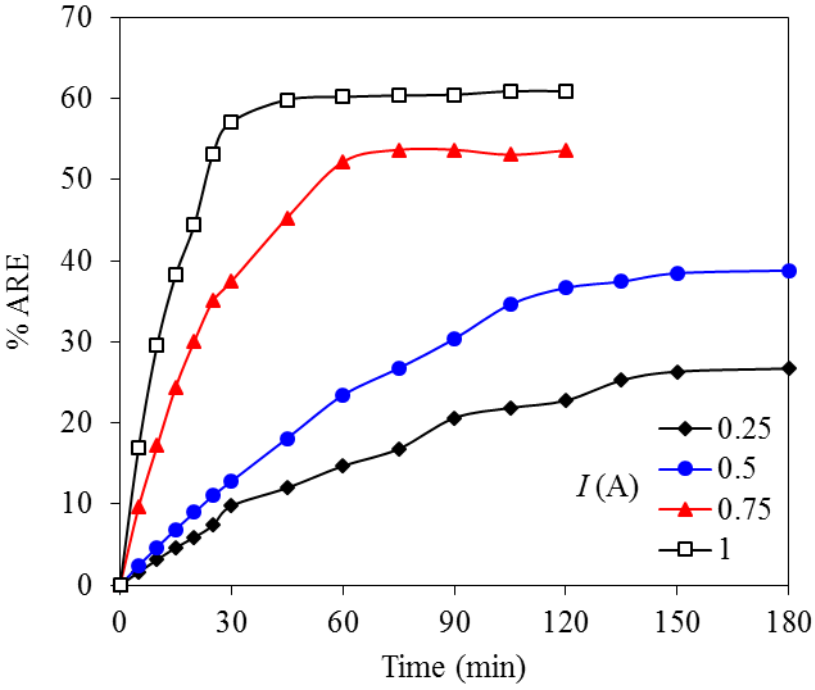

(a)

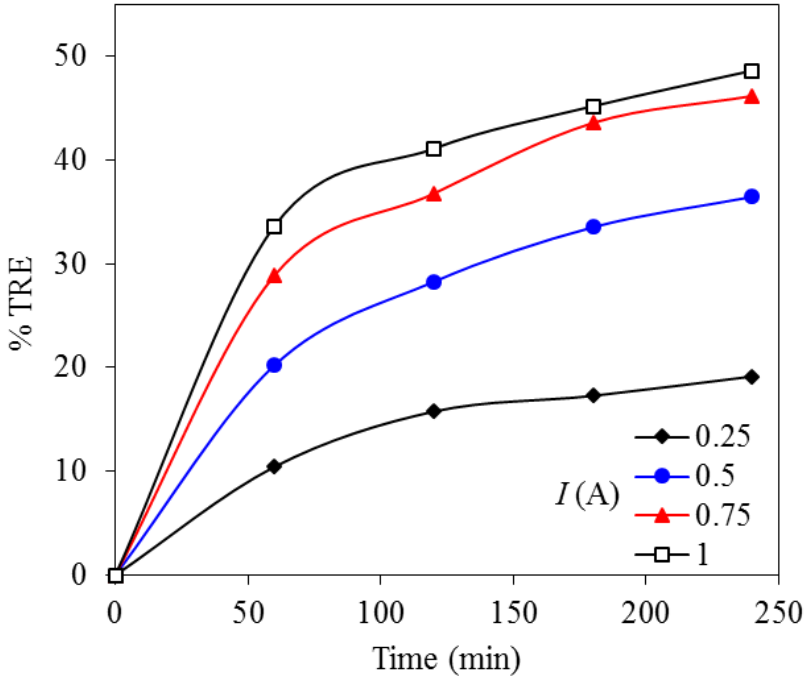

(b)

Fig. 4.12. Effect of applied current (*I*) on (a) %ARE, and (b) %TRE for EO treatment of AMT wastewater.

Efficiency of EO for TOC abatement was tested in the same range of applied current (0.25 A – 1.0 A) for prolonged electrolysis time up to 240 min (Fig. 4.12b). TRE values of 19.15%, 36.46%, 46.18% and 48.62% were achieved for current values of 0.25 A, 0.5 A, 0.75 A and 1 A, respectively in 240 min of EO. Threefold escalation in %TRE was observed, when applied current was increased from 0.25 A to 1.0 A. In neutral pH range, physisorbed active oxygen and HOCl play the key role in mineralization of organic species. The amount of these oxidants improved significantly with increase in applied current, hence resulting in substantial improvement in %TRE values.

Comparative analysis of %MCE and SEC for different values of applied *I* after 120 min of EO is shown if Fig. 4.13. For different values of applied *I*, SEC increased from 0.228 to 0.558 kW h (g TOC removed)$^{-1}$ with an increase in *I* (0.25 A to 1.0 A). However, %MCE decreased from 11.77% to 7.67% for the same values of applied *I* (A). Even though, TOC removal rate was enhanced with the increase in values of applied current, still the energy consumption of EO system increased because of elevation in average EO cell potential, *U* from 3.1 V to 5.2 V, with increase in *I* from 0.25 A to 1.0 A. As discussed above, the unescapable reaction of oxygen evolution (Eqs. 4.15 and 4.16) is enhanced at higher current intensities which competitively consumes the extra electrons. Although, at higher *I*, the rate of generation of •OH radicals is elevated, the unreacted radicals tend to form hydrogen peroxide and hydroperoxyl radical according to Eqs. 4.13 and 4.14 (Brillas and Martinez-Huitle, 2015), whose oxidation power is much less as compared to that of hydroxyl radical (Moreira et al., 2017). Aggravation of such parasitic reactions at higher current intensity causes the loss in mineralization efficiency of EO process, thus increasing the overall cost of treatment.

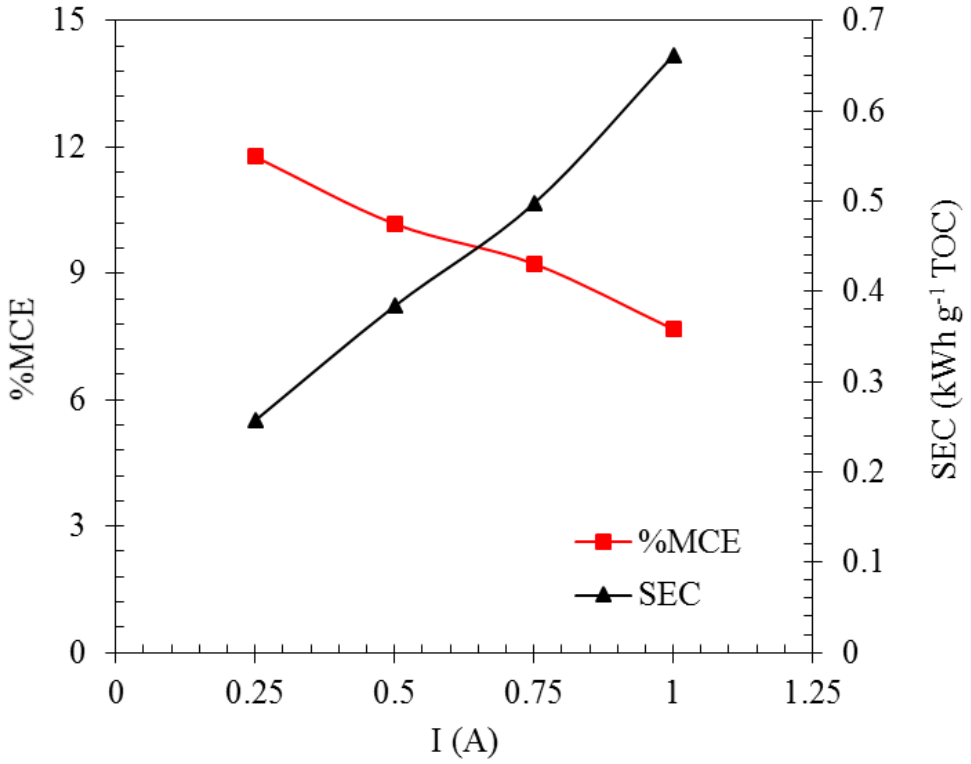

Fig. 4.13. Effect of applied current (*I*) on %MCE and SEC (kW h (g TOC removed)$^{-1}$) for EO treatment of AMT wastewater.

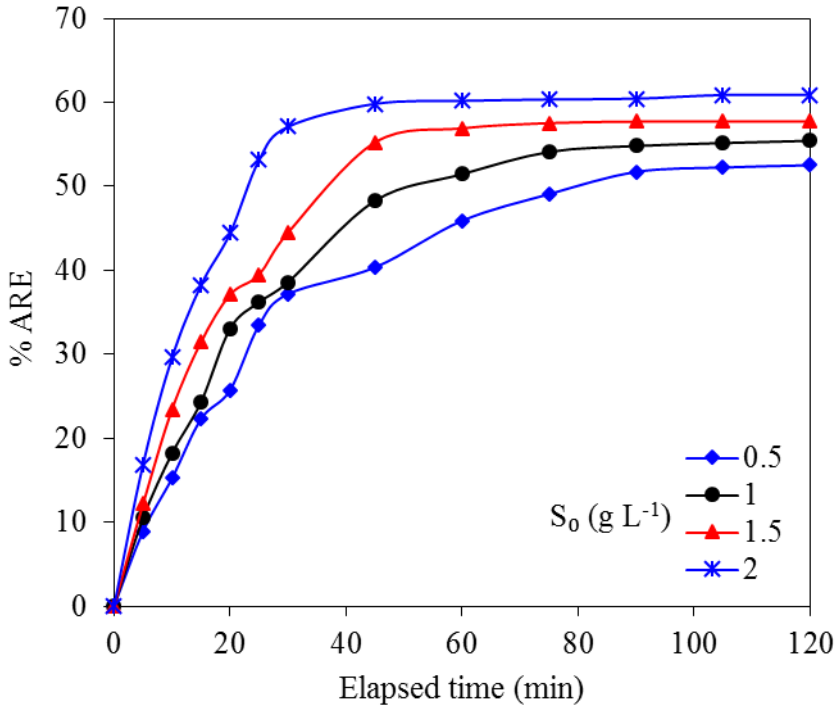

(a)

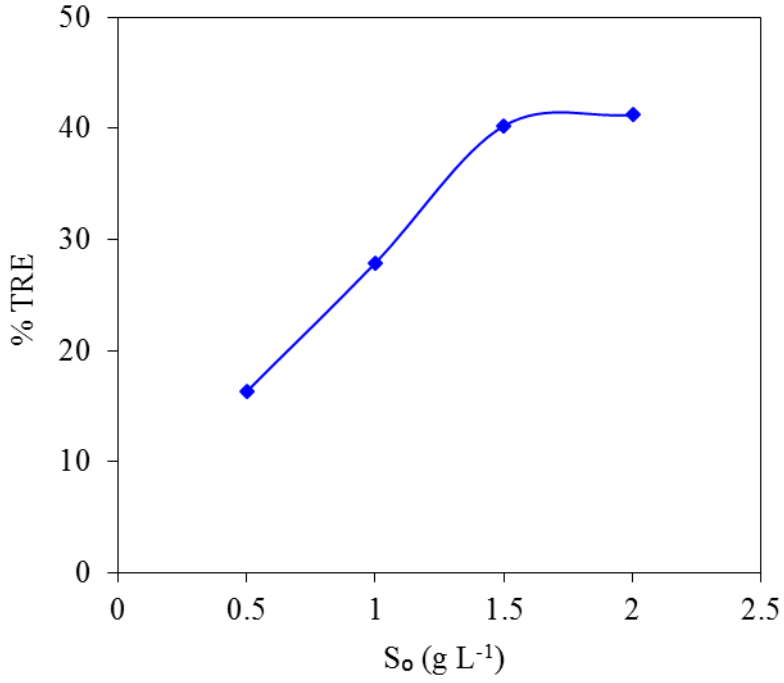

(b)

Fig. 4.14. Effect of NaCl concentration (S_0) on (a) %ARE, and (b) %TRE for EO treatment of AMT wastewater.

4.3.3. Effect of Supporting Electrolyte Concentration (S_0)

In order to study the effect of supporting electrolyte concentration on performance of EO process, a range of 0.5 to 2 g L^{-1} of NaCl concentration (S_0) in synthetic wastewater was selected. Other operating parameters were set as: I = 1 A, pH = 7, C_0 = 50 mg L^{-1}. As depicted in Fig. 4.14a and b, the increase in S_0 resulted in increase in both %ARE and %TRE values. ARE value got enhanced from 52.51% to 60.88% after 120 min of electrolysis, when S_0 was increased from 0.5 to 2 g L^{-1} (Fig. 4.14a). For the same set of S_0 values and electrolysis time, %TRE values also showed threefold improvement from 16.31% to 48.67% (Fig. 4.14b). As conferred in section 4.2.3, the mediated oxidation of AMT was carried out by the oxy-chloro species generated at the Ti/RuO_2 surface according to Eqs. 4.6 – 4.11. It was evident that the amount of these reactive chloro oxidants increased with the increase in concentration of NaCl in synthetic wastewater, thus enhancing the efficiency of EO for removal of AMT and TOC.

Correlation of S_0, %MCE and SEC is shown in Fig. 4.15. %MCE increased with exponential decay in SEC (kW h (g TOC removed)$^{-1}$), when S_0 (g L^{-1}) was increased. With increase in amount of NaCl, the conductivity of synthetic wastewater got significantly increased from 1.32 mS cm^{-1} (S_0 = 0.5 g L^{-1}) to 4.08 mS cm^{-1} (S_0 = 2 g L^{-1}), thus lowering the average cell potential (U) from 10.2 V (S_0 = 0.5 g L^{-1}) to 5.2 V (S_0 = 2 g L^{-1}), which in turn decreased the amount of energy consumed by the electrolytic system. Higher quantity of NaCl amplified the generation rate of chloro-oxidant species in wastewater, consequently increasing the TOC decay rate, and thus the mineralization efficiency of EO by Ti/RuO_2 anodes. Therefore, the overall cost of EO treatment method decreased and the %MCE increased, when the amount of NaCl in synthetic wastewater was increased from 0.5 g L^{-1} to 2 g L^{-1}.

4.3.4. Effect of Initial AMT Concentration (C_0) and Decay Kinetics

Degradation of AMT antibiotic by EO treatment technique at any instant of time (t) can be demonstrated by pseudo-first-order kinetic as Eq. 4.18. However, as there is always a fraction of AMT in treated wastewater even after attaining equilibrium. Therefore, a modified equation of pseudo-first order kinetic model (Eq. 4.19) has been used as explained in section 4.2.4. Non-linear regression using Marquardt's percent standard deviation (MPSD) error function was performed by fitting the experimental data in Eq. 4.20.

Kinetic study for degradation of AMT was performed by varying the initial concentration of AMT (C_0) in the range of 10 – 50 mg L^{-1} at I = 1 A, pH = 7.0, S_0 = 2 g L^{-1} and also by varying applied current in the range of 0.25 – 1.0 A at same experimental conditions with C_0 = 50 mg L^{-1}.

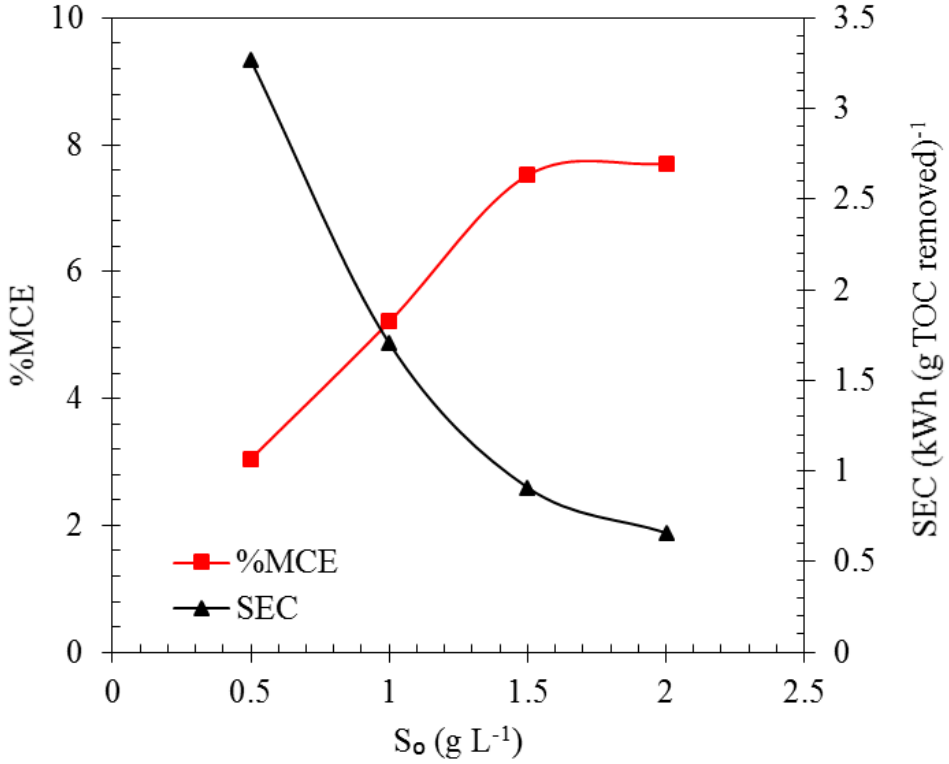

Fig. 4.15. Effect of NaCl concentration (S_0) on %MCE and SEC (kW h (g TOC removed)$^{-1}$) for EO treatment of AMT wastewater.

Table 4.3. Kinetic parameters for AMT degradation at different operating conditions.

Parameter	k_f (min^{-1})	$C_{Re, exp}$ (mg L^{-1})	$C_{Re, cal}$ (mg L^{-1})	R^2	MPSD
C_0 (mg L^{-1})					
10	0.14	3.3	3.25	0.997	3.56
20	0.12	11.23	11.23	0.994	10.53
30	0.08	16.1	16.3	0.999	4.34
40	0.07	21.1	21.02	0.992	5.04
50	0.06	30.22	30.39	0.996	6.88
***I* (A)**					
0.25	0.01	13.35	14.12	0.997	9.28
0.50	0.01	19.39	20.29	0.997	12.17
0.75	0.04	26.78	27.44	0.998	6.46
1.00	0.06	30.44	30.46	0.996	6.88

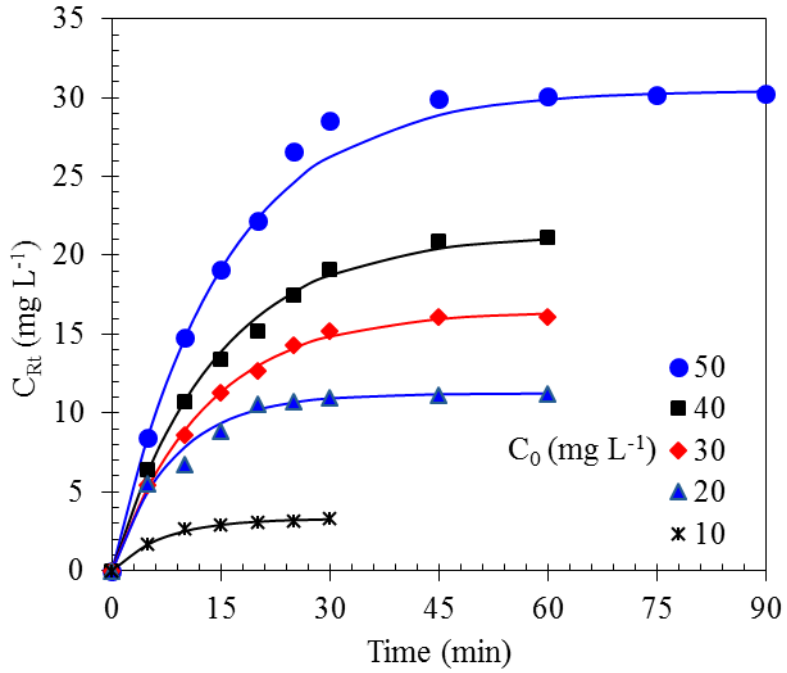

(a)

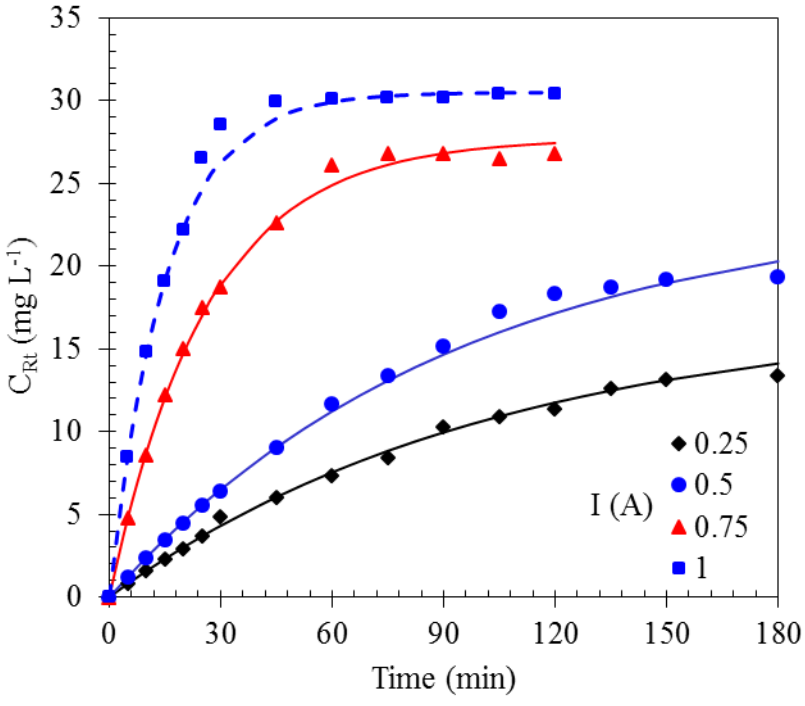

(b)

Fig. 4.16. Degradation kinetics of AMT (a) Effect of initial AMT concentration (C_0) (b) Effect of applied current (*I*).

The kinetic data fitted to pseudo-first-order kinetic model by varying C_0 and *I* are shown by solid line in Fig. 4.16a and b, respectively. The best fit values of rate constant, correlation coefficient and MPSD are shown in Table 4.3. The equilibrium condition was achieved in 30 min for C_0 = 10 mg L^{-1}, 60 min for C_0 = 20, 30 and 40 mg L^{-1}, and 90 min for C_0 = 50 mg L^{-1}. Hence, the time range for the kinetic study of AMT degradation was set accordingly as presented in Fig. 4.16a. As evident from data in Table 4.3, R^2 values (~0.99) and low MPSD values justify the aptness of pseudo-first-order kinetic model for AMT degradation by EO using Ti/RuO_2 electrodes. Furthermore, the proximity of $C_{Rt,exp}$ and $C_{Rt,cal}$ values reinforces the fitness of pseudo-first-order kinetic model for current study.

The values of k_f decreased from 0.14 to 0.06 min^{-1}, with the increase in C_0 from 10 to 50 mg L^{-1} (Table 4.3). These results suggest that the degradation rate of AMT by EO at its lower concentration levels was faster than its higher concentration levels. The nature and amount of oxidation species (•OH, HOCl, ClO^-, H_2O_2, HO_2•, etc.) generated at the anode surface and in the bulk solution remains the same when a fixed current value (*I*) is supplied to the EO system. When substrate (AMT) concentration in wastewater is low, the oxidants attacking its molecules for degradation are in plenty, thus resulting in faster removal. Conversely, the ratio of substrate concentration and oxidants decreases for higher values of AMT concentration, causing the slower degradation rate, and thus lower k_f values.

When *I* was increased from 0.25 A to 1.0 A, the value of k_f also increased from 0.01 to 0.06 min^{-1} (Table 4.3). The increase in value of applied current intensity amplifies the generation of oxidants (•OH, HOCl, ClO^-, H_2O_2, HO_2•, etc.) responsible for degradation of AMT molecules in synthetic wastewater, which is well elucidated in sections 4.2.2 and 4.3.2. This in turn leads to faster degradation of AMT, and hence, higher values of pseudo-first-order rate constant.

4.3.5. Identification of Transformation Products and Proposed Degradation Pathway

In order to derive the degradation scheme of AMT during EO process by Ti/RuO_2 electrodes, synthetic wastewater with 200 mg L^{-1} of AMT was taken in the reactor for electrolysis at neutral pH, 1 A of applied current and 2 g L^{-1} of NaCl. Samples before and after electrolysis reaction were collected for analysis by UPLC-Q-TOF-MS. The mass spectrum of initial sample before EO treatment (Fig. 4.17) shows peaks corresponding to AMT molecule and its fragmentation ions. The mass/charge ratio (m/z) of 366 corresponds

to the protonated molecule of AMT $[M + H]^+$. Additional peak at m/z value of 349 represents the fragmentation ion AF 1 $[M – NH_3 + H]^+$ of AMT molecule. The opening of β-lactam ring of AMT leads to formation of other two fragments AF 2 and AF 3, corresponding to m/z values of 208 and 160, respectively (Table 4.4). Besides, m/z value of 388 is attributable to the sodium adduct ion $[M + Na]^+$. The retention time of AMT was 0.87 min (Fig. 4.18).

The UPLC chromatogram of sample withdrawn after 15 min of EO reaction is shown in Fig. 4.19. Three major AMT degradation products (ADPs) were identified, whose retention time, elemental composition and proposed structure is shown in Table 4.4. The plausible degradation/mineralization pathway of AMT by EO using Ti/RuO_2 electrodes is depicted in Fig. 4.20.

The reactions occurring during EO process are quite complex and involve a number of oxidant species, such as •OH, HOCl and Cl_2, which degrade the organic pollutants via direct or mediated oxidation. Based on the information gathered from UPLC-Q-TOF-MS analysis of samples, a possible reaction pathway for AMT degradation was proposed. As shown in Fig. 4.20, loss of NH_3 group, and attack of active chlorine leading to decarboxylation of AMT molecule, resulted in formation of a reaction intermediate ADP 1 (m/z = 339). Subsequent hydroxylation of ADP 1 by active oxygen in the form of hydroxyl radicals, generated another degradation product, ADP 3 with m/z = 325. The replacement of entire aromatic moiety of AMT molecule by active chlorine formed ADP 2 (m/z = 269). Alternative route for formation of ADP 2 could also be via direct attack of Cl^- ions on the AMT molecule, thus leading to decarboxylation, loss of aromatic moiety and amine group. Further attack of oxidation species on degradation products would lead to formation of aliphatic acids and inorganic ions (SO_4^- and NH_4^+). Chlorinated transformation products underwent reduction at the Ti/RuO_2 cathode, thus resulting in their de-chlorination. Finally, mineralization occurred after oxidation of aliphatic acids to form CO_2 and H_2O. Mineralization efficiency of nearly 48% was achieved at optimum conditions of EO in 4 h of reaction, signifying the amount of carbon content in synthetic wastewater which got converted to CO_2 (inorganic carbon).

4.3.6. Operating Cost Analysis

At optimum conditions for EO treatment of AMT (I = 1 A, pH = 7.0, S_0 = 2 g L^{-1}), 0.404 kW h of electrical energy was consumed for removal of 1 g of TOC from wastewater in 1 h of EO. The average cost of electrical energy in Punjab, India is INR 5 per kW h. Therefore, the price of electrical energy (C_{EE}) comes out to be INR 2.02 (g of TOC removed)$^{-1}$.

Ti/RuO_2 electrodes (10 cm × 8.5 cm; thickness: 1.5 mm) used in present study were procured for INR 2,500 each. Two electrodes were employed as anodes for EO treatment of AMT. According to the manufacturer, the life of these electrodes was 2.5 years at optimum experimental conditions (I = 1 A, pH = 7.0, S_0 = 2 g L^{-1}). Using EO technique under optimum conditions, ~34% TOC was removed from wastewater comprising AMT in 1 h. The electrode cost (C_{EL}) hence comes out to be INR 26.86 (g of TOC removed)$^{-1}$. Therefore, the total cost of EO treatment (C_{EE} + C_{EL}) for removal of 1 g of TOC is INR 28.88 (~ $ 0.44).

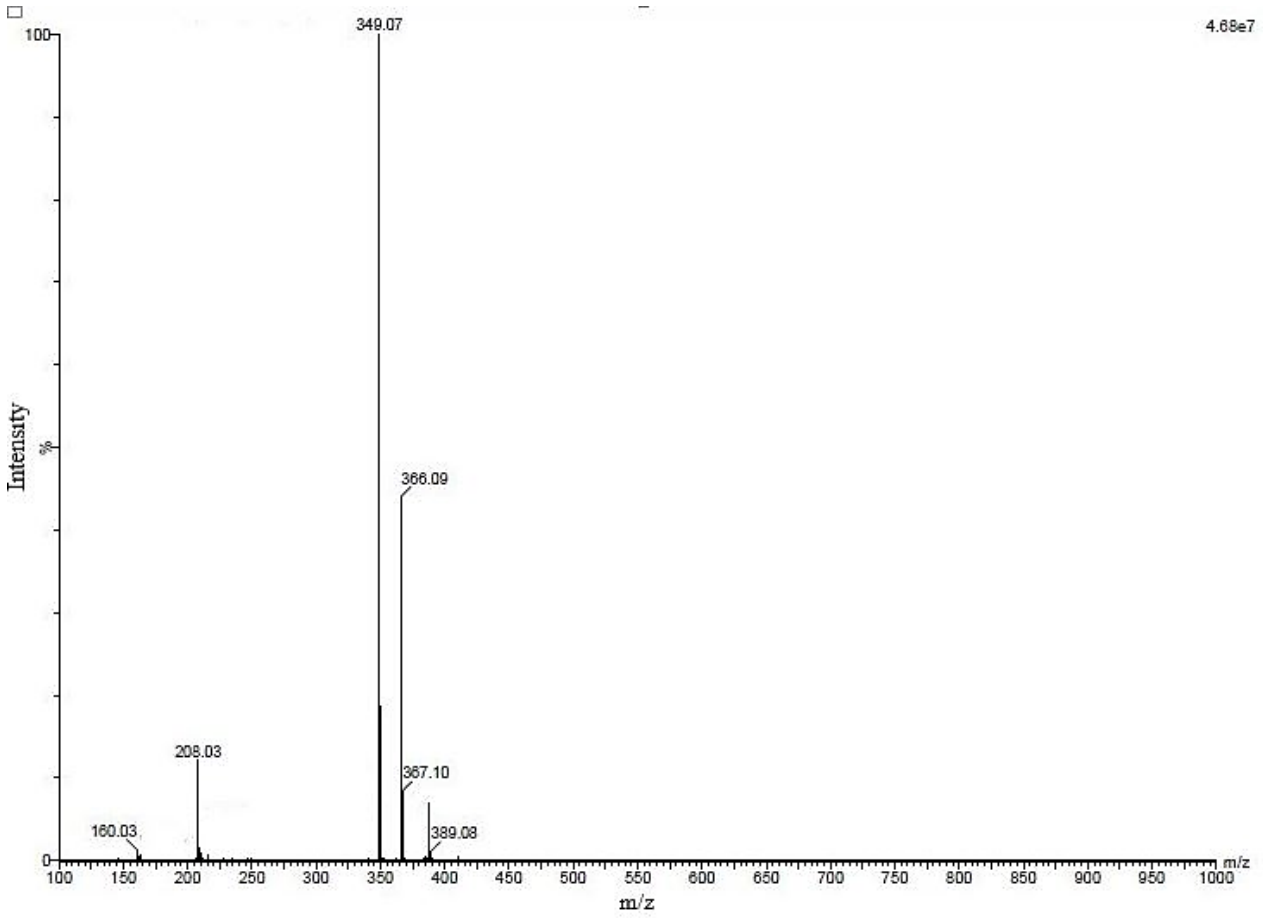

Fig. 4.17. Mass spectrum of AMT (m/z $[M+H]^+$ = 366).

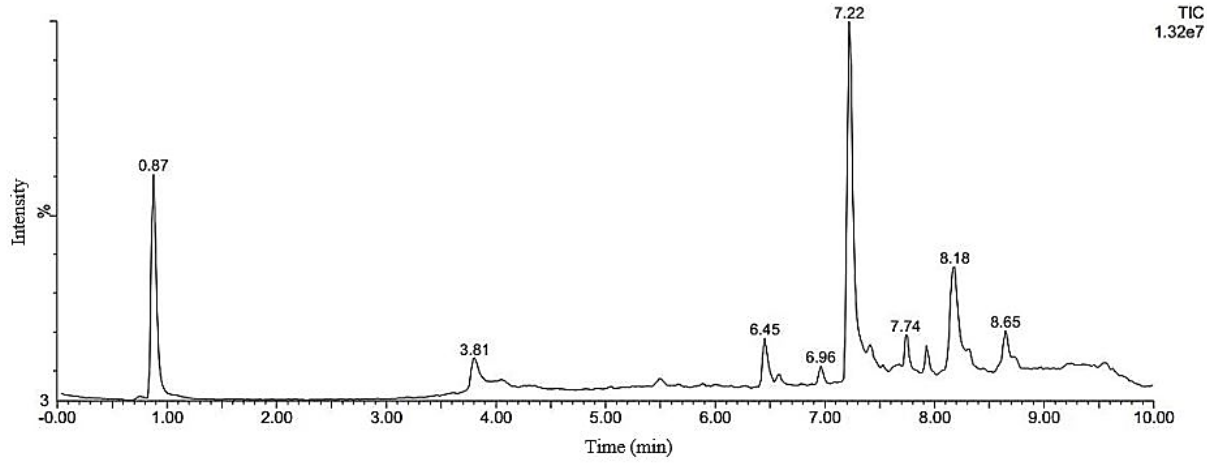

Fig. 4.18. UPLC-Q-TOF-MS chromatogram of AMT (Retention time = 0.87 min).

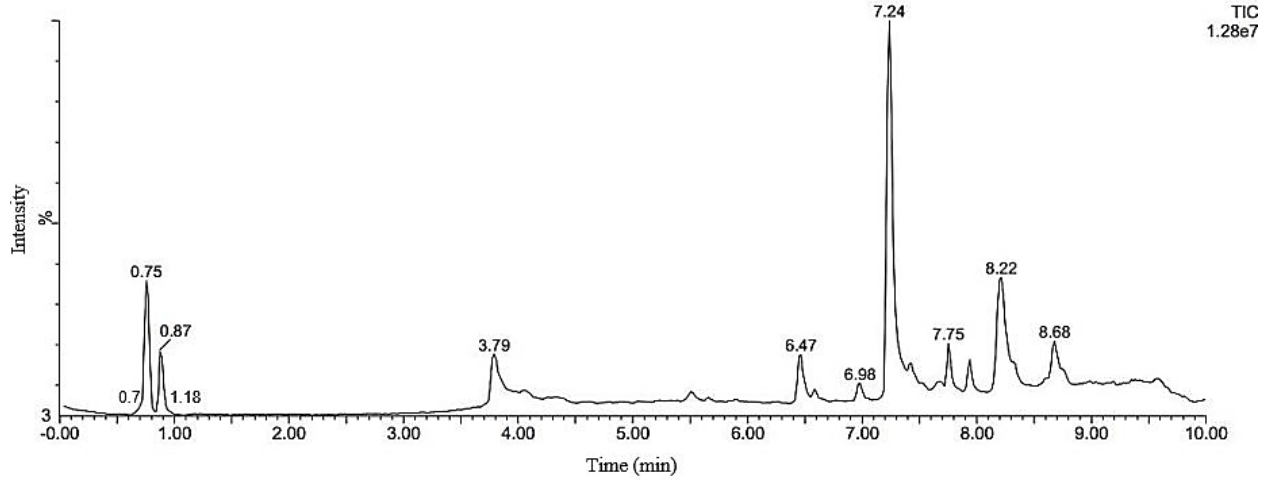

Fig. 4.19 UPLC-Q-TOF-MS chromatogram of sample taken after 15 min of EO treatment of AMT wastewater.

Table 4.4. Major AMT degradation products (ADPs) formed during batch EO process.

Compound	R_T (min)	m/z $[M+H]^+$	Elemental composition	Proposed Structure
ADP 1	0.703	339	$C_{15}H_{15}ClN_2O_3S$	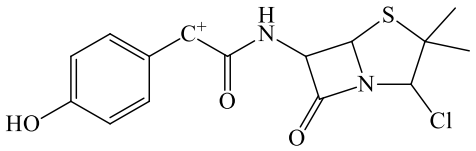
ADP 2	0.754	269	$C_8H_{10}Cl_2N_2O_2S$	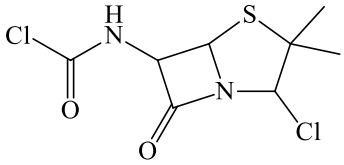
ADP 3	1.18	325	$C_{13}H_{12}N_2O_6S$	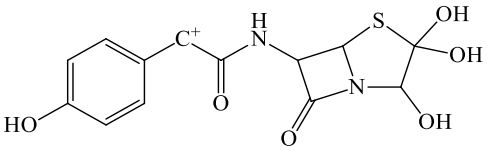
AMT	0.87	366	$C_{16}H_{19}N_3O_5S$	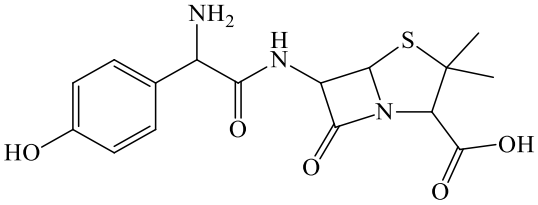
AF1	-	349	$C_{16}H_{16}N_2O_5S$	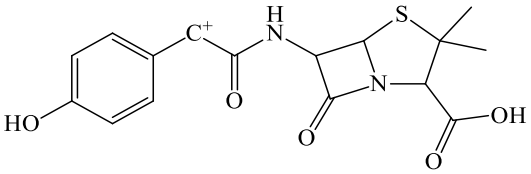
AF2	-	208	$C_{10}H_{11}N_2O_3$	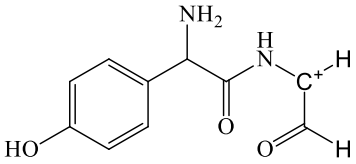
AF3	-	160	$C_6H_9NO_2S$	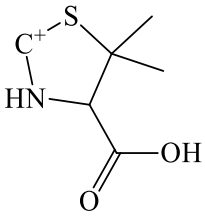

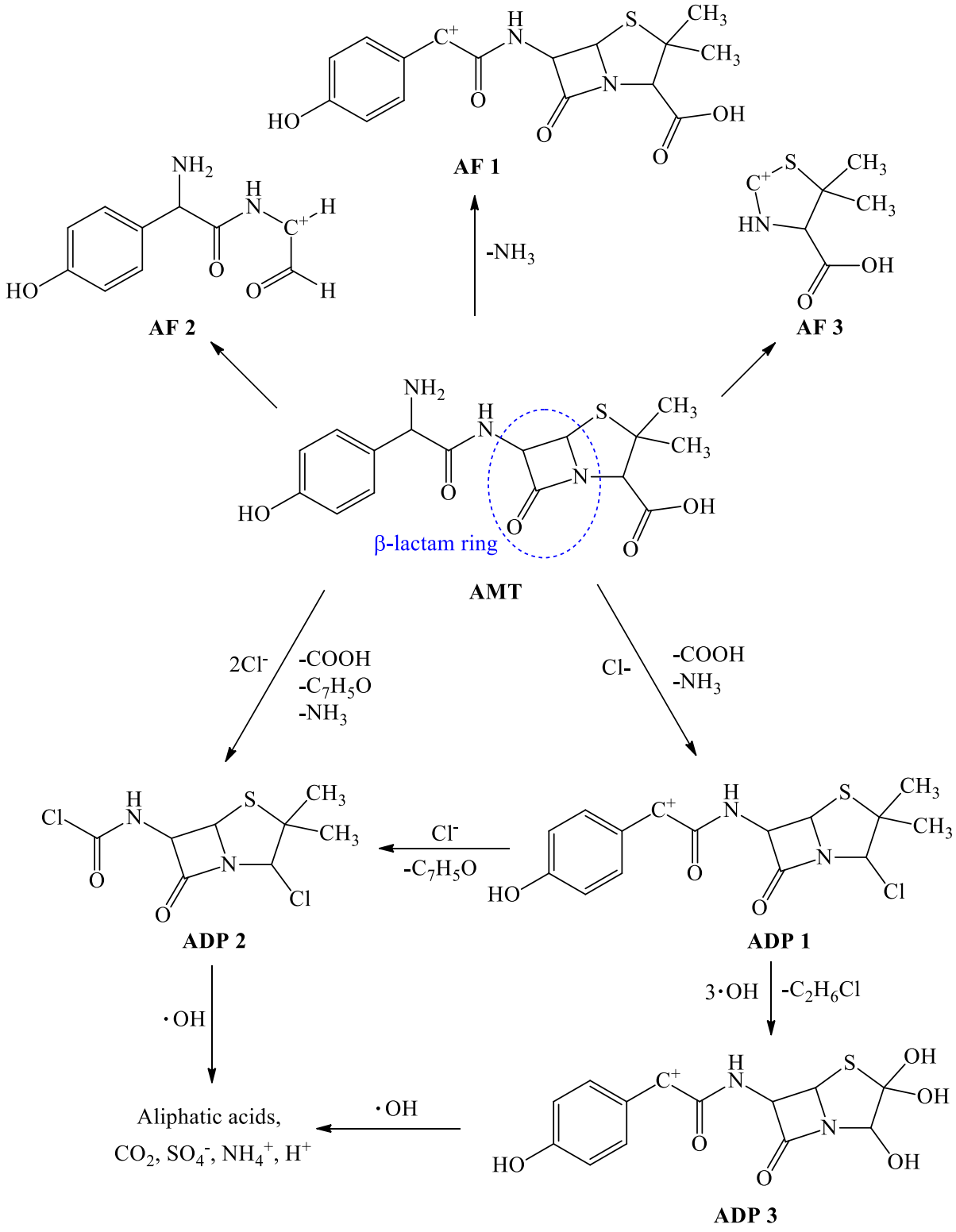

Fig 4.20. Proposed pathway for degradation of AMT during batch EO treatment.

4.4. CONTINUOUS EO TREATMENT OF WASTEWATER COMPRISING OFLX

4.4.1. Model fitting and analysis of variance (ANOVA)

Continuous EO experiments were designed using five level CCD by RSM software. The effects of four independent variables: initial pH (2 – 10); applied current, I (0.25 – 1.25 A); retention time, R_T (15 – 195 min); and elapsed time, t (20 – 180 min), on the responses TOC removal efficiency (%) (Z_1), OFLX removal efficiency (%) (Z_2) and SEC (kW h (g TOC removed)$^{-1}$) (Z_3) were investigated. Total 30 experiments were conducted for this study, with 6 replications at the center point, for which the response values are shown in Table 4.5. The Design-Expert software suggested that the quadratic model the best fitted the experimental responses values. The significance and quadratic model adequacy was justified using ANOVA (Tables 4.7a, b, c). The values of (Prob > F) for model were <0.0001 for all the responses (Z_1, Z_2 and Z_3), implying that the model are significant. Value of (Prob > F) less than 0.05 indicates that the corresponding model term is significant. Based on this confidence level, responses values Z_1, Z_2 and Z_3 were calculated in terms of significant model terms, excluding the insignificant model terms as shown in Eqs.4.22 – 4.24. Moreover, the "Lack of fit" values of the model were insignificant, which is desired, for the responses Z_1, Z_2 and Z_3.

$$Z_1 = -33.08 + (5.9 \times pH) + (44.11 \times I) + (0.047 \times R_T) + (0.15 \times t) - (0.48 \times pH^2) - (16.28 \times I^2) - (1.41 \times pH \times I) \quad \textbf{(4.22)}$$

$$Z_2 = 54.42 + (3.36 \times pH) + (35.48 \times I) - (0.03 \times R_T) + (5.43 \times 10^{-3} \times t) - (0.48 \times pH^2) - (18.87 \times I^2) \quad \textbf{(4.23)}$$

$$Z_3 = 2.06 - (0.48 \times pH) - (1.86 \times I) - (1.18 \times 10^{-3} \times R_T) + (1.72 \times 10^{-3} \times t) + (0.04 \times pH^2) + (0.79 \times I^2) - (1.89 \times 10^{-5} \times t^2) + (0.16 \times pH \times I) + (7.77 \times 10^{-3} \times I \times t) \quad \textbf{(4.24)}$$

The signal to noise ratio (adequate precision) was found to be 20.53, 25.83 and 32.34 for the responses Z_1, Z_2 and Z_3, respectively, signifying adequate signal (> 4), and thus proving the capability of the model to navigate the design space. Coefficient of determination (R^2) values for the models were determined by ANOVA as: 0.967 (Z_1), 0.971 (Z_2) and 0.987 (Z_3), which justify the model, as only 3.31%, 2.92% and 1.32% of the total variations were unexplained by the model, respectively. Furthermore, the values of predicted R^2 were in agreement with the values of adjusted R^2 (Table 4.6). The quadratic model was further validated by the plots between (1) normal % probability versus

studentized residuals (Fig. 4.21), and (2) predicted versus actual values (Fig. 4.22), for responses Z_1, Z_2 and Z_3. All the analysis verified the adequacy and accuracy of the models for the three responses.

Table 4.5. Design matrix and experimental responses of continuous EO of OFLX.

Standard order	Run	pH	*I* (A)	R_T (min)	*t* (min)	Z_1	Z_2	Z_3
29	1	6	0.75	105	100	18.48	76.24	0.699
5	2	4	0.5	150	60	11.54	74	0.398
26	3	6	0.75	105	100	17.21	73.1	0.751
16	4	8	1	150	140	19.08	71.84	1.518
3	5	4	1	60	60	14.83	74.9	0.728
19	6	6	0.25	105	100	10.33	66.48	0.306
24	7	6	0.75	105	180	26.18	79	0.889
7	8	4	1	150	60	16.77	78.56	0.644
9	9	4	0.5	60	140	16	74.9	0.670
21	10	6	0.75	15	100	16.25	74	0.796
13	11	4	0.5	150	140	17.33	76.33	0.619
11	12	4	1	60	140	20.91	77.72	1.206
10	13	8	0.5	60	140	15.18	66.85	0.742
15	14	4	1	150	140	22.16	80.16	1.138
8	15	8	1	150	60	12.45	68.07	1.034
22	16	6	0.75	195	100	20.81	78.6	0.621
4	17	8	1	60	60	10.83	64.73	1.146
30	18	6	0.75	105	100	18.19	74.3	0.711
23	19	6	0.75	105	20	6.77	72.6	0.322
14	20	8	0.5	150	140	17.58	69.56	0.641
6	21	8	0.5	150	60	9.89	65.92	0.488
25	22	6	0.75	105	100	17.98	75.42	0.719
18	23	10	0.75	105	100	8.14	56.98	1.694
20	24	6	1.25	105	100	18.65	75.54	1.541
17	25	2	0.75	105	100	13.77	78.98	0.939
1	26	4	0.5	60	60	8.58	73.08	0.536
27	27	6	0.75	105	100	18.62	76.14	0.694
12	28	8	1	60	140	18.29	68.1	1.584
2	29	8	0.5	60	60	8.04	63.79	0.601
28	30	6	0.75	105	100	19.8	75.21	0.653

Table 4.6. R^2, adjusted R^2 and predicted R^2 values for responses as suggested by CCD.

Responses	R^2	Adjusted R^2	Predicted R^2
Z_1	0.97	0.94	0.83
Z_2	0.97	0.94	0.87
Z_3	0.99	0.97	0.93

Table 4.7a. ANOVA of %TOC removal (Z_1) for continuous EO of OFLX wastewater.

Source	Sum of Squares	DF	Mean Square	F – Value	Prob > F
Model	651.01	14	46.50	31.34	< 0.0001
pH	32.76	1	32.76	22.08	0.0003
I	95.28	1	95.28	64.22	< 0.0001
R_T	22.54	1	22.54	15.19	0.0014
t	371.46	1	371.46	250.36	< 0.0001
pH^2	99.17	1	99.17	66.84	< 0.0001
I^2	28.41	1	28.41	19.15	0.0005
R_T^2	0.0016	1	0.0016	0.0011	0.9740
t^2	4.31	1	4.31	2.90	0.1089
pH × *I*	7.92	1	7.92	5.34	0.0355
pH × R_T	0.04	1	0.04	0.028	0.8686
pH × *t*	1.12	1	1.12	0.76	0.3979
I × R_T	0.54	1	0.54	0.36	0.5552
I × *t*	0.38	1	0.38	0.26	0.6182
R_T × *t*	0.42	1	0.42	0.28	0.6014
Residual	22.25	15	1.48		
Lack of Fit	18.61	10	1.86	2.549	0.1567
Pure Error	3.64	5	0.73		
Cor Total	673.27	29			

Table 4.7b. ANOVA of %OFLX removal (Z_2) for continuous EO of OFLX wastewater.

Source	Sum of Squares	DF	Mean Square	F – Value	Prob > F
Model	841.21	14	60.08	35.67	< 0.0001
pH	549.03	1	549.03	326.01	< 0.0001
I	59.44	1	59.44	35.29	< 0.0001
R_T	36.43	1	36.43	21.63	0.0003
t	51.65	1	51.65	30.67	< 0.0001
pH^2	102.93	1	102.93	61.12	< 0.0001
I^2	38.17	1	38.17	22.66	0.0003
R_T^2	0.56	1	0.56	0.33	0.5729
t^2	0.008	1	0.008	0.001	0.9436
pH × I	2.56	1	2.56	1.52	0.2359
pH × R_T	0.75	1	0.75	0.45	0.5140
pH × t	1.73	1	1.73	1.031	0.3261
I × R_T	2.24	1	2.24	1.33	0.2666
I × t	0.03	1	0.03	0.018	0.8930
R_T × t	0.004	1	0.004	0.0027	0.9592
Residual	25.26	15	1.68		
Lack of Fit	18.13	10	1.81	1.27	0.4177
Pure Error	7.13	5	1.42		
Cor Total	866.47	29			

Table 4.7c. ANOVA of SEC (Z_3) for continuous EO of OFLX wastewater.

Source	Sum of Squares	DF	Mean Square	F – Value	Prob > F
Model	3.91	14	0.28	80.17	< 0.0001
pH	0.46	1	0.46	132.14	< 0.0001
I	1.91	1	1.91	548.45	< 0.0001
R_T	0.048	1	0.048	13.98	0.0020
t	0.56	1	0.56	161.54	< 0.0001
pH^2	0.59	1	0.59	171.32	< 0.0001
I^2	0.06	1	0.06	19.05	0.0006
R_T^2	0.0005	1	0.0005	0.16	0.6948
t^2	0.025	1	0.025	7.21	0.0170
pH × I	0.11	1	0.11	31.17	< 0.0001
pH × R_T	0.00015	1	0.00015	0.045	0.8344
pH × t	0.00075	1	0.00075	0.21	0.6481
I × R_T	0.0003	1	0.0003	0.094	0.7633
I × t	0.096	1	0.096	27.69	< 0.0001
R_T × t	0.001	1	0.001	0.45	0.5085
Residual	0.0522	15	0.0034		
Lack of Fit	0.047	10	0.0047	4.51	0.0552
Pure Error	0.005	5	0.00104		
Cor Total	3.96	29			

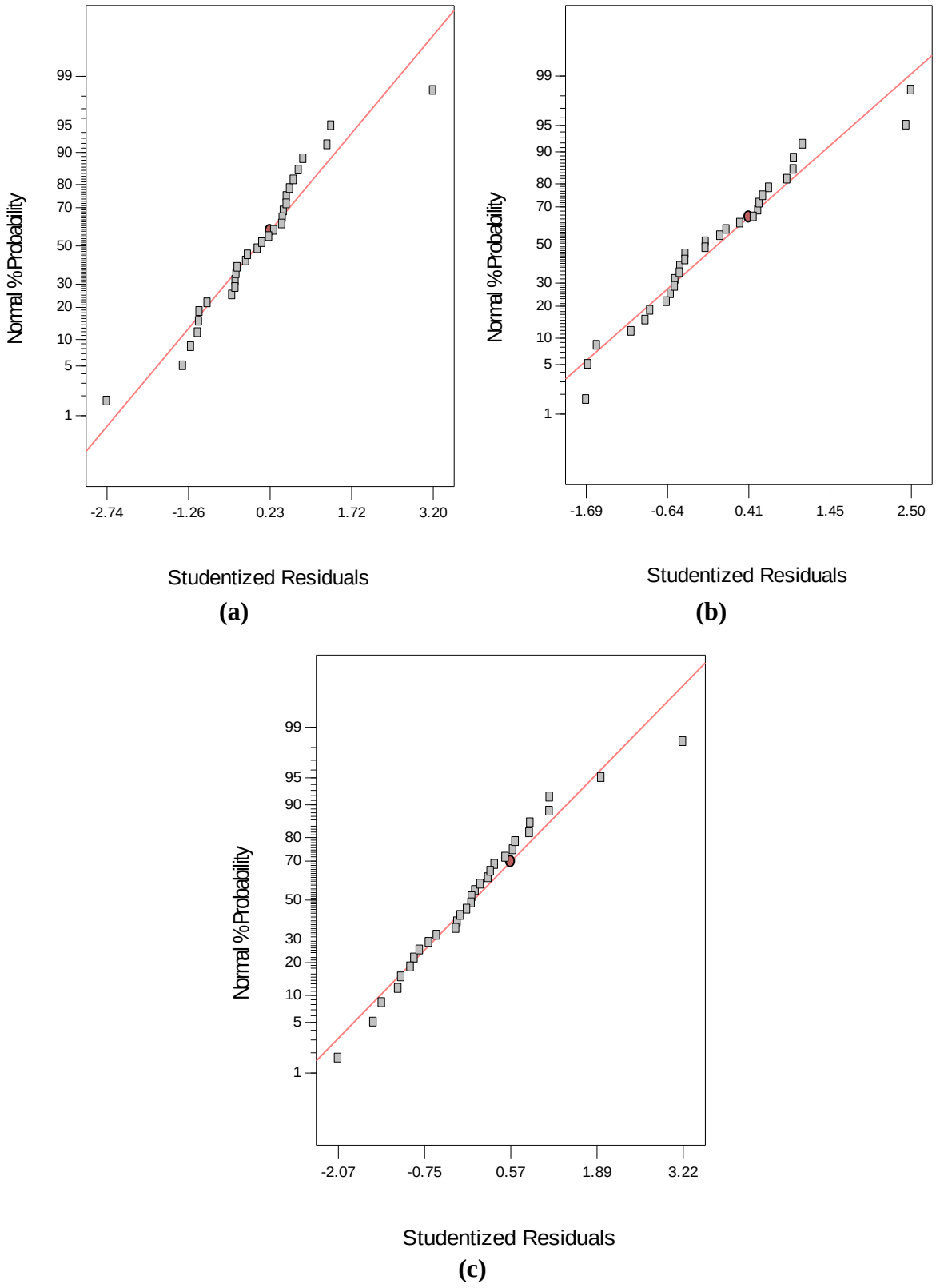

Fig. 4.21. Normal % probability versus studentized residuals plots for (a) %TOC removal (Z_1), (b) %OFLX removal (Z_2) and (c) SEC (kW h (g TOC removed)$^{-1}$) (Z_3).

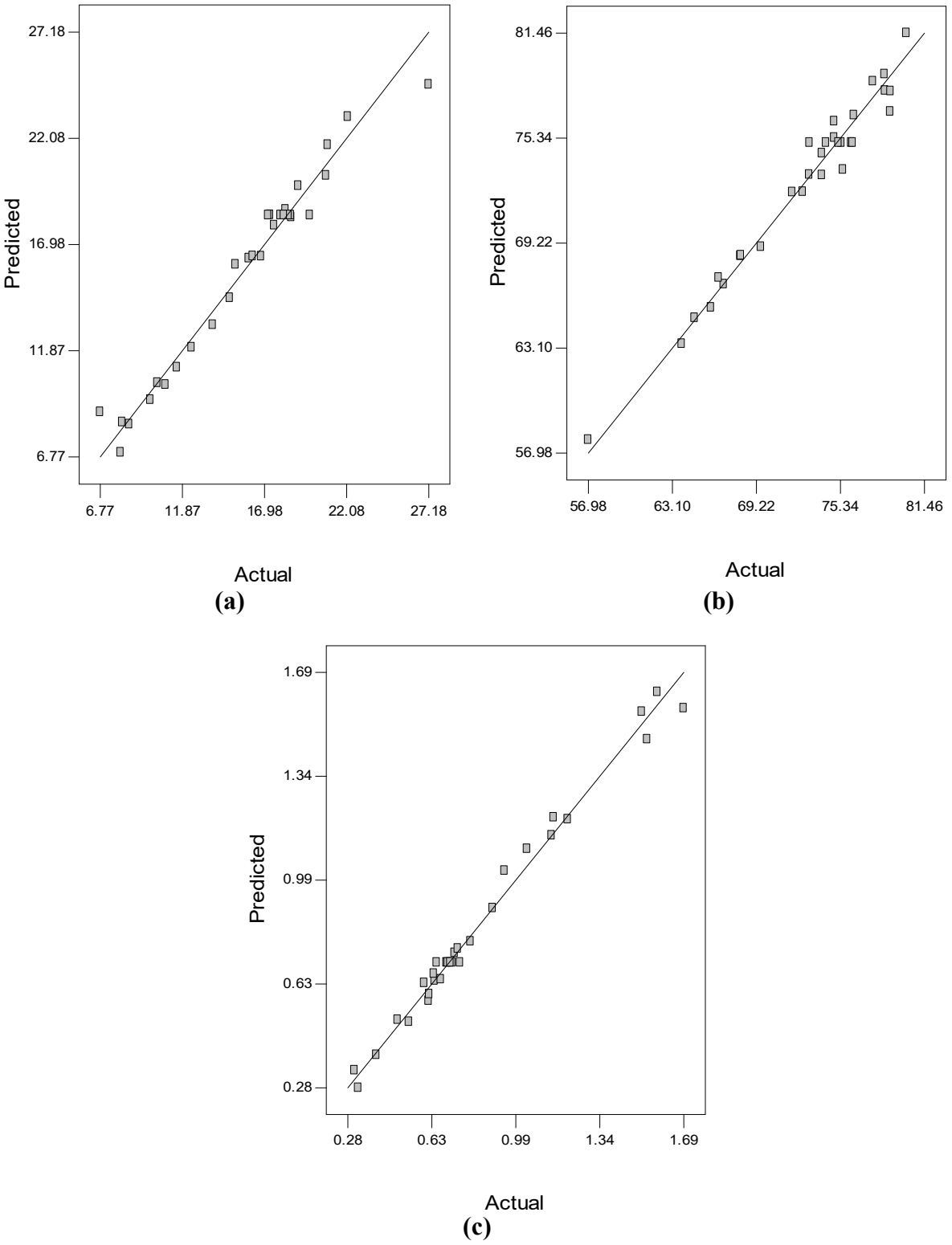

Fig. 4.22. Predicted versus actual plots for (a) %TOC removal (Z_1), (b) %OFLX removal (Z_2) and (c) SEC (kW h (g TOC removed)$^{-1}$) (Z_3).

4.4.2. Effect of Operating Parameters and Optimization

The individual and interactive effects of operating parameters (independent variables: pH, *I* (A), R_T (min) and *t* (min)) on %TOC removal (Z_1), %OFLX removal (Z_2) and SEC (kW h (g TOC removed)$^{-1}$) (Z_3) were analysed with the help of 3-D response surface plots as illustrated in Figs. 4.23 – 4.25. As found through ANOVA (Table 4.7a – 4.7c), the operating parameters were statistically significant because the P (Prob > F) value was less than 0.05 for each one of them. Fig. 4.23 represents the effects of parameters on Z_1. As shown in Fig. 4.23a, TOC removal efficiency increased when the pH was increased from 2 to 7. Maximum Z_1 was attained in the neutral pH zone. Further increase in pH led to negative effect on Z_1, which was true for entire range of *I* as well as *t* (Fig. 4.23d). A sharp increase in Z_1 was observed when applied current *I* was increased from 0.25 A to ≈1 A. Marginal decrease in Z_1 was observed when *I* was further increased up to 1.25 A. Fig. 4.23b shows the interactive effect of applied current and elapsed time on Z_1. Linear increase in Z_1 was observed when the reaction time (*t*) was increased from 20 to 180 min for all values of *I*. One important aspect of continuous treatment system is the interaction between R_T and *t*. Z_1 increased with the increase in R_T and *t* (Fig. 4.23c). However the effect of *t* was found to be more prominent than that of R_T on TOC removal efficiency. The interactive effect of R_T with pH and *I* is shown in Figs. 4.23 d and f, respectively. Z_1 always increased with increase in R_T for all values of pH and *I*.

The effects of operating parameters on OFLX removal efficiency are shown in Fig. 4.24. Z_2 value was observed to be similar in the range of pH from 2 to ≈4, and was found to decrease with further rise in pH for entire range of *I* under study. Sharp decrease in Z_2 was observed for pH above 8 (Fig. 4.24a). A substantial enhancement in Z_2 value was seen when *I* was increased from 0.25 A to ≈ 1 A. For *I* values higher than 1 A, slight decrement in Z_2 was observed. Z_2 increased with increase in both *t* and R_T (Fig. 4.24c). Nonetheless, the effect of elapsed time was much protruding in case of Z_1 than Z_2, as can be seen in Fig 4.24c. The steady state for OFLX removal was attained in ≈1 h of elapsed time. However, the TOC removal required quite longer period of time to attain the equilibrium state. Therefore, OFLX removal by continuous EO is much rapid than TOC removal from the wastewater. The interactive effect of pH and R_T (Fig. 4.23d) and pH and *t* (Fig. 4.23e) followed similar trend, showing maximum Z_2 at acidic pH and continuous increase in Z_2 with increasing R_T

and *t* values. The effect of R_T became stronger towards higher values of *I*, with maximum Z_2 value at ≈1 A (Fig. 4.23f).

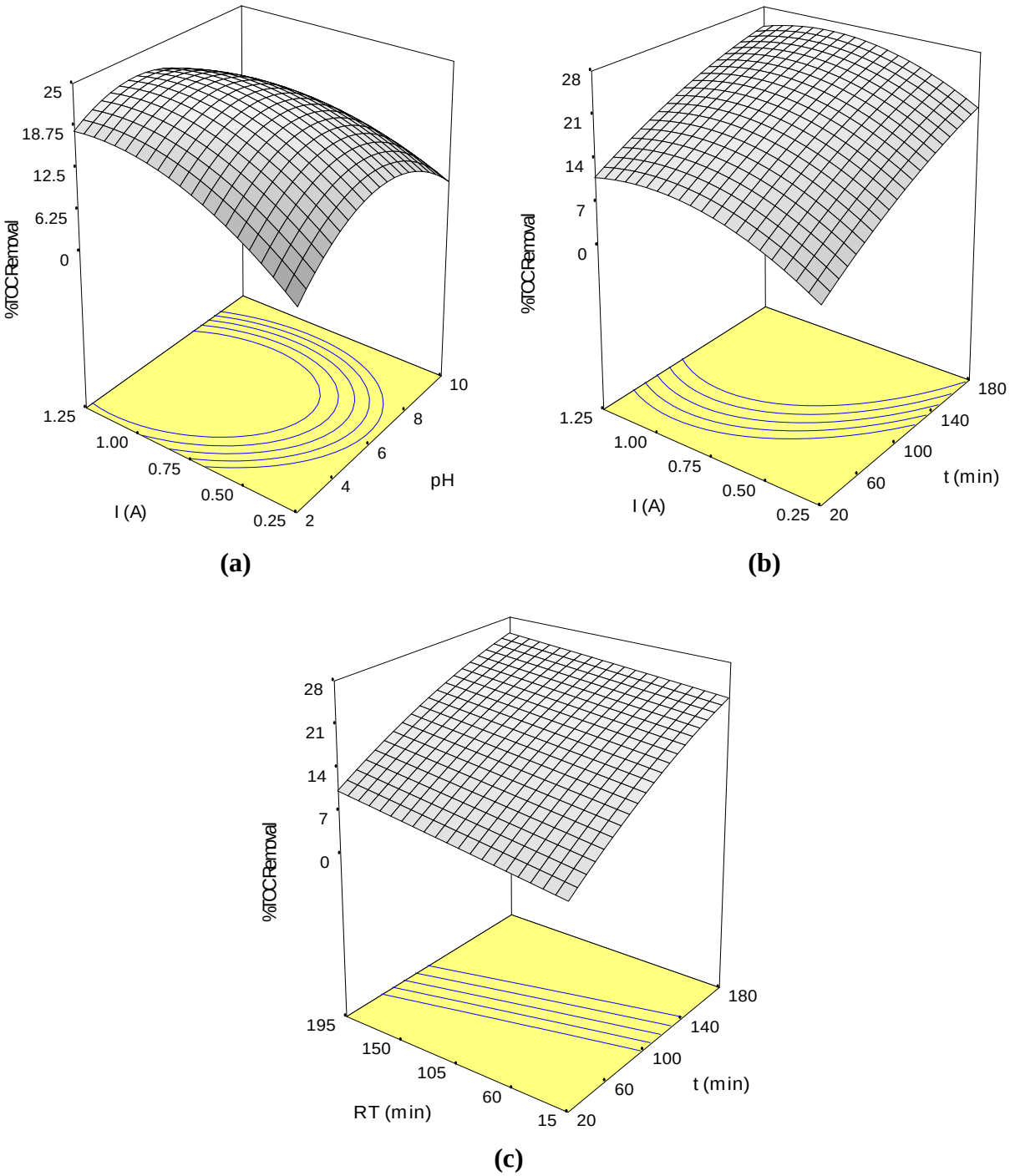

Fig. 4.23(a – c). 3D response surface graphs for %TOC removal as function of independent variables pH, *I*, R_T and *t*.

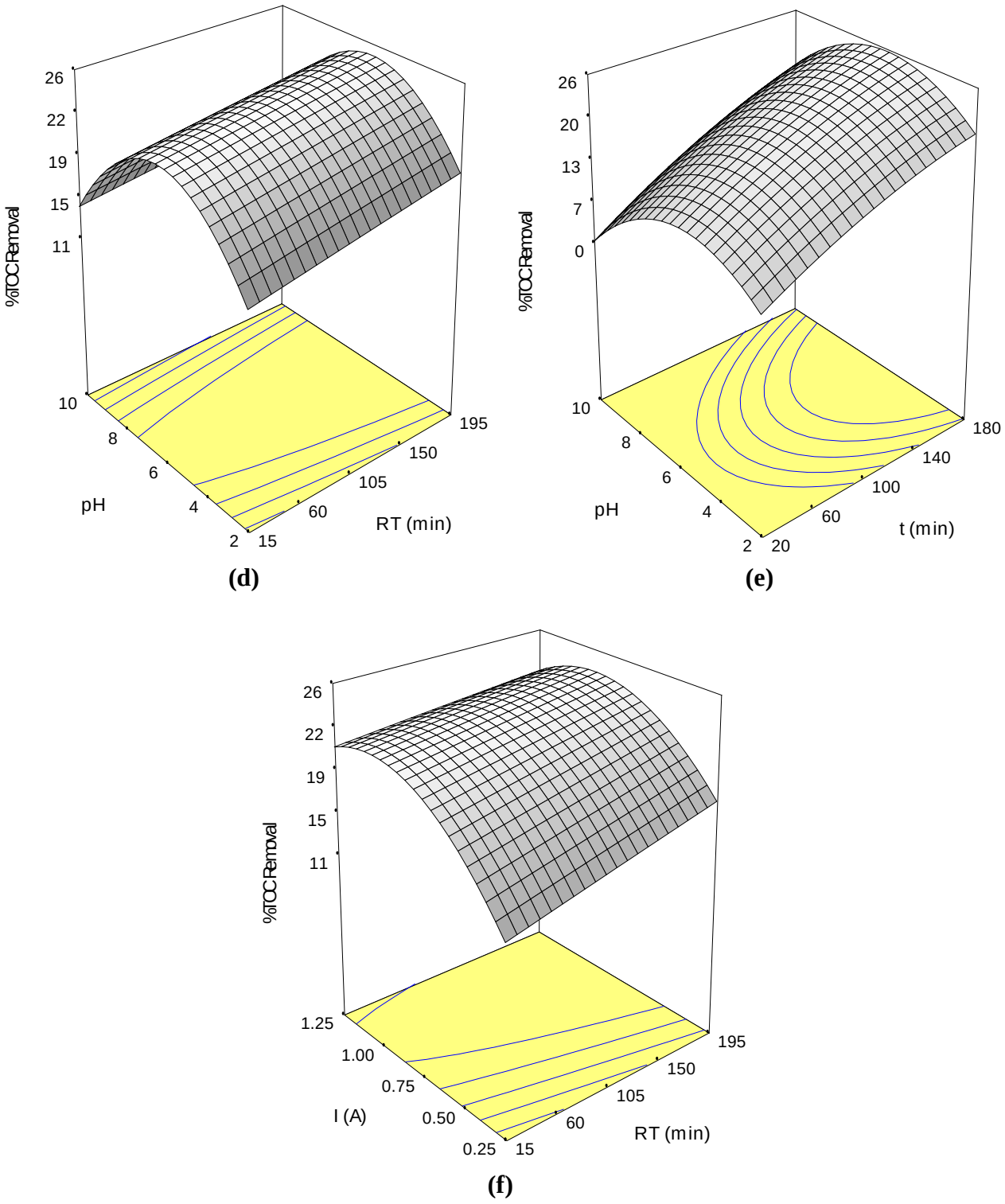

Fig. 4.23 (d – f). 3D response surface graphs for %TOC removal (Z_1) as function of independent variables pH, *I*, R_T and *t*.

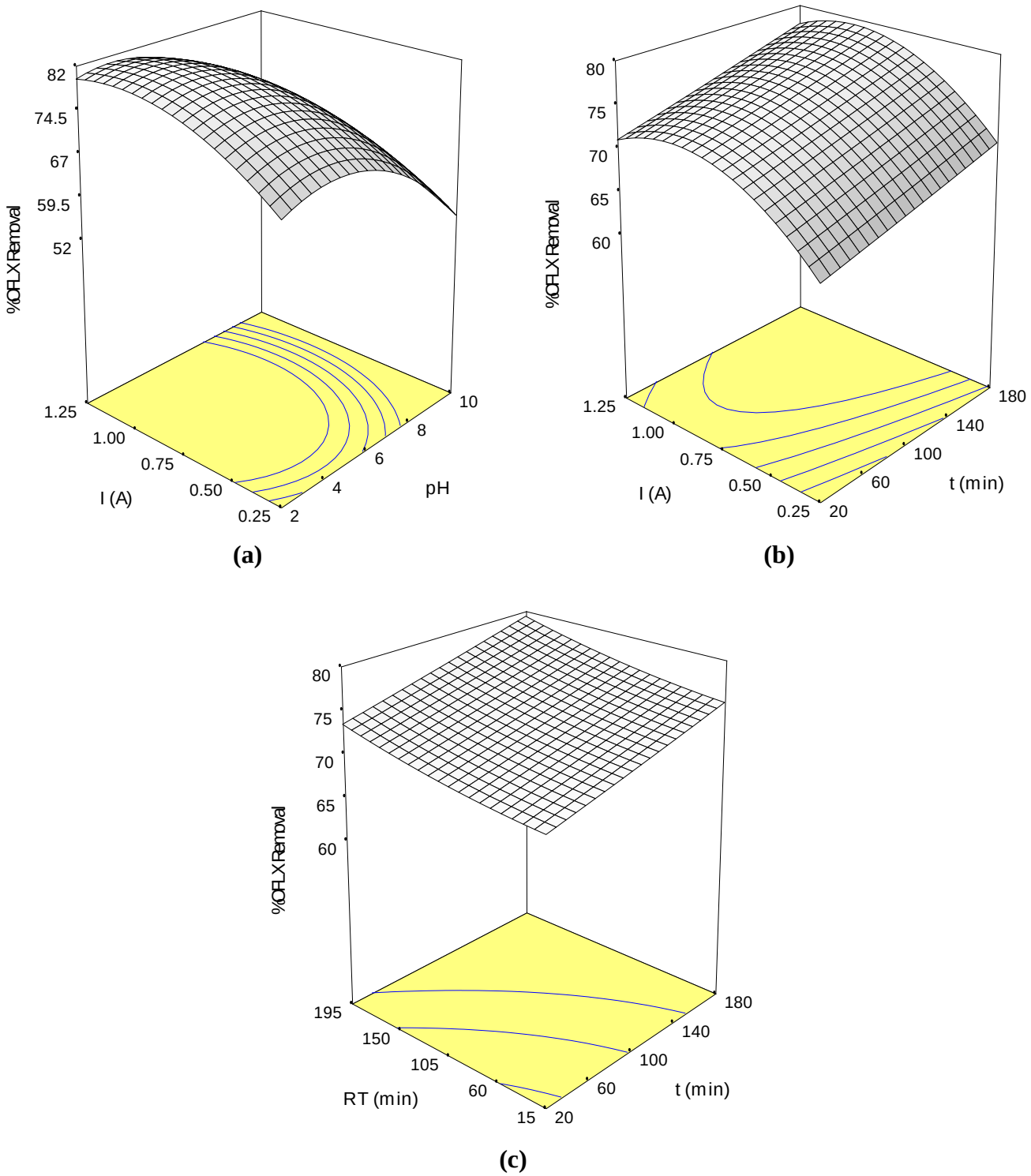

Fig. 4.24 (a – c). 3D response surface graphs for %OFLX removal (Z_2) as function of independent variables pH, *I*, R_T and *t*.

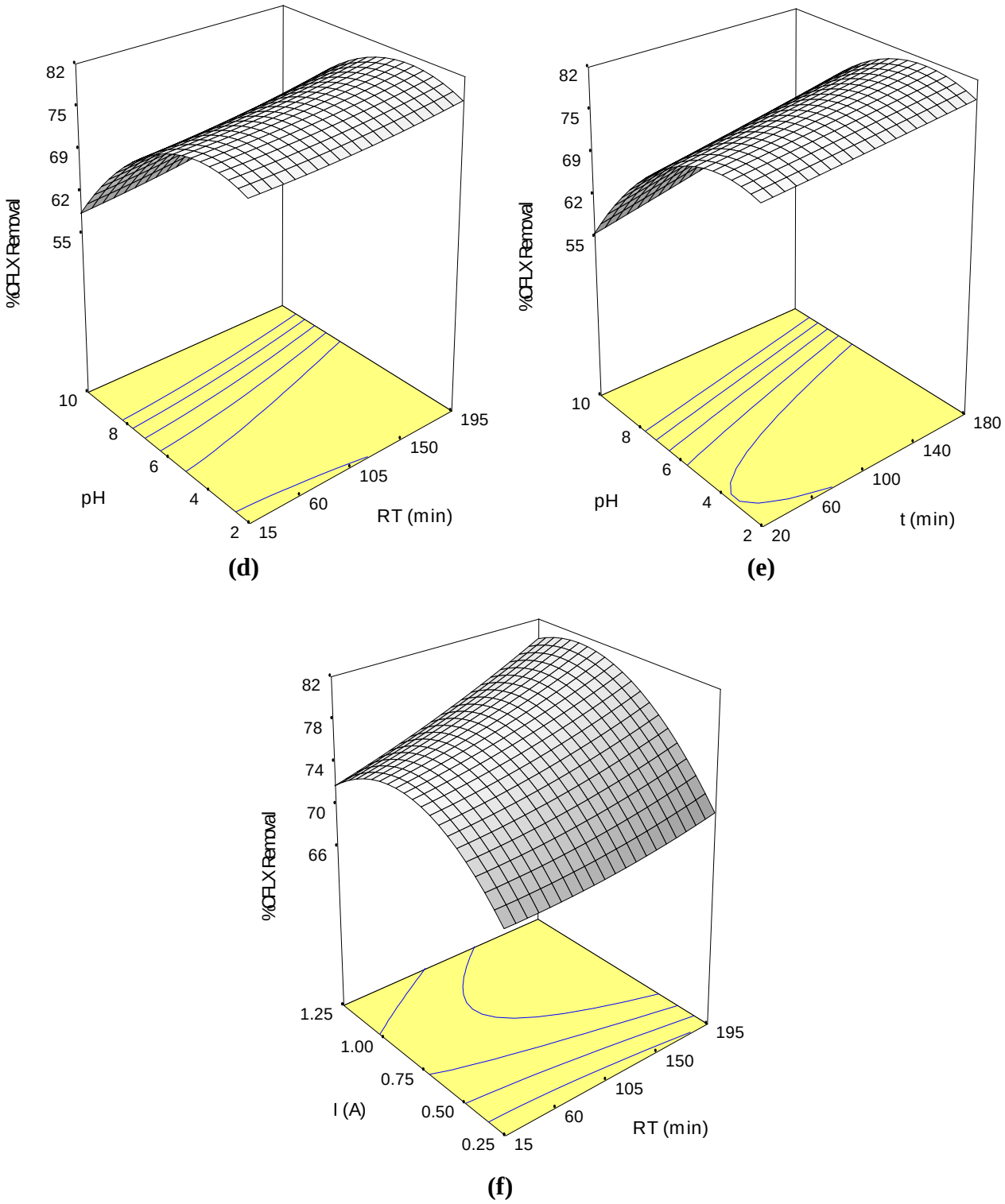

Fig. 4.24 (d – f). 3D response surface graphs for %OFLX removal (Z_2) as function of independent variables pH, *I*, R_T and *t*.

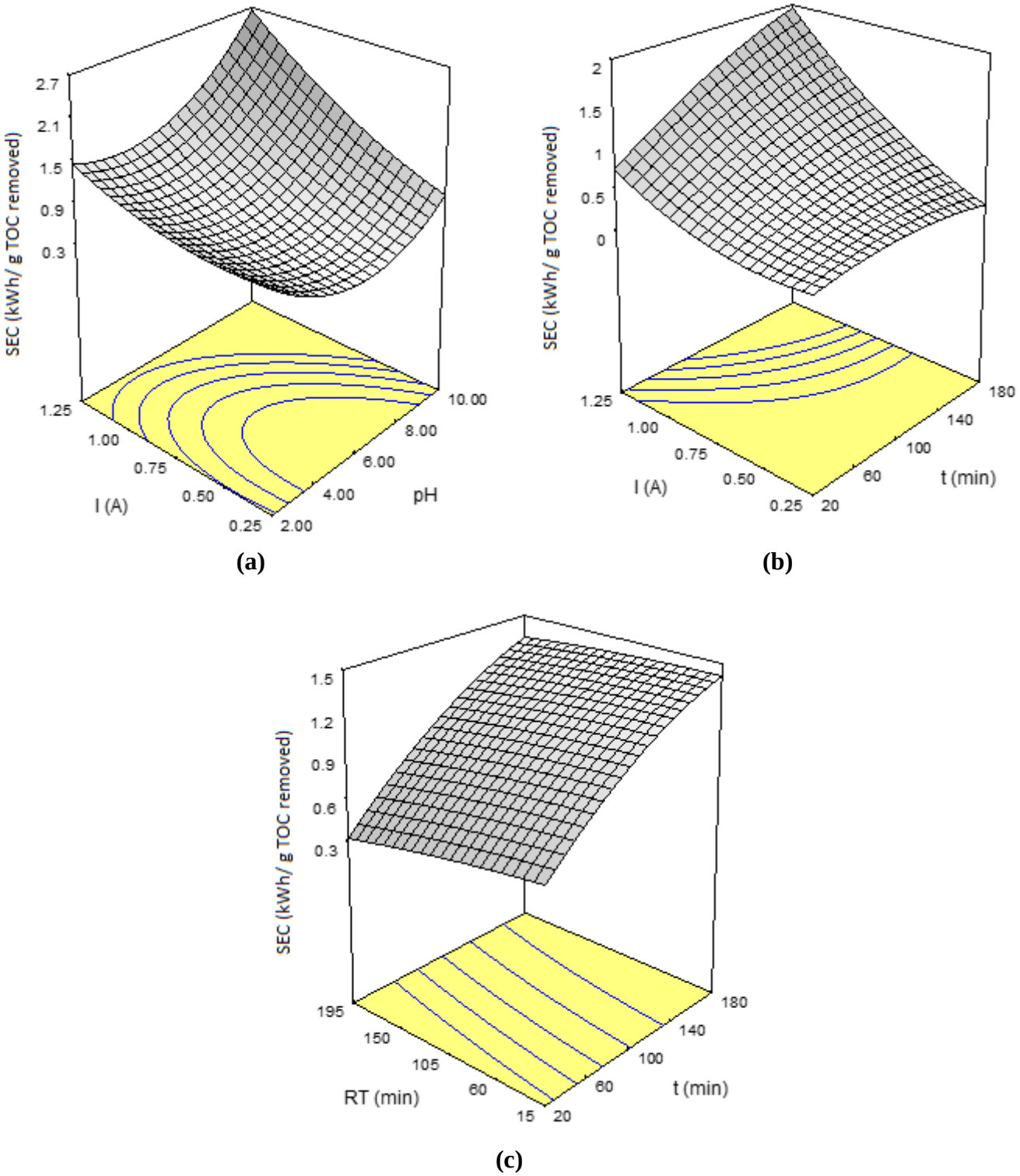

Fig. 4.25 (a – c). 3D response surface graphs for SEC (kW h (g TOC removed)$^{-1}$) (Z_3) as function of independent variables pH, *I*, R_T and *t*.

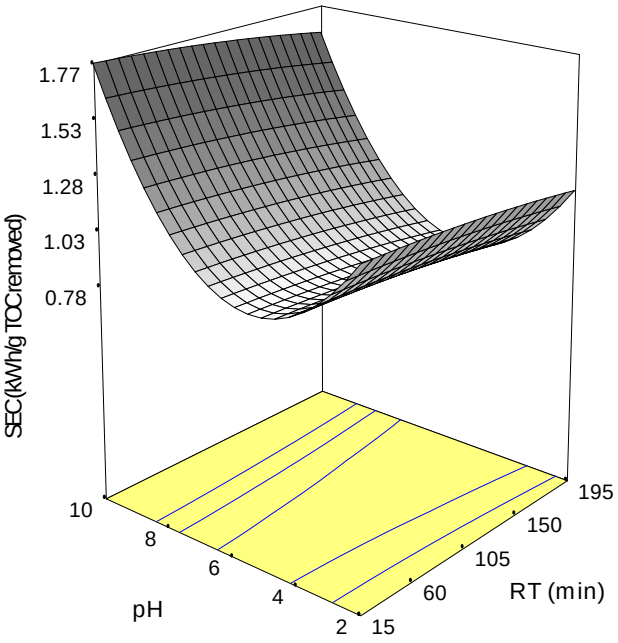

(d)

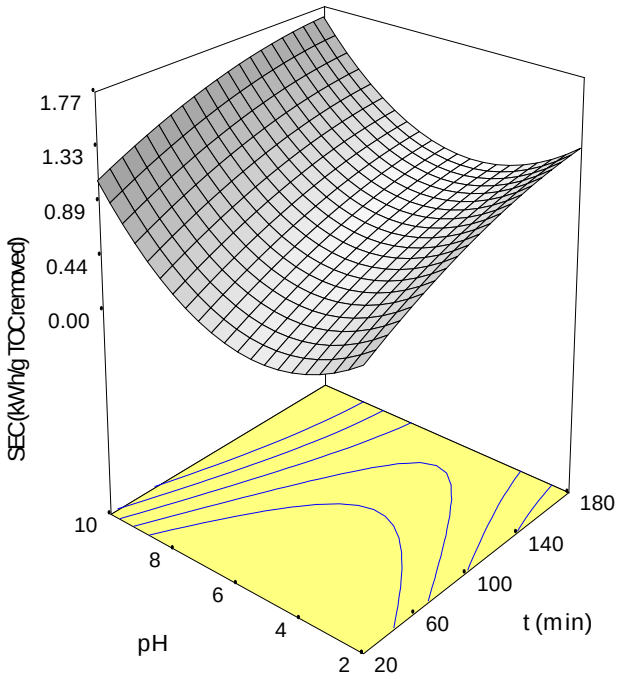

(e)

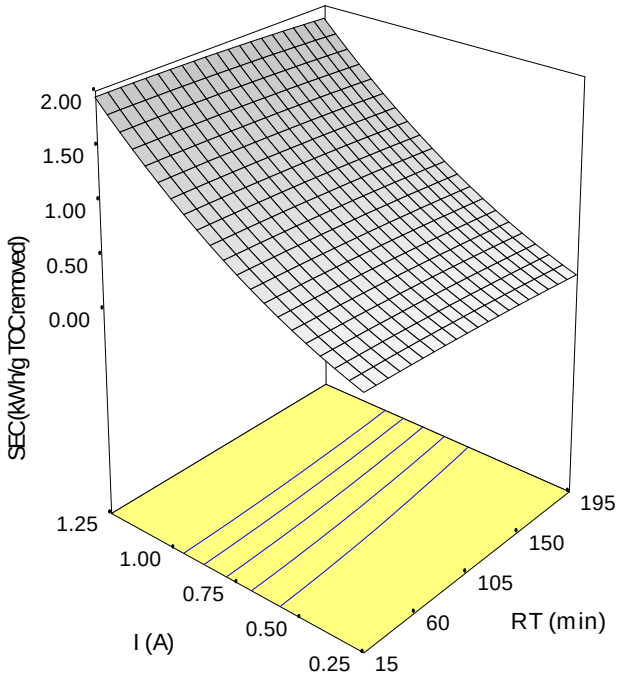

(f)

Fig. 4.25 (d – f). 3D response surface graphs for SEC (kW h (g TOC removed)$^{-1}$) (Z_3) as function of independent variables pH, *I*, R_T and *t*.

The behaviour and pattern of degradation process by Ti/RuO_2 anode, discussed above, can be explained by the characteristic properties of this electrode for generation of variety of oxidant species depending on the nature of wastewater. OFLX either gets oxidized at the anode surface itself by "direct oxidation" (Eq. 4.1 – 4.5) or through "indirect oxidation" in the bulk solution through oxidants generated at the anode surface (Eq. 4.6 – 4.11), which is well explained in section 4.2.1.

In acidic conditions, maximum OFLX removal efficiency was achieved, however the amount of TOC removed under the same conditions was certainly low. The chemisorbed hydroxyl radicals on Ti/RuO_2 surface are predominant in acidic environment. The OFLX was thus degraded to form its transformation products according to Eq. 4.5. Additionally, indirect oxidation of OFLX also took place via Cl_2 and HOCl, which might have formed intermediates resisting further degradation at given experimental conditions. Evidently, in acidic conditions, conversion of OFLX was more prevalent than its combustion/mineralization, subsequently resulting in poor TOC removal efficiency. Nevertheless, pH values around neutral conditions (pH 6 – 7) were found to be favourable for TOC removal from the wastewater comprising OFLX. The TOC abatement occurred according to Eq. 4.4 through the prime oxidizing species active at this pH i.e., physisorbed active oxygen. Alkaline pH (8 – 10) had negative impact on both Z_1 and Z_2. This could be attributed to the fact that the EO was driven by species having low oxidation potentials for organic pollutants. The conversion of OFLX was occurring to some extent, with just meagre amount of the same being mineralized.

Current intensity plays a vital role during the EO treatment method. The values of Z_1 and Z_2 were seen increasing when the applied current was increased from 0.25 A to ≈1 A. This could be owed to higher generation rate of oxidant species at higher applied current, which in turn destroyed the OFLX. However, with further increase in *I* to 1.25 A, both Z_1 and Z_2 were found to decrease. The reason could be other side reactions, such as oxygen evolution at anode (Eqs. 4.15, 4.16) and hydrogen evolution at cathode (Eq. 4.25), taking place at such high current intensity along with degradation and mineralization of OFLX. Besides, the excess production of hydroxyl radicals also increases the production of hydroperoxyl radical (Eq. 4.14), which further reacts with hydroxyl radical according to Eq. (4.26). Such reactions consumed an important part of energy and hence lower the OFLX and TOC removal rates (Fabianska et al., 2014).

$$2H_2O + 2e^- \rightarrow H_2 + 2OH^- \quad \textbf{(4.25)}$$

$$HO_2\bullet + \bullet OH \rightarrow H_2O + O_2 \quad \textbf{(4.26)}$$

The third response, SEC (kW h (g TOC removed)$^{-1}$, stands essential to test the economic feasibility of continuous EO process for abatement of OFLX antibiotic from wastewater. Fig. 4.25 represents the interactive effects of pH, *I* (A), R_T (min) and *t* (min) on Z_3. Minimum energy was consumed when pH was around the neutral zone (6 – 7) and at lower values of applied current intensity (Fig. 4.25a). For *I* value of ≈ 0.75 A and above, and pH above ≈7, a sharp increase in value of Z_3 could be observed. This particular area of the plot signifies that in alkaline pH and higher applied current, most of the energy was consumed in side reactions (Eqs. 4.14 – 4.16, 4.25 and 4.26) rather than mineralization of OFLX. Fig. 4.25b represents the interactive effect of *I* (A) and *t* (min) on Z_3. For lower values of applied current between 0.25 A and 0.5 A, there was no visible impact of elapsed time on Z_3. However, when *I* was further increased above 0.5 A, a sharp increase in Z_3 value with elapsed time was observed. Increase in *I* always increased the SEC (Figs. 4.25 a, b and f). Nonetheless, the amplification in SEC was much enhanced for higher values of *t*. Z_3 always decreased to some extent with increase in R_T value for all values of t, pH and *I* (Figs. 4.25 c, d and f), but increased significantly when *t* was increased (Fig. 4.25 b, c and e).

In order to optimize the values of operating parameters, the target was set to maximize Z_1 (%TOC removal) and Z_2 (%OFLX removal), while keeping Z_3 (SEC) minimum. As a result, the optimum condition was found by RSM was: pH = 6.0, *I* = 0.64 A, R_T = 157.68 min and *t* = 170 min with predicted responses as: Z_1 = 78.16%, Z_2 = 23.94% and Z_3 = 0.658 kW h (g TOC removed)$^{-1}$. A set of three experiments was conducted at these optimal conditions to verify the suitability of optimization analysis, and the average value came out to be: Z_1 = 76.78%, Z_2 = 23.85% and Z_3 = 0.706 kWh/g TOC removed, which were in good agreement with the predicted values.

The mineralization of OFLX antibiotic takes place according to Eq. 3.4. The %MCE value for the optimum run of EO came out to be 5.07%. This signifies that only 5.07% of the current supplied to continuous EO reactor was utilized for mineralization of OFLX or TOC abatement, and rest of the applied current got utilized in formation of degradation/transformation products of OFLX and other side reactions such as oxygen and hydrogen evolution.

4.4.3 Decay kinetics in continuous EO treatment

At optimum condition of continuous EO of synthetic wastewater, decay kinetics of OFLX and TOC was explored by applying pseudo-first order kinetic model equations modified as:

$$C_{R_t} = C_{R_e}[1 - e^{k_f t}] \quad \textbf{(4.27)}$$

$$TOC_{R_t} = TOC_{R_e}[1 - e^{k_f t}] \quad \textbf{(4.28)}$$

Where, C_{Rt} (mg L^{-1}) and TOC_{Rt} (mg L^{-1}) are the amounts of OFLX and TOC removed from the wastewater by EO at any time *t*, respectively, C_{Re} (mg L^{-1}) and TOC_{Re} (mg L^{-1}) are the amounts of OFLX and TOC removed at equilibrium conditions, and k_f denotes pseudo-first order rate constant. Marquardt's percent standard deviation (MPSD) (Eq. 4.20) was applied as an error function for fitting the experimental data using non – linear regression as described in section 4.2.4. C_{Rt} values in Eq. 4.20 were replaced by TOC_{Rt} values to compute the error function corresponding to TOC removal kinetics.

Fig. 4.26 depicts the kinetic data for OFLX and TOC removal using continuous EO treatment at optimum condition (pH = 6.0, *I* = 0.64 A, R_T = 157.68 min, *t* = 170 min), fitted to pseudo-first order kinetic model. The values of k_f were found to be 5.3×10^{-2} and 1.5×10^{-2} min^{-1} for OFLX removal and TOC removal, respectively. Clearly, OFLX removal was more than three times faster than TOC removal from the wastewater undergoing continuous EO treatment using Ti/RuO_2 anodes. Breaking down of organic intermediates of high molecular masses into smaller organic compounds and then to CO_2 could take longer interval of time, thus resulting into slow TOC removal. The experimental and calculated values of OFLX and TOC concentration removed from wastewater were very close to each other, which resulted into R^2 values of 0.997 (%OFLX removal) and 0.999 (%TOC removal), and rather low values of MPSD (8.06 for %OFLX removal; 5.53 for %TOC removal), hence supporting the aptness of pseudo-first order kinetic model.

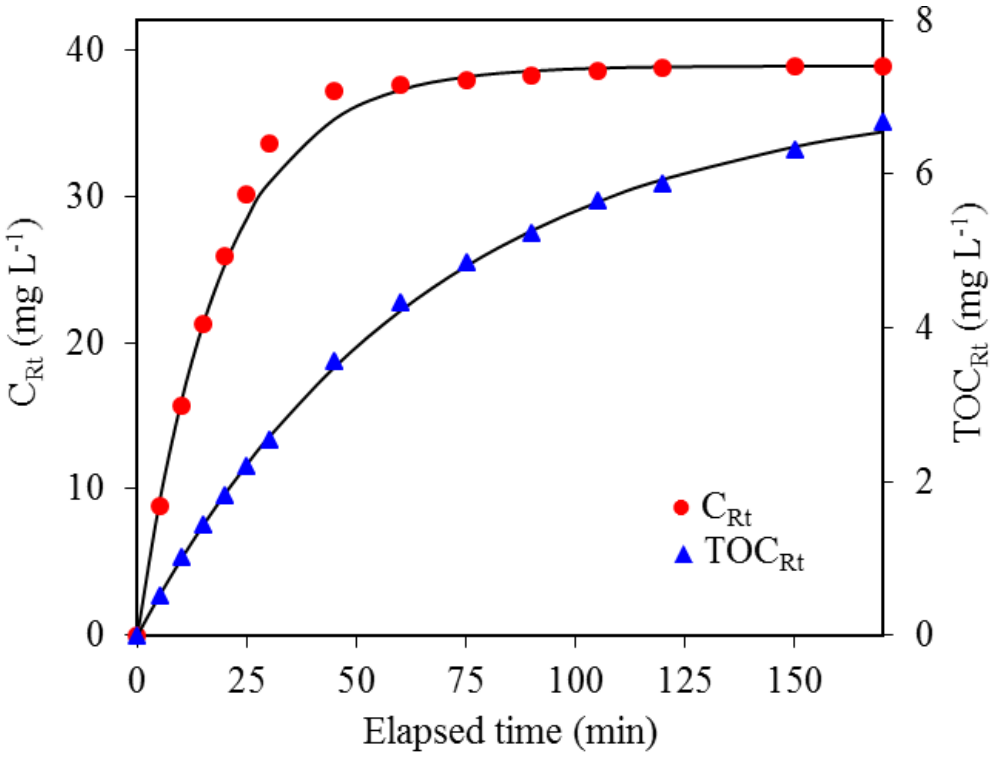

Fig. 4.26. Kinetics of TOC and OFLX removal at optimum condition of continuous EO treatment.

4.4.4. Identification of transformation products and proposed degradation pathway

There are a number of reactions taking place during electro-oxidation of a pollutant via number of oxidation species (•OH, Cl_2, HOCl, H_2O_2, etc.) generated in the EO reactor (Section 4.2.1). This causes the formation of different transformation products in the wastewater. In order to identify the OFLX transformation products and create a possible scheme for degradation pathway, synthetic wastewater was subjected to EO at optimum conditions determined by RSM under CCD, and the samples collected from the outlet were then analyzed by UPLC-Q-TOF-MS. The retention time for OFLX came out to be 5.5 min (Fig. 4.27). The corresponding mass spectrum of OFLX (molar mass = 361) comprised of peaks with mass/charge (m/z) ratio of 362, 318 and 261 (Fig. 4.28), which were explained in detail in section 4.2.5. The chromatograms obtained from the UPLC-Q-TOF-MS of samples collected after 15, 45 and 90 min of continuous EO are shown in Figs. 4.29a, b and c, respectively. These plots revealed the presence of seven transformation products or reaction intermediates of OFLX or ORIs (ORI 1 – ORI 7). The m/z ratio, retention time, elemental composition and proposed structure of these intermediates are mentioned in Table 4.8. It was found that six ORIs were similar to those detected during batch EO treatment of OFLX using Ti/RuO_2 electrodes (Section 4.2.5, Table 4.2). However, ORI 6 (m/z = 297) was formed during continuous treatment of OFLX and was detected in sample withdrawn after 45 min of EO (Fig. 4.29b).

A plausible degradation scheme of OFLX antibiotic was derived on the basis of identified ORIs (Fig. 4.30). As discussed in section 4.2.1, OFLX could either be degraded by direct anodic oxidation or by indirect oxidation through active oxygen or active chloro species. The degradation of OFLX by Ti/RuO_2 electrodes in a continuous EO reactor could follow two different pathways under indirect oxidation mechanism: (1) Hydroxylation leading to de-fluorination and subsequent opening of piperazinyl ring; (2) Decarboxylation by active chlorine and subsequent hydroxylation and opening of piperazinyl ring.

4.4.4.1. Direct anodic oxidation via hydroxylation and de-fluorination: In first degradation pathway, an intermediate product was formed due to "ipso attack" of •OH radical to replace fluorine, in a similar fashion as batch EO of OFLX (Section 4.2.5). Further, the nitrogen atoms in piperazinyl moiety were attacked by hydroxyl radicals, resulting in opening of the piperazinyl ring and formation of two different reaction intermediates – ORI 2 (m/z = 337)

and ORI 3 (m/z = 326). In subsequent reactions, attack of active chlorine species on ORI 2 would completely replace the leftover of piperazinyl moiety and form ORI 5 (m/z = 304). In another route, hydroxylation of ORI 2 would lead to its dealkylation and active chlorine's attack would lead to its decarboxylation, thus forming ORI 6 (m/z = 297).

4.4.4.2. Indirect oxidation via decarboxylation and hydroxylation: In second pathway, ORI 1 (m/z = 352) was formed form decarboxylation of OFLX molecule by active chlorine. Subsequent hydroxylation would open the piperazinyl ring and form ORI 4 (m/z = 314) after demethylation. ORI 7 (m/z = 269) could either be formed by hydroxylation, dealkylation and replacement of fluorine in ORI 4; or simply via dealkylation of ORI 6.

4.4.4.3. Cathodic reduction: The ORIs comprising Cl^- (R–Cl) would further undergo cathodic Reduction through hydrogen atom generated by electrolytic dissociation of water and chemisorbed on to the cathode surface (Eq. 4.29) (Sun et al., 2011; Goyal et al., 2017). The reduction of chloro-compounds adsorbed on anode surface (Eq. 4.30) takes place on the cathode as demonstrated in Eqs. 4.31 and 4.32.

$$Ti/RuO_2 + H_2O + e^- \rightarrow Ti/RuO_2.(H)_{ad} + OH^- \quad \textbf{(4.29)}$$

$$Ti/RuO_2 + R–Cl \rightarrow Ti/RuO_2.(R–Cl)_{ad} \quad \textbf{(4.30)}$$

$$Ti/RuO_2.(R–Cl)_{ad} + Ti/RuO_2.(H)_{ad} \rightarrow Ti/RuO_2.(R–H)_{ad} + HCl \quad \textbf{(4.31)}$$

$$Ti/RuO_2.(R–H)_{ad} \rightarrow R–H + Ti/RuO_2 \quad \textbf{(4.32)}$$

The reduced ORIs undergo further oxidation via action of hydroxyl radicals and other oxidants generated at the anode and in the bulk solution. It is evident from the UPLC chromatograms, the intensity of peaks of ORIs with higher m/z values is very high in sample withdrawn after 15 min of EO, which thereafter subsided for the samples withdrawn after 45 min of EO, and completely vanished in chromatogram of sample taken after 90 min of EO. However, the intensity and peak area of ORIs with lower m/z values intensified with time. The results were also supported by the values of TOC removal efficiencies attained in the study.

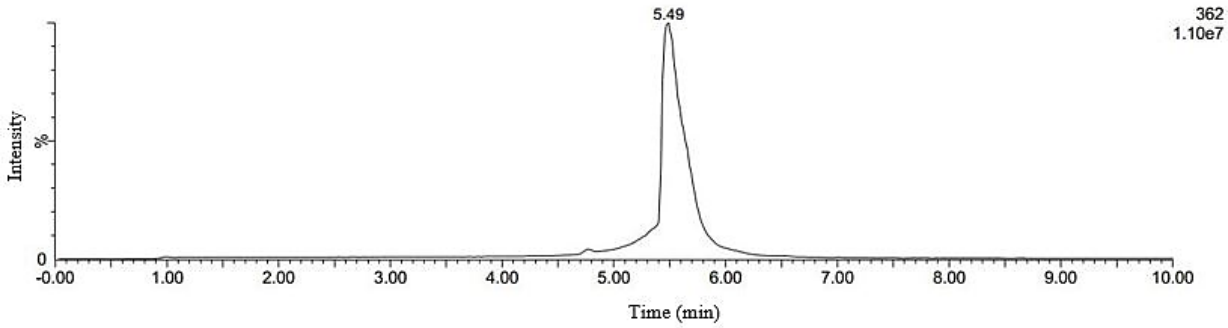

Fig. 4.27. UPLC-Q-TOF-MS chromatogram of OFLX (Retention time = 5.5 min).

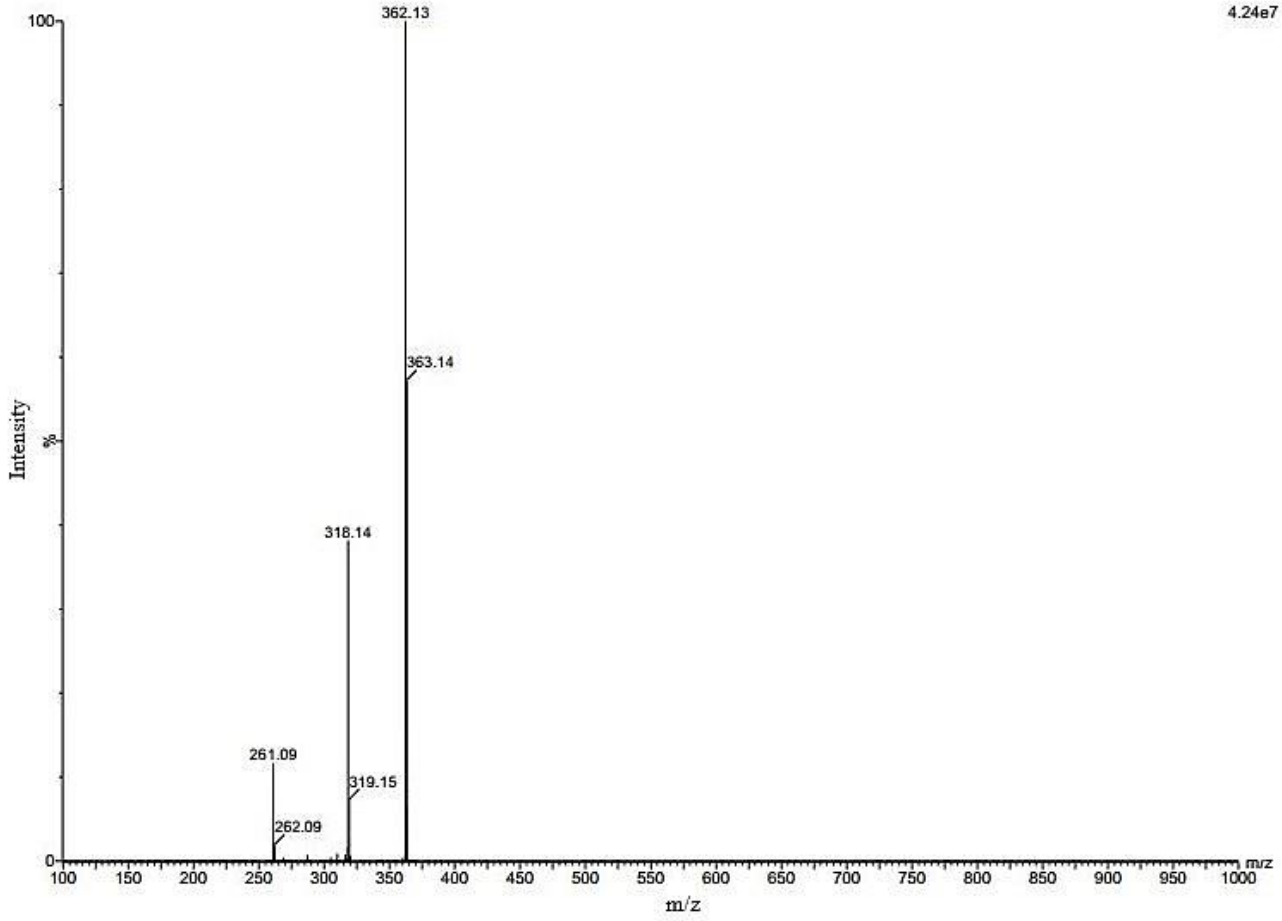

Fig. 4.28. Mass spectrum of OFLX (m/z $[M+H]^+$ = 362).

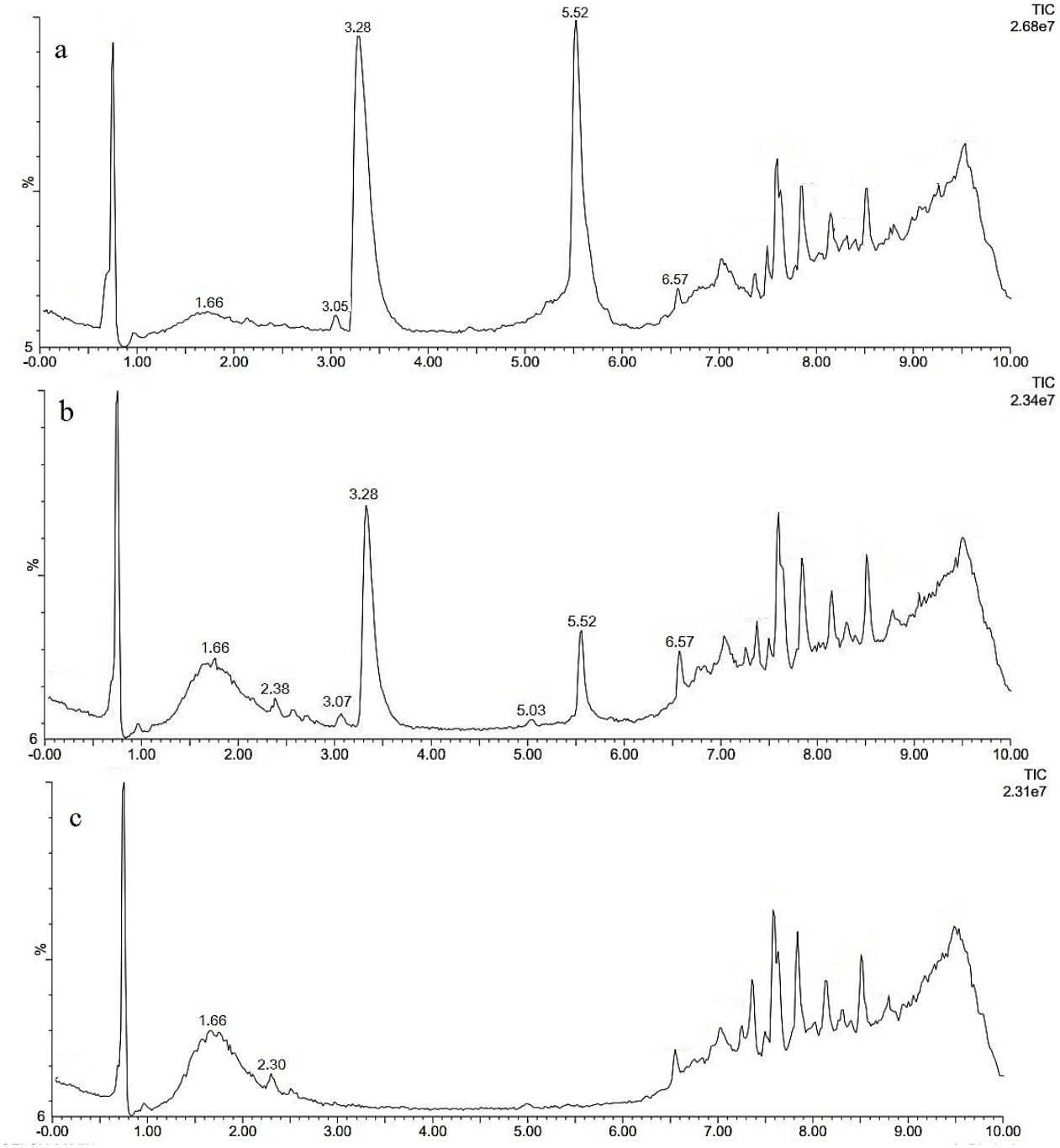

Fig. 4.29. UPLC-Q-TOF chromatograms of samples taken after (a) 15 min, (b) 45 min and (c) 90 min of continuous EO treatment of OFLX wastewater.

Table 4.8. Major OFLX reaction intermediates (ORIs) formed during continuous EO process.

Compound	Retention time (min)	m/z $[M+H]^+$	Elemental composition	Proposed Structure
ORI 1	3.28	352	$C_{17}H_{19}N_3O_2FCl$	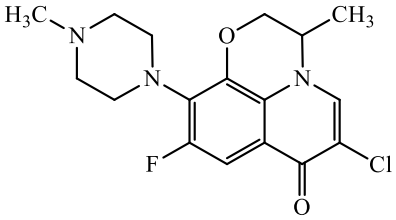
ORI 2	2.38	337	$C_{15}H_{16}N_2O_7$	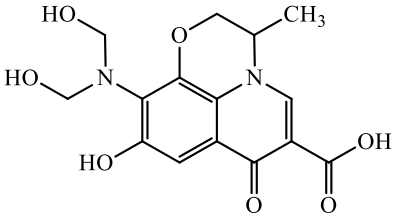
ORI 3	3.05	326	$C_{13}H_{15}N_3O_7$	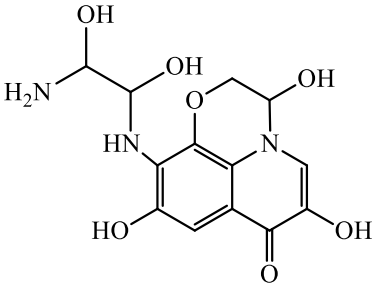
ORI 4	2.30	314	$C_{13}H_{13}N_3O_3FCl$	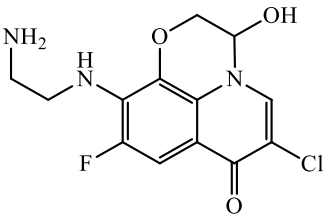
ORI 5	1.66	304	$C_{11}H_7NO_5Cl_2$	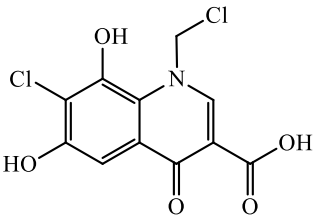
ORI 6	5.03	297	$C_{13}H_{13}ClN_2O_4$	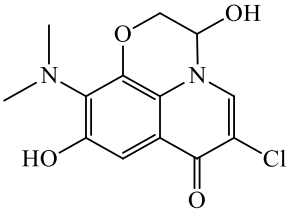
ORI 7	6.57	269	$C_{11}H_9N_2O_4Cl$	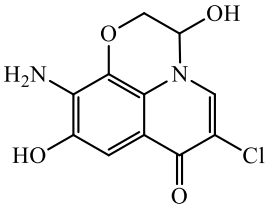

4.4.5. Operating Cost Analysis

Major cost driving factors in continuous EO treatment of wastewater include the cost of energy consumption (C_{EE}) and cost of electrodes (C_{EL}) incorporated in the process. During optimum run of continuous EO treatment of OFLX wastewater, 0.658 kW h of energy was consumed for removing 1 g of TOC. The average cost of electrical energy in Punjab, India is INR 5 per kW h. Therefore, the cost of electrical energy consumption (C_{EE}) came out to be INR 3.29. As per manufacturer's claim, Ti/RuO_2 anodes possess a life of 2.5 years if operated under the optimum condition (I = 0.64 A, pH = 6.0). Two Ti/RuO_2 plates served as anode during EO treatment, each costing INR 2,500. As 23.94% of TOC abatement was achieved during optimum run in 170 min of continuous EO, the cost of electrodes (C_{EL}) came out to be INR 99.4.The total operating cost will therefore be (C_{EE} + C_{EL}) INR 102.69 (US $ 1.57).

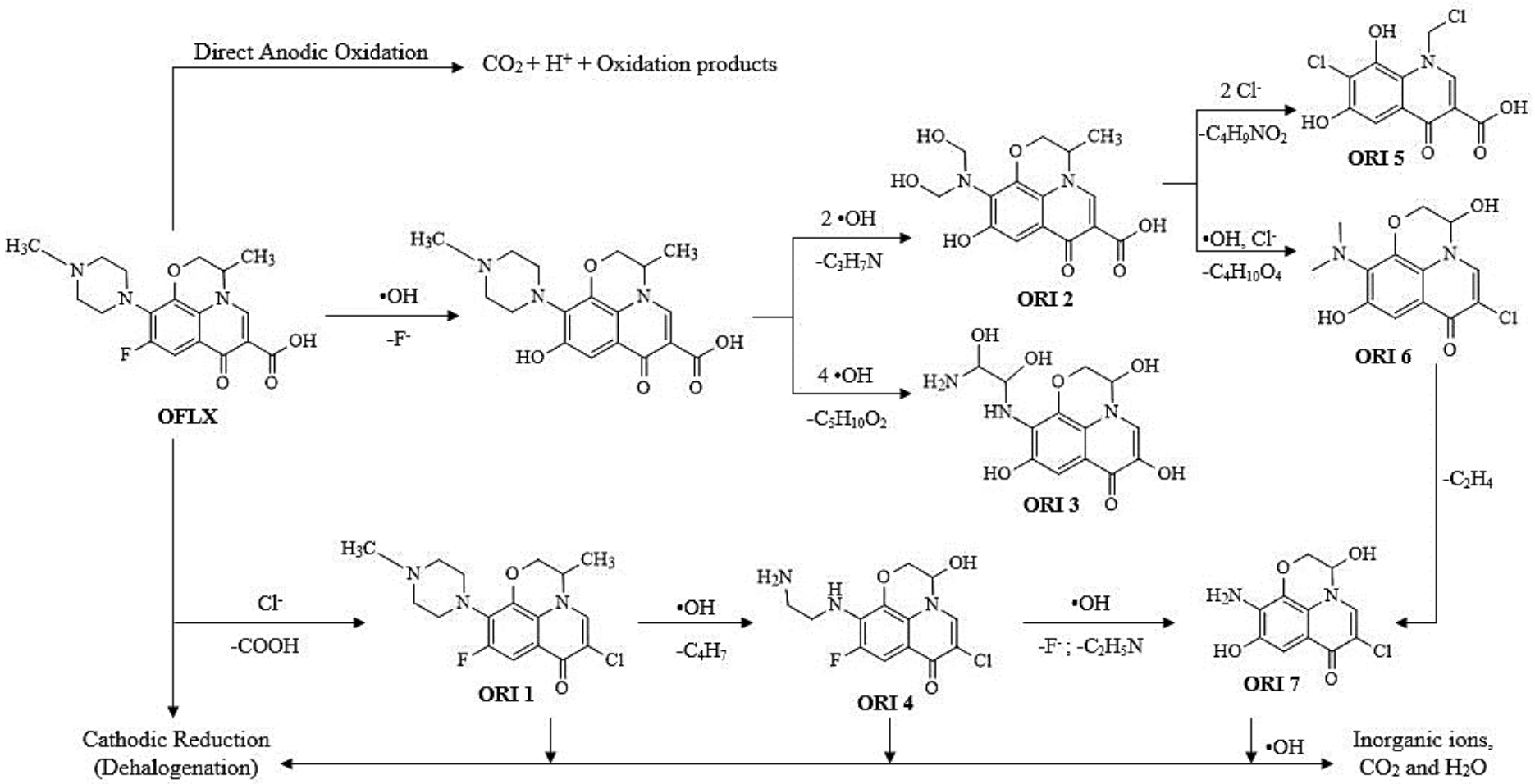

Fig. 4.30. Plausible degradation mechanism of OFLX during continuous EO treatment.

4.5. CONTINUOUS EO TREATMENT OF WASTEWATER COMPRISING AMT

4.5.1. Model fitting and analysis of variance (ANOVA)

Experiments were designed based on five level central composite design (CCD), by response surface methodology (RSM). The design required 30 experiments with 6 replications at the center point to determine the effect of operating parameters or independent variables, i.e. pH, I (A), R_T (min) and t (min), on %TOC removal (Z_1), %AMT removal (Z_2) and SEC (kWh (g TOC removed)$^{-1}$) (Z_3) (Table 4.9). The correlation of responses and independent variables was estimated using quadratic model (which also includes linear model), according to second order polynomial equation (Table 4.10). Along with the equation, experimental data were processed for ANOVA to analyze significance of model terms and the interaction between operating parameters and responses (Tables 4.11a (Z_1), b (Z_2) and c (Z_3)). Model F values of 86.38, 53.12 and 500.19 for Z_1, Z_2 and Z_3, respectively, along with P value (Prob > F) <0.0001, signify that the models are significant for all three responses under consideration. "Lack of fit" F values of 4.12, 2.95 and 2.72 were insignificant for %TOC removal, %AMT removal and SEC, respectively, which is desired for the model. For a model term, if P value < 0.05, then it is significant. Therefore, based on this confidence level and data given in Tables 4.11a, b and c, the response values were calculated in terms of significant model terms (Eqs. 4.33 – 4.35). The adequate precision (signal to noise ratio) values were 36.05, 29.35 and 85.13 for X_1, X_2 and X_3, respectively, which signify that the models have a very strong signal to be used for optimization.

$$Z_1 = -77.81 + (15.77 \times pH) + (80.43 \times I) + (6.43 \times 10^{-3} \times R_T) + (0.21 \times t) - (0.92 \times pH^2) - (48.73 \times I^2) + (-9.08 \times 10^{-4} \times t^2) + (0.13 \times I \times t) \quad \textbf{(4.33)}$$

$$Z_2 = -30.46 + (10.32 \times pH) + (63.02 \times I) - (9.19 \times 10^{-3} \times R_T) + (0.08 \times t) - (0.58 \times pH^2) - (33.99 \times I^2) \quad \textbf{(4.34)}$$

$$Z_3 = 1.41 - (0.39 \times pH) - (0.55 \times I) - (3.34 \times 10^{-4} \times R_T) + (2.56 \times 10^{-3} \times t) + (0.03 \times pH^2) + (0.61 \times I^2) + (1.18 \times 10^{-4} \times pH \times R_T) + (2.69 \times 10^{-3} \times I \times t) \quad \textbf{(4.35)}$$

The quality of fit of the quadratic model was justified on the basis of R^2 (coefficient of determination) values: 0.99 (Z_1), 0.98 (Z_2) and 0.99 (Z_3). Moreover, the values of predicted R^2 were in agreement with the values of adjusted R^2 (Table 4.10). The CV values for all the responses were in acceptable range (Z_1: 5.47, Z_2: 3.41, Z_3: 3.17), thus implying enhanced reproducibility. Furthermore, the models were validated using plots between (a) normal %

probability *vs* studentized residuals (Fig. 4.31), and (b) predicted *vs* actual values (Fig. 4.32), for responses Z_1, Z_2 and Z_3. The adequacy and accuracy of models was thus verified.

Table 4.9. Design matrix and experimental responses of continuous EO of AMT.

Standard order	Run	pH	*I* (A)	R_T (min)	*t* (min)	Z_1	Z_2	Z_3
29	1	6	0.75	105	100	32.23	45.58	0.374
5	2	4	0.5	150	60	11.15	30.33	0.323
26	3	6	0.75	105	100	30.97	43.8	0.387
16	4	8	1	150	140	38.91	52.86	0.706
3	5	4	1	60	60	13.79	32.51	0.644
19	6	6	0.25	105	100	12.45	30.09	0.204
24	7	6	0.75	105	180	36.21	49.67	0.605
7	8	4	1	150	60	16.12	34.46	0.568
9	9	4	0.5	60	140	14.63	33.25	0.61
21	10	6	0.75	15	100	30.27	42.29	0.395
13	11	4	0.5	150	140	16.51	35.75	0.553
11	12	4	1	60	140	24.37	37.89	0.934
10	13	8	0.5	60	140	27.88	45.22	0.371
15	14	4	1	150	140	26.94	39.88	0.856
8	15	8	1	150	60	30.2	45.53	0.395
22	16	6	0.75	195	100	36.09	48.44	0.338
4	17	8	1	60	60	27.8	43.2	0.41
30	18	6	0.75	105	100	32.89	45.29	0.367
23	19	6	0.75	105	20	18.16	36.21	0.104
14	20	8	0.5	150	140	31.55	50.26	0.332
6	21	8	0.5	150	60	27.45	44.56	0.161
25	22	6	0.75	105	100	31.74	44.36	0.379
18	23	10	0.75	105	100	30.17	45.81	0.423
20	24	6	1.25	105	100	29.18	42.52	0.909
17	25	2	0.75	105	100	6.33	25.14	1.353
1	26	4	0.5	60	60	9.14	28.47	0.375
27	27	6	0.75	105	100	32.05	44.86	0.376
12	28	8	1	60	140	36.16	49.66	0.755
2	29	8	0.5	60	60	25.43	42.48	0.172
28	30	6	0.75	105	100	33.19	46.42	0.364

Table 4.10. R^2, adjusted R^2 and predicted R^2 values for responses as suggested by CCD.

Responses	R^2	Adjusted R^2	Predicted R^2
Z_1	0.99	0.98	0.93
Z_2	0.98	0.96	0.90
Z_3	0.99	0.99	0.99

Table 4.11a. ANOVA of %TOC removal (Z_1) for continuous EO of AMT wastewater.

Source	Sum of Squares	DF	Mean Square	F – Value	Prob > F
Model	2384.95	14	170.35	86.38	< 0.0001
pH	1072.14	1	1072.14	543.64	< 0.0001
I	294.07	1	294.07	149.11	< 0.0001
R_T	40.74	1	40.74	20.659	0.0004
t	352.43	1	352.43	178.71	< 0.0001
pH^2	372.9	1	372.9	189.08	< 0.0001
I^2	254.47	1	254.47	129.03	< 0.0001
R_T^2	0.056	1	0.056	0.028	0.8681
t^2	57.94	1	57.94	29.38	< 0.0001
pH × *I*	5.09	1	5.096	2.58	0.1288
pH × R_T	0.26	1	0.26	0.13	0.7202
pH × *t*	4.65	1	4.65	2.36	0.1453
I × R_T	0.013	1	0.014	0.007	0.9344
I × *t*	27.74	1	27.74	14.07	0.0019
R_T × *t*	0.28	1	0.28	0.14	0.7125
Residual	29.58	15	1.97		
Lack of Fit	26.38	10	2.64	4.12	0.06
Pure Error	3.2	5	0.64		
Cor Total	2414.53	29			

Table 4.11b. ANOVA of %AMT removal (Z_2) for continuous EO of AMT wastewater.

Source	Sum of Squares	DF	Mean Square	F – Value	Prob > F
Model	1466.5	14	104.75	53.12	< 0.0001
pH	846.92	1	846.92	429.46	< 0.0001
I	106.38	1	106.38	53.95	< 0.0001
R_T	46.06	1	46.06	23.36	0.0002
t	205.04	1	205.04	103.97	< 0.0001
pH^2	149.16	1	149.16	75.64	< 0.0001
I^2	123.79	1	123.79	62.77	< 0.0001
R_T^2	0.54	1	0.54	0.27	0.61
t^2	5.95	1	5.95	3.02	0.1
pH × I	4.21	1	4.21	2.14	0.16
pH × R_T	1.18	1	1.18	0.59	0.45
pH × t	0.09	1	0.09	0.05	0.83
I × R_T	0.25	1	0.25	0.13	0.72
I × t	2.21	1	2.21	1.12	0.31
R_T × t	1.27	1	1.27	0.64	0.43
Residual	29.58	15	1.97		
Lack of Fit	25.29	10	2.53	2.95	0.12
Pure Error	4.29	5	0.86		
Cor Total	1496.08	29			

Table 4.11c. ANOVA of SEC (Z_3) for continuous EO of AMT wastewater.

Source	Sum of Squares	DF	Mean Square	F – Value	Prob > F
Model	1.65	14	0.12	500.19	< 0.0001
pH	0.27	1	0.27	1129.57	< 0.0001
I	0.59	1	0.59	2508.16	< 0.0001
R_T	0.009	1	0.009	38.98	< 0.0001
t	0.42	1	0.42	1773.33	< 0.0001
pH^2	0.31	1	0.31	1324.31	< 0.0001
I^2	0.04	1	0.04	167.93	< 0.0001
R_T^2	0.0001	1	0.0001	0.45	0.5102
t^2	0.0009	1	0.0009	3.81	0.0698
pH × I	0.0002	1	0.0002	0.66	0.4287
pH × R_T	0.002	1	0.002	7.65	0.0144
pH × t	0.0002	1	0.0002	0.66	0.4287
I × R_T	0.0003	1	0.0003	1.29	0.2726
I × t	0.01	1	0.01	48.94	< 0.0001
R_T × t	0.0005	1	0.0005	2.14	0.1638
Residual	0.003	15	0.0002		
Lack of Fit	0.003	10	0.0003	2.72	0.1405
Pure Error	0.0005	5	0.0001		
Cor Total	1.66	29			

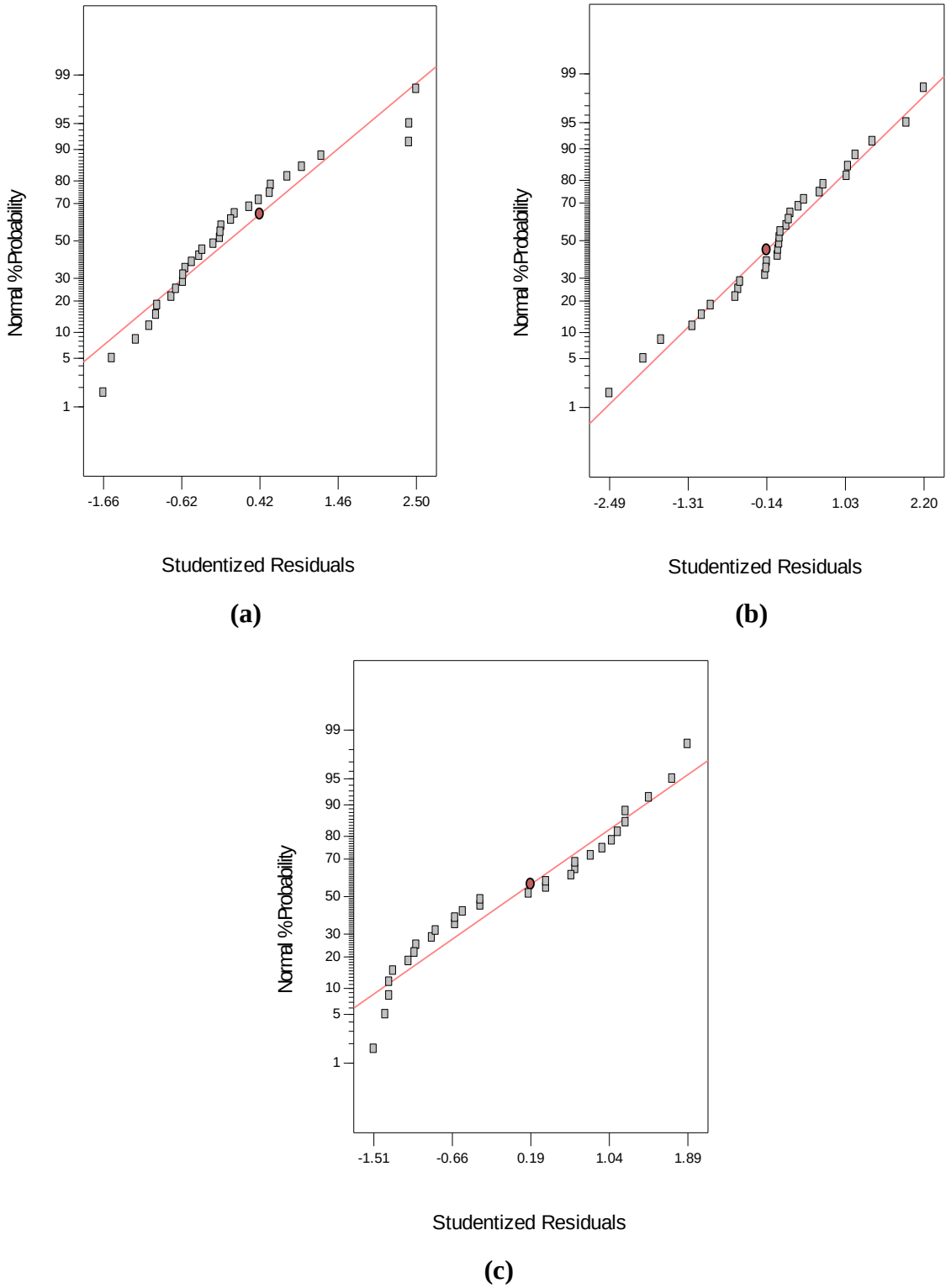

Fig. 4.31. Normal % probability versus studentized residuals plots for (a) %TOC removal (Z_1), (b) %AMT removal (Z_2) and (c) SEC (kW h (g TOC removed)$^{-1}$) (Z_3).

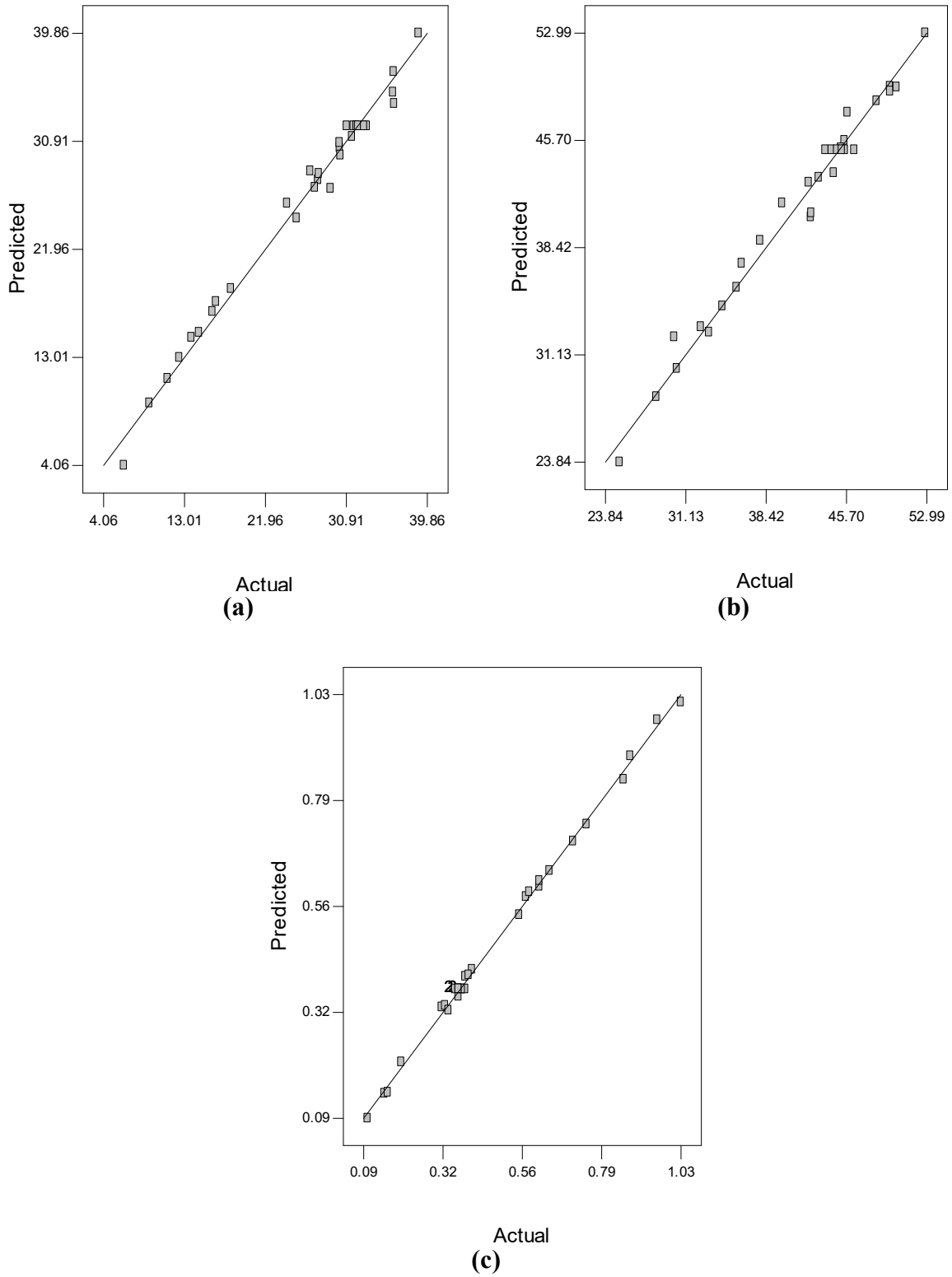

Fig. 4.32. Predicted versus actual plots for (a) %TOC removal (Z_1), (b) %AMT removal (Z_2) and (c) SEC (kW h (g TOC removed)$^{-1}$) (Z_3).

4.5.2. Effect of Operating Parameters and Optimization

The three dimensional response surface plots (Figs. 4.33 – 4.35) were used to analyse the individual and interactive effects of independent variables (pH, *I* (A), R_T (min), *t* (min)) on responses: %TOC removal (Z_1), %AMT removal (Z_2) and SEC (kW h (g TOC removed)$^{-1}$) (Z_3). As shown in Fig. 4.33a, the TOC removal efficiency was very poor in highly acidic medium, i.e. pH 2 – 4. With further increase in pH, Z_1 was found to increase up to pH value of ≈7. Thereafter, in alkaline environment (pH 8 – 10), the TOC removal efficiency slightly decreased. For all the values of *I* (A), maximum Z_1 was attained in the neutral pH range only. Z_1 was extremely poor at for low applied current of 0.25 A (current density, i = 1.47 mA cm^{-2}). However, Z_1 increased with the increase in *I* value from 0.5 to ≈1.0 A (i = 2.94 to 5.88 mA cm^{-2}). Further increase in *I* value up to 1.25 A (i = 7.35 mA cm^{-2}), had an undesirable effect on Z_1, as there was marginal diminution in mineralization. The interactive effect of applied current and elapsed reaction time is shown in Fig. 4.33b. TOC removal efficiency increased with increase in EO reaction time. However, the enhancement in Z_1 value with time was more prominent for higher values of applied current (0.5 – 1.25 A), than low applied current value ≈ 0.25 A. However, as discussed earlier, Z_1 was comparatively lower for highest value of applied current (1.25 A). Retention time is an important parameter in continuous EO treatment process. As shown in Fig. 4.33c, Z_1 was found to increase with both *t* and R_T. Nonetheless, it is clear that the effect if *t* on X_1 was slightly more prominent than the effect of R_T. The interactive effects of pH – R_T and *I* – R_T on TOC removal is shown in Fig. 4.33d and 4.33f, respectively. As discussed previously, Z_1 increased with increase in R_T, over entire range of applied *I* and initial pH of wastewater. Fig. 4.33e depicts the interactive effect of elapsed time and initial pH on Z_1. Maximum TOC removal efficiency was achieved in neutral pH range for elapsed time ≈ 150 min.

Fig. 4.34a depicts the interactive effect of *I* and pH on Z_2. Substantial improvement in AMT removal efficiency was seen when initial pH of wastewater was increased from 2 to ≈7, for all values of *I*. However, further increase in pH up to 10 resulted in almost no change in Z_2. Similarly, over entire range of elapsed time, *t*, maximum AMT removal was attained at pH≈7 (Fig. 4.34e). The effect of *I* on Z_2 followed the same trend as Z_1. Hence, maximum AMT removal was achieved in neutral pH range at applied current ≈ 1.0 A. As shown in Fig. 4.34b, Z_2 increased with increase in *I* values from 0.25 to 1.0 A, and then decreased for *I* = 1.25 A, irrespective of elapsed time. Increment in Z_2 value followed a linear trend when *t* value was increased from 20 to 180 min, for all values of applied current. Z_2 value improved when both

t and R_T were increased from 20 to 180 min, and 15 to 190 min, respectively (Fig. 4.34c). Z_2 always increased with increase in R_T irrespective of solution pH and applied current (Fig. 4.34d and f).

EO technique involves generation of a number of oxidants on anode surface for destruction of target pollutant either on the anode surface or in the bulk solution. The pH of wastewater plays a key role in generation of different types of oxidant species, particularly in chloride rich wastewaters. Moreover, Ti/RuO_2 anode is known for its strong electro-catalytic activity for generation of chloro-oxidant species (Cl_2, HOCl. OCl^-), whose dominance is sturdily pH dependent (Comninellis, 1994; Deborde and Gunten, 2008; Sires et al., 2014).

In present study, best results for Z_1 and Z_2 were attained in the neutral pH range. Nevertheless, efficiency in terms of AMT and TOC removal was quite low in acidic pH range. Degradation of AMT antibiotic in acidic medium primarily occurred through chemisorbed hydroxyl radicals (Eq. 4.3) and active chlorine in the form of Cl_2. Oxidation potential of Cl_2 is comparatively lower than other oxidants. Moreover, chemisorbed •OH results in partial conversion of AMT to its intermediates (ARIs) (Eq. 4.5). Furthermore, chlorine reduction takes place in acidic conditions according to Eq. 4.21, and oxygen gets evolved (Trasatti et al., 1987).

Thus, indirect oxidation of AMT by Cl_2 and partial conversion by chemisorbed hydroxyl radicals resulted in to poor values of Z_1 and Z_2 in acidic conditions. Physisorbed hydroxyl radicals are predominant in neutral pH range, thus resulting into maximum AMT removal and TOC removal according to Eq. 4.4. Furthermore, HOCl is dominant in neutral pH, whose oxidation potential is higher than that of Cl_2, thus resulting in improved values of Z_1 and Z_2. Alkaline pH (8 – 10) had a meagre undesirable impact on Z_1, but Z_2 remained unaffected. This could be attributed to lower oxidation potential of species, such as hydrogen peroxide and hydroperoxyl radical (Eq. 4.13 and 4,14) responsible for AMT abatement in alkaline pH conditions (Martinez-Huitle and Ferro, 2006; Yavuz and Kaporal, 2006; Brillas and Martinez-Huitle, 2015).

The amount of current applied during EO has a strong influence on different outcomes of this process. Both Z_1 and Z_2 were found to increase with increase in *I* value from 0.25 to ≈1.0 A. The results are justified, since the rate of generation of oxidant species on the anode surface is directly proportional to the amount of current supplied to the EO reactor system, thus giving enhanced values of %AMT and %TOC removal at higher values of applied current. Nonetheless, this was found to be true up to a certain level of applied current. When *I* was further raised up to 1.25 A, Z_1 and Z_2 tend to decrease. During EO process, there are two

inevitable reactions of oxygen and hydrogen evolution taking place on anode and cathode, respectively (Eqs. 4.36 and 4.37).

$$H_2O \rightarrow 1/2O_2 + 2H^+ + 2e^- \quad \textbf{(4.36)}$$

$$2H_2O + 2e^- \rightarrow H_2 + 2OH^- \quad \textbf{(4.37)}$$

Furthermore, with increase in applied current, the generation rate of •OH increases, and excess hydroxyl radicals react to form hydrogen peroxide and hydroperoxyl radical (Brillas and Martinez-Huitle, 2015; Moreira et al., 2017). Consequently, at higher applied current, its significant portion got exhausted in these undesirable but inevitable side reactions, thus resulting in diminutive performance of EO in terms of AMT and TOC removal.

EO is an energy intensive process. In order to check its feasibility on economic grounds, the third response, specific energy consumption (Z_3) was evaluated. Fig. 4.35 shows the individual and interactive effects of independent variables on Z_3. SEC increased with the increase in value of *I*, for all values of pH and R_T (Fig. 4.35a, 4.35f). The average cell potential increased with the increase in applied current, thus resulting in higher values of SEC. Minimum SEC was found in neutral pH range (6 – 8). This is because maximum mineralization took place in this pH range. Maximum energy was consumed in acidic conditions, again due to poor mineralization, because SEC is inversely proportional to the amount TOC removed from the wastewater (Eq. 3.3). This signifies that most part of the energy supplied during EO was consumed in parasitic reactions. As shown in Fig. 4.35b, there is no visible effect on SEC with elapsed time (20 – 180 min) for lower values of applied current (0.25 to ≈0.75 A). However, with further increase in *I* value up to 1.25 A, Z_3 value always increased. The increment in Z_3 was however quite sharp towards higher values of elapsed time, *t*. SEC always increased with increase in elapsed time, but decreased with the increase in retention time (Fig. 4.35c, 4.35f). Fig. 4.35d depicts the interactive effect of pH and R_T on Z_3. For acidic pH range from 2 to ≈5, SEC decreased with the increase in value of R_T. However, when the pH approaches neutral zone, the effect of R_T on SEC diminishes. In alkaline pH zone, SEC remained almost unaffected by R_T. Nevertheless, SEC always increased with increase in elapsed time for all values of pH (Fig. 4.35e).

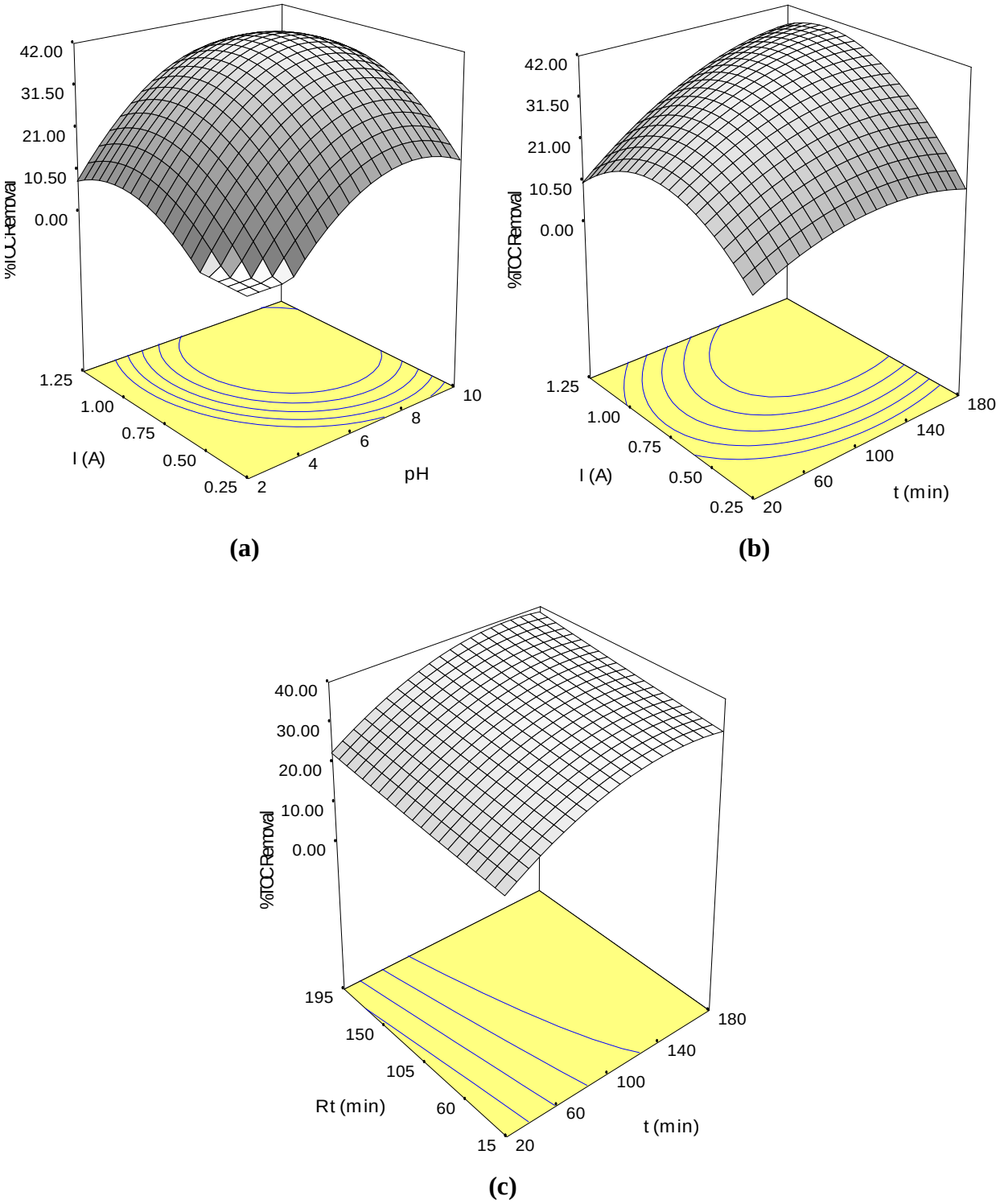

Fig. 4.33 (a – c). 3D response surface graphs for %TOC removal as a function of independent variables pH, *I*, *t* and R_T.

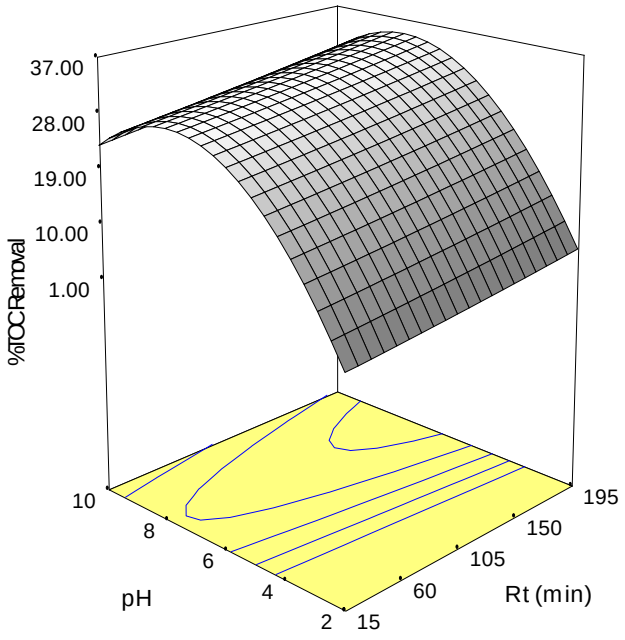

(d)

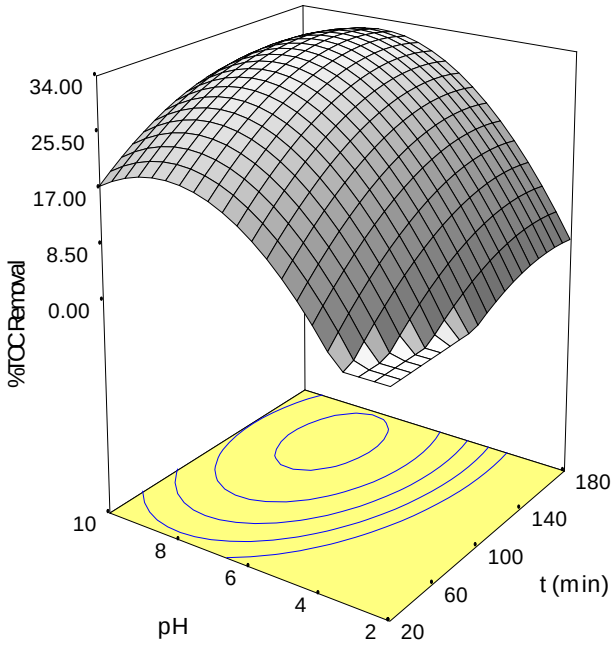

(e)

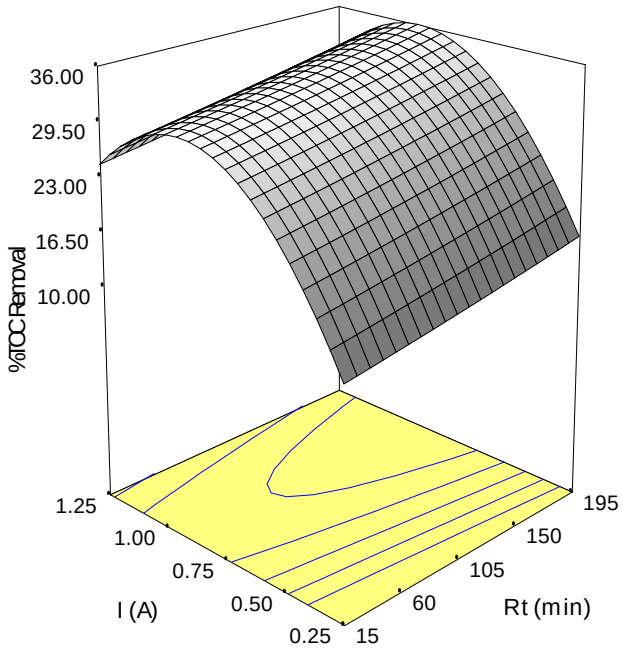

(f)

Fig. 4.33 (d – f). 3D response surface graphs for %TOC removal as a function of independent variables pH, *I*, *t* and R_T.

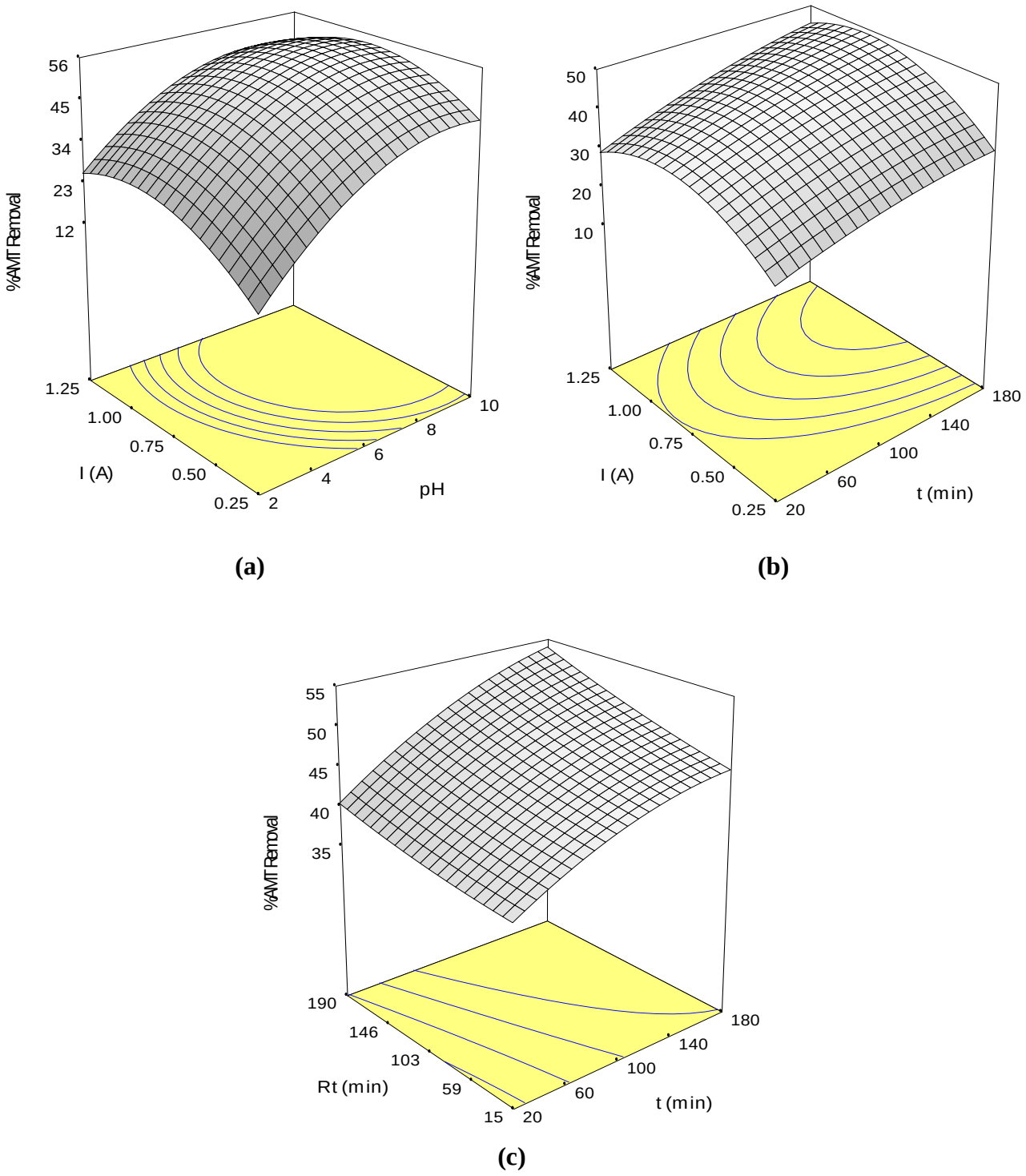

Fig. 4.34 (a – c). 3D response surface graphs for %AMT removal as a function of independent variables pH, *I*, *t* and R_T.

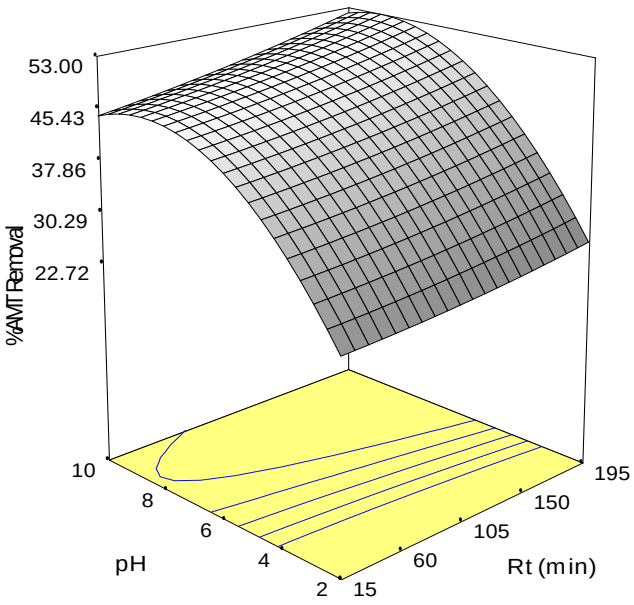

(d)

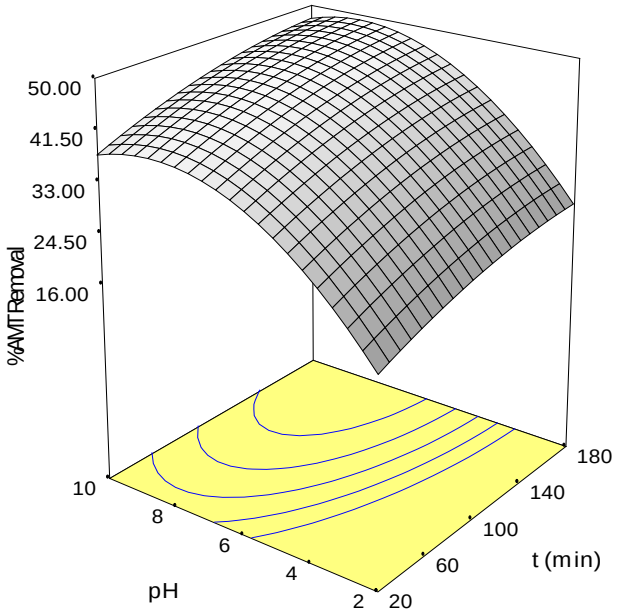

(e)

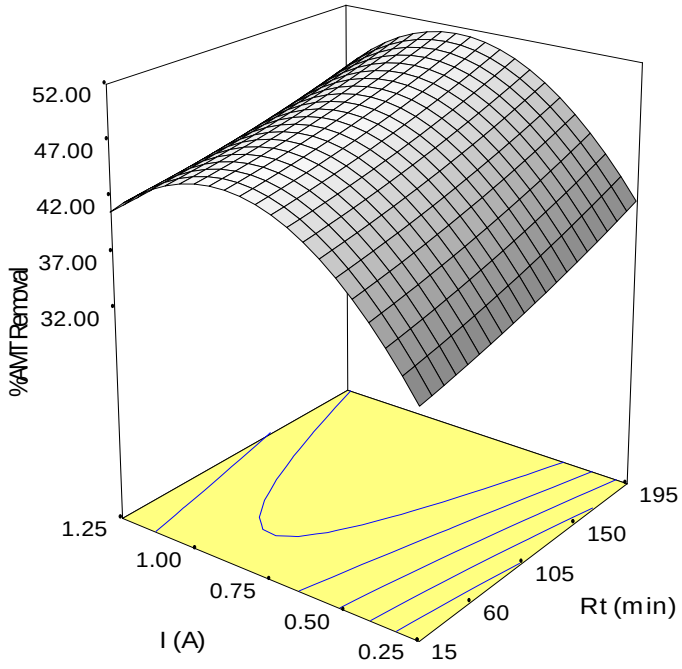

(f)

Fig. 4.34 (d – f). 3D response surface graphs for %AMT removal as a function of independent variables pH, *I*, *t* and R_T.

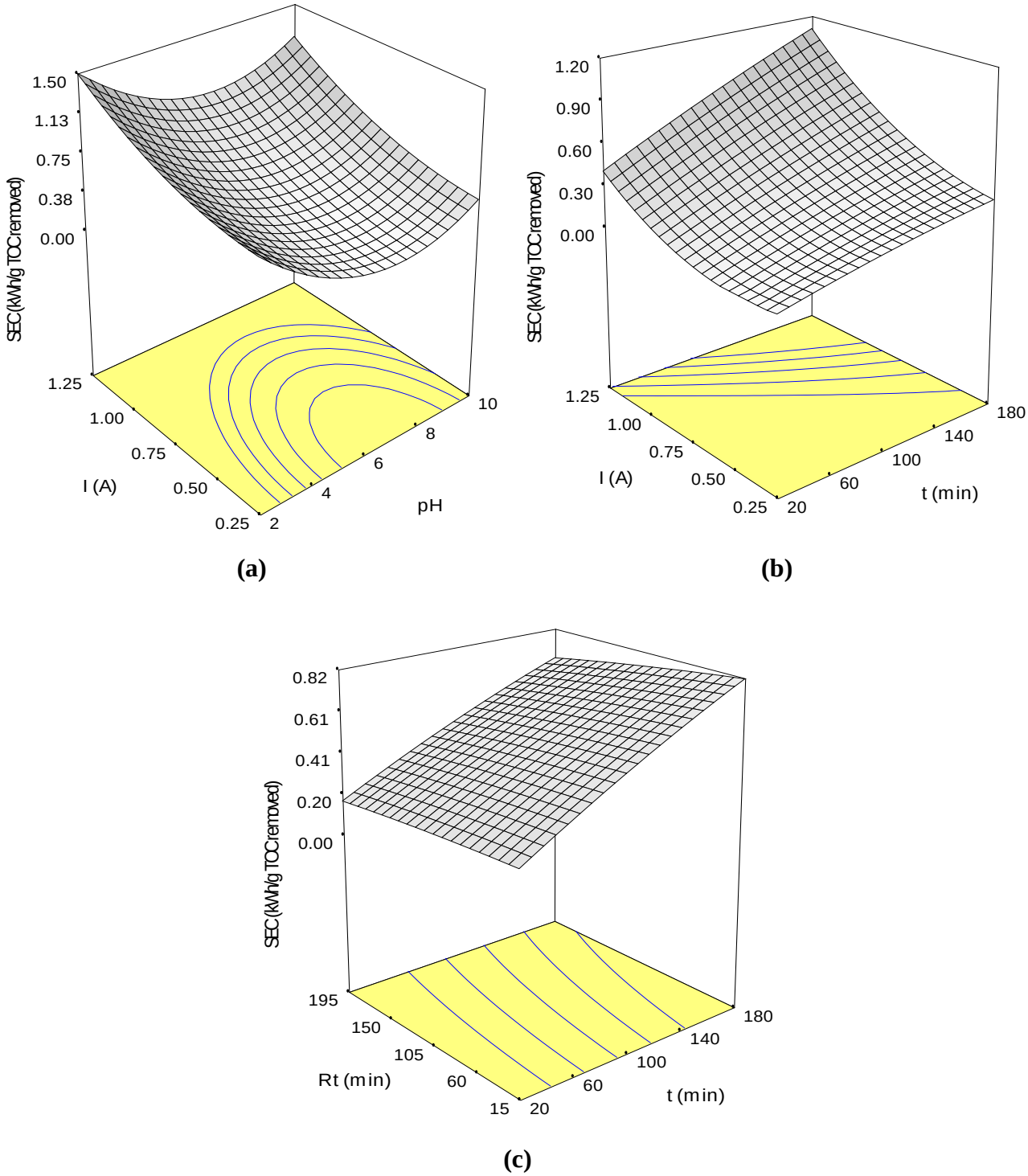

Fig. 4.35 (a – c). 3D response surface graphs for SEC (kW h (g TOC removed)$^{-1}$) as a function of independent variables pH, *I*, *t* and R_T.

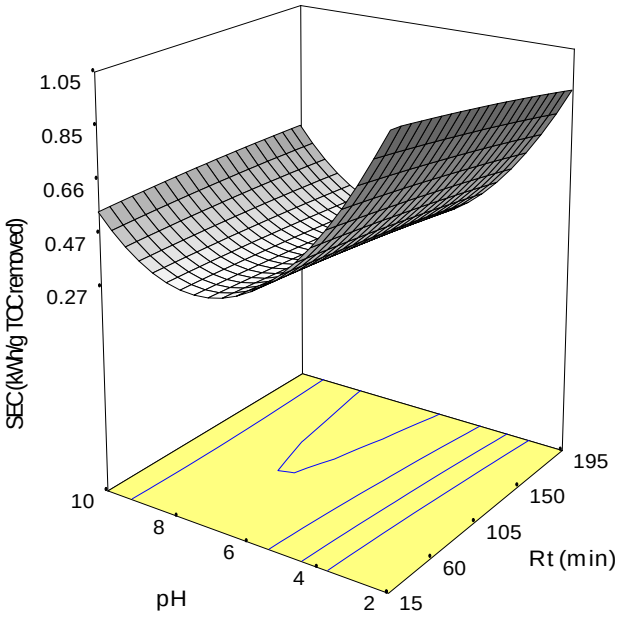

(d)

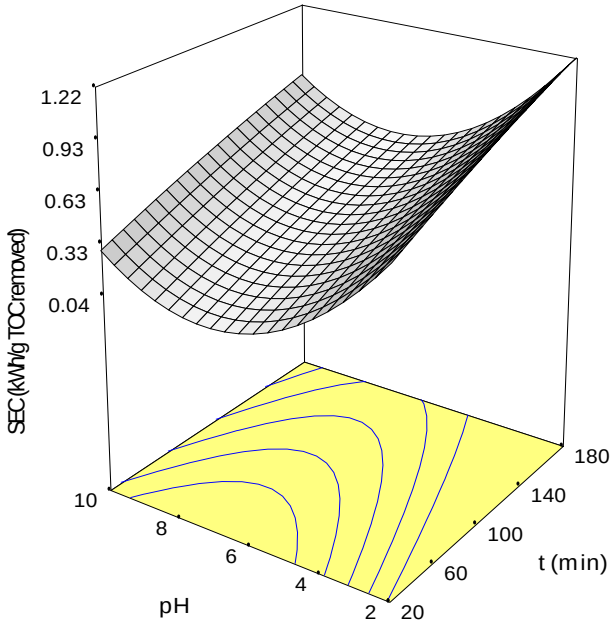

(e)

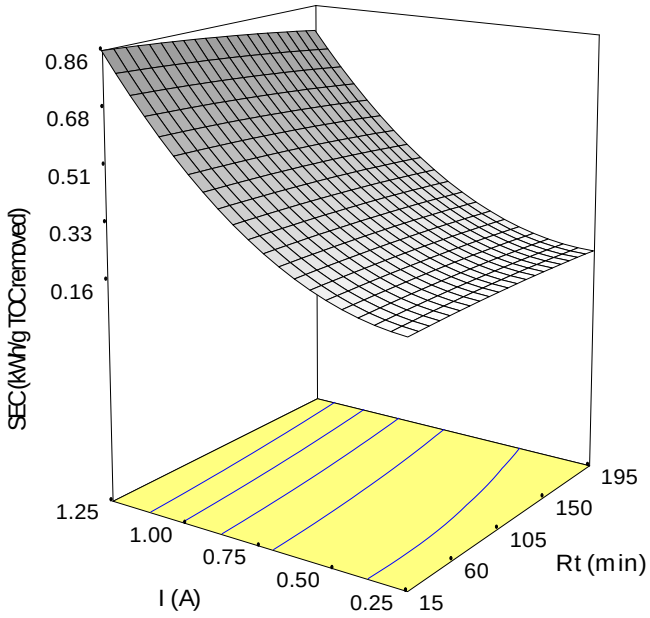

(f)

Fig. 4.35 (d – f). 3D response surface graphs for SEC (kW h (g TOC removed)$^{-1}$) as a function of independent variables pH, *I*, *t* and R_T.

The operating conditions for continuous EO treatment were optimized in order to achieve maximum %AMT and %TOC removal, and minimum SEC (kW h (g TOC removed)$^{-1}$). The optimum condition achieved by RSM for given target was: pH = 7.53, I = 0.7 A, R_T = 175.6 min, and t = 128.89 min. The values of responses at this condition were predicted by RSM as: Z_1 = 52.86%, Z_2 = 38.36% and Z_3 = 0.385 kW h (g TOC removed)$^{-1}$). In order to verify the suitability of this optimization, a set of three experiments was performed at the given optimum conditions. The mean values of responses thus obtained were: Z_1 = 51.64%, Z_2 = 37.82% and Z_3 = 0.408 kWh (g TOC removed)$^{-1}$). The experimental values of responses were found to be in good agreement with their predicted values, thus validating the optimization analysis done by RSM.

The mineralization current efficiency (%MCE) of continuous EO process was calculated for optimum run using Eq. 3.6. The computed value of MCE for experiment conducted at optimum conditions came out to be 9.81%, implying that this much part of total current supplied to the EO cell was utilized in mineralization of AMT, and the rest was consumed in side reactions occurring during the treatment process.

4.5.3. Decay Kinetics in Continuous EO Treatment

A continuous EO experiment was run at optimum conditions (pH = 7.53, I = 0.7 A, R_T = 175.6 min, t = 128.89 min), and 10 mL samples of synthetic wastewater were collected from the reactor outlet after fixed intervals of time, for studying the AMT and TOC decay kinetics using modified equations (Eqs. 4.27 and 4.28) of pseudo-first order kinetic model (Lucas and Perez, 2009). Marquardt's percent standard deviation (MPSD) (Eq. 4.20) was employed as an error function to fit the experimental data using non – linear regression (Marquardt, 1963). C_{Rt} values in Eq. 4.20 were replaced by TOC_{Rt} values to compute the error function corresponding to TOC removal kinetics.

The AMT and TOC removal data obtained at optimum conditions for continuous EO was fitted on to pseudo-first order kinetic model according to Eqs. 4.27 and 4.28, and is demonstrated in Fig. 4.36. R^2 value was found to be 0.998 for both AMT and TOC removal, which substantiates the fit of pseudo-first order kinetic model. Moreover, MPSD values were as low as 6.87 and 9.84 for AMT and TOC removal, respectively, adding to the validation of the kinetic model. The values of k_f were found to be 4.4 × 10^{-2} min^{-1} (AMT removal) and 9.1 × 10^{-3} min^{-1} (TOC removal). This signifies that AMT removal from the synthetic wastewater was almost five times faster than TOC removal using Ti/RuO_2 electrodes in continuous EO method.

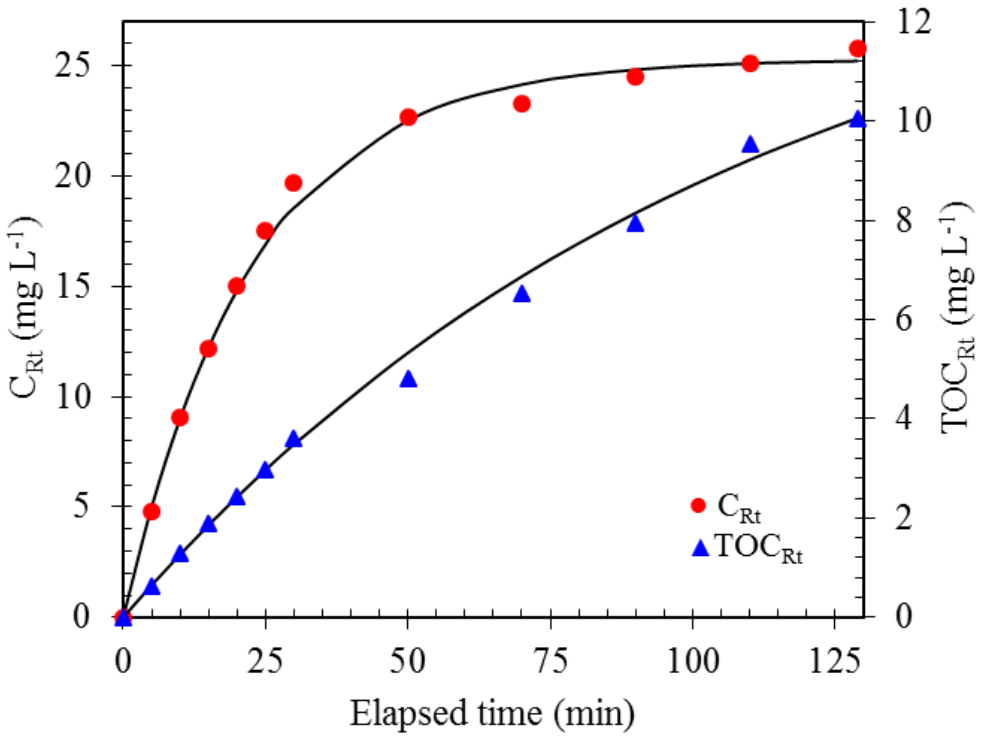

Fig. 4.36. Kinetics of TOC and AMT removal at optimum condition of continuous EO treatment.

As discussed earlier, EO is a complex process involving a number of oxidants and their reactions with organic pollutants. Ti/RuO_2 anodes majorly demonstrate active behavior resulting in to oxidation or electrochemical conversion of pollutant species. The reaction intermediates thus formed further undergo oxidation and break into organic entities with lower molecular weights. The process continues till their mineralization, i.e. conversion to CO_2. Hence, TOC removal process was found to be slower as compared to degradation of target pollutant.

4.5.4. Identification of Transformation Products and Proposed Degradation Pathway

In order to degrade and mineralize the target pollutant, there are a number of reactions taking place at the anode and in the bulk solution during EO process, resulting in to formation of different reaction intermediates. Degradation of AMT by Ti/RuO_2 electrodes also resulted in to formation of certain reaction intermediates (ARIs), which were identified by subjecting the samples collected during optimum run to UPLC-Q-TOF-MS analysis (Table 4.11). Subsequently, a plausible AMT degradation pathway was proposed (Fig. 4.40).

The retention time of AMT was 0.93 min (Fig. 4.37). The corresponding mass spectra of initial sample yielded signals at mass/charge ratio (*m/z*) values of 366 and 388, corresponding to protonated AMT molecule $[M + H]^+$ and its sodium adduct $[M + Na]^+$, respectively. Signals at *m/z* values of 349, 208 and 160 corresponding to three AMT fragments $[M – NH_3 + H]^+$, $[M – C_6H_{10}N_2O_3 + H]^+$ and $[M – C_{10}H_{10}N_2O_3 + H]^+$, respectively, were also detected (Fig. 4.38). These fragments were formed as a consequence of loss of amine group and opening of β-lactam ring of AMT molecule. The UPLC chromatograms of samples extracted from the reactor after 15 and 30 min (Fig. 4.39a and b) of electrolysis revealed the presence of 8 ARIs (ARI 1 – ARI 8). The details of retention time, *m/z* ratio, elemental composition and proposed structure of these ARIs are presented in Table 4.11. In batch electrolysis of synthetic wastewater comprising AMT using Ti/RuO_2 electrodes (Section 4.3.5), revealed the presence of three major reaction intermediates. However, in present study, out of 8 ARIs detected during continuous EO of AMT, two were found to be similar as reported earlier (corresponding to *m/z* ratio = 339 and 269), and 6 of them were detected only during continuous EO treatment of AMT. Based on the identified ARIs, a tentative degradation scheme of AMT antibiotic was derived and is shown in Fig. 4.40.The degradation of AMT on Ti/RuO_2 electrodes followed different routes such as direct anodic oxidation via hydroxylation and decarboxylation, and opening of β-lactam ring via indirect oxidation.

4.5.4.1. Direct anodic oxidation: In direct anodic degradation, electron transfer from the Ti/RuO_2 anode to the AMT molecule adsorbed on to its surface took place, leading to its degradation/mineralization according to Eq. 4.38.

$$Ti/RuO_2 + AMT \rightarrow Ti/RuO_2.(AMT)_{ads} \rightarrow nCO_2 + \text{other degradation products} + zH^+ \qquad \textbf{(4.38)}$$

Apart from direct electron transfer to AMT molecule, its degradation occurred through highly reactive hydroxyl radicals. Direct oxidation via hydroxylation of AMT led to its de-alkylation and formation of ARI 1 (*m/z* 368). Subsequent hydroxylation and decarboxylation

of ARI 1 generated ARI 5 (*m/z* 340). ARI 2 (*m/z* 453) was formed by attack of multiple hydroxyl radicals on different bonds of AMT molecule resulting in to its demethylation.

4.5.4.2. Indirect oxidation via opening of β-lactam ring: In another route of degradation pathway, attack of hydroxyl radicals and active chlorine on AMT molecule resulted in its β-lactam ring opening and decarboxylation, respectively, and thus forming ARI 4 (*m/z* 412). Subsequent hydroxylation and replacement of entire aromatic moiety of ARI 4 led to ARI 7 (*m/z* 300). Furthermore, the instability of ARI 4 molecule and action of active oxygen yielded ARI 8 (*m/z* 334). Alternatively, combined attack of active oxygen and active chlorine species on ARI 5 also resulted in to formation of ARI 8. Loss of amine ($-NH_3$) group and decarboxylation by active chlorine from AMT molecule consequently formed ARI 3 (*m/z* 339). Replacement of entire aromatic moiety by Cl^- in ARI 3 resulted in generation of ARI 6 (*m/z* 269). Further attack of hydroxyl radicals, would lead to mineralization of the reaction intermediates (ARI 1 – 8) to CO_2 and inorganic ions such as SO_4^{2-} and NH_4^+.

4.5.4.3. Direct cathodic reduction: The chlorinated ARIs (R−Cl) (ARI 3, 4, 6 and 8) would further undergo cathodic degradation, through hydrogen generated due to water dissociation (Eq. 4.29) and chemisorbed on to cathode surface, leading to their de-chlorination according to Eqs. 4.30 and 4.31. The reduced entities would further undergo either direct anodic oxidation or indirect oxidation in the bulk via different chloro-oxidant species, further lowering the amount of TOC in the wastewater.

Possible degradation routes of AMT by EO using non-active anodes such as Ti_4O_7 and BDD were explored by Ganiyu et al., 2016 and Frontistis et al., 2017. In both the cases, hydroxylation via physisorbed •OH, was clearly the prime force behind degradation and mineralization of AMT antibiotic. However, in present work active chlorine and hydroxyl radicals, both play their parts in AMT abatement process. Degradation by EO thus follows different routes depending on the type of electrode employed for the purpose.

4.5.5. Operating Cost Analysis

The operating cost of continuous EO treatment o synthetic wastewater comprising AMT was calculated on the basis of two major costs: (1) cost of electrical energy consumed (C_{EE}) (2) cost of anodes (C_{EL}). During optimum run of continuous EO treatment, 0.385 kW h of energy was consumed for removing 1 g of TOC from wastewater. The average cost of electrical energy in Punjab, India is INR 5 per kW h. Therefore, the cost of electrical energy

consumption (C_{EE}) came out to be INR 1.92. As per manufacturer's claim, Ti/RuO_2 anodes possess a life of 2.5 years if operated under the optimum condition (I = 0.7 A, pH = 7.53). Two Ti/RuO_2 plates served as anode during EO treatment, each costing INR 2,500. As 38.36% of TOC abatement was achieved during optimum run in ≈129 min of continuous EO, the cost of electrodes (C_{EL}) came out to be 54.58 INR .The total operating cost will therefore be (C_{EE} + C_{EL}) INR 56.5(US $ 0.87).

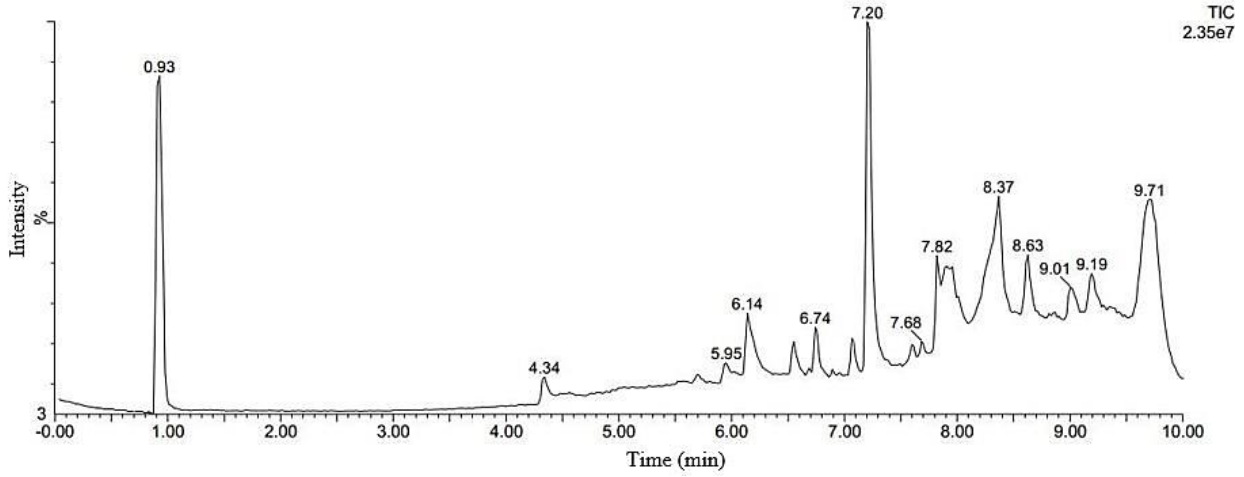

Fig. 4.37 UPLC-Q-TOF-MS chromatogram of AMT (Retention time = 0.93 min).

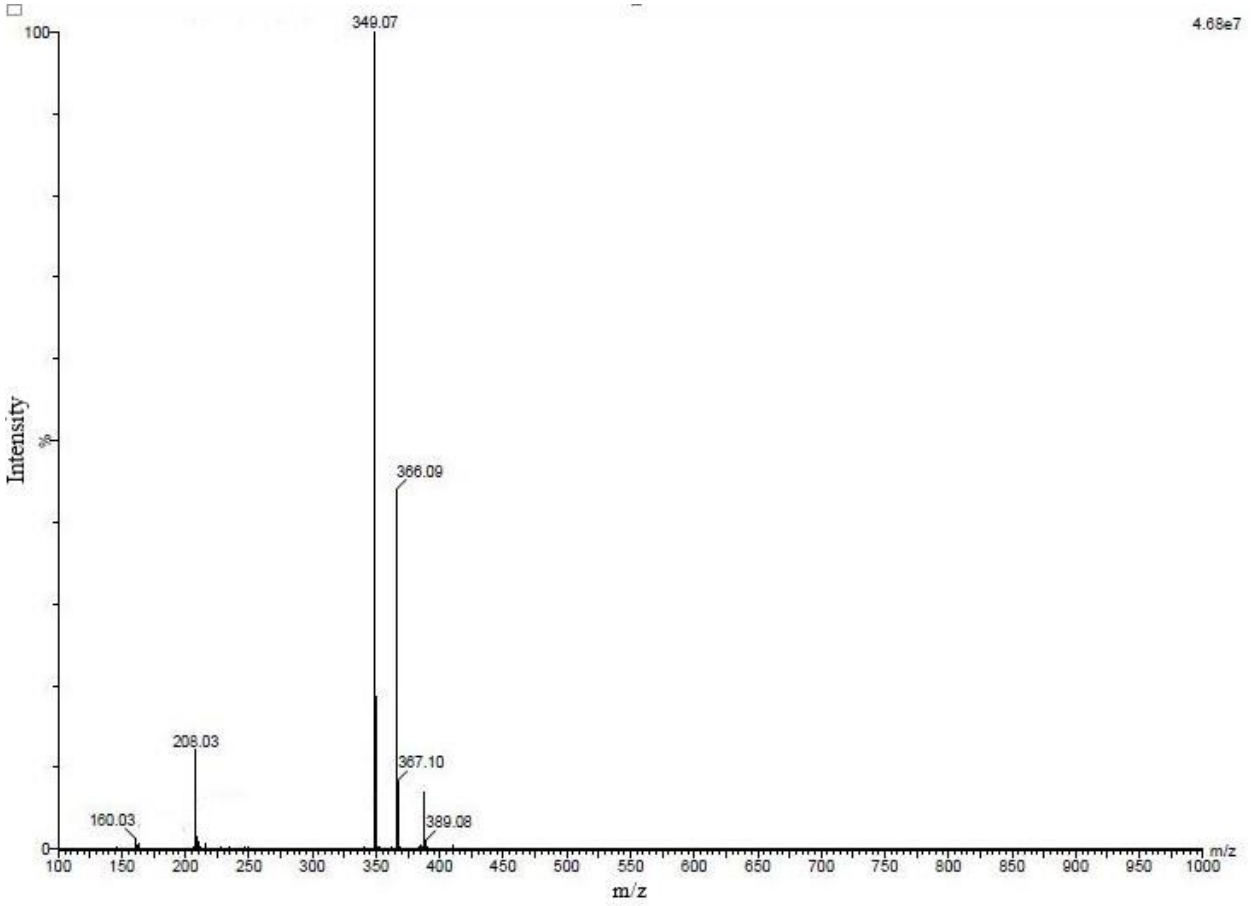

Fig. 4.38 Mass spectrum of AMT (m/z $[M+H]^+$ = 366).

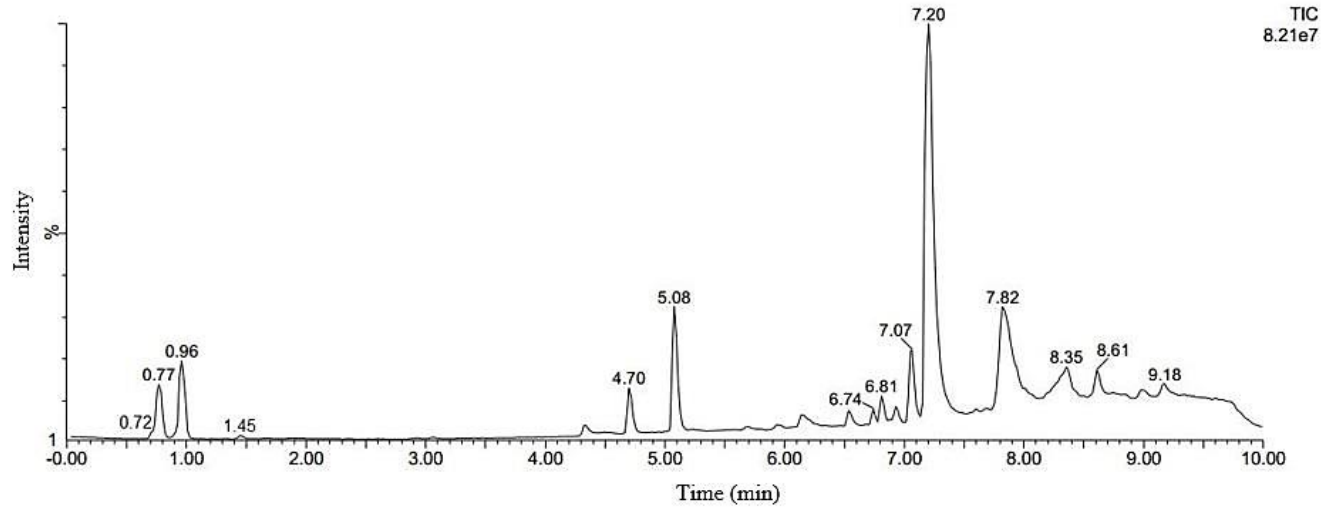

(a)

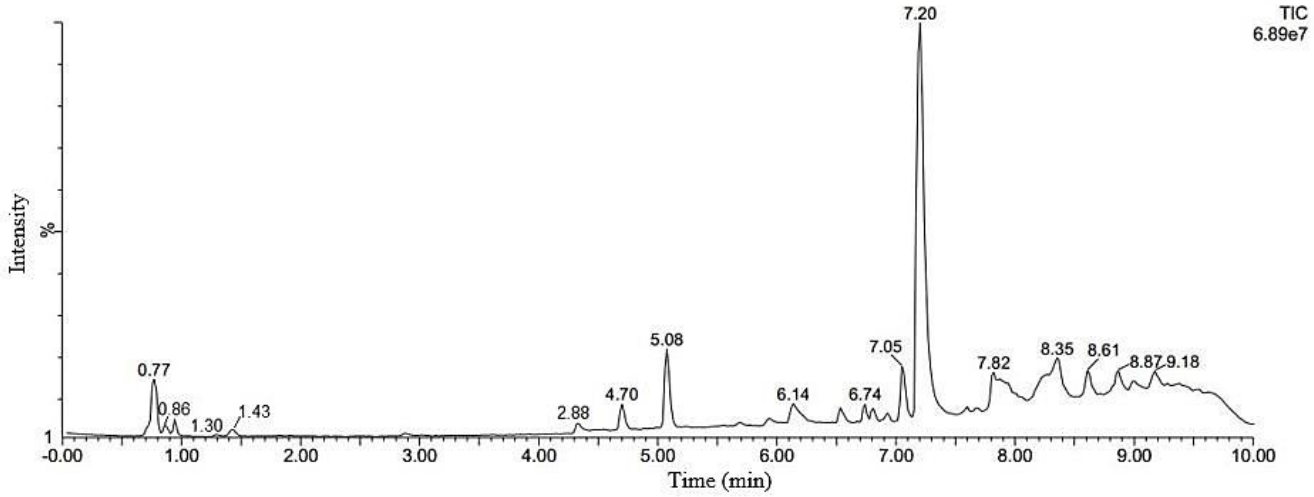

(b)

Fig. 4.39. UPLC-Q-TOF chromatograms of samples taken after (a) 15 min and (b) 30 min of continuous EO treatment of AMT wastewater.

Table 4.12. Major AMT reaction intermediates (ARIs) formed during continuous EO process.

Compound	R_t (min)	*m/z* $[M+H]^+$	Elemental composition	Proposed Structure
ARI 1	1.30	368	$C_{15}H_{17}N_3O_6S$	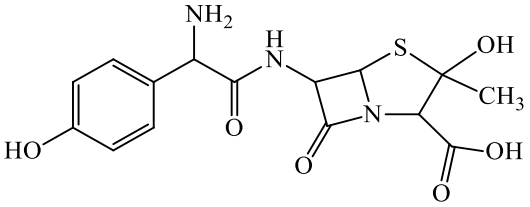
ARI 2	4.70	453	$C_{14}H_{18}N_3O_{12}S$	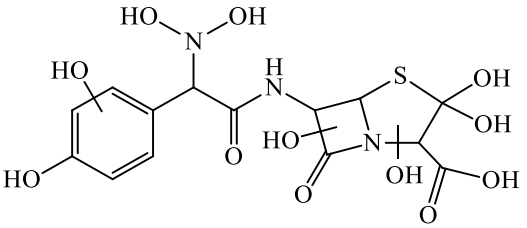
ARI 3	0.72	339	$C_{15}H_{15}ClN_2O_3S$	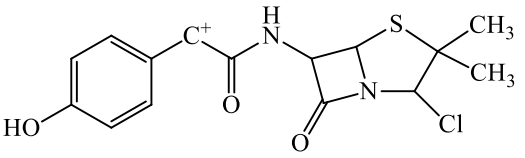
ARI 4	0.86	412	$C_{15}H_{15}Cl_2N_3O_6S$	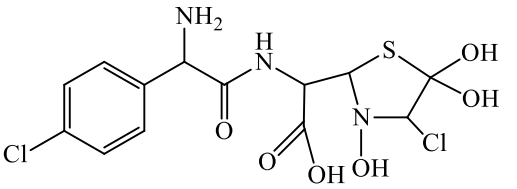
ARI 5	5.08	340	$C_{14}H_{17}N_3O_5S$	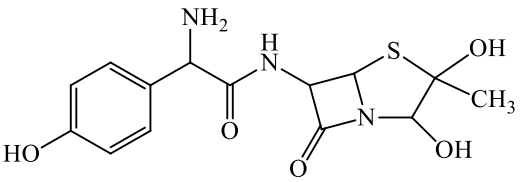
ARI 6	0.77	269	$C_8H_{10}Cl_2N_2O_2S$	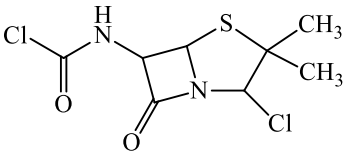
ARI 7	1.45	300	$C_7H_{13}N_3O_8S$	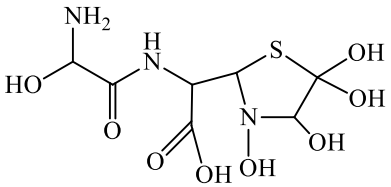
ARI 8	2.88	334	$C_{12}H_{16}ClN_3O_4S$	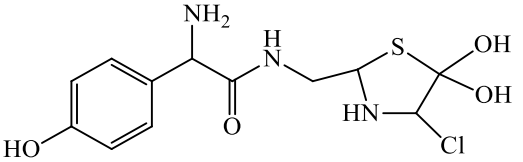

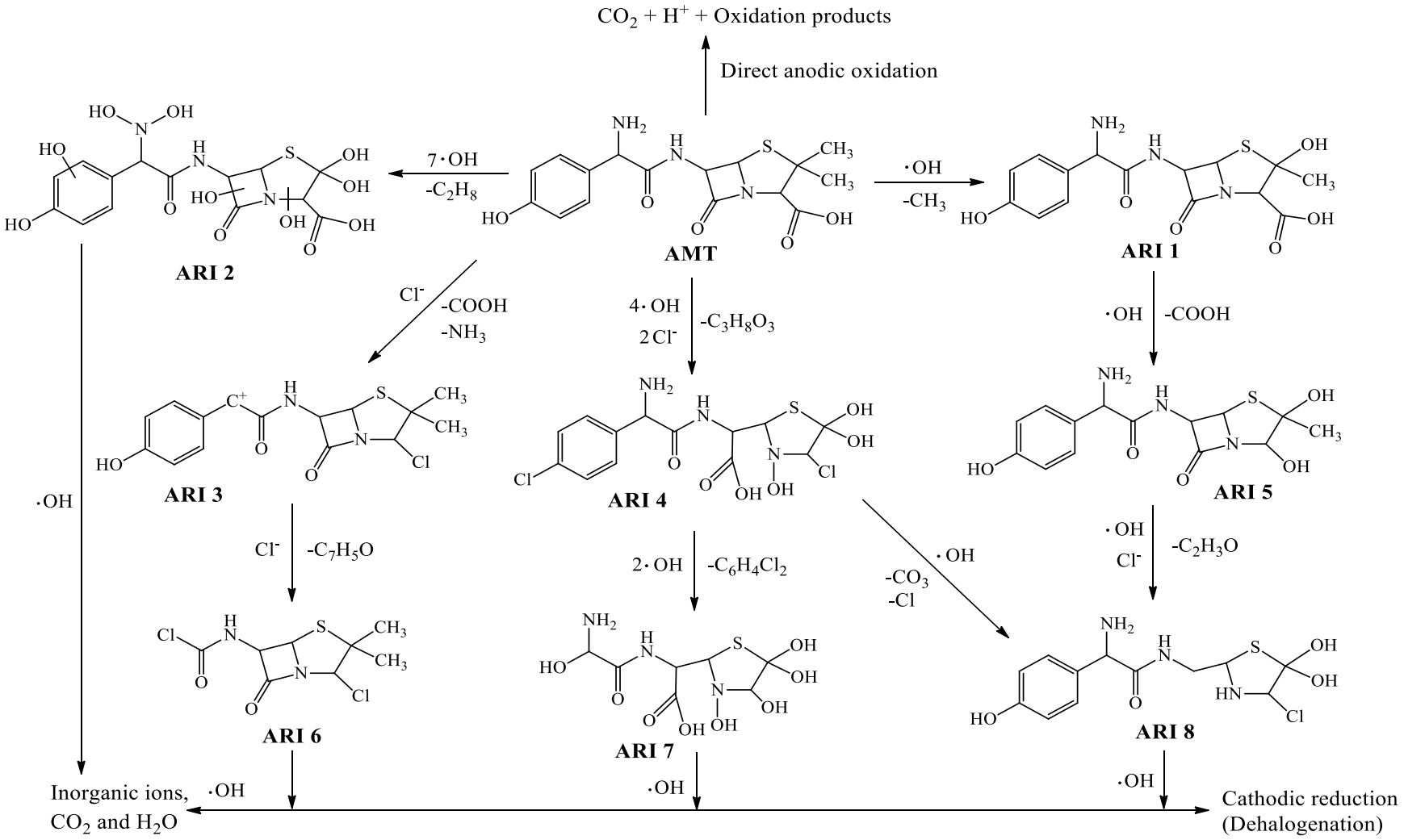

Fig. 4.40. Plausible degradation mechanism of AMT during continuous EO treatment.

4.6. CHARACTERIZATION OF Ti/RuO_2 ELECTRODES

In order to study the effect of EO treatment on electrode material, physico-chemical characterization of fresh Ti/RuO_2 anode and used Ti/RuO_2 anode (after all sets of experiments) was performed. The characterization techniques used for the purpose were: SEM, EDX and XRD.

The composition and surface morphology of Ti/RuO_2 anode before and after its usage for EO treatment of synthetic pharmaceutical wastewater comprising antibiotics was determined using SEM and EDX. The morphology of anode was found to be similar in both the cases (Fig. 4.41), however, diminutive loss of RuO_2 coating could be seen in SEM image (× 1000 magnification) of used electrode (Fig. 4.41b). Besides, the cracks in SEM image of electrode used in nearly 200 EO experiments were comparatively wider. EDX was used to study the elemental distribution on the surface of fresh and used Ti/RuO_2 anode. EDX study revealed the presence of Ti (34.09 %), Ru (12.49 %), O (44.54%) and C (3.26 %) on the surface of fresh anode as shown in Fig. 4.42a. EDX analysis of used anode showed the presence of Ti (29.88 %), Ru (9.22 %), O (40.34 %) and C (15.14 %) (Fig. 4.42b). Loss in % weight of Ti and Ru elements is evident in case of EDX analysis of used anode, which explains anode's limited life of 2.5 years. However, there is significant increase in amount of carbon content on anode surface after EO treatment, which signifies degradation/mineralization of organic contaminants.

The micro structure of anode material was studied using X-ray diffraction (XRD). The XRD pattern of fresh and used Ti/RuO_2 anode is shown in Fig. 4.43. Ti, RuO_2 and TiO_2 rich broad and symmetric peaks were attained (Nan et al., 1994; Zubavichus et al., 2002). The intensity of peaks is slightly less in case of used electrode, however, peak positions remain intact, signifying unaltered micro structure of Ti/RuO_2 anode after its usage for wastewater treatment. Moreover, it indicates that the RuO_2 coating on Ti plate was stable after even 200 EO experiments performed in batch and continuous reactor for degradation of antibiotics.

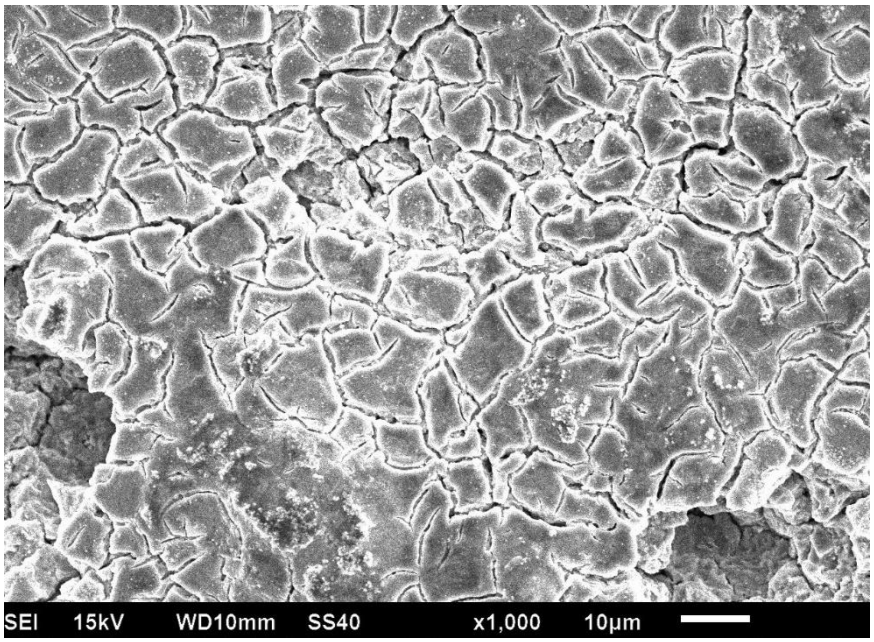

(a)

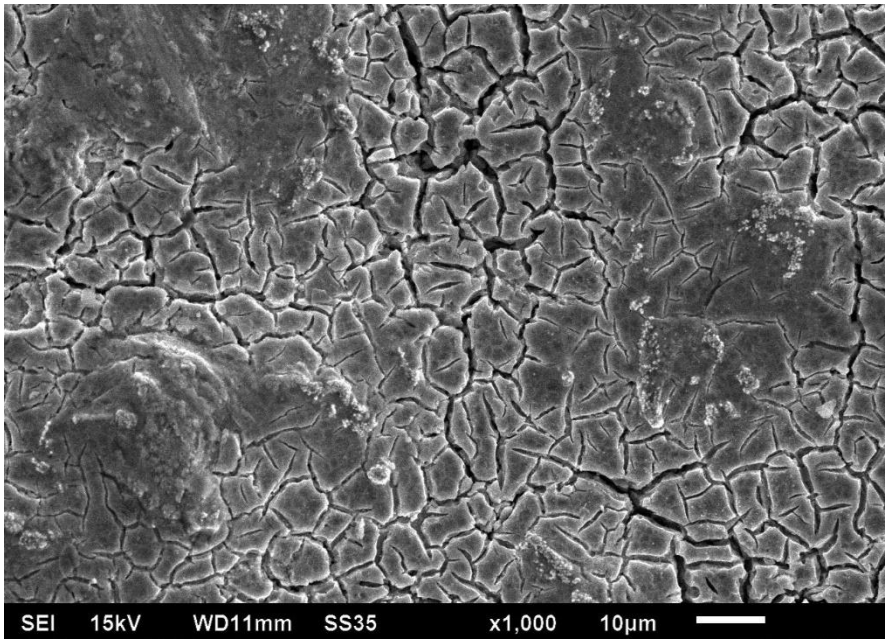

(b)

Fig. 4.41. SEM images of (a) fresh Ti/RuO_2 anode and (b) used Ti/RuO_2 anode.

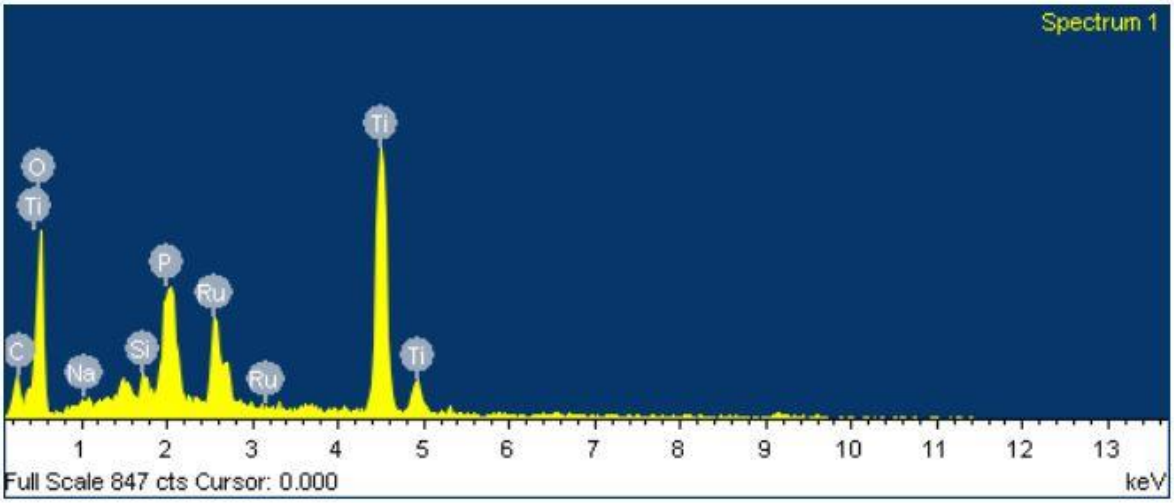

(a)

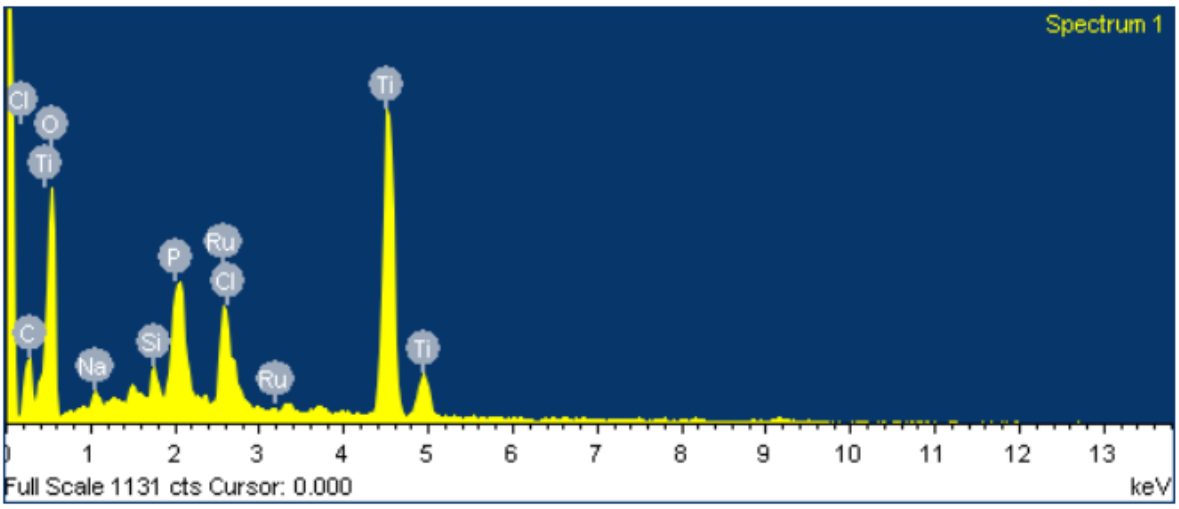

(b)

Fig. 4.42. EDX spectrum of (a) fresh Ti/RuO_2 anode and (b) used Ti/RuO_2 anode.

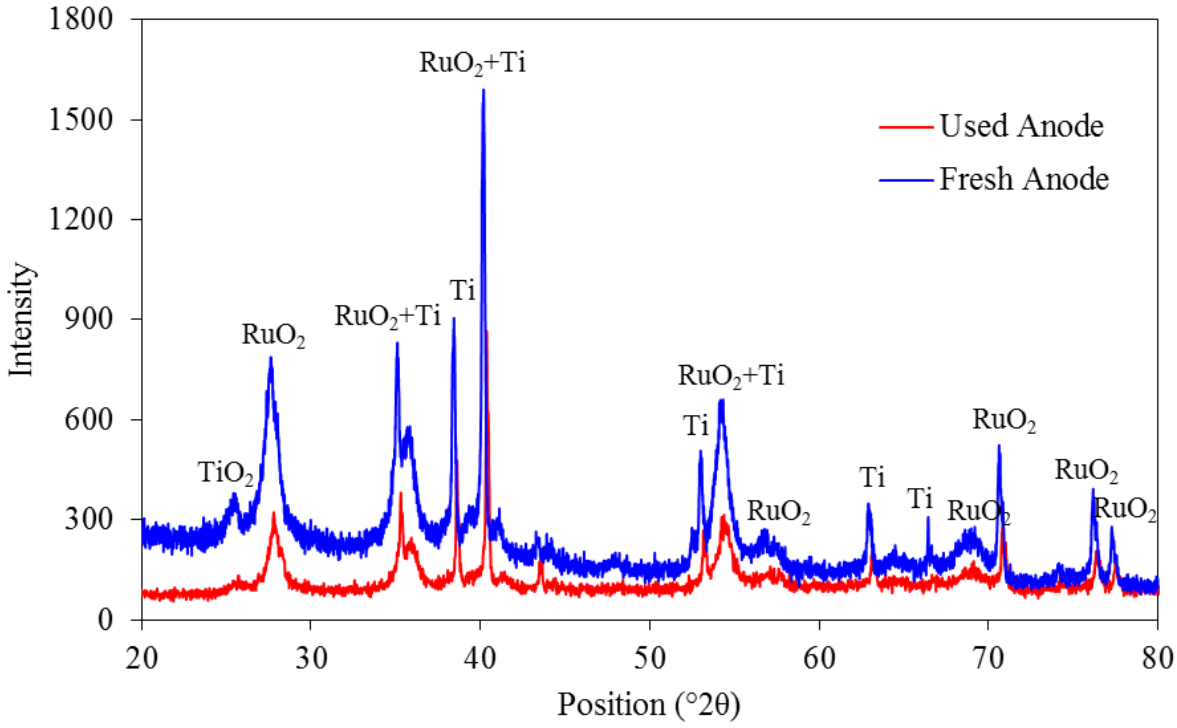

Fig. 4.43 XRD patterns of fresh and used Ti/RuO_2 anode.

Chapter – 5

CONCLUSION

On the basis of results obtained from the present study of EO treatment of pharmaceutical wastewater comprising antibiotics, following major conclusions were drawn.

5.1. BATCH ELECTRO-OXIDATION

- Highly acidic pH favoured OFLX degradation/transformation, while maximum mineralization was achieved at neutral pH. However, in case of AMT, both degradation and mineralization were maximum in case of neutral pH. Therefore, the optimum pH was found to be the neutral pH. The mineralization of antibiotics at neutral pH was achieved chiefly by direct oxidation via physisorbed •OH on Ti/RuO_2 anode, and mediated oxidation via HOCl, ClO^-, H_2O_2 and HO_2•.
- Increase in applied current increased the degradation efficiency of EO cell by generating extra oxidant species. However, the MCE decreased in case of EO treatment of both OFLX and AMT, with the increase in applied current. This could be attributed to the amplification in undesirable but inevitable reactions like oxygen and hydrogen evolution taking place during electrolysis. Therefore, a significant part of applied current was consumed by these reactions.
- Increase in NaCl amount improved the conductivity of wastewater and boosted the drug degradation via generating higher amount of active chlorine species through Ti/RuO_2 anodes. With the increase in S_0, SEC value for EO treatment significantly decreased because of decrease in average cell potential. Furthermore, MCE value was enhanced with increase in S_0 value due to improvement in mineralization of EO cell.
- At optimum condition of OFLX degradation (pH = 6.8 ± 0.1, I = 1 A, S_0 = 2 g L^{-1}), 80% ARE and 46.3% TRE were achieved in 30 and 240 min of EO treatment, respectively. Similarly, at optimum condition of AMT degradation (pH = 7, I = 1 A, S_0 = 2 g L^{-1}), 60% ARE and 48% TRE were achieved in 60 and 240 min of EO treatment, respectively.

- Degradation of antibiotics always followed pseudo-first order kinetics. The value of rate constant k_f increased with the increase in applied current because of rapid degradation by increased number of oxidant species at higher current. The ratio of oxidant species to substrate concentration decreased with the increase in antibiotic concentration, thus resulting in decrease in values of k_f.
- The operating cost of batch EO treatment of antibiotics using two Ti/RuO_2 anodes came out to be INR 38.38 (OFLX) and INR 28.88 (AMT) for 1 g TOC removal.
- UPLC-Q-TOF-MS analysis of treated sample of OFLX wastewater revealed the presence of 7 major transformation products formed during its EO treatment by Ti/RuO_2 electrodes. However, in case of EO treatment of AMT, 3 major reaction intermediates were detected. Based on these reaction intermediates, plausible degradation pathways for both the antibiotics were proposed.
- Degradation of OFLX followed the route of de-fluorination, breaking of piperazinyl ring and further dealkylation or replacement by •OH or Cl^-.
- Attack of active chlorine on aromatic moiety and subsequent hydroxylation of AMT molecule by active oxygen lead to degradation of AMT.

5.2. CONTINUOUS ELECTRO-OXIDATION

- Continuous EO treatment experiments were performed based on CCD by RSM. ANOVA revealed that quadratic model best fitted the experimental data obtained for antibiotic removal (OFLX and AMT) (Z_1), TOC removal (Z_2) and SEC (Z_3). The experimental data obtained at optimum conditions identified by RSM were found to be in good agreement with the response values predicted by RSM.
- Optimum condition determined by RSM for in order to achieve maximum Z_1 and Z_2 and minimum Z_3 for OFLX antibiotic was: pH = 6.0, I = 0.64 A, R_T = 157.68 min and t = 170 min. OFLX removal efficiency of 76.78%, TOC removal efficiency of 23.85% and SEC value of 0.706 kW h (g TOC removed)$^{-1}$ were attained at optimum conditions of continuous EO treatment.
- In case of AMT antibiotic, the optimum condition given by RSM was: pH = 7.53, I = 0.7 A, R_T = 175.6 min and t = 128.89 min; for which the response values came out to be: AMT removal = 51.64%, TOC removal = 37.82% and SEC = 0.408 kW h (g TOC removed)$^{-1}$.

- During EO continuous treatment, both antibiotic removal and TOC removal followed pseudo-first order kinetics in case of both the antibiotics. However, the k_f values revealed that antibiotic degradation was almost five times faster than TOC abatement.
- According to data obtained for optimum runs, the operating costs of continuous treatment of antibiotics came out to be: INR 102.69 (OFLX) and INR 56.5 (AMT) for 1 g TOC removal for 1 g TOC removal.
- UPLC-Q-TOF-MS analysis of treated sample of OFLX wastewater in continuous EO cell revealed the presence of 7 major transformation products of the antibiotic. The degradation mechanism of OFLX followed direct oxidation via hydroxylation and de-fluorination; or indirect oxidation via decarboxylation and hydroxylation. The chlorinated transformation products underwent cathodic reduction at Ti/RuO_2 cathode.
- In case of AMT degradation in continuous EO cell, 8 major transformation products were identified. Apart from direct anodic oxidation of AMT molecule via generated •OH radicals, indirect oxidation via active chlorine led to opening of its beta-lactam ring. The chlorinated species further got reduced at the Ti/RuO_2 cathode surface.

FUTURE RECOMMENDATION

- Toxicity study of degradation by-products in treated effluent from EO treatment cell should be performed in order to its disposability.
- Applicability of Ti/RuO_2 electrodes for EO treatment of real pharmaceutical wastewater should be studied.
- Since the drugs, in this study, are not completely mineralized and present in its degraded from, the EO treatment in combination with other advanced oxidation method is recommended.

REFERENCES

Anglada, A., Urtiaga, A., Ortiz, I., 2009. Contributions of electrochemical oxidation to waste-water treatment: fundamentals and review of applications. Journal of Chemical Technology and Biotechnology 84, 1747–1755.

Baghel, R., Upadhyaya, S., Chaurasia, S.P., Singh, K., Kalla, S., 2018. Optimization of process variables by the application of response surface methodology for naphthol blue black dye removal in vacuum membrane distillation, Journal of Cleaner Production, 199, 900-915.

Behera, S.K., Kim, H.W., Oh, J.E., Park, H.S., 2011. Occurrence and removal of antibiotics, hormones and several other pharmaceuticals in wastewater treatment plants of the largest industrial city of Korea. Science of the Total Environment 409, 4351-4360.

Benito-Pena, E., Partal-Rodera, A.I., Leon-Gonzalez, M.E., Moreno-Bondi, M.C., 2006. Evaluation of mixed mode solid phase extraction cartridges for the pre-concentration of beta-lactam antibiotics in wastewater using liquid chromatography with UV-DAD detection. Analytica Chimica Acta 556, 415– 422.

Bocos, E., Oturan, N., Sanroman, M.A., Oturan, M.A., 2016. Elimination of radiocontrast agent diatrizoic acid from water by electrochemical advanced oxidation: Kinetics study, mechanism and mineralization pathway. Journal of Electroanalytical Chemistry 772, 1–8.

Bocos, E., Pazos, M., Sanromán, M. A., 2014. Electro-Fenton decolourization of dyes in batch mode by the use of catalytic activity of iron loaded hydrogels. Journal of Chemical Technology & Biotechnology, 89(8), 1235-1242.

Bocos, E., Pérez-Álvarez, D., Pazos, M., Rodríguez-Argüelles, M. C., Sanromán, M. Á. 2016. Coated nickel foam electrode for the implementation of continuous electro-Fenton treatment. Journal of Chemical Technology & Biotechnology, 91(3), 685-692.

Boudreau, J., Bejan, D., Bunce, N. J., 2010b. Competition between electrochemical advanced oxidation and electrochemical hypochlorination of acetaminophen at

boron-doped diamond and ruthenium dioxide based anodes. Canadian Journal of Chemistry 88, 418- 425.

Boudreau, J., Bejan, D., Li, S., Bunce, N. J., 2010a. Competition between electrochemical advanced oxidation and electrochemical hypochlorination of sulfamethoxazole at a boron-doped diamond anode. Industrial and Engineering Chemistry Research 49, 2537 – 2542.

Brillas, E., 2014, Electro-Fenton, UVA Photoelectro-Fenton and Solar Photoelectro-Fenton Treatments of Organics in Waters Using a Boron-Doped Diamond Anode: A Review. Journal of Mexican Chemical Society 58(3), 239-25.

Brillas, E., Garcia-Segura, S., Skoumal, M., Arias, C., 2010. Electrochemical incineration of diclofenac in neutral aqueous medium by anodic oxidation using Pt and boron-doped diamond anodes. Chemosphere 79, 605-612.

Brillas, E., Martinez-Huitle, C.A., 2015. Decontamination of wastewaters containing synthetic organic dyes by electrochemical methods. An update. Rev. Applied Catalysis B: Environmental 166–167, 603–643.

Brillas, E., Sires, I., Arias, C., Cabot, P. L., Centellas, F., Rodriguez, R. M., Garrido, J. A., 2005. Mineralization of paracetamol in aqueous medium by anodic oxidation with a boron- doped diamond electrode. Chemosphere 58, 399-406.

Brinzilla, C.I., Pacheco, M.J., Ciriaco, L., Ciobanu, R.C., Lopes, A., 2012. Electrodegradation of tetracycline on BDD anode. Chemical Engineering Journal 209, 54–61.

Brown, K.D., Kulis, J., Thomson, B., Chapman, T.H., Mawhinney, D.B., 2006. Occurrence of 24 antibiotics in hospital, residential, and dairy effluent, municipal wastewater, and the Rio Grande in New Mexico. Science of the Total Environment 366, 772–783.

Cannizares, P., Martinez, F., Jimenez, C., Lobato, J., Rodrigo, M.A., 2006. Coagulation and electrocoagulation of wastes polluted with dyes. Environmental Science and Technology 40(20), 6418 – 6424.

Cavalcanti, E.B., Garcia–Segura, S., Centellas, F., Brillas, E., 2013. Electrochemical incineration of omeprazole in neutral aqueous medium using a platinum or boron-

doped diamond anode: Degradation kinetics and oxidation products. Water Research 47, 1803–1815.

CDDEP, 2015. The State of the World's Antibiotics, 2015. Washington DC: Center for Disease Dynamics, Economics & Policy, 2015.

Cha, J.M., Yang, S., Carlson, K.H., 2006. Trace determination of β-lactam antibiotics in surface water and urban wastewater using liquid chromatography combined with electrospray tandem mass spectrometry. Journal of Chromatography A 1115, 46 – 57.

Chen, G., 2004. Electrochemical technologies in wastewater treatment. Separation and Purification Technology 38, 11-41.

Chen, T.S., Kuo, Y.M., Chen, J.L., Huang, K.L., 2013. Anodic degradation of ofloxacin on a boron-doped diamond electrode. International Journal of Electrochemical Science 8, 7625-7633.

Ciriaco, L., Anjo, C., Correia, J., Pacheco, M.J., Lopes, L., 2009. Electrochemical degradation of Ibuprofen on Ti/Pt/PbO_2 and Si/BDD electrodes. Electrochimica Acta 54, 1464–1472.

Comninellis, C., 1994. Electrocatalysis in the electrochemical conversion of organic pollutants for wastewater treatment. Electrochimica Acta 39, 1857–1862.

Coria, G., Nava, J.L., Carreno, G., 2014. Electrooxidation of diclofenac in synthetic pharmaceutical wastewater using an electrochemical reactor equipped with a boron doped diamond electrode. Journal of Mexican Chemical Society 58(3), 303-308.

Costanzo, S.D., Murby, J., Bates, J., 2005. Ecosystem response to antibiotics entering the aquatic environment. Marine Pollution Bulletin 51, 218 – 223.

Da Silva, S.W., Navarro, E.M.O., Rodrigues, M.A.S., Bernardes, A.M., Perez-Herranz, V., 2019. Using p-Si/BDD anode for the electrochemical oxidation of norfloxacin. Journal of Electroanalytical Chemistry 832, 112–120.

De Amorim, K.P., Romualdo, L.L., Andrade, L.S., 2013. Electrochemical degradation of sulfamethoxazole and trimethoprim at boron-doped diamond electrode:

Performance, kinetics and reaction pathway. Separation and Purification Technology 120, 319-327.

De Amorim, K.P., Romualdo, L.L., Andrade, L.S., 2014. Performance and kinetic-mechanistic aspects in the electrochemical degradation of sulfadiazine on boron-doped diamond electrode. Journal of Brazilian Chemical Society 25(8), 1484 – 1492.

De Vidales, M.J.M., Robles-Molina, J., Dominguez-Romero, J.C., Canizares, P., Saez, C., Molina-Diaz, A., Rodrigo, M.A., 2012. Removal of sulfamethoxazole from waters and wastewaters by conductive-diamond electrochemical oxidation. Journal of Chemical Technology and Biotechnology 87, 1441 – 1449.

Deborde, M., and Von Gunten, U., 2008. Reactions of chlorine with inorganic and organic compounds during water treatment-kinetics and mechanisms: a critical review. Water Research 42, 13-51.

Dirany, A., Sires, I., Oturan, N., Oturan, M.A., 2010. Electrochemical abatement of the antibiotic sulfamethoxazole from water. Chemosphere 81, 594–602.

Diwan, V, Tamhankar, A.J., Aggarwal, M., Sen, S., Khandal, R.K., Stalsby-Lundborg, C., 2009. Detection of antibiotics in hospital effluents in India. Current Science 97, 1752–1755.

Dominguez, J.R., Gonzalez, T., Palo, P., Sanchez-Martin, J., 2010. Anodic oxidation of ketoprofen on boron-doped diamond (BDD) electrodes. Role of operative parameters. Chemical Engineering Journal 162, 1012–1018.

El-Ghenymy, A., Cabot, P. L., Centellas, F., Garrido, J. A., Rodriguez, R. M., Arias, C., Brillas, E., 2013b. Electrochemical incineration of the antimicrobial sulfamethazine at a boron-doped diamond anode. Electrochimica Acta 90, 254-264.

El-Ghenymy, A., Garrido, J.A., Rodriguez, R.M., Cabot, P.L., Centellas, F., Arias, C., Brillas, E., 2013a. Degradation of sulfanilamide in acidic medium by anodic oxidation with a boron-doped diamond anode. Journal of Electroanalytical Chemistry 689, 149-157.

Fabianska, A., Bialk-Bielinska, A., Stepnowski, P., Stolte, S., Siedlecka, E.M., 2014. Electrochemical degradation of sulfonamides at BDD electrode: Kinetics, reaction pathway and eco-toxicity evaluation. Journal of Hazardous Materials 280, 579-587.

Feng, Y., Wang, C., Liu, J., Zhang, Z., 2010. Electrochemical degradation of 17-alpha-ethinylestradiol (EE2) and estrogenic activity changes. Journal of Environmental Monitoring 12, 404 – 408.

Fick, J., Soderstrom, H., Lindberg, R.H., Phan, C., Tysklind, M., Larsonn, D.G.J., 2009. Contamination of surface, ground, and drinking water from pharmaceutical production. Environmental Toxicology and Chemistry 28, 2522-2527.

Fill, B.A., Boncukcuoglu, R., Yilmaz, A.E., Bayar, S., 2014. Electro-oxidation of pistachio processing industry wastewater using graphite anode. Clean 42(9), 1232 – 1238.

Frontistis, Z., Antonopoulou, M., Venieri, D., Konstantinou, I., Mantzavinos, D., 2017. Boron- doped diamond oxidation of amoxicillin pharmaceutical formulation: Statistical evaluation of operating parameters, reaction pathways and antibacterial activity. Journal of Environmental Management 195, 100–109.

Gadipelly, C., Perez-Gonzalez, A., Yadav, G.D., Ortiz, I., Ibanez, R., Rathod, V.K., Marathe, K.V., 2014. Pharmaceutical industry wastewater: review of the technologies for water treatment and reuse. Industrial and Engineering Chemistry Research, 53, 11571–11592.

Ganiyu, S.O., Oturan, N., Raffy, S., Cretin, M., Esmilaire, R., Hullebusch, E.V., Esposito, G., Oturan, M.A., 2016. Sub-stoichiometric titanium oxide (Ti_4O_7) as a suitable ceramic anode for electrooxidation of organic pollutants: A case study of kinetics, mineralization and toxicity assessment of amoxicillin. Water Research 106, 171-182.

Ganzenko, O., Huguenot, D., Hullebusch, E.D., Esposito, G., Oturan, M.A., 2014. Electrochemical advanced oxidation and biological processes for wastewater treatment: a review of the combined approaches. Environmental Science and Pollution Research 21, 8493–8524.

Gonzalez T., Dominguez J.R., Palo P., Sanchez-Martin J., Cuerda-Correa E.M., 2011. Development and optimization of the BDD-electrochemical oxidation of the antibiotic trimethoprim in aqueous solution. Desalination 280, 197-202.

Goyal, A., Srivastava, V.C., 2017. Treatment of highly acidic wastewater containing high energetic compounds using dimensionally stable anode. Chemical Engineering Journal 325, 289–299.

Goyne, K.W., Chorover, J., Kubicki, J.D., Zimmerman, A.R., Brantley, S.L., 2005. Sorption of the antibiotic ofloxacin to mesoporous and nonporous alumina and silica. Journal of Colloidal Interface Science 283, 160-170.

Gros, M., Petrovik, M., Ginebreda, A., Barcelo, D., 2010. Removal of pharmaceuticals during wastewater treatment and environmental risk assessment using hazard indexes. Environment International 36, 15–26.

Guillette, L.J., Crain, D.A., Gunderson, M.P., Kools, S.A.E., Milnes, M.R., Orlando, E.F., Rooney, A.A., Woodward, A.R., 2000. Alligators and Endocrine Disrupting Contaminants: A Current Perspective, Integrative and Comparative Biology 40(3), 438–452.

Guinea, E., Brillas, E., Centellas, F., Canizares, P., Rodrigo, M.A., Saez, C., 2009. Oxidation of enrofloxacin with conductive-diamond electrochemical oxidation, ozonation and Fenton oxidation. A comparison. Water Research 43, 2131–2138.

Guinea, E., Garrido, J.A., Rodriguez, R.M., Cabot, P., Arias, C., Centellas, F., Brillas, E., 2010. Degradation of the fluoroquinolone enrofloxacin by electrochemical advanced oxidation processes based on hydrogen peroxide electrogeneration. Electrocimica Acta 55, 2101–2115.

Haidar, M., Dirany, A., Sires, I., Oturan, N., Oturan, M.A., 2013. Electrochemical degradation of the antibiotic sulfachloropyridazine by hydroxyl radicals generated at a BDD anode. Chemosphere 91, 1304–1309.

Heberer, T., 2002. Occurrence, fate, and removal of pharmaceutical residues in the aquatic environment: review of recent research data. Toxicology Letters 131, 5–17.

Hirsch, R., Ternes, T., Haberer, K., Kratz, K.L., 1999. Occurrence of antibiotics in the aquatic environment. Science of the Total Environment 225, 109–118.

Homem, V., Santos, L., 2011. Degradation and removal methods of antibiotics from aqueous matrices – A review. Journal of Environmental Management 92, 2304–2347.

Hussain, S., Gul, S., Steter, J.R., Miwa, D.W., Motheo, A.J., 2015. Route of electrochemical oxidation of the antibiotic sulfamethoxazole on a mixed oxide anode. Environmental Science and Pollution Research 22, 15004–15.

Jara, C.C., Fino, D., 2010. Cost optimization of the current density for electroxidation wastewater processes. Chemical Engineering Journal 160, 497–502.

Jara, C.C., Fino, D., Specchia, V., Saracco, G., Spinelli, P., 2007. Electrochemical removal of antibiotics from wastewaters. Applied Catalysis B 70, 479-487.

Jeong, J., Kim, C., Yoon, J., 2009. The effect of electrode material on the generation of oxidants and microbial inactivation in the electrochemical disinfection process. Water Research 43, 895–901.

Kakkar, M., Rogawski, L., 2013. Antibiotic Use and Residues in Chicken Meat and Milk Samples from Karnataka and Punjab, India. New Delhi, India: Public Health Foundation of India.

Kaur P., Sangal V. K., Kushwaha J. P., 2015. Modeling and evaluation of electro-oxidation of dye wastewater using artificial neural networks. RSC Advances 5, 34663–34671.

Kaur, P., Kushwaha, J.P., Sangal, V.K., 2017. Evaluation and disposability study of actual textile wastewater treatment by electro-oxidation method using Ti/RuO_2 anode. Process safety and Environmental Protection 111, 13–22.

Kaur, P., Kushwaha, J.P., Sangal, V.K., 2018. Electrocatalytic oxidative treatment of real textile wastewater in continuous reactor: degradation pathway and disposability study. Journal of Hazardous Materials 346, 242–252.

Kemper, N., 2008. Veterinary antibiotics in the aquatic and terrestrial environment. Ecological Indicators 8, 1–13.

Khetan, S.K., Collins, T.J., 2007. Human pharmaceuticals in the aquatic environment: a challenge to green chemistry. Chemical Reviews 107, 2319–2364.

Kim, S., Choi, S.K., Yoon, B.Y., Lim, S.K., Park, H., 2010. Effects of electrolyte activities of RuO_2/Ti and Sb-SnO_2/Ti anodes for water treatment. Applied Catalysis B 97, 135-141.

Kim, S.C., Carlson, K., 2007. Temporal and spatial trends in the occurrence of human and veterinary antibiotics in aqueous and river sediment matrices. Environmental Science and Technology 41, 50–57.

Kitazono, Y., Ihara, I., Yoshida, G., Toyoda, K., Umetsu. K., 2012. Selective degradation of tetracycline antibiotics present in raw milk by electrochemical method. Journal of Hazardous Materials 243, 112–116.

Klavarioti, M., Mantzavinos, D., Kassinos, D., 2009. Removal of residual pharmaceuticals from aqueous systems by advanced oxidation processes. Environment International 35, 402-417.

Klein, E.Y., Van Boeckel, T.P., Martinez, E.M., Pant, S., Gandra, S., Levin, S.A., Goossens, H., Laxminarayan, R., 2018. Global increase and geographic convergence in antibiotic consumption between 2000 and 2015. PNAS, 115, E3463-E3470.

Korbahti, B.K., Tasyurek, S., 2015. Electrochemical oxidation of ampicillin antibiotic at boron-doped diamond electrodes and process optimization using response surface methodology. Environmental Science and Pollution Research 22, 3265-3278.

Kumar, S., Singh, S., Srivastava, V.C., 2015. Electro-oxidation of nitrophenol by ruthenium oxide coated titanium electrode: Parametric, kinetic and mechanistic study. Chemical Engineering Journal 263, 135-143.

Kummerer, K., 2001. Drugs in the environment: emission of drugs, diagnostic aids and disinfectants into wastewater by hospitals in relation to other sources – a review. Chemosphere 45, 957–969.

Kummerer, K., 2009. Antibiotics in aquatic environment – A review – Part I. Chemosphere 75, 417-434.

Kushwaha, J.P., Srivastava, V. C., Mall, I. D., 2010. Organics removal from dairy wastewater by electrochemical treatment and residue disposal. Separation and Purification Technology 76, 198–295.

Larsson, D.G.J., De Pedro, C., Paxeus, N., 2007. Effluent from drug manufacturers contains extremely high levels of pharmaceuticals. Journal of Hazardous Materials 148, 751–755.

Larsson, D.G.J., Fick, J., 2009. Transparency throughout the production chain: A way to reduce pollution from the manufacturing of pharmaceuticals? Regulatory Toxicology and Pharmacology 53, 161–163.

Laxminarayan, R., Chaudhury, R.R., 2016. Antibiotic resistance in India: Drivers and opportunities for action. PLoS Medicine 13, e1001974.

Laxminarayan, R., Matsoso, P., Pant, S., Brower, C., Rottingen, J.A., Klugman, K., Davies, S., 2016a. Access to effective antimicrobials: a worldwide challenge. Lancet 387, 168–175.

Li S., Bejan D., McDowell M. S., Bunce N. J., 2008. Mixed first and zero order kinetics in the electrooxidation of sulfamethoxazole at a boron-doped diamond (BDD) anode. Journal of Applied Electrochemistry 38, 151-159.

Lin, A. Y., Tsai, Y., 2009. Occurrence of pharmaceuticals in Taiwan's surface waters: Impact of waste streams from hospitals and pharmaceutical production facilities. Science of the Total Environment 407, 3793–3802.

Lin, H., Niu, J., Xu, J., Li, Y., Pan, Y., 2013. Electrochemical mineralization of sulfamethoxazole by Ti/SnO_2-Sb/Ce-PbO_2 anode: Kinetics, reaction pathways, and energy cost evolution. Electrochimica Acta 97, 167-174.

Lucas, M.S., Peres, J.A., 2009. Removal of COD from olive mill wastewater by Fenton's reagent: Kinetic study. Journal of Hazardous Materials 168, 1253–1259.

Marquardt, D.W., 1963. An algorithm for least-squares estimation of nonlinear parameters. Journal of the Society for Industrial and Applied Mathematics 11, 431–441.

Martinez-Huitle, C., Ferro, S., 2006. Electrochemical oxidation of organic pollutants for the wastewater treatment: direct and indirect processes. Chemical Society Reviews 35, 1324–1340.

Martinez-Huitle, C.A., Panizza, M., 2018. Electrochemical oxidation of organic pollutants for wastewater treatment. Current Opinion in Electrochemistry 11, 62–71.

Michael, I., Rizzo, L., McArdell, C.S., Manaia, C.M., Merlin, C., Schwartz, T., Dagot, C., Fatta-Kassinos, D., 2013. Urban wastewater treatment plants as hotspots for the release of antibiotics in the environment: a review. Water Research 47, 957-995.

Miyata, M., Ihara, I., Yoshid, G., Toyod, K., Umetsu, K., 2011. Electrochemical oxidation of tetracycline antibiotics using a Ti/IrO_2 anode for wastewater treatment of animal husbandry. Water Science and Technology 63(3), 456–461.

Mora-Gomez, J., Ortega, E., Mestre, S., Perez-Herranz, V., Garcia-Gabaldon, M., 2019. Electrochemical degradation of norfloxacin using BDD and new Sb-doped SnO2 ceramic anodes in an electrochemical reactor in the presence and absence of a cation-exchange membrane. Separation and Purification Technology 208, 68–75.

Moreira, F.C., Boaventura, R.A.R., Brillas, E., Vilar, V.J.P., 2017. Electrochemical advanced oxidation processes: a review on their application to synthetic and real wastewaters. Applied Catalysis B: Environmental, 202, 217–261.

Motoc, S., Manea, F., Pop, A., Pode, R., Teodosiu, C., 2012. Electrochemical degradation of pharmaceutical effluents on carbon-based electrodes. Environmental Engineering and Management Journal 11(3), 627–634.

Murugananthan, M., Latha, S.S., Raju. G.B., Yoshihara, S., 2010. Anodic oxidation of ketoprofen – An anti-inflammatory drug using boron-doped diamond and platinum electrodes. Journal of Hazardous Materials 180, 753–758.

Murugananthan, M., Yoshihara, S., Rakuma, T., Uhera, N., Shirakashi, T., 2007. Electrochemical degradation of 17β-estradiol (E2) at boron-doped diamond (Si/BDD) thin film electrode. Electrochimica Acta 52, 3242–3249.

Mutiyar, P.K., Mittal, A.K., 2013. Occurrences and fate of an antibiotic amoxicillin in extended aeration-based sewage treatment plant in Delhi, India: a case study of emerging pollutant. Desalination and Water Treatment 51, 6158–6164.

Mutiyar, P.K., Mittal, A.K., 2014. Risk assessment of antibiotic residues in different water matrices in India: key issues and challenges. Environmental Science and Pollution Research 21(12), 7723–7736.

Nan, H., Chen, Y.R., Luo, J.M., Jin, Y., Rong, L., Jing, X., Liu, X.H., 1994. In vitro investigation of blood compatibility of Ti with oxide layers of rutile structure. Journal of Biomaterials Applications 8(4), 404 – 412.

Nideesh, P.V., Divyapriya, G., Oturan, N., Trellu, C., Oturan, M.A., 2019. Environmental appliactions of boron-doped diamond electrodes: 1. Application in water and wastewater treatment. ChemElectroChem 6, 1–20.

Nikolaou, A., Meric, S., Fatta, D., 2007. Occurrence patterns of pharmaceuticals in water and wastewater environments. Analytical and bioanalytical chemistry 387(4), 1225–1234.

Nordmann, P., Naas, T., Poirel, L., 2011. Global spread of Carbapenemase - producing Enterobacteriaceae. Emerging Infectious Diseases 17(10), 1791–8.

Oaks, J. L., Gilbert, M., Virani, M. Z., Watson, R. T., Meteyer, C. U., Rideout, B. A., Mahmood, S., 2004. Diclofenac residues as the cause of vulture population decline in Pakistan. Nature 427(6975), 630.

Oturan, N., Wu, J., Zhang, H., Sharma, V.K., Oturan, M.A., 2013. Electrocatalytic destruction of the antibiotic tetracycline in aqueous medium by electrochemical advanced oxidation processes: Effect of electrode materials. Applied Catalysis B: Environmental 140–141, 92–97.

Panizza, M. and Cerisola, G., 2009. Direct and mediated anodic oxidation of organic pollutants. Chemical Reviews 109, 6541-6569.

Petrie, B., Barden, R., Kaspryzk-Hordern, B., 2015. A review on emerging contaminants in wastewaters and the environment: Current knowledge, understudied areas and recommendations for future monitoring. Water Research 72, 3–27.

Petrie, B., Barden, R., Kaspryzk-Hordern, B., 2015. A review on emerging contaminants in wastewaters and the environment: Current knowledge, understudied areas and recommendations for future monitoring. Water Research 72, 3–27.

Petrovic, M., Hernando, M.D., Diaz-Cruz, M.S., Barcelo, D., 2005. Liquid chromatography–tandem mass spectrometry for the analysis of pharmaceutical

residues in environmental samples: a review. Journal of Chromatography A 1067, 1–14.

Pillai, L.M.S., Gupta, A.K., 2017. Performance analysis of a continuous serpentine flow reactor of electrooxidation of synthetic and real textile wastewater: energy consumption, mass transfer coefficient and economic analysis. Journal of Environmental Management 193, 524–531.

Rahmani, A.R., Nematollahi, D., Samarghandi, M.R., Samadi, M.T., Azarian, G., 2018. A combined advanced oxidation process: electrooxidation-ozonation for antibiotic ciprofloxacin removal from aqueous solution. Journal of Electroanalytical Chemistry 808, 82–89.

Rajkumar, D., Palanivelu, K., Mohan, N., 2003. Electrochemical degradation of resorcinol using mixed oxide coated titanium electrode for wastewater treatment – A kinetic study. Indian Journal of Chemical Technology 10, 396–401.

Rivera-Utrilla, J., Sanchez-Polo, M., Ferro-Garcia, M.A., Prados-Joya, G., Ocampo-Perez, R., 2013. Pharmaceuticals as emerging contaminants and their removal from water. A review. Chemosphere 93, 1268 – 1287.

Rossi, A., Alves, V.A., Da Silva, L.A., Oliveira, M.A., Assis, D.O.S., Santos, F.A., Miranda, R.R.S., 2009. Electrooxidation and inhibition of the antibacterial activity of oxytetracycline hydrochloride using a RuO2 electrode. Journal of Applied Electrochemistry 39, 329–337.

Sacher, F., Gabriel, S., Metzinger, M., Stretz, A., Wenz, M., Lange, F.T., Brauch, H.J., Blankenhorn, I., 2002. Active pharmaceutical ingredients in ground water – the results of a monitoring program in Baden Württemberg (Germany). Vom Wasser 99, 183–196.

Sahu, O., Mazumdar, B., Chaudhari, P.K., 2019. Electrochemical treatment of sugar industry wastewater: process optimization by response surface methodology. International Journal of Environmental Science and Technology, 16, 1527–1540.

Sanchez-Montes, I., Neto, J.R.F., Silva, B.F., Silva, A.J., Aquino, J.M., Rocha-Filho, R.C., 2018. Evolution of the antibacterial activity and oxidation intermediates during the electrochemical degradation of norfloxacin in a flow cell with a PTFE-doped β-

PbO2 anode: Critical comparison to a BDD anode. Electrochimica Acta, 284, 260–270.

Santoke, H., Song, W., Cooper, W.J., Greaves, J., Miller, E., 2009. Free-radical induced oxidative and reductive degradation of fluoroquinolone pharmaceuticals: Kinetic studies and degradation mechanism. Journal of Physical Chemistry A 113, 7846–7851.

Santos, I.D.D., Afonso, J.C., Dutra, A.J., 2011. Electrooxidation of phenol on a Ti/RuO_2 anode: effect of some electrolysis parameters. Journal of the Brazilian Chemical Society, 22(5), 875–883.

Sarmah, A.K., Meyer, M.T., Boxall, A.B., 2006. A global perspective on the use, sales, exposure pathways, occurrence, fate and effects of veterinary antibiotics (VAs) in the environment. Chemosphere 65(5), 725–759.

Silva, F., Saez, C., Lanza, M., Canizares, P., Rodrigo, M., 2019. The Role of Mediated Oxidation on the Electro-irradiated Treatment of Amoxicillin and Ampicillin Polluted Wastewater. Catalysts, 9(1), 9.

Singh, S., Srivastava, V.C., Mall, I.D., 2013. Mechanism of dye degradation during electrochemical treatment. Journal of Physical Chemistry C 117, 15229-15240.

Sires, I., Brillas, E., Oturan, M.A., Rodrigo, M.A., Panizza, M., 2014. Electrochemical advanced oxidation processes: today and tomorrow. A review. Environmental Science and Pollution Research 21, 8336-8367.

Sires, I., Cabot, P.L., Centellas, F., Garrido, J.A., Rodriguez, R.M., Arias, C., Brillas, E., 2006. Electrochemical degradation of clofibric acid in water by anodic oxidation: comparative study with platinum and boron-doped diamond electrodes. Electrochimica acta, 52(1), 75–85.

Smith, A.J., Balaam, J.L., Ward, A., 2007. The development of a rapid screening technique to measure antibiotic activity in effluents and surface water samples. Marine Pollution Bulletin 54, 1940–1946.

Sopaj, F., Rodrigo, M.A., Oturan, N., Podvorica, F.I., Pinson, J., 2015. Influence of the anode materials on the electrochemical oxidation efficiency. Application to

oxidative degradation of the pharmaceutical amoxicillin. Chemical Engineering Journal 262, 286–294.

Steter, J.R., Dionisio, D., Lanza, M.R.V., Motheo, A.J., 2014. Electrochemical and sonoelectrochemical processes applied to the degradation of the endocrine disruptor methyl paraben. Journal of Applied Electrochemistry 44, 1317–1325.

Sun, Z.R., Gao, M., Peng, Y.Z., Hu, X., 2011. Electrochemical dechlorination of 2,4-dichlorophenol in aqueous solution on palladium-loaded meshed titanium electrode, Water Science and Technology 63, 199.

Sundarapandiyan, S., Chandrasekar, R., Ramanaiah, B., Krishnan, S., Saravanan, P., 2010. Electrochemical oxidation and reuse of tannery saline wastewater. Journal of Hazardous Materials 180, 197–203.

Tamtam, F., Mercier, F., Le Bot, B., Eurin, J., Dinh, Q.T., Clement, M., Chevreuil, M., 2008. Occurrence and fate of antibiotics in the Seine River in various hydrological conditions. Science of the Total Environment 393, 84–95.

Trasatti, S., 1987. Progress of the understanding of the mechanism of chlorine evolution at oxide electrodes. Electrochimica Acta 32, 369–382.

Van Boeckel, T.P., Gandra, S., Ashok, A., Caudron, Q., Grenfell, B.T., Levin, S.A., Laxminarayan, R., 2014. Global antibiotic consumption 2000 to 2010: an analysis of national pharmaceutical sales data. Lancet Infectious Diseases 14, 742-750.

Vasilie S., Manea, F., Baciu, A., Pop, A., Dual use of boron-doped diamond electrode in antibiotics-containing water treatment and process control, 2018. Process Safety and Environmental Protection 117, 446-457.

Vedenyapina, M.D., Borisova, D.A., Streltsova, E.D., Rakishev, A.K., & Vedenyapin, A.A., 2014. Electrochemical degradation and mineralization of tetracycline on a boron-doped diamond electrode. Russian Chemical Bulletin 63(8), 1843-1847.

Vidal, J., Huilinir, C., Santander, R., Silva-Agredo, J., Torres-Palma, R.A., Salazar, R., 2019. Degradation of ampicillin antibiotic by electrochemical processes: evaluation of antimicrobial activity of treated water. Environmental Science and Pollution Research 26(5), 4404–4414.

Wachter, N., Aquino, J.M., Denadai, M., Barreiro, J.C., Silva, A.J., Cass, Q.B., Rocha-Filho, R.C., Bocchi, N., 2019. Optimization of the electrochemical degradation process of the antibiotic ciprofloxacin using a double-sided β-PbO2 anode in a flow reactor: kinetics, identification of oxidation intermediates and toxicity evaluation. Environmental Science and Pollution Research 26, 4438–4449.

Wang, Y., Shen, C., Zhang, M., Zhang, B., Yu, Y., 2016. The electrochemical degradation of ciprofloxacin using a SnO_2-Sb/Ti anode: Influencing factors, reaction pathways and energy demand. Chemical Engineering Journal 296, 79–89.

Waterson, K., Wang, J.W., Bejan, D., Bunce, N.J., 2006. Electrochemical waste water treatment: Electrooxidation of acetaminophen. Journal of Applied Electrochemistry 36, 227–232.

Watkinson, A.J., Murby, E.J., Kolpin, D.W., Constanzo, S.D., 2009. The occurrence of antibiotics in an urban watershed: From wastewater to drinking water. Science of the Total Environment 407, 2711–2723.

Wirzal, M.D.H., Yusoff, A.R.M., Zima, J., Barek, J., 2013. Degradation of ampicillin and penicillin G using anodic oxidation. International Journal of Electrochemical Science 8, 8978-8988.

Wu, J., Zhang, H., Oturan, N., Wang, Y., Chen, L., Oturan, M.A., 2012. Application of response surface methodology to the removal of the antibiotic tetracycline by electrochemical process using carbon-felt cathode and DSA (Ti/RuO_2-IrO_2) anode. Chemosphere 87, 614–620.

Xie, R., Meng, X., Sun, P., Niu, J., Jiang, W., Bottomley, L., Crittenden, J., 2017. Electrochemical oxidation of ofloxacin using a TiO2-based SnO2-Sb/polytetrafluoroethylene resin-PbO2 electrode: Reaction kinetics and mass transfer impact. Applied Catalysis B: Environmental 203, 515–525.

Xu, W.H., Zhang, G., Zou, S.C., Li, X.D., Liu, Y.C., 2007. Determination of selected antibiotics in the Victoria Harbour and the Pearl River, South China using high performance liquid chromatography – electrospray ionization tandem mass spectrometry. Environmental Pollution 145, 672–679.

Yahiaoui, I., Aissani-Benissad, F., Fourcade, F., Amrane, A., 2013. Removal of tetracycline hydrochloride from water based on direct anodic oxidation (Pb/PbO_2 electrode) coupled to activated sludge culture. Chemical Engineering Journal 221, 418–425.

Yavuz, Y. and Koparal, A.S., 2006. Electrochemical oxidation of phenol in a parallel plate reactor using ruthenium mixed metal oxide electrode. Journal of Hazardous Materials 136, 296-302.

Yu, X., Zhou M., Hu, Y., Serrano, K.G., Yu, F., 2014. Recent updates on electrochemical degradation of bio-refractory organic pollutants using BDD anode: a mini review. Environmental Science and Pollution Research 21, 8417–8431.

Zaviska, F., Drogui, P., Blais, J.F., Mercier, G., d'Auzay, S.D.L.R., 2013. Electrochemical oxidation of chlorotetracycline using Ti/IrO_2 and Ti/PbO_2 anode electrodes: Application of experimental design methodology. Journal of Environmental Engineering 139, 810-821.

Zhang, H., Liu, F., Wu, X., Zhang, J., Zhang, D., 2009. Degradation of tetracycline in aqueous medium by electrochemical method. Asia-Pacific Journal of Chemical Engineering 4, 568–573.

Zhao, X., Hou, Y., Liu, H., Qiang, Z., Qu, J., 2009. Electrooxidation of diclofenac at boron doped diamond: Kinetics and mechanism. Electrochimica Acta 54, 4172–4179.

Zhu, L., Santiago-Schubel, B., Xiao, H., Hollert, H., Kueppers, S., 2016. Electrochemical oxidation of fluoroquinolone antibiotics: Mechanism, residual antibacterial activity and toxicity change. Water Research 102, 52-62.

Zorita, S., Martensson, L., Mathiasson, L., 2009. Occurrence and removal of pharmaceuticals in a municipal sewage treatment system in the south of Sweden. Science of the total environment 407(8), 2760–2770.

Zubavichus, Y.V., Slovokhotov, Y.L., Nazeeruddin, M.K., Zakeeruddin, S.M., Gratzel, M., Shklover, V., 2002. Structural characterization of solar cell prototypes based on nanocrystalline TiO_2 anatase sensitized with Ru complexes. X-ray diffraction, XPSand XAFS spectroscopy study. Chemistry of Materials 14(8), 3556 – 3563.

RESEARCH PUBLICATIONS

SCI Journals

1. Kaur, R., Kushwaha, J.P., Singh, N., Electrooxidation of Ofloxacin antibiotic by dimensionally stable Ti/RuO_2 anode: Evaluation and mechanistic approach, 2018. ***Chemosphere*** 193, 685-694. **(Impact Factor: 5.108)**
2. Kaur, R., Kushwaha, J.P., Singh, N., Amoxicillin Electro-catalytic oxidation using Ti/RuO_2 Anode: Mechanism, Oxidation Products and Degradation Pathway, 2019. ***Electrochimica Acta*** 296, 856-866. **(Impact Factor: 5.383)**
3. Kaur, R., Kushwaha, J.P., Singh, N., Electro-catalytic oxidation of Ofloxacin antibiotic in continuous reactor: Evaluation, Transformation products and Pathway, 2019. ***Journal of the Electrochemical Society*** 166(6), H250-H261. **(Impact Factor: 3.120)**
4. Kaur, R., Kushwaha, J.P., Singh, N., Electro-oxidation of amoxicillin trihydrate in continuous reactor by Ti/RuO_2 anode, 2019. ***Science of the Total Environment*** 677, 85-97. **(Impact Factor: 5.589)**

International Conferences

1. Kaur, R., Kushwaha, J.P., Singh, N., Antibiotics Removal from Wastewater by Electro-oxidation Method. *CHEMCON 2016 – Chemical Engineering towards Sustainable Development* (December 27–30, 2016), organized by Indian Institute of Chemical Engineers, Chennai, India **(BEST PAPER AWARD)**.

2. Kaur, R., Kushwaha, J.P., Singh, N., Antibiotics Removal from Wastewater In a Continuous Electro-oxidation Reactor: Kinetic Study. *CHEMCON 2018 – Seamless Chemical Engineering in Service of Humanity: Innovations, Opportunities & Challenges* (December 27–30, 2018), organized by Dr. B. R. Ambedkar National Institute of Technology, Jalandhar, India

National Conference

1. Kaur, R., Kushwaha, J.P., Singh, N., Kinetic Study for the Removal of Ofloxacin from Pharmaceutical Wastewater by Electrochemical Method. *National Conference on Advances in Chemical and Environment Engineering - 2016 (ACEE 2016)* (April 22–23, 2016), organized by Dr. B. R. Ambedkar National Institute of Technology, Jalandhar, India.